CR-172082

Conceptual Design of a Lunar Oxygen Pilot Plant

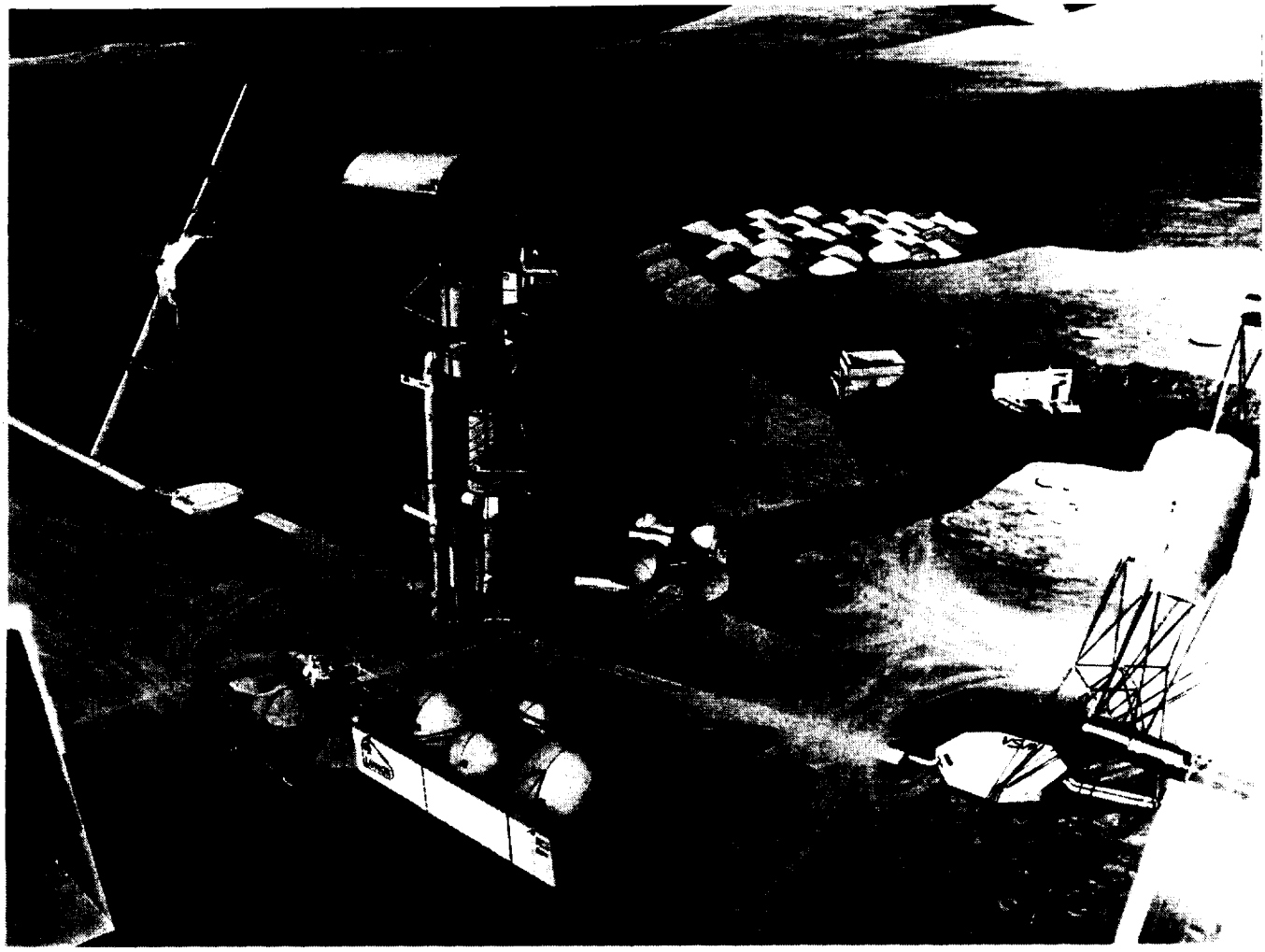

NASA Contract Number NAS9-17878
EEI Report 88-182
July 1, 1988

Conceptual Design of a Lunar Oxygen Pilot Plant

Lunar Base Systems Study (LBSS) Task 4.2

Prepared under NASA Contract NAS9-17878 for the

Advanced Programs Office

NASA Johnson Space Center

by

Eagle Engineering, Inc.

Houston, Texas

EEI Contract TO-87-57

Task 4.2 Report

EEI Report No. 88-182

July 1, 1988

Foreword

This study was conducted between December 1, 1987 and July 1, 1988 by Eagle Engineering, Inc. (EEI) for the Advanced Programs Office at the NASA Johnson Space Center (JSC). The Conceptual Design of a Lunar Oxygen Production Facility was performed to support the JSC Lunar Base Surface Systems (LBSS) study intended to provide planning for a Lunar Base near the year 2000. The purpose of this study was to (1) provide a list of candidate lunar oxygen production processes, (2) develop a rationale for selecting two processes for further study, (3) produce conceptual designs of pilot plants based on the two leading processes, (4) determine impacts of pilot and production plants on base operations, (5) determine the feasibility of recovering solar wind implanted hydrogen from the lunar regolith.

Dr. John W. Alred was the NASA JSC technical manager for this study. The NASA JSC task monitors for this task were Mr. James Sturm and Mr. Kyle O. Fairchild.

EEI personnel participating in this task included:

Project Manager:	Mr. William R. Stump
Task Manager:	Mr. Eric L. Christiansen
Technical Contributors:	Mr. John Euker
	Mr. Karl Maples
	Dr. Charles H. Simonds
	Mr. Scott Zimprich
Illustration Support:	Mr. Mark W. Dowman
	Mr. Mike Stovall

Table of Contents

Table of Contents (Cont.)

Table of Contents (Cont.)

List of Figures

List of Figures (Cont.)

List of Tables

List of Abbreviations

A&R	Automation & Robotics
ASTS	Advanced Space Transportation System
atm	atmospheres (1 atm = 14.696 psi)
°C	Celsius (temperature)
cm	centimeter
DDT&E	Design, Development, Test, and Evaluation
EVA	Extravehicular Activity
°F	Fahrenheit (temperature)
FL	Front-end Loader
g or gm	grams
h or hr	hours
IVA	Intravehicular Activity
°K	Kelvin (temperature)
kg	kilograms
km	kilometers
ksi	kips per square inch (1 ksi = 1000 psi)
kw	kilowatts
kwe	kilowatts electric
kwh	kilowatt-hours
kwt	kilowatts thermal
lbs or lb_m	pounds mass
lb_f	pounds force
LEO	Low Earth Orbit
LH_2	Liquid Hydrogen
LLO	Low Lunar Orbit
LOX	Liquid Oxygen
LS	Lunar Surface
m	meters
mt	metric tons (1 mt = 1000 kg or 2,204.6 lb_m)
MPa	Megapascals (1 MPa = 145.04 psi)
MW	Megawatts
MWe	Megawatts electric
MWh	Megawatt-hours
MWt	Megawatts thermal
N	Newtons (1 N = 0.224809 lb_f)
Pa	Pascal (1 Pa = 1 N/m^2, 6,894.7 Pa = 1 psi)
Poise	Poise (100 centipoise = 100 cp = 0.1 $N\text{-}s/m^2$ = 1 g/cm-s)
psi	pounds-force per square inch
PV	Photovoltaic Solar Power System
OTV	Orbital Transfer Vehicle
RFC	Regenerative Fuel Cell Power System
s or sec	seconds
w	watts
wh	watt-hours
yr	years

1.0 Executive Summary

The primary objective of this study was to develop conceptual designs of two pilot plants to produce oxygen from lunar materials. A lunar pilot plant will be used to generate engineering data necessary to support an optimum design of a larger scale production plant. Lunar oxygen would be of primary value as spacecraft propellant oxidizer. In addition, lunar oxygen would be useful for servicing non-regenerative fuel cell power systems, providing requirements for life support, and to makeup oxygen losses from leakage and airlock cycling.

Numerous processes to produce oxygen from lunar materials have been proposed. Thirteen different lunar oxygen production methods are described in this report. Comparisons are complicated because many variations of each process exist, and some produce multiple byproducts with potential uses at a later stage of lunar base development. Based on process simplicity and well understood reaction chemistry, hydrogen reduction of ilmenite was selected for conceptual design studies. Based on recovery of an important "byproduct", a second process pathway to oxygen, extraction of solar-wind hydrogen from bulk lunar soil, was also selected for conceptual design. Thermal recovery of solar-wind hydrogen liberates water, which is subsequently electrolyzed to produce oxygen (water is a reaction product of hydrogen and ilmenite contained in the soil), as well as hydrogen. Thus, hydrogen recovery offers a process that produces both oxidizer and fuel propellants for lunar landers and other spacecraft.

Computer models of both processes were prepared that utilize equipment scaling relations, mass and energy balances, and thermodynamic relationships to estimate mass and power requirements for oxygen production plants. Trades and sensitivity analyses were performed with these models. Studies on the hydrogen reduction of ilmenite process included:

- Evaluation of feedstock alternatives: high-titanium mare soil or basalt.
- Effect of solar and nuclear-electric power sources.
- Effect on pilot plant mass/power to simply vent the product oxygen gas instead of liquefying and storing it (since the pilot plant is a research tool).
- Comparison between delivering a series of small self-contained, modular production plants to increase oxygen production versus constructing a single, large plant.
- Difference between using unbeneficiated feedstock or using magnetic or electrostatic separation to feed an ilmenite concentrate to the reactor.
- Sensitivity of process mass and power to oxygen production rate.
- Sensitivity of process mass and power to feedstock conditions such as ilmenite abundance in soil or ilmenite grain size in basalt.

Drawings of a 2 metric ton/month LOX pilot plant conceptual design, employing hydrogen reduction of ilmenite, were produced. Plant mass is 24.7 metric tons (54,400 lb_m) including a power system that uses solar photovoltaic arrays to provide 146 kwe for the process and for regenerating fuel cell reactants. Baseline plant operating strategy is mining and continuous processing during the lunar day, and no mining with processing units on hot standby during the lunar night. The major process equipment is delivered to the lunar surface in an integrated package that manifests easily into a Shuttle payload pallet with outside dimensions of 14' diameter x 45' long. However, additional volume is required to deliver the power systems. Since it is assumed that the purpose of the pilot plant is to provide long-term, 1/6-g equipment performance data, the plant will be operated for continuous periods without on-site human attention. Thus, extensive automation and robotics applications are anticipated for the pilot plant, such as teleoperated mining

vehicles and equipment servicers. These would have numerous applications in other areas of lunar base operations.

Studies of the optimum temperature for solar-wind hydrogen extraction and the sensitivity of plant mass/power to production rates were also completed. Mass of a pilot plant designed to produce 2 metric ton/month LOX and 1.2 metric ton/month LH_2 is 60 metric tons (132,200 lb_m). The mass estimate includes a nuclear power plant providing 1.7 MWe for the process.

2.0 Introduction

Groundrules and assumptions for the study are listed in Section 3. Thirteen candidate lunar oxygen processes were identified and described in Section 4. Although the list is not complete (other reagents have been suggested) and there are many variations possible for each process, the descriptions are representative of the processes most favored for lunar oxygen extraction.

Two candidates were selected for further study and conceptual design: reduction of ilmenite by hydrogen and extraction of solar wind volatiles. After describing the distribution of lunar sources of ilmenite and solar wind hydrogen in Section 5, Sections 6 and 7 describe the conceptual designs for these two processes. A concluding summary of results and recommendations is given in Section 8.

Scaling equations used for sizing equipment in the hydrogen reduction of ilmenite process are documented in Appendix A. Appendix B provides a sample output of the sizing program. Appendix C presents scaling equations unique to the hydrogen extraction plant, while Appendix D gives a sample output of the program. Appendix E contains information on an assessment of lunar oxygen production for supplying a low Earth orbit market (referenced from Section 6.7).

3.0 Study Groundrules

1. The pilot plant will be designed to have a maximum liquid oxygen production rate of 2 metric tons/month (1) at a 90% plant utility.

2. The pilot plant will be operated during Phase II of the lunar base buildup program (1). This phase is defined as the human-tended period (2000-2005) before a permanently occupied lunar base (1, 83, 84). It is assumed the pilot plant will require long operating periods to generate an adequate engineering and operating performance database for production plant design. Therefore, the pilot plant will operate without on-site human attention.

3. The baseline liquid oxygen production rate for program analyses of a full-scale production plant ranges from 100-1,000 metric tons/year. A 1,000 mt/yr LOX plant will supply the annual Earth-Moon advanced space transportation system (ASTS) requirements and provides some margin for other purposes (Mars missions, etc.). A conceptual design for a reusable lunar lander with a maximum landed payload of 25 mt (no ascent), or 14 mt with inert mass returned to lunar orbit, requires approximately 30 mt propellant: 25.7 mt LOX and 4.3 mt LH_2 at a 6:1 oxidizer to fuel ratio (50). A roundtrip for a lunar mission stack of two reusable orbital transfer vehicles delivering a 35 mt cargo to LLO (and returning empty) requires 73.5 mt LOX and 10.5 mt LH_2 at a 7:1 mixture ratio (3). A lunar base may require 5-7 roundtrips/year.

4.0 Candidate Processes for Production of Oxygen from Lunar Materials

Many processes have been proposed to recover oxygen from lunar raw materials (16-23) including:

Thermochemical Reduction

1. Hydrogen reduction of Ilmenite.
2. Carbothermal reduction of ilmenite and other oxides with coke, methane, carbon monoxide, or other hydrocarbons.
3. Recovery of solar wind hydrogen followed by hydrogen reduction of oxides.
4. Hydrogen sulfide reduction of Ca, Fe, and Mg oxides.

Thermochemical Reduction/Oxidation

5. Carbochlorination.

Thermochemical Oxidation

6. Fluorine exchange.

Note: The above thermochemical processes often employ electrolytic methods to regenerate the chemical reagents (e.g. water electrolysis for ilmenite reduction), however, thermochemical regeneration alternatives usually also exist.

Reactive Solvent

7. Hydrofluoric acid leach.

Electrochemical Reduction

8. Direct electrolytic reduction of oxide melt.
9. Electrolytic reduction of oxide/caustic solution.
10. Reduction of metal oxides by lithium or sodium followed by electrolysis of the lithium or sodium oxide melt.
11. Reduction of anorthite by aluminum followed by staged electrolysis steps to recover silicon, aluminum, calcium, and oxygen.

Thermal/Physical

12. Vapor phase reduction.
13. Ion separation.

Other chemical pathways to oxygen have been proposed (82) but the above represent those processes described in some detail in the literature. A comparison of these processes is complicated because many processing variations and equipment options exist for each, effecting process mass, power, volume, manpower, and other considerations. In addition, many produce byproducts (metals, ceramics, etc.). For a fair comparison, the demand and/or value for each of these byproducts must be established, and the cost for separating and processing the byproducts into useful end products must be determined.

4.1 Process Descriptions

Process chemistry and processing conditions, and major advantages and disadvantages of several lunar oxygen extraction techniques are described in the following subsections.

4.1.1 Hydrogen Reduction of Ilmenite

Ilmenite feedstock reacts endothermically with hydrogen to produce water. A reaction temperature of 900-1,000°C has typically been reported necessary to achieve sufficient rates of reaction. Product water is then electrolytically or thermochemically split to regenerate reactant hydrogen and liberate oxygen. The reactions are expressed as:

$$FeTiO_{3(s)} + H_{2(g)} = Fe_{(s)} + TiO_{2(s)} + H_2O_{(g)} \qquad \text{Reduction}$$

$$H_2O_{(g)} + \text{electricity} = H_{2(g)} + 1/2\ O_{2(g)} \qquad \text{Electrolysis}$$

An alternative to the electrolysis step is a thermochemical cycle to regenerate hydrogen reductant gas. One of dozens of possible thermochemical cycles is the DeBeni Carbon-Iron Process that catalytically decomposes water by the following reaction sequence (7,8):

Reaction	Reaction Temp. (K)
$C + H_2O = CO + H_2$	920
$CO + 2\ Fe_3O_4 = C + 3\ Fe_2O_3$	520
$3\ Fe_2O_3 = 2\ Fe_3O_4 + 1/2\ O_2$	1670

$H_2O = H_2 + 1/2\ O_2$	

Such a reaction sequence reportedly involves less energy than does electrolysis (7, p.101). However, thermochemical separation of water increases the complexity of the water separation step, requiring more process equipment such as individual reaction vessels for each process step.

A simplified schematic of the process is depicted in Figure 4-1a. A fluidized bed reactor has been proposed for the reduction step (14, 16). Gibson & Knudsen's (14) concept of a three-stage fluidized bed reactor system is given in Figure 4-1b.

An energy-efficient hydrogen reduction scheme has been proposed (14; 16, pp.228-237) using vapor-phase water electrolysis to allow both reactor and electrolysis to operate at the same temperature. The use of high-temperature, solid-state electrolytic cells probably represents the greatest technology development requirement for this process although experimental work on this technology is progressing (24-27, 118). High temperature electrolysis using a solid ceramic electrolyte has been experimentally researched for fuel cells (25); electrolysis of mixtures of water, carbon dioxide, and carbon monoxide (26, 27); Mars atmospheric in-situ propellant production (24); carbon dioxide reduction in life support systems (118); and in the technology development of another lunar propellant production technique (64). Conventional water electrolysis systems can be used but will result in a less energy efficient process. Thus, synergism (and the inherent advantages for system commonality) could exist between solid-state electrolysis units for the hydrogen-reduction process and regenerative fuel cells in the power system (26), and even with the proposed Mars surface propellant manufacture systems (24, 34-37).

Pros and Cons

The major advantages for the process are:

- Process chemistry is uncomplicated and has been verified in laboratory testing (9-13). Necessary technology development efforts need only be directed at reducing plant mass and energy requirements, not at proving the process will work from a chemical basis.

- Oxygen generation and hydrogen reductant recovery is accomplished in one step by water electrolysis. This reduces complexity, increasing the probability of a low mass, reliable system.

- Resupply mass for reagent makeup of process losses is expected to be small due to the low density of hydrogen gas.

- Direct terrestrial counterparts exist for the major process equipment, such as the reactor. Continuous fluidized-bed and counter-current gas-solid flow reactors of the type contemplated for the reduction reaction have been operated terrestrially (13-15). Thus, industrial operating experience can be drawn on by NASA during the design and development process of exterrestrial extraction plants using this chemical process.

- Process temperatures are below the melting point of the ilmenite feed which reduces reactor materials problems.

- Iron production is possible but would probably require melting the solid residue of iron and rutile.

The major disadvantages of the process are:

- Only ilmenite is reduced in the hydrogen reduction process. To decrease the amount of material handled and process heat requirements, ilmenite must be separated from the bulk regolith.

- The kinetics for the hydrogen reduction reaction is relatively slow: 1 hour at 1,000°K is required to remove approximately 70 percent of the oxygen associated with divalent iron in ilmenite (13; 16, p.232,234). Another researcher reported that unoxidized ilmenite required 2 hours at 873°K and 0.25 hours at 1,073°K to completely reduce the iron oxide in ilmenite assuming the reaction rate is controlled by kinetics (9). In any case, the hydrogen reduction reactor must be made long enough to provide the required solid's residence time to accomplish the reduction reaction. The slower the kinetics, the longer (and heavier) a reactor must be for a given reaction temperature and production rate.

  The thermodynamics of hydrogen reduction impose rather low equilibrium per-pass conversions of H_2 to H_2O: 10.5 percent (molar) at 1,000°C and 7 percent at 900°C (14, p.547, Figure 2). As per-pass conversions decrease, the reductant gas flow rate through the system must be increased for a given production rate, which then requires larger reactor and gas piping diameters (and mass penalties).

Figure 4-1a. Simplified Schematic of Hydrogen Reduction of Ilmenite Process

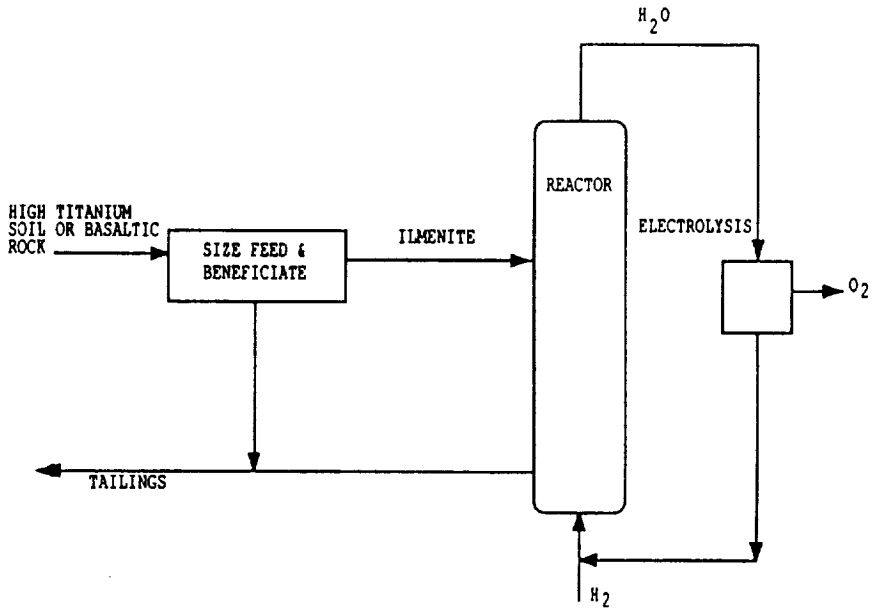

Figure 4-1b. Three-Stage Fluidized Bed Reactor Concept for Ilmenite Reduction (Ref.14)

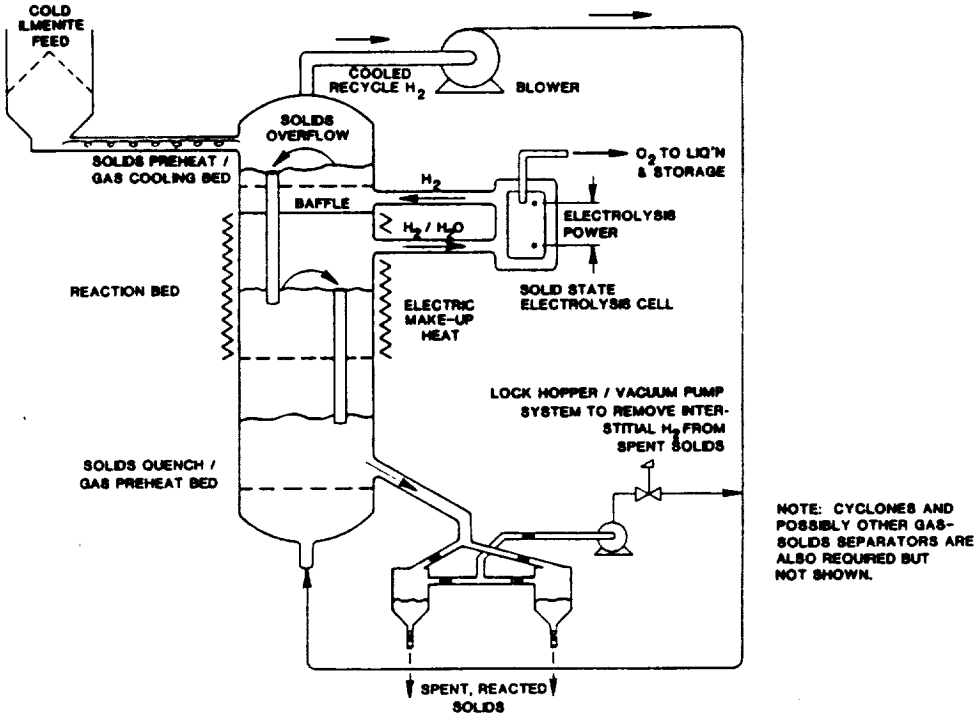

4.1.2 Carbothermal Reduction

Reduction of lunar oxides (ilmenite, pyroxenes, olivines) by carbonaceous reductants has been studied for several decades (28-30). Experimental work by Rosenburg, et al. (28, 31) was performed on the reduction of molten magnesium silicates by methane with the following process chemistry:

$$Mg_2SiO_4 + 2\ CH_4 = 2\ CO + 4\ H_2 + Si + 2\ MgO$$ (olivine) — Reduction @ 1,625°C / 2,960°F

and,

$$MgSiO_3 + 2\ CH_4 = 2\ CO + 4\ H_2 + Si + MgO$$ (pyroxene) — Reduction @ 1,625°C / 2,960°F

Lunar fines are first melted, then methane is injected to reduce iron oxides and the more stable silicates. Carbon monoxide (CO) and hydrogen products are reacted at lower temperature and over a nickle catalyst with additional hydrogen to regenerate methane and produce water.

$$2\ CO + 6\ H_2 = 2\ CH_4 + 2\ H_2O$$ — Catalytic Redox @ 250°C / 480°F

Oxygen and hydrogen can be electrolytically produced from water after it is separated from the methane/water product. A process schematic is given in Figure 4-2.

Carbothermal reduction of anorthite is possible (32), but at extremely high temperatures (2,500°K, 4,000°F). Besides the unattractiveness of high temperature materials and corrosion problems, process chemistry for this reaction scheme is severly complicated by the presence of metallic and oxide gaseous species (Al_2O, SiO, Al, Si, Ca) and condensed carbide phases (SiC, Al_4C_3, Al_4O_4C). It is not considered further.

Cutler, et al. (30), has proposed an oxygen and iron production scheme using coke (devolatilized carbon) to reduce molten ilmenite. The proposed process utilizes concepts and technology from the iron/steel making and petrochemical refining industries. A process flow diagram is given in Figure 4-3. The process includes three major steps: ilmenite smelting, iron decarburization (steelmaking), and hydrocarbon reforming. Ilmenite is melted (1,640°K, 2,500°F) in the smelting step and reacts endothermically with carbonaceous materials to form iron by the following reaction:

$$FeTiO_3 + C = Fe + CO + TiO_2$$ (slag-metal bath reaction)

This step is reminiscent of the conditions in the lower part of the iron-making blast furnace. Anorthite (10 percent) is added to form a quaternary slag (TiO_2, SiO_2, Al_2O_3, CaO) with a melting point below iron. Because the anorthite will have to be melted, it constitutes an energy penalty. The energy requirement for this step was proposed to be provided by induction heaters or via electric arc heating using carbon electrodes (30). The electrodes would be consumed during operation, but would only provide 2-4 percent of the required carbon reductant (at an electrode consumption rate of 5-10 kg/mt Fe).

Four to five percent carbon will alloy with the iron (15) and recovery is required for efficient reactant recycling. After the molten iron product is tapped from the smelter,

decarburization is accomplished by injecting some of the oxygen product into the iron bath to form carbon monoxide.

$$C_{(soln.)} + 1/2\ O_2 = CO \qquad \text{(iron decarburization)}$$

This step is identical to terrestrial basic oxygen steelmaking furnaces. The decarburization reaction is highly exothermic and thus requires no additional energy. However, the amount of oxygen injected must be carefully controlled to avoid excessive re-oxidation of the iron. The result of the process is a low-carbon steel which, however, requires further downstream forming operations before it would be suitable for lunar base structural applications. The iron-rich slag from the steelmaking process should be recycled to the smelter to recover iron units and oxygen.

Carbon monoxide from the smelter and steelmaking units is reacted with hydrogen in a reforming step to produce water and hydrocarbons. This step is exothermic and requires a nickel catalyst to promote a specific gas product. One possible hydrocarbon product is methane:

$$CO + 3\ H_2 = H_2O + CH_4 \qquad \text{(reforming)}$$

Typical terrestrial methanators operate at 300-400°C (8). Higher pressures (6 atm.) increase the yield of methane by reducing (by up to 50 percent) the quantity of carbon dioxide produced by competitive reactions (28). The reforming step actually will involve additional major equipment besides a CO/H_2 reactor; possibly staged condensers and distillation columns to produce a reasonably pure water stream. The water stream is electrolytically separated into oxygen and hydrogen. Hydrogen from the electrolysis step is fed to the reformer. It was proposed that hydrocarbons from the reformer could be coked or cracked to form the carbon electrodes for the smelter if electric arc reduction is performed (30). Electrode manufacture will undoubtedly require several steps and several separate unit operations other than implied by simple thermal decomposition or catalytic cracking of a hydrocarbon.

Pros and Cons

The major advantage of carbonaceous reduction of molten oxides is that in principal, less mining and lower loads on downstream equipment (and thus potentially smaller process units) are required than the hydrogen reduction of ilmenite scheme because reduction of silicates is possible. However, this advantage comes at the price of greater system complexity (more process units, less reliability).

Advantages include:

- Rosenburg's proposed process (28, 31) reduces silica and ferrous oxide in lunar pyroxene, olivine, and ilmenite minerals. Thus, less lunar material need be mined in comparison to hydrogen reduction (Section 4.1.1) and Cutler's (30) carbon reductant process which requires ilmenite. Trades for system mass with and without mineral beneficiation are needed.

- Terrestrial counterparts exist for a number of the proposed process steps: smelters, steelmaking, and hydrocarbon reforming. Extensive process operational experience exists.

- At temperatures proposed for these processes, carbon extracts 1.33 times its mass in oxygen, while thermodynamics limits hydrogen extraction of oxygen to 0.56 to 0.84 times its mass at the temperatures proposed for hydrogen reduction (900°C and 1,000°C, respectively). This implies a larger inventory of hydrogen and perhaps larger gas handling systems. However, this may not be significant in an overall systems mass statement.

- Silicon is a byproduct of Rosenburg's process (28,31). However, purification and fabrication into useful products would take many more steps.

Disadvantages include:

- The ilmenite or other oxides must be molten. This requires thermal energy to heat and melt the solids and heavy-duty refractories to protect reaction vessels and piping. In addition, molten silicates and metal are extremely corrosive, limiting refractory service life. Typical blast furnace campaigns (continuous operating lifetime) are 2-5 years in length, with the life of the refractory lining the practical limitation (15). The refractory lining is then completely replaced (including carbon refractories used in the furnace hearth) in a very labor intensive operation lasting several weeks to months. Active cooling loops were suggested (30) as a means to stablize refractory wear. Such techniques are used on modern furnaces to extend refractory life. However, process heat demands will increase if active cooling is implemented.

- Although steel is a necessary byproduct of ilmenite reduction by coke, additional processing, working, and quality assurance will be required to fabricate useful steel structural forms. In addition, steelmaking is a batch process. Thus, the economy and ease of automation for a continuous process is probably not possible for a major part of the proposed ilmenite reduction process (30).

- Recovery of the carbonaceous reductant is difficult for the proposed (28,30) processes. Cutler (30) includes two major process steps (iron decarburization and hydrocarbon reforming) while Rosenburg (28) adds one (methanation) to recover carbon. Each of these steps would involve one or more separate process vessels (and thus weight). In addition, Rosenburg (28) measured carbon loss in the slag and metal phases of 10-30 percent by weight of the carbon charged. Additional processing would be necessary to recover this carbon. Thus, although less solids handling is required for Rosenburg's proposal (28,31), the added complexity of recovering carbon requires more equipment and weight. Trades are possible between the degree of recovery and the cost of importation of the carbonaceous reductant.

  It should be noted that although the carbon that alloys with the iron or metal phase can be recovered, a significant amount, up to 20 percent as reported by Rosenburg (28), of the carbon charge also goes into solution with the slag from the reduction reactor. No process for recovery of carbon from slag has been proposed, but is likely to be extremely difficult.

  Another problem in carbon recovery is the catalyst used in the hydrocarbon reforming/-methanation steps of the proposed processes (28,30). Catalysts are susceptible to poisoning by impurities in the gas feed. In practice, catalysts generally lose activity or selectivity (governing the composition of the product gases) with time. Thus,

catalyst lifetimes are limited (variable but typically 2-3 years) after which the reactor's catalyst is dumped and a fresh catalyst charge added.

One possible solution to the high temperature and carbon recovery problems is to use carbon monoxide as the reductant gas and maintain temperatures below approximately 1000°C (below the melting point of feed materials). Ilmenite would be the feedstock of choice. Product gases would primarily contain CO and CO_2 (product composition with temperature is given in Figure 4-4). The three-stage fluidized bed concept illustrated in Figure 4-1b could be used with few changes. A high temperature, solid-state, ceramic electrolyte electrolysis cell could be used to produce oxygen and recover the carbon monoxide reductant gas in one step, and for energy efficiency as used so advantageously in the hydrogen reduction concept. This type of electrolysis cell has been studied extensively recently for possible application to a Mars surface atmospheric processor that would produce oxygen and CO fuel from the Martian carbon dioxide atmosphere (24, 34-37).

Using methane to reduce ilmenite at less than 1,000°C is another possibility. Friedlander (38, p.615) reports that 85-90 percent reduction of small ilmenite particles (0.25-0.5 mm) in a fluidized bed was obtained in 5-7 minutes by natural gas (primarily methane) at 1,000-1,030°C. However, if kinetics permit, carbon monoxide reductant gas is preferred because the electrolysis, cryogenic, and gas systems of the process would closely resemble most major elements of a Martian propellant production plant. Thus, lessons learned for propellant production on the lunar surface could significantly reduce the development and costs of Mars surface propellant production.

Figure 4-2. Carbothermal Process with Methane Reductant (from Ref. 22, slightly modified)

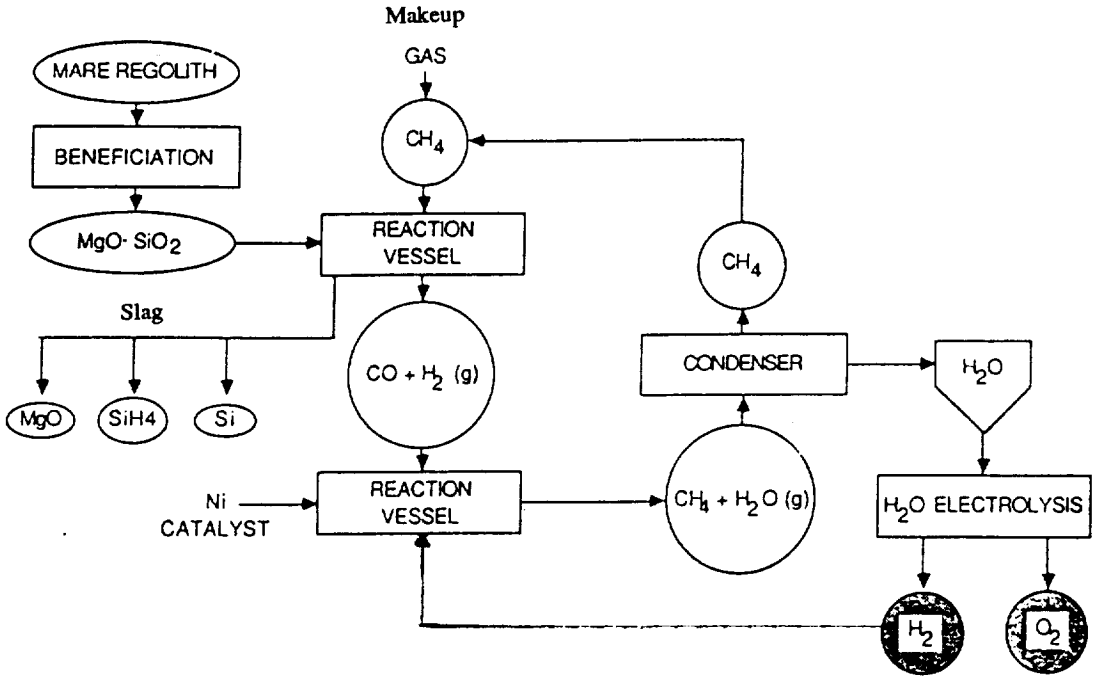

Figure 4-3. Carbothermal Process with Carbon Reductant (from Ref. 30, slightly modified)

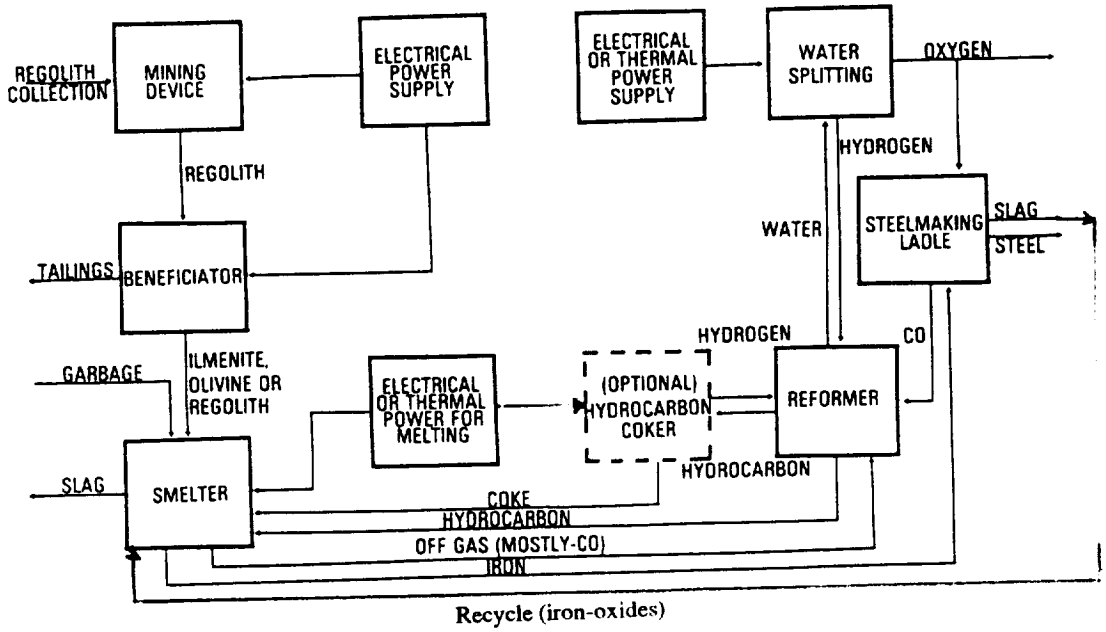

Figure 4-4. Equilibrium for CO and H_2 Reduction of Ilmenite
(Equilibrium conversion of pure CO or H_2 feed is indicated, which equals the CO_2 mole fraction or H_2 mole fraction in product gas. Derived from thermodynamic properties given in Ref.119)

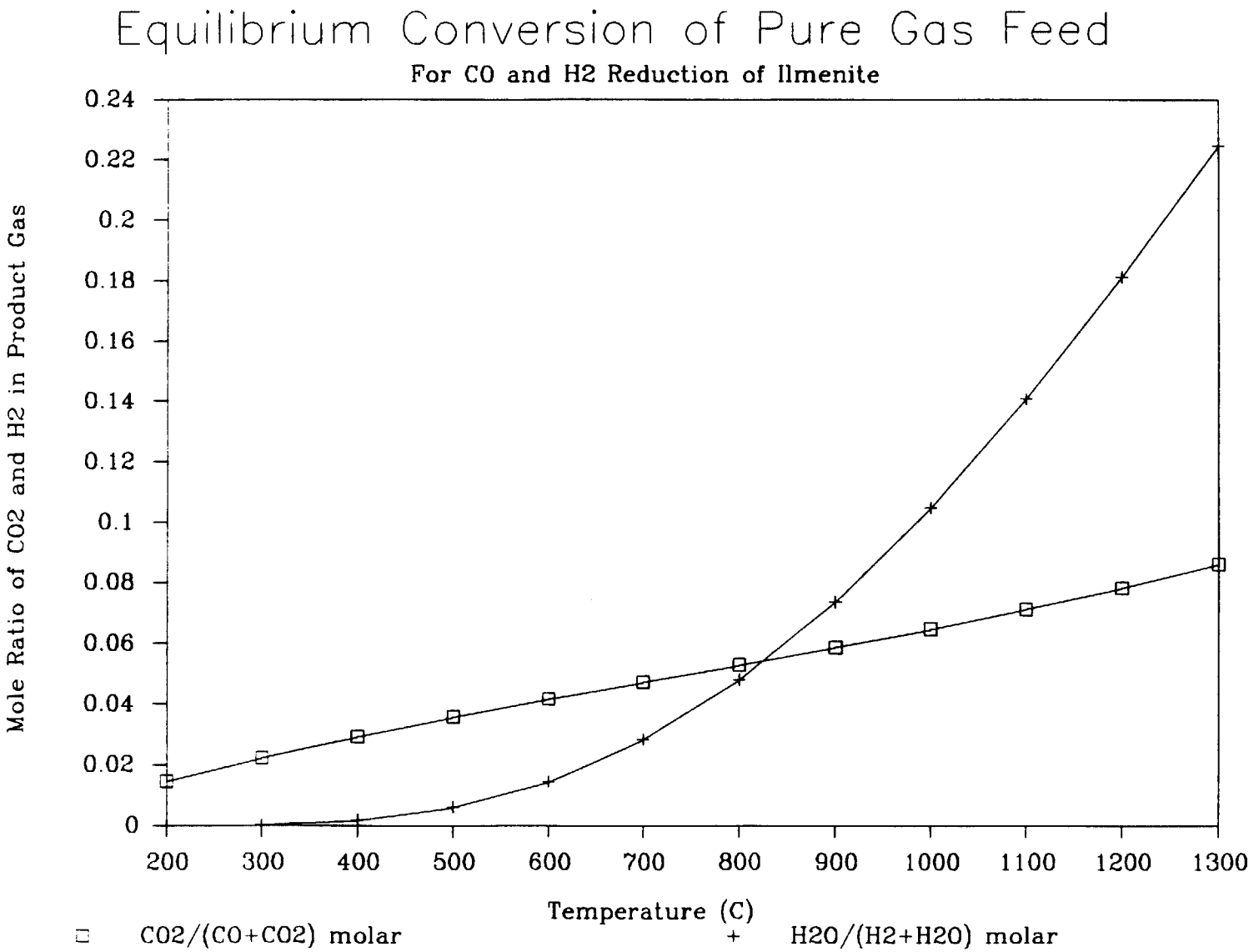

4.1.3 Hydrogen Extraction

Hydrogen deposited by the solar wind in lunar surface materials can be extracted upon heating (39-41). Essentially all hydrogen is released by heating the soil to 900°C (40). Depending on temperature, a portion of this hydrogen will react with ferrous oxides in ilmenite to produce water, which can be electrolyzed to oxygen and hydrogen. Thus, a hydrogen recovery process would extract oxygen as well. Conceptual designs of hydrogen extractors have been proposed using solar energy (19,46), microwave generators (42), and microbial action (43).

Hydrogen Content

The solar wind flux at the Moon's surface is about 3×10^8 protons/second/m^2, or 1 gram hydrogen in a square meter in 63 million years. Solar wind hydrogen penetrates less than 2000 angstroms (0.2 microns) into lunar surface materials (44) and is concentrated in the outer 200 angstroms (41). Small particles, with large surface area to volume ratios, are significantly enriched in solar wind gases (2,40,41,45). As given in Gibson et al. (40), the total hydrogen abundance (from H_2 and H_2O) in five bulk lunar soils range from 26 to 54 μg H/g (see Section 5.2). Over 80 percent of the hydrogen is found in the sub-45 micron size fraction (40). Thus, a hydrogen concentrate can be produced by separating the fine grain material. The mass and power of beneficiation equipment to do the size separation should be traded against the energy saved in the thermal processing of the soil.

Although, bulk soil samples have been analyzed with greater than 100 μg H/g, because of mixing due to cratering, a 50 μg H/g average bulk soil content is used for design purposes in this study. JSC laboratories have collected data on the gas release from soil samples heated at 6°C/minute (39). For practical purposes, complete release can be achieved by 900°C (40) and about 80 percent of the hydrogen is released below 600°C (41).

Pros and Cons

Advantages of a solar wind hydrogen extraction process:

- Both oxygen and hydrogen propellant can be produced. Only moderate temperatures are required to release hydrogen (600-900°C), although the quantity of oxygen extracted depends on the ilmenite reduction water/hydrogen equilibrium constant which increases with temperature. Thermal energy requirements could conceivably be provided by solar collectors.

- Efficient oxygen and hydrogen production can conceivably enable the economic supply of lunar oxygen to a low Earth orbit (LEO) market (48). Justifying the transportation of lunar oxygen to LEO on an economic basis (when the price competition is the transportation cost of a heavy launch vehicle, which will probably be developed to transport a lunar base/production plant in the first place) is much more difficult unless lunar hydrogen is produced (48).

- The same hydrogen/oxygen extraction process equipment can form the basis of sintering equipment to bond lunar soil into useful structural shapes (49). Sintering is the process of binding granular materials into solids at temperatures below the melting point without the addition of binding agents such as cement, plastics, or fluxes. Lunar soils sinter relatively easily because of their large glass component.

Sintering temperature varies with composition. The high-titanium mare soils characteristic of the Apollo 11 and 17 landing sites will sinter in less than 20 minutes at about 630°C while the aluminous soils of the lunar highlands (observed at Apollo 16) require temperatures of nearly 930°C to achieve the same effect.

Forming sintered products could thus be combined with hydrogen extraction of bulk soils since process temperatures are similar and little additional equipment is required. Note that sintering could not be applied to feedstocks consisting of fine grain ilmenite (a possible hydrogen concentrate). Sintered products would be useful for load bearing construction such as roadway tiles, mounts for modules and surface equipment, and blocks or bricks to build walls for bunkers near launch pads (to protect equipment from debris kicked up by rocket exhaust), for shading radiators and cryogenic storage tanks from the sun, and for radiation protection around modules.

Disadvantages:

- Large amounts of soil mechanical and thermal processing is necessary to extract hydrogen. At 50 ppm H, 20,000 mt of soil must be mined, heated to 600-900°C (requiring 159 kw-hr/mt soil at 600°C and 254 kw-hr/mt soil at 900°C), and discarded to recover 1 mt of hydrogen at 100 percent efficiency. To provide the 4.3 mt hydrogen fuel load required for one roundtrip by a reusable lunar lander (50), the soil contained in a pit 150 m x 150 m x 2 m deep would be processed. This corresponds to the amount of material excavated in about 1.4 miles of interstate highway.

  Thermal processing requirements can be decreased by: 1) recovering thermal energy from heated soil fines by using staged fluidized beds, and/or 2) decreasing the quantity of soil processed by concentrating the 45μm and smaller particles which contain 80 percent of the hydrogen (40). Possibly fines can be separated in cyclone separators or mechanical gas-classifiers using the hydrogen gas evolved from the process as a carrier fluid (after it has been cooled by pre-heating cold solid concentrate).

4.1.4 Hydrogen Sulfide Reduction

Reduction of iron, calcium, and magnesium oxides by hydrogen sulfide gas was proposed by Dalton, et al. (18) and others (17) as a method to increase the efficiency of the thermochemical oxygen production and decrease the amount of soil handling. It becomes much more practical to use bulk lunar soil without beneficiation for this process. The general reaction sequence is (where M = metals: Fe, Ca, Mg):

$MO + H_2S = MS + H_2O$ (reduction)

$MS + heat = M + S$ (thermal decomposition)

$H_2O + electricity = H_2 + 1/2\ O_2$ (electrolysis)

$H_2 + S = H_2S$ (hydrogen sulfide regeneration)

Advantages:

- Soil mining and processing is reduced from hydrogen reduction of ilmenite because the process yields more oxygen per unit soil mass.

- Iron, calcium, and magnesium can be produced besides oxygen, although additional separation and purification steps would be necessary.

Disadvantages:

- Thermal decomposition of metal sulfides will require elevated temperatures and process yield is uncertain. Considerable development is anticipated (18).
- If oxygen is used in environmental systems, oxygen purification steps are necessary due to the toxic nature of H_2S.

4.1.5 Carbochlorination

The carbochlorination process was proposed as a way to produce aluminum, iron, and oxygen from the reduction of anorthite, $CaAl_2Si_2O_8$, and ilmenite, $FeTiO_3$ (32). A fluidized bed reactor operating at 770°C (below the melting point of a reaction product, $CaCl_2$) is proposed to react carbon and chlorine gas with anorthite and ilmenite:

$$CaAl_2Si_2O_{8(s)} + 8\ C_{(s)} + 8\ Cl_{2(g)} = CaCl_{2(s)} + 2\ AlCl_{3(g)} + 2\ SiCl_{4(g)} + 8\ CO_{(g)}$$

$$FeTiO_{3(s)} + C_{(s)} + 3/2\ Cl_{2(g)} = FeCl_{3(g)} + TiO_{2(s)} + CO_{(g)}$$

$$2\ SiCl_4 + 4\ CO_{(g)} = 2\ SiO_{2(s)} + 4\ C_{(s)} + 4\ Cl_{2(g)}$$

As shown by the process flowsheet in Figure 4-5, staged condensation steps are used to separate the gas components. A condenser at 225°C removes $FeCl_3$ as a liquid, another at 90°C is used to liquefy and separate $AlCl_3$, and a third operates at -30°C to remove $SiCl_4$. The silicon chloride is recycled back to the carbochlorination reactor where its concentration builds to a steady-state value by reacting with CO back to silica. The residual solids from the reactor, SiO_2 and $CaCl_2$, are heated to 800°C to melt the $CaCl_2$, and separated in a centrifuge. The chlorine in $CaCl_2$ is recovered by first hydrolysis of $CaCl_2$ followed by calcination:

$$CaCl_{2(s)} + 2\ H_2O_{(g)} = Ca(OH)_{2(s)} + H_{2(g)} + Cl_{2(g)} \qquad \text{hydrolysis @ 400°C}$$

$$Ca(OH)_{2(s)} = CaO_{(s)} + H2O_{(g)} \qquad \text{calcination @ 600°C}$$

The iron chloride, $FeCl_3$, can be reduced directly by hydrogen gas at 700°C to produce metallic iron and hydrochloric acid (HCl), or it can be oxidized to hematite, Fe_2O_3, which is then reduced by hydrogen or carbon below 1000°C to obtain low-carbon iron via the following reactions:

$$FeCl_{3(g)} + 3/4\ O_{2(g)} = 1/2\ Fe_2O_{3(s)} + 3/2\ Cl_{2(g)} \qquad \text{oxidation @ 300°C}$$

$$1/2\ Fe_2O_{3(s)} + 3/2\ H_{2(g)} = Fe_{(s)} + 3/2\ H_2O_{(g)} \qquad \text{reduction @ 1,000°C}$$

The chlorine in $AlCl_3$ is recovered, along with aluminum, by an electrolytic process developed by Alcoa (32). The electrolysis takes place in a refractory lined vessel operating at 700-750°C using graphite electrodes and mixed alkali/alkaline earth chloride fluxing agents.

Carbon monoxide and water products from the various reactions can be reduced to hydrogen (recycled to reduction of hematite), carbon (recycled to carbochlorination reactor), and oxygen product by a variety of thermochemical and electrolytic methods.

Pros and Cons

Advantages:

- Reduction of alumina and ferrous oxides in the lunar soil is possible, reducing the amount of solids handling necessary over hydrogen reduction of ilmenite.
- Production of aluminum and low-carbon iron or steel is a necessary byproduct of the reaction to recover carbon and chlorine reactants.

Disadvantages:

- The recovery of carbon and chlorine reactants involves a large number of processing steps with an attendantly large quantity and mass of necessary equipment. Other process concerns include systems reliability, reactant recovery efficiency, and materials corrosion considerations in a high temperature, chlorine-rich environment.

Figure 4-5. Carbochlorination Process Flowsheet (from Ref. 32)

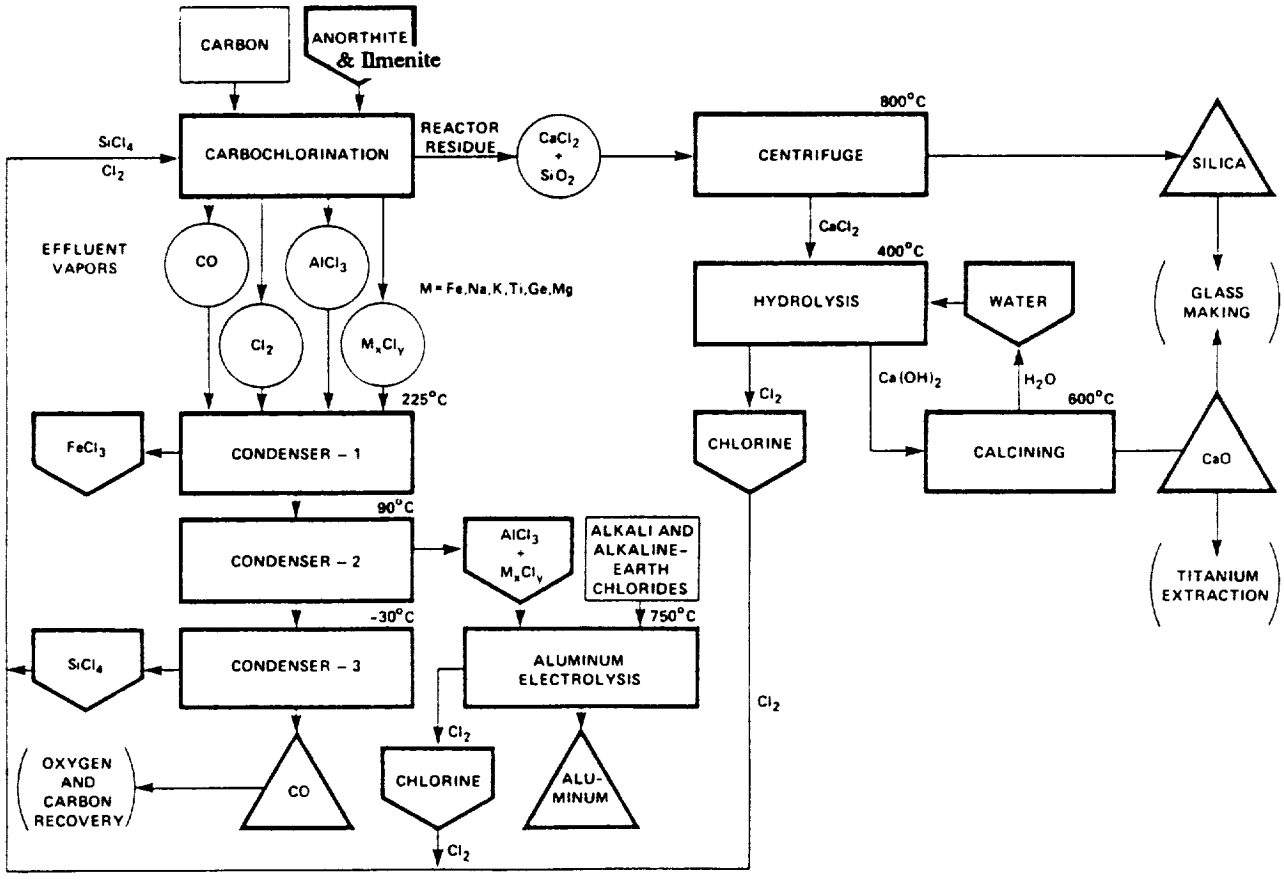

4.1.6 Fluorine Exchange

Because fluorine gas, F_2, reacts with all oxides to liberate oxygen and form metal fluorides, its use in an oxygen/metal production process has been suggested (16, 17, 56-58). Generalized reactions are summarized (16):

M oxides + F_2 = M fluoride + O_2	(fluorine exchange @ 500°C)
M fluorides + K = Metals + KF	(reduction of fluorides w/ potassium vapor)
KF + electricity = K + 1/2 F_2	(electrolysis of potassium fluoride @ 846°C, KF melting point)

where M = Ca, Al, Fe, Si, Mg, Ti

Burt (58) proposed fluorination of an anorthite ($CaAl_2Si_2O_8$) concentrate to avoid process complexities created by trying to recover fluorine for recycling from a mixture of many metal fluorides. Other mineral concentrates (e.g. ilmenite) are also possible feedstocks. Fluorination proceeds rapidly at 500°C and is safely carried out in nickle reaction vessels (58). The first step in the proposed process (58) could be conducted in the first of a two-stage fluidized bed reactor. Only partial fluorination of the pure anorthite feed is completed in this step because the input reactant gas stream is F_2-"lean" since the purpose of this first step is to scrub excess fluorine from the product gas of the second stage by using the second stage product gas as the first stage feed gas:

$$CaAl_2Si_2O_8 + 2\ F_2 = CaF_2 + Al_2SiO_4F_2 + SiO_2 + O_{2(g)} \qquad (1a)$$

Fresh fluorine (in excess) is fed into the bottom of the second stage where it reacts with the solids from the second stage:

$$CaF_2 + Al_2SiO_4F_2 + SiO_2 + 6\ F_2 = CaAlF_5 + AlF_3 + 2\ SiF_{4(g)} + 3\ O_{2(g)} \qquad (1b)$$

The product gas from this reactor is passed through a bed of NaF to scrub out the SiF_4 gas:

$$2\ SiF_4(g) + 4\ NaF_{(s)} = 2\ Na_2SiF_6 \qquad (2)$$

The sodium silicofluoride is separated and reduced by sodium metal to silicon and sodium fluoride at above 992°C (NaF melting point):

$$2\ Na_2SiF_6 + 8\ Na_{(g)} = 2\ Si_{(s)} + 12\ NaF_{(l)} \qquad (3)$$

The NaF is separated, a third recycled to step 2 while the remainder is routed to the electrolysis cell (step 8). The fluorination reactor residual solids/liquids are also reduced by sodium metal at 992°C:

$$CaAlF_5 + AlF_{3(s)} + 6\ Na_{(g)} = CaF_{2(s)} + 2\ Al_{(l)} + 6\ NaF_{(l)} \qquad (4)$$

Sodium fluoride is separated and transferred to the electrolysis cell (step 8) while fluorite (CaF_2 melting point = 1,330°C) reacts with sodium monoxide (mp = 1,275°C, sublimes) at high temperature by the following reaction:

$$CaF_2 + Na_2O = CaO + 2\ NaF \qquad (5)$$

Solid-solid reactions are typically slow (mass diffusion rate limited), therefore this reaction may require temperatures in excess of 1,275°C to proceed. The sodium fluoride product is transferred to the electrolysis cell while CaO can be used to scrub the final traces of F_2 from the oxygen product if required by oxygen propellant purity specifications:

$$CaO + F_2 = CaF_2 + O_2 \quad (6)$$

Sodium monoxide for step 5 is produced by oxidation of sodium:

$$2\,Na + 1/2\,O_2 = Na_2O \quad (7)$$

The sodium fluoride generated in steps 3-5 is electrolyzed to yield Na and F_2 for recycling:

$$16\,NaF_{(l)} + \text{electricity} = 16\,Na_{(l\text{ or }v)} + 8\,F_{2(g)} \quad (8)$$

Burt (58) suggests that this cell can operate at 992°C (the melting point of NaF) or at lower temperatures if CaF_2 is added to form a binary mixture (down to 818°C) or ternary mixtures of NaF, CaF_2, and LiF (down to 615°C).

Pros and Cons

The major advantage with fluorine extraction is that it works with all lunar oxides. However, the recovery of fluorine is a complicated operation requiring several processing steps. Fluorine recovery is absolutely essential because 2.375 tons of fluorine are required for each ton of oxygen produced (58).

Advantages:

- Fluorine reacts rapidly with all lunar oxides above 500°C (58), thus promising less mining and solids handling than processes that reduce only selected oxides. Nickel or steel process vessels can safely contain fluorine below 500°C (58).

- Oxygen is liberated directly as a concequence of the fluorine exchange reaction, unlike thermochemical reduction processes which require splitting off oxygen that is chemically bonded to the reductant (i.e. H_2O, CO, CO_2, etc.).

- Relatively purified aluminum, silicon, and CaO are byproducts from the fluorine recovery processing.

Disadvantages:

- The proposed fluorine exchange process is complicated and will require eight reactor vessels (58) not including other major process units to perform component separations. The complexity is due to the difficulty of fluorine recovery for recycling. Many steps are required, each involving separate process units since they operate at different processing conditions or handle separate chemical species. Some are likely to be energy intensive since they operate at elevated temperature (to 1,200°C+ in some cases) or require electric energy for electrolysis. However, estimates of process mass and energy requirements are not known for comparison purposes.

  The very reason that fluorine extraction is attractive leads to the difficulty of separating and recovering fluorine. Burt proposed separating anorthite from bulk

lunar soil or rock, to avoid the complications of separating a multicomponent (6 or more) mixture of metal fluorides. Processing anorthite only will obviously require additional mining for a given oxygen production rate over using bulk lunar soil, as well as requiring anorthite beneficiation equipment. The additional mining and beneficiation adds mass to the process. Although the effort to reduce processing complexity is needed, the suggestion (58) for extracting oxygen from a concentrated anorthite feed effectively negates the advantage of using fluorine extraction in the first place. However, since anorthite is more common in lunar soils than ilmenite, particularily in highland regions, less soil would be required per oxygen unit than an ilmenite reduction scheme. Highland soils contain 40-60 percent by volume anorthositic components, with up to 90 percent of this anorthite that is available without further grinding or liberation (2, pp.246-247). Available ilmenite concentration, on the other hand, is only 5-9 volume percent of high-titanium mare region soils (2, p.249).

- Considerable technology development, including laboratory bench scale study of the chemistry of some process steps, is required (58). In particular, the NaF electrolysis step represents unproven technology (58). Development of a fluorine corrosion resistant electrode material, such as lanthanide-doped fluorite, CaF_2 is suggested (58).

- Although oxygen is produced directly by fluorine exchange, it must be separated from another gaseous product of complete fluorination, SiF_4. Trace fluorine should be scrubbed from the product oxygen to levels that will avoid corrosion in space vehicle propulsion systems.

A similar process is possible using chlorine (Cl_2) gas exchange instead of fluorine. This halide, however, will only react with iron oxide (such as in ilmenite) and chlorine is difficult to recover for recycling (16, p.220).

4.1.7 Hydrofluoric Acid Leach

Waldron, et al. (18, 59-60) has proposed an acid leach process that depends on the corrosive nature of hydrofluoric acid, HF, to dissolve and react with raw lunar soil forming mixed metal fluorides and water. A series of acid leach reactors would operate in batch mode at 110°C (60, p.II-160) producing steam and SiF_4 vapor, and precipitate metal fluorides. SiF_4 must be separated from the product water vapor before producing oxygen/hydrogen. Fluorine and HF are recovered from the metal fluorides in a complex procedure with multiple unit operations involving high temperature hydrolysis (1,000°C+), electrolysis, ion exchange, distillation, centrifuges, and drying steps. A process schematic and major reactions are given in Figure 4-6. Other leachants are mentioned as possible alternatives to HF including mixed hydrofluoric/sulfuric acid (HF/H_2SO_4) solution and molten ammonium salts: NH_4FHF, $(NH_4)_2SiF_6$, or $(NH_4)_2TiF_6$ (59, pp.90-91), but they tend to increase the complexity of the separations over just HF.

Pros and Cons

Advantages:

- All lunar oxides can be fluorinated at low temperatures in aqueous acid solution. Thus, fewer raw lunar fines are required per unit oxygen product than a reaction utilizing only specific lunar minerals.

- As a consequence of recovering fluorine for recycle, various metals can be produced, particularly aluminum, iron, and silicon.

- Most of the process chemistry has been investigated in the laboratory, and 75% of the process steps have been conducted in a "comparable" or "equivalent" pilot- or commercial-scale terrestrial process (18, p.126).

Disadvantages:

- The acid leach reactors and possibly some downstream equipment (centrifuges) are operated in a batch mode on a 30 minute leach cycle making automation more difficult and losing production at either end of each cycle.

- Additional process chemistry investigations are required to verify that the process is workable. In particular, separation and purification of the fluoro compounds for later processing to recover fluorine requires additional investigation and testing (18, p.125). Many processes are available to recover HF involving ion-exchange and electrolytic steps, but they all require multiple steps, many pieces of equipment, and greater electric energy consumption than simple water electrolysis.

  The application of a large number of different unit operations (HF acid leach tanks, hydrolyzers, strippers, distillation columns, ion-exchange beds, crystallizers, centrifuges, dryers, molten sodium hydroxide electrolysis cells, etc.) to the lunar environment will require greater design, development, test, and evaluation (DDT&E) costs than processes that require fewer (albeit larger) unit operations. A major effort to reduce the complexity of this process is needed.

- Columns using ion exchange resins have been proposed (18, p.124; 60, p.II-163,165) for several reaction steps (e.g., converting sodium fluoride, NaF, to sodium hydroxide, NaOH). At least two columns are required for each ion-exchange application. While one bed is on a separation cycle, the other is on a regeneration cycle. Systems to recycle regeneration solution must be provided. In addition, the lifetime of the exchange resins are typically limited to a few years (60, p.II-49) with replacement requiring a time consuming manual operation.

  Alternatives to resins include ion-exchange membranes which require much more development work (60, p.II-99) and multistep, thermochemical techniques which are energy intensive.

- Reagent (as HF) loss rates of 1.5 kg per metric ton input soil feed are estimated (60, p.II-171). Energy-intensive exhaustive drying is required to reduce moisture and HF contents in residual solids.

- Materials inert to HF (carbon brick, phenolic/graphite, or CaF_2 liners) and F_2 corrosion must be used throughout much of the process. Liner materials compatibility problems with other process conditions (high temperature steam such as in hydrolyzers) and with mechanical erosion are likely.

- A modification of the Castner cell used terrestrially for electrolysis of molten NaOH has been proposed that uses a diaphragm and vacuum drying of the anolyte to remove water from the Castner cell and avoid hydrogen generation/handling (18, p.124). Testing of this concept would be necessary.

Figure 4-6. HF Acid Leach Process Schematic (Ref. 18)

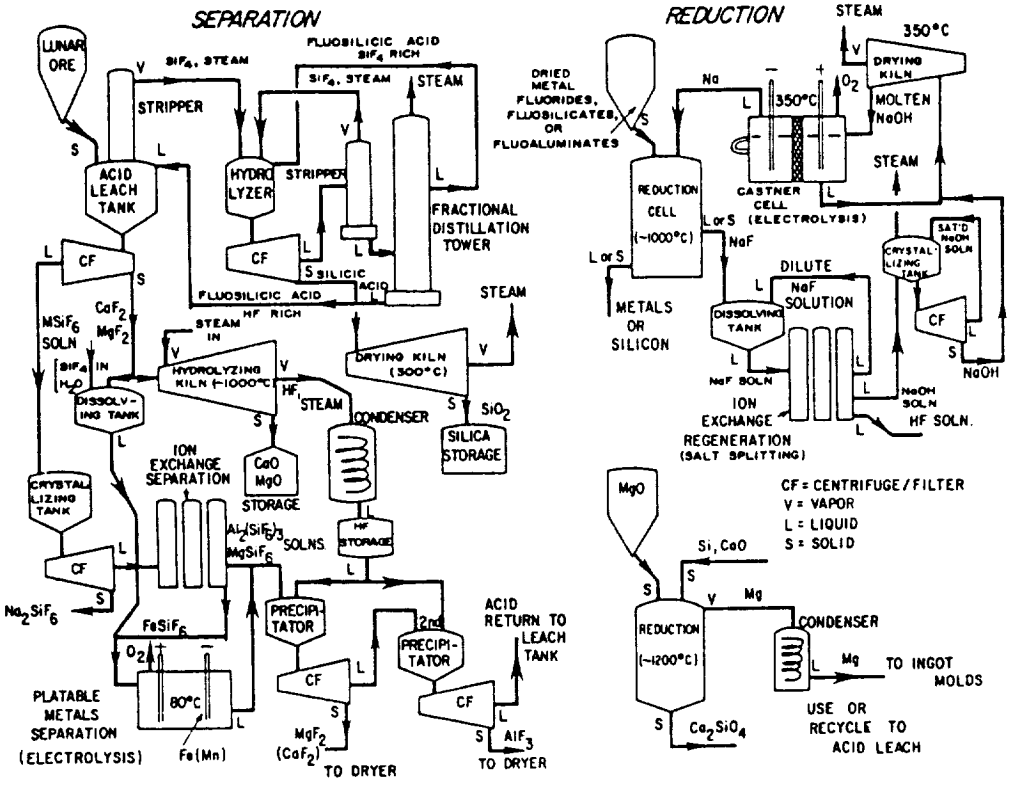

HF ACID LEACH PROCESS EQUATIONS

(1) $xMO \cdot SiO_2 + (4 + 2x)\ HF = xMF_2 + SiF_4\ (aq) + (2 + x)\ H_2O$

(1a) $xMO \cdot SiO_2 + (5 + 2x)\ HF = xMF_2 + HSiF_5\ (aq) + (2 + x)\ H_2O$

(2) $SiF_4\ (aq) + NH_2O = SiF_4\ (v) + nH_2O(v)$

(2a) $HSiF_5\ (aq) + nH_2O = SiF_4\ (v) + HF\ (aq) + nH_2O(v)$

(3) $(1-y)\ [SiF_4\ (v) + 4H_2O = Si\ (OH)_4 + 4\ HF]$

(3a) $(1-y)\ [SiF_4\ (v) + 2H_2O = SiO_2 + 4HF]$

(4) $(1-y'z)\ [xMF_2 + H_2O = xMO + 2xHF]$

(5) $y\ [SiF_4 + 4Na = Si + 4NaF]$

(6) $y'[xMF_2 + 2xNa = xM + 2xNaF]$

(7) $z[xMF_2 + xSiF_4\ (aq) = xMSiF_6\ (aq)]$

(8) $z[xMSiF_6\ (aq) + xH_2O + \text{electrical energy} = (x/2)O_2 + xM + xH_2SiF_6]$

(8a) $z[xMSiF_6\ (aq) + M'SO_3R^* = xM'SiF_6(aq) + xMSO_3R^*]$

(9) $mNaF + mR^*OH = mNaOH + mR^*F$

(9a) $mNaF + (m/2)\ Ca\ (OH)_2 = mNaOH +)(m/w)\ CaF_2$

(10) $mNaOH + \text{electrical energy} = mNa + (m/4)O_2 + (m/2)H_2O$

(11) $(1-y)\ [Si\ (OH)_4 = SiO_2 + 2H_2O]$

Note: R^* = ion-exchange; $m = 4y + 2xy'$

4.1.8 Direct Electrolytic Reduction

Experimental investigations (61) have established that molten basalt is conductive enough to support electrolysis without fluxing agents. Oxygen is released at the anode and molten iron at the cathode. Temperatures of 1,300°C or greater are required to maintain the cell constituents in a molten state. Higher temperatures increase the conductivity of the melt (61) and decrease melt viscosity (improving fluid transfer and processibility). Direct electrolytic reduction of silica and alumina was suggested as a possibility requiring additional study (61, p.3-6). A lunar magma electrolysis cell might be operated in a continuous mode (at low feed rates) with resistance losses providing the thermal energy required to melt solid feed. A modification of industrial electric arc furnace startup procedures could be used to initiate and enlarge a molten pool in a cold furnace at the beginning of a campaign (61). After forming a molten pool, the primary electrodes would be activated, solid feed begun, and oxygen, liquid metal product, and slag continuously withdrawn. However, in practice, operation may be limited to batch mode (64).

An experimental cell for molten basalt electrolysis studies (61) contained a molybdenum anode (central rod) and cathode (crucible) with a 1 cm wide annulus. A test at 1,550°C and current density of 1.25 A/cm^2 (of the original anode) had greater than 95% electrolytic efficiency with the remainder of the energy converted to heat due to resistance losses in the cell (61). The approximately 1.5 cm long x 0.625 cm diameter Mo anode immersed in the melt was completely oxidized (to mainly molybdenum dioxide) in 1.4 hr. The conductivity of basalt was measured (61) at 1,450°C to be 0.43 $[ohm\text{-}cm]^{-1}$ (conductivity follows arrhenius rule with conductivity at 1,200°C measured at 0.08 reciprocal ohm-cm).

The advantages of magma electrolysis are:

- No fluxing agents (e.g. NaOH, fluorides) are used to lower the melting temperature, reduction voltages, and viscosity of the oxides. Mass penalties are therefore not incurred to supply flux for the initial charge and for makeup of process losses. Also, the additional process equipment to recover and recycle the flux is avoided.

- Production of iron is possible although it will likely be alloyed with aluminum and silicon. Regardless, additional processing will be necessary to convert the iron into useful products.

- The number of process steps and equipment is low.

Disadvantages:

- Much more investigation is required to specify optimum process conditions, feed rate, and feedstock. Continuous operation may not be practical. Expected oxygen extraction efficiency also needs further study before meaningful design parameters can be specified.

- At the high temperatures required for the process (1,500-1,700°C), anode oxidation and corrosion problems are severe. Platinum was suggested as a possible anode material although it was not tested and has potential melting point problems (Pt m.p. 1,772°C) especially during furnace temperature transients (61). Other experimenters have used platinum successfully (63, 64) although long term behavior and operation during furnace upsets should be researched. If suitable corrosion-resistant refractory anode materials cannot be found, sacrificial anodes such as graphite or SiC could

be used. However, they would generate CO or CO_2 gas requiring subsequent processing to liberate oxygen, as well as needing to be recycled or supplied from Earth.

The cathode also sustained considerable corrosion from molten iron during experimental testing (61). A thermally stablized iron skull cathode emulating industrial experience was proposed as a possible solution (the skull is a solid skin of iron product that forms around the cathode). This requires active cooling to solidify iron onto the cathode material for protection. After thermal equilibrium is established, the cathode would transition from molten iron in the interior of the cell, to solid iron and solid cathode. Of course, this solution will result in greater cell electrical energy demands to makeup thermal losses.

- Oxygen generated at the anodes will be difficult to completely separate from the molten silicates under lunar gravity conditions (64). This will decrease cell productivity.

4.1.9 Electrolytic Reduction of Oxide/Caustic Solution

This process uses molten sodium hydroxide (NaOH) at 400°C to dissolve oxides from bulk lunar soil (16). The solution is electrolyzed to produce oxygen at the anode and sodium at the cathode. Sodium will immediately reduce lunar oxides to produce Na_2O and metals which precipitate near the cathode. The process was proposed as a batch process. Continuous operation is possible but will require separate units for the solution of caustic with lunar oxides and for the electrolysis step. A mixed caustic and solid products would be withdrawn continuously from near the cathode of the reactor. Another unit would be required to separate and recycle the caustic to the pre-electrolysis solution tank.

Advantages:

- Oxygen yield is high since reduction of nearly all oxides appears possible (16, 17) except for magnesium and calcium oxides (62).

- Metals production is possible but multiple steps would be required to separate the mixed metal product.

- Although requiring additional research, sodium in lunar materials could conceivably be used to makeup for process sodium losses.

Disadvantages:

- Nickel electrodes used on initial experimental investigations of the process were consumed (16, p.221). Inert material alternatives are needed.

- Additional work is required to develop a quantitative database of process conditions and oxygen yield before meaningful process design is possible.

- Caustic recovery from reactor residual solids is another area requiring additional research. Separation of the metals product and electrolyte solution may require centrifuges and dryers to minimize electrolyte loss resulting in significant equipment mass penalties. Sodium must also be separated from the residual metals from the electrolysis cell and reconstituted to caustic with water.

- The long term performance of the electrolyzer cell requires additional investigation. Gradual degradation of electrolytes may require continuous fresh electrolyte makeup and mass/energy penalties for caustic recovery (20, p.7-51).

- Development of electrochemical strategies to avoid dendritic growth of metals deposited at the cathode that could eventually short the cell are required (64), otherwise cell lifetimes will be limited.

A possible process alternative is potassium hydroxide (KOH) flux (62). A NaOH basic leach process was proposed that uses non-electrolytic, pyrochemical reduction routes for the separation of oxygen and metals and recovery of caustic reagent (18). However, this process appears particularily complex with multiple steps (some at temperatures of 1,100°C) and the need for additional carbon reagents.

4.1.10 Reduction by Lithium or Sodium

An indirect electrochemical reduction of lunar oxides has been proposed (64, 65) that uses lithium (or sodium) to reduce oxides to metal and Li_2O, removing Li_2O selectively, and electrolytically separating it to lithium and oxygen. A process diagram is given in Figure 4-7. Lithium will reduce FeO, TiO_2, and SiO_2 via the general reaction,

$$2Li + MO = Li_2O + M \qquad \text{(where M = metals/oxides of Si, Fe, Ti)}$$

but will not reduce Al_2O_3, CaO, or MgO (64). The reduction reaction would take place between liquid lithium (m.p. = 186°C) and either bulk lunar soil or mineral separates (e.g. ilmenite). Reduction at 727°C for ilmenite was suggested (64). The expected reaction products (metals, unreduced oxides, and Li_2O) are all solids at reaction temperature which makes separating lithium oxide difficult. Sublimation of Li_2O under reduced pressure, at 700°C and near-vacuum pressure of 0.02 mm Hg, was proposed (64). Using the readily available lunar vacuum to maintain the reduced pressure is possible but would result in some Li_2O loss. After separation, the lithium oxide would be solidified, and fed into a solid-state electrolytic cell containing a molten ternary melt of LiF (66.3 mole percent), LiCl (28.5 percent), and Li_2O (5 percent) at approximately 900°C. The lithium oxide is reduced in the electrolytic cell while LiF and LiCl are required fluxing agents to reduce the melt temperature (and viscosity) and permit high ionic conductivity. Liquid lithium forms at the cathode (304 SS or $FeSi_2$). After removal from the surface of the melt, it would be recycled to the reduction reactor. Oxygen gas evolves at the anode. In experimental testing (64), the anode was made of strontium doped lanthanum manganite ($La_{0.89}Sr_{0.10}MnO_3$). A solid electrolyte, made of CaO or yttria stablized zirconia supported on porous zirconia or alumina, is used.

Advantages:

- The process reduces silica as well as iron and titanium oxides. Production of oxygen would be essentially independent of the location of a lunar base site since silicates predominate in all areas of the lunar surface. Typical lunar soils contain 40% or more SiO_2 (4). Less lunar soil per unit oxygen production is required over processes reducing only ilmenite or other specific mineral.

- Iron, titanium, and silicon production is possible, but a separation strategy has not been developed to recover these elements from the mixed metal and oxides in the lithium reactor's solid residue.

Disadvantages:

- Lithium oxide recovery from the lithium reduction reactor's solid product will be difficult. Sublimation of Li_2O under reduced pressure may require an extensive vacuum pump system if process losses using lunar vacuum are severe. Research is required to quantify Li_2O recovery as a function of sublimation process conditions (time, temperature, pressure). The size of a Li_2O vapor system at 0.02 mm Hg (proposed in Ref. 64) is expected to be large. Resolidification of Li_2O vapor will require energy for compression or active cooling in condensers incurring a thermal energy loss (that will need to be added later).

- Long term Li_2O electrolysis cell stability at operational temperatures (900°C) requires further research. Cells have been operated in excess of 125 hours at 650°C (64). Degradation of materials in the electrolysis cell melt will require LiF and LiCl makeup to renew the flux (20, p.7-51). Quantification of flux loss through degradation, through entrainment in the lithium product stream, or by other mechanisms is needed.

- Long-term anode, cathode, and cell corrosion at operational temperature and conditions needs to be assessed.

- The sensitivity of the solid ceramic electrolyte material (yttria stablized zirconia) to mechanical damage should be considered. The desire to minimize the thickness of the solid electrolyte for lower resistance losses (64) may make the cells too brittle to withstand launch loads or vibrations/mechanical cycling due to plant operating conditions.

Figure 4-7. Indirect Electrochemical Reduction With Lithium (Ref. 64)

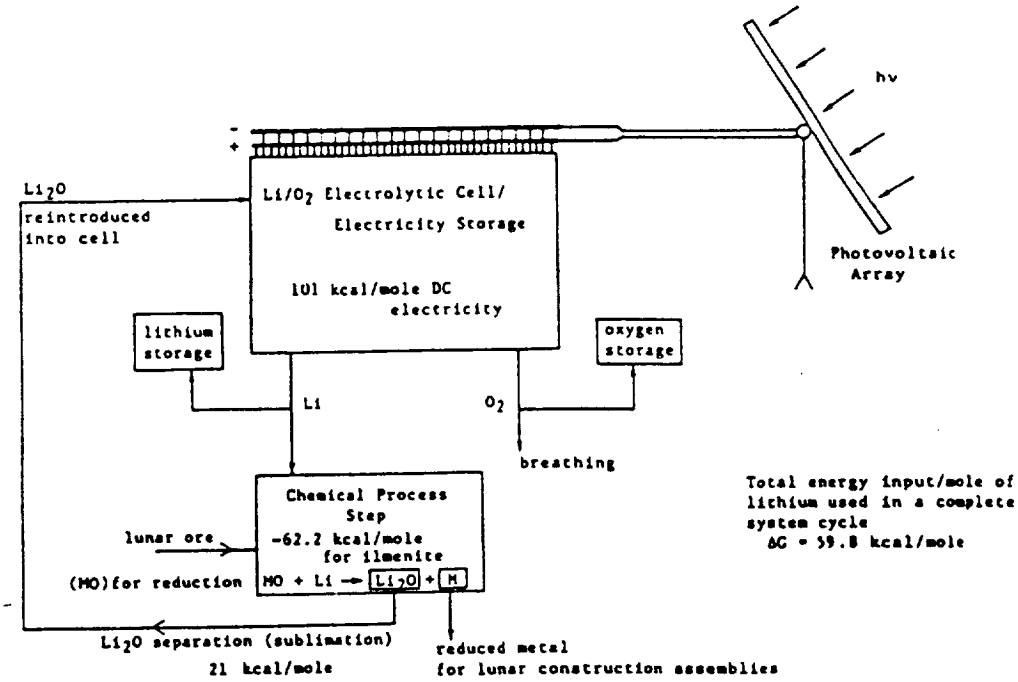

4.1.11 Reduction by Aluminum

Anorthite, concentrated from lunar highlands soils, can be reduced in a series of chemical and electrochemical steps to produce oxygen, aluminum, and silicon as given in Figure 4-8 (66, 67). In the first step, anorthite is dissolved in a cryolitic melt (90%-100% cryolite Na_3AlF_6 with remainder CaF_2, AlF_3, Al_2O_3, or BaF_2) at approximately 1,000°C. Aluminum, added to the melt, reduces silica to silicon:

$$3\ (CaO{\cdot}Al_2O_3{\cdot}2\ SiO_2) + 8\ Al = 6\ Si + 3\ CaO + 7\ Al_2O_3$$

Excess aluminum is added to react with all available silica. The silicon product forms solid crystals in the solution (67). At cryolite-alumina-silica solution concentrations of more than 20% alumina, two solid phases (alumina and silicon) result (67, p.14). Cooling the solution to 680-700°C, results in formation of solid silicon and an aluminum-silicon eutectic (an Al-Si alloy remaining liquid to 577°C) containing about 12.6% silicon (66, 67). It seems necessary, therefore, that filtration of the reaction solution using centrifuges, hydrocones, or other liquid/solid separators to remove solid silicon crystals must be performed between 700-1,000°C to separate silicon cleanly. Reactor alumina concentration must also be controlled below 20% to avoid alumina precipitation and loss of alumina (and aluminum reagent) in the solid silicon stream. The above reaction is apparently complete after approximately 1 hour (67). Therefore, a stirred-tank reactor large enough to allow a residence time of at least an hour is required, otherwise the reactor will necessarily be operated in batch mode.

After silicon is completely removed, the cryolite solution with CaO, alumina, and unreacted aluminum is pumped to a electrolysis cell where alumina is reduced. This step of the process is based on an advanced aluminum production process still under development by the Department of Energy (66, 67 p.41). A major goal is the development of anodes inert to high-temperature oxidizing conditions by application of cermet materials (cermets are ceramic/metallic composites, such as zirconia/nickle activated by lanthanum-doped cerium oxide). The products of the electrolysis step are oxygen evolved at the anode, and aluminum produced at the cathode which sinks and is collected from the bottom of the cell. This step may be difficult to perform in a continuous mode. For 1,000 mt/year of oxygen, 1.4 MW electric power is estimated to be required (66).

A major portion of the remaining CaO in the residual electrolyte solution must be removed prior to recycling the cryolite back to the aluminum reduction reactor. Alternative approaches include electrolytic reduction of CaO in another electrolysis cell, CaO separation from cryolite, or formation and removal as calcium aluminate, $CaO{\cdot}Al_2O_3$.

Advantages:

- The first step of the process, reduction of anorthite by aluminum, has been demonstrated experimentally (66, 67). Quantitative yields and optimum operating conditions require additional research.
- Production of silicon and aluminum is possible.

Disadvantages:

- Beneficiation equipment is required to separate anorthite from anorthisitic materials (e.g. soils in highland regions).

- Clean separations of silicon require careful control of the alumina content of the aluminum reduction reactor and exit stream temperature. High temperature (700-1000°C) solid/liquid filter equipment will be required.
- The alumina electrolytic reduction process using inert cermet anodes is still under development.
- Recovery of cryolite flux is difficult and expensive in terms of potentially large penalties in electrical energy and equipment mass. A suitable strategy to separate CaO from the electrolyte melt has not been developed.

Figure 4-8. Step Wise Reduction of Anorthite to Produce Si, Al, and Oxygen (Ref. 66)

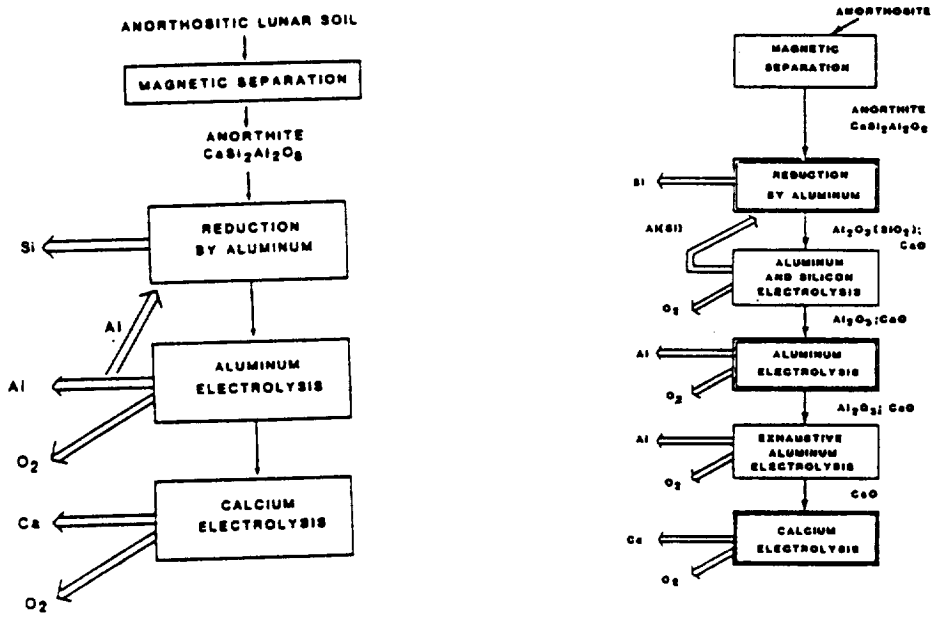

4.1.12 Vapor-Phase Reduction

Vapor-phase reduction refers to the property that vaporized oxides will partially dissociate into monoxides and oxygen which can subsequently be collected upon cooling. The process concept that has been theoretically studied to-date is illustrated in Figure 4-9 (68). Lunar oxide fines are heated to 3,000°K by solar concentrators or induction heaters. The equilibrium pressure of the vaporized oxides at 3,000°K is 0.26 atm assuming that the feedstock oxides consist of 15 wt.% Al_2O_3, 50 wt.% SiO_2, 10 wt.% TiO_2, 25 wt.% FeO (68). The oxides at these elevated temperatures are reduced to a lower oxidation state and approximately 20 wt.% of the inlet feed is released as oxygen. Since FeO does not dissociate, it is suggested that beneficiation of feed to remove the FeO content of the soil would increase oxygen yield (68). Rapid cooling of the vapor is a key process requirement to remove the reduced oxides before they recombine with oxygen. Figure 4-9 shows the oxygen stored in a balloon at 10 mm Hg. However, just 1 mt of oxygen at 0°C and 10 mm Hg would fill a 48 m diameter balloon. Compression and liquefaction of the oxygen product is probably more viable. At 20% oxygen yield, energy requirements for the process were estimated as 35.5 MW-hr/mt oxygen produced, including 25.5 MW-hr/mt O_2 for vaporization of the feed material and 10 MW-hr/mt O_2 for operating cooling/-condensing equipment (68). At 24% yield (resulting from removing the FeO content in the feed in a beneficiation step), energy requirements were estimated as 29.6 MW-hr/mt O_2 for feed vaporization and product separation (energy for mining, beneficiation, oxygen liquefaction, etc. was not included).

Advantages:

- Bulk lunar soil serves as process feedstock. However, higher oxygen yields are expected (24%) if the FeO content of the soil is discarded prior to vaporization because FeO remains essentially unreduced at process temperatures.
- The process does not require a supply of reagents from Earth.

Disadvantages:

- It is an energy intensive process. Extreme temperatures (3,000°K) are required. Containment materials problems will be severe.
- All studies of the concept have been analytical/theoretical. No laboratory-scale process demonstrations have been performed. Recombination of the dissociated constituents back into their original oxides may be a severe problem. Removal of reduced oxides from condenser surfaces may not be difficult. Long-term fouling of condenser surfaces will lower process oxygen production efficiency because the longer periods of time before condensation occurs will allow oxide recombination rates to increase.
- Low process pressures require large equipment volumes (and mass) for a given oxygen production rate.
- No terrestrial analogs for the process exist. Operational lessons learned from practical experience is not available.

4.1.13 Ion Separation

If lunar oxides are heated to even higher temperatures (7,000-10,000°K) than in vapor-phase reduction, the oxide dissociation products are ionized, although the extent of ionization differs depending on elemental species. At 8,000°K, over 90% of the metallic dissociation products (Fe, Ti, Al, Mg) and 25% of the silicon are ionized, while ionization occurs in only 1% of the oxygen (68). At 10,000°K, oxygen ionization increases to 2.6%, while 72% of the silicon ionizes and metals ionization approaches 100%. This "ionization gap" forms the basis of the vapor-ion separation process which extracts highly ionized metals by electrostatic or electromagnetic fields while essentially neutral oxygen continues to flow downstream for recovery (Figure 4-10). Based on a soil feedstock content given in Section 4.1.12, theoretical oxygen yields of 28 wt.% of the feedstock at 8,000°K (and 37% metals) and 38 wt.% oxygen at 10,000°K (51% metals) were calculated (68). Energy requirements were estimated as 34.5 MW-hr/mt oxygen produced including 33 MW-hr/mt O_2 for heating the oxides to 10,000°K and 1.5 MW-hr/mt O_2 for electrostatic separation of the charged metal ions (68).

Advantages:

- Higher oxygen yield than the vapor reduction scheme.
- Independance from Earth-supplied reagents.

Disadvantages:

- The concept represents theoretical efforts not substantiated by experimental work.
- The high temperatures will present extreme materials problems.
- Condensers to remove non-ionized metals and silicon (28% of the feed silicon is not ionized at 10,000°K - Ref.68) will be required to produce pure oxygen. Condenser energy requirements were not included in the process energy estimate or in Figure 4-10.
- Separation of condensed metals and oxides from electrostatic and condenser elements will be difficult.

Figure 4-9. Vapor-Phase Reduction Process Schematic (Ref. 68)

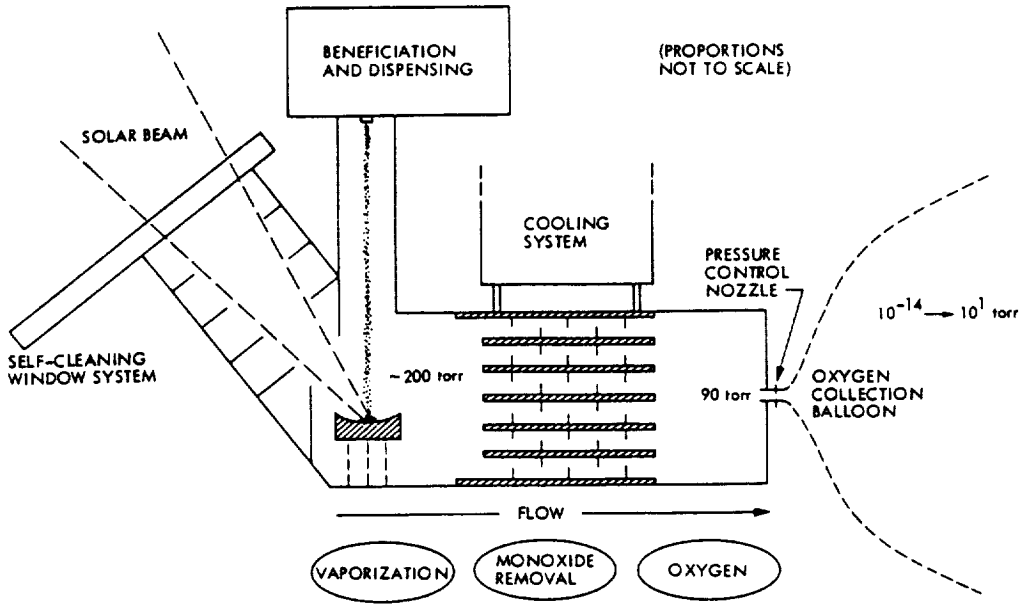

Figure 4-10. Ion Separation Process Concept (Ref. 68)

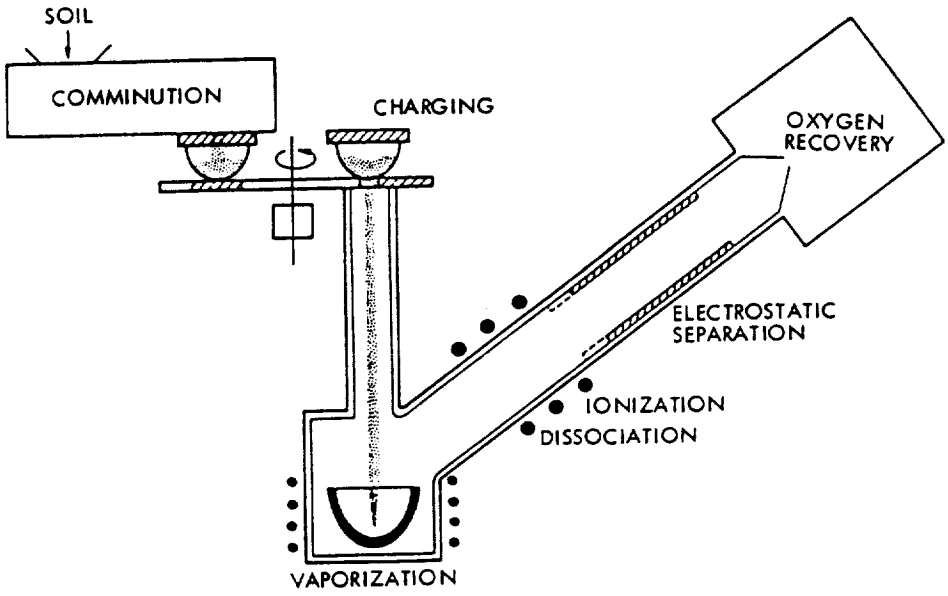

4.2 Selection Criteria and Application

Several possible ways to compare the alternative oxygen production processes are:

- Life-cycle lunar base program savings for the production plant.
- Life-cycle cost per unit oxygen produced.
- Technology readiness, process reliability, manpower requirements, maintainability, safety.
- Plant mass, power, manpower, volume, and other plant physical characteristics.

Life-Cycle Savings

This comparison is based on the difference between savings in launch costs for delivery of propellant to the lunar surface without oxygen production and the cost of developing, transporting, and operating the process. Savings in launch costs will depend on the type/costs of Earth launch and orbital transfer vehicles. The basing mode for the lunar lander (whether at Space Station, in low lunar orbit, or on the lunar surface) will also influence launch cost savings. Because certain processes produce byproducts which could be made into useful structural elements, the costs and program savings for using available byproducts should also be factored into life-cycle savings.

Life-Cycle Costs

Considering only the cost side of the life-cycle savings equation, alternative processes can be assessed based on the average cost per unit oxygen produced over the process lifetime. Life-cycle costs would include design, development, test, and evaluation (DDT&E), transportation, setup, operation, resupply, and maintenance costs. DDT&E depends on the technology readiness, complexity, and number and size of the process units. Operation cost for a process depends on the efficiency and productivity of the process (continuous versus batch mode), mining requirements, the extent of automation, and other factors, but basically is determined by process manpower requirements. Resupply costs reflect the transportation costs incurred for reagents required to makeup process losses. Maintenance costs include the labor and hardware required for process equipment replacement and repair. These costs depend on the complexity and quantity of equipment and interfaces, the amount of rotating machinery, the severity of process conditions, and the extent of corrosion and wear. Trades are possible, for instance between higher DDT&E costs to incorporate more automation and reduced manpower requirements/operations costs. Life-cycle costs are, of course, related to process equipment lifetime which depends on many of the same factors: process severity, corrosion and wear, etc., but also on the expenditure level during the DDT&E phase, as well as costs incurred for maintenance and repair.

Technology Readiness and other factors

The various processes can be compared on the basis of the laboratory and bench scale research necessary to prove the process is viable. Technology that exists or will likely exist prior to delivery (circa 2000-2005) should also be accounted for. Other factors (safety, reliability, maintainability) are also important in determining if a process will perform as expected in the lunar environment.

Process Mass and Power

A basic component of the required data, process mass and power, is difficult to attain from literature on a consistent basis for comparison purposes, as given in Table 4-1. In some cases, such as vapor-phase reduction and ion separation, adequate data is not yet available to produce a plant design for meaningful equipment mass estimates. In other cases, process mass and power estimates may not include mining, beneficiation, complete processing, oxygen liquefaction and storage, or power system estimates. Table 4-2 lists the efficiency of each process in terms of the ratio of process mass and energy to annual oxygen production based on the data in Table 4-1. Because these ratios should decrease (efficiency increases) as plant capacity increases, comparison of the processes is not valid (even if the original mass estimates included the same equipment systems) unless oxygen production rates are nearly equivalent.

Processes Selected for Conceptual Design

For this study, two process attributes were considered of overriding importance for successful development of lunar oxygen production: 1) reliability and 2) efficiency.

Reliability can be attributed to process viability, simplicity, and maintainability. Although many other factors are involved, each of the reliability attributes was defined by a basic process characteristic: viability is defined by the technology readiness of the process, simplicity by the number of process steps (the more process steps, the more equipment required, and the greater likelihood of a breakdown somewhere in the chain), and maintainability by the severity of processing conditions (the higher the temperature or more corrosive the conditions, the more likely equipment lifetime will be limited). Process efficiency is defined by the plant mass, power, and consumables consumption required for a given production rate. Because consistent values for these are not available to make a realistic comparison (see Tables 4-1 and 4-2), the same criterion defining process simplicity-the number of process steps-was chosen.

All identified oxygen processes were rated by the 3 characteristics: technology readiness (as applied to the overall process, not to the design of individual pieces of equipment), number of major process steps, and severity of process conditions. As given in Table 4-3, the two top rated processes selected for conceptual design studies were hydrogen reduction of ilmenite and solar wind hydrogen extraction with concurrent reduction of ilmenite to produce oxygen.

The rationale for selecting hydrogen reduction of ilmenite was based on the comparison and on:

- The reduced complexity associated with this process when compared to the alternative processes. Fewer process units will be required since oxygen can be produced and hydrogen recovered in a single electrolysis step following reaction (only direct electrolytic reduction of an oxide melt would require approximately the same number of process units). Fewer units and interfaces translates into operational advantages in terms of higher reliability and lower maintenance costs.

- The chemical reactions have been characterized well enough in the laboratory to assign realistic bounds to expected oxygen yields as a function of process conditions.

- Potential synergism for portions of a lunar oxygen production plant based on this process and major components of a Martian atmospheric processor.

Solar wind hydrogen extraction was also selected based on:

- The high desirablity of combined oxygen and fuel production from lunar resources.
- Possible synergisms between hydrogen extraction and oxygen production plants.
- Potential production with low mass penalties of hot-pressed sintered ceramic products as a byproduct of hydrogen extraction.

Of course, these selections were made with limited data and on minimal selection criteria. Additional analytical and experimental study of these processes is warranted to better define the most appropriate lunar oxygen process.

Table 4-1. Process Mass and Power Requirements as Reported in Literature

Process	O_2 Prod.	Feedstock Requirements	Plant Mass (mt)	Energy Req. Total	Electrical	Thermal	Reactant Requirements	Ref.
1. H_2 reduction of Ilmenite								
1-A.	10 mt	662 mt	1.83 mt(1)	50.8 MWh	43.2 MWh	7.6 MWh	0.01 mt(2)	22
1-B.	9 mt/month	365 mt/month	-	0.65 MW	0.15 MW	0.5 MW		16
1-C.	1000 mt/yr	160,000 mt/yr	400 mt(3)	5 MW				10,14,69
1-D.	150 mt/mon.	20,200 mt/mon.	439 mt(4)	6 MW				70
1-E.(5)	1.82 mt/day		35.4-51.0 mt					19
	0.91 mt/day		21.3-34.8 mt					19
	0.012 mt/day		0.279-0.578 mt					19
1-F.(6)	293 mt/yr	44,000 mt/yr	119.6 mt	1.68 MW				21
1-G.(7)	2 mt/month	370 mt/month(8)	24.7 mt	146 kw			24 kg/yr	72
	1000 mt/yr	327,000 mt/yr(9)	225 mt	3.0 MW			968 kg/yr	72
2. Carbothermal Reduction								
2-A.(10)	10 mt	292.4 mt	12 mt	211.7 MWh	43.2 MWh	168.5 MWh	5.1 mt CH_4	22
2-B.(11)	9 mt/month	29.7 mt/month	-	1.36 MW	0.26 MW	1.1 MW		16
2-C.(12)	1000 mt/yr	100,000 mt/yr	104.6 mt	2.4 MW			-	30
3. Solar Wind Hydrogen Extraction								
3-A.	1.3 kg H_2	24.2 mt						22
3-B.	1 mt H_2	13,582 mt(13)						41
3-C.(14)	5.34 kg H_2O	1 mt						46
3-D.(15)	83 mt/yr H_2	9,600 mt/day	556 mt	111 MW	31 MW	80 MW		73
3-E.(16)	2 mt/mon. O_2	29.4 kmt/mon.	60 mt	1.7 MW				72
4. Hydrogen Sulfide Reduction								
4-A.	9 mt/month	162 mt/month	-	1.25 MW	0.15 MW	1.1 MW		16

Notes:

(1) Mass & Power estimates for 1-A include reactor and water electrolysis units only.

(2) 0.31 mt H_2 required if no recovery, 95% recovery assumed (22).

(3) Plant & power system included in process mass estimate for 1-C. Power system 45% of total mass. Feedstock calculated by 10 acre x 2 m x 2 mt/m^3 (from Ref.10).

(4) Mass & power estimates for 1-D include mining, beneficiation, process equipment, liquefaction and storage, power and thermal systems, and habitat for crew support.

(5) All production rates for 1-E at 50% duty cycle (thus, actual production is given rate * 0.5 * time period). Mass estimates based on beneficiation, process, liquefaction & storage, power & thermal (mining systems not included).

(6) Lowest mass ilmenite reduction scheme in Ref.21 that uses mobile miner/electrostatic separation beneficiation equipment (74) and assumed 4000 hr/yr production (46% duty cycle or 73 kg/hr O_2 production rate).

(7) Results from this report (Section 6). Pilot plant (2 mt/month production) based on solar photovoltaic/regenerative fuel cell power system and 45% process plant duty cycle, and includes mining, beneficiation, process, liquefaction/-storage, power and thermal systems. Production plant (1000 mt O_2/year) based on nuclear power and 90% duty cycle, and includes mass/power estimates for mining, beneficiation, process, liquefaction/storage, power and thermal systems.

(8) High-Ti basalt feedstock, 45% process duty cycle, PV/RFC power system.

(9) High-Ti soil (mare region) feed, 90% process duty cycle, nuclear power system.

(10) Based on reduction of pyroxene ($MgSiO_3$) by methane. 10 mt silane (SiH_4) and 4.35 mt silicone byproducts also produced (22). Methane (CH_4) reactant resupply requirements based on 15 mt methane needed at 66% recovery (22).

(11) Based on reduction by methane of bulk lunar oxides.

(12) Reduction of ilmenite by carbonaceous reductants (methane or coke). 3680 mt of iron (steel) byproduct also produced (30). Estimates based on nuclear power and 90% process duty cycle. Mass includes mining, beneficiation, process and power (60% of total mass) systems. Process power estimate does not include mining or beneficiation power requirements.

(13) Assuming 100 ppm H in bulk soil, 90.9% of H in -20μm fraction, 81% recovery of H upon heating to 600°C, 23 wt.% of fines in -20μm fraction, 3,124 tons of concentrate heated yielding 73.6% of the hydrogen (41).

(14) Basis is concentrate of -20μm fraction soil, enhanced 10x in H over bulk soil, heated to 1000°C generating 5.34 kg water, corresponding to 0.60 kg H_2 and 4.74 kg O_2 (46).

(15) Used "90% certainity" plant estimate (from Ref.73) w/ estimate basis of recovering 50 ppm H_2 from bulk lunar soil by heating to 700°C releasing 50% of contained hydrogen, solar heating in vacuum to 500°C (25 mt of solar heaters) @ 70% solar heating efficiency, induction-heating from 500 to 700°C @ 90% electric efficiency (300 mt of solar-electric systems and 31 mt of RF generators).

(16) Plant produces 1.2 mt H_2, 2 mt O_2 per month. Bulk lunar soil feed w/ 50 ppm hydrogen, 80% of hydrogen recovered at 927°C extraction temperature, 50% of thermal energy requirements recovered in staged fluidized beds, 75% of process reactor thermal requirements supplied by nuclear power waste heat.

Table 4-1 (Cont). Process Mass and Power Requirements as Reported in Literature

Process	O_2 Prod.	Feedstock Requirements	Plant Mass (mt)	Energy Req. Total	Electrical	Thermal	Reactant Requirements	Ref.
5. Carbochlorination								
5-A.(17)	10 mt	238 mt	12.45 mt	125.4 MWh	43.2 MWh	82.2 MWh	57 mt Cl_2	22
5-B.(18)	10 mt	238 mt	13.4 mt	162.3 MWh	78.6 MWh	83.7 MWh	26 mt Cl_2	22
6. Fluorine Exchange								
6-A.(19)	9 mt/month	22.5 mt/month	-	1.05 MW	0.25 MW	0.8 MW		16
6-B.	1.82 mt/day		34.7-50 mt					19
	0.91 mt/day		20.9-34.2 mt					19
	0.012 mt/day		0.204-0.425 mt					19
7. HF Acid Leach								
7-A.(20)	10 mt	23.6 mt	2.85 mt	69.9 MWh	43.2 MWh	26.7 MWh	27.5 mt HF	22
7-B.(21)	10 mt	87.3 mt	11.73 mt	249.7 MWh	119.8 MWh	129.9 MWh	16.5 mt HF	22
7-C.	10 mt	60.2 mt	15.93 mt	203.2 MWh	96.4 MWh	106.8 MWh	14.4 mt HF, 0.5 mt CaO, 0.1 mt Si	22
7-D.(22)	10570 mt/yr	30,000 mt/yr	220 mt	30 MW			30 mt/yr	18,71
7-E.	293 mt/yr	1440 mt/yr	86.6 mt	2.68 MW				21
8. Magma (Direct) Electrolysis								
8-A.(23)	10 mt	1325 mt	0.98 mt	155.6 MWh	92.9 MWh	62.7 MWh		22
9. Electrolytic Reduction of Caustic Solution								
9-A.	9 mt/month	21.6 mt/month	-	0.85 MW	0.35 MW	0.5 MW		16
10. Reduction with Lithium								
10-A.(24)	1000 mt/yr	31,645 mt/yr	-	3.0 MW				64
11. Reduction with Aluminum								
11-A.(25)	1000 mt/yr			1.4 MW				66
12. Vapor Phase Reduction								
12-A.(26)	10 mt	24.2 mt	15 mt	34 MWh/mt O_2				22
12-B.	1 mt	5 mt		29.6 MWh	10.4 MWh	19.2 MWh		68
13. Ion Separation								
13-A.(27)	10 mt	24.2 mt	15 mt	44 MWh/mt				22
13-B.(28)	10 mt	24.2 mt	15 mt	96 MWh/mt				22
13-C.	1 mt	2.6 mt		34.5 MWh				68

(17) Reactants required: 95.8 mt Cl_2 with 40% recovered, 16.3 mt C with 100% recovered.
(18) 8.5 mt Al also produced. Reactants required: 95.8 mt Cl_2 with 73% recovered, 16.3 mt C with 100% recovered.
(19) All production rates for 6-B at 50% duty cycle (thus, actual production is given rate * 0.5 * time period). Mass estimates based on beneficiation, process, liquefaction & storage, power & thermal (mining systems not included).
(20) 5.9 mt Al also produced. Reactants required: 27.5 mt HF @ 40% recovery efficiency and 26.2 mt NaOH @ 100% recovery.
(21) 4.7 mt Al and 2.35 mt Mg also produced. Reactants required: 30.6 mt HF @ 53% recovery, 18.2 mt NaOH @ 100% recovery, 5.42 mt CaO @ 90% recovery, 1.35 mt Si @ 90% recovery.
(22) Anorthosite feedstock baselined (18,71). Assumed products CaO and 90% yield from other oxides. Plant mass includes 120 mt for power, 20 mt for reagents, 24 mt for radiators, and 56 mt for process equipment (no mining, water electrolysis, O_2 liquefaction or storage equipment included). The process requires 336 mt of water, HF, and NaOH reagents (Ref.71) which are made during a special startup campaign from H_2, F_2, and Na brought from Earth (66 mt of Earth reagents required in Ref.71). 30 mt/yr of reagent makeup are estimated required (Ref.71).
(23) Assumes ilmenite feedstock and includes only magma electrolysis cell in mass estimate (22). Power estimate only includes requirements to heat feed to 1350°K and dissociation energy (no efficiencies included).
(24) Ilmenite feedstock basis. Electrical requirements include only L_2O electrolytic cell (2.6 MW) and L_2O separation (0.35 MW) energy requirements (no mining, oxygen purification or liquefaction).
(25) 500 mt Si and 500 mt Al also produced. Only Al electrolysis cell in power estimate (not included is power for mining, Al reduction reactor, calcium electrolysis, oxygen liquefaction, and other process requirements).
(26) Mg, Fe, and Al byproducts also. Process facility mass was not calculated, estimate only (22).
(27) Mg, Fe, Al byproducts. Mass estimated not calculated. Ion separation based on electrostatic methods.
(28) Mg, Fe, Al byproducts. Mass estimated not calculated. Ion separation based on electromagnetic methods.

Table 4-2. Process Mass and Power Ratios (Derived from Data in Table 4-1)

Process	O_2 Prod. (mt/yr)	Feedstock per O_2 Prod.[2] (mt/mt O_2)	Plant Mass per O_2 Prod. (mt-yr/mt O_2)	Energy per O_2 Prod. (kw-yr/mt)	Annual Resupply Reactants per O_2 Production (mt/mt O_2)
1. H_2 Reduction of Ilmenite					
1A.	120?	66.2	0.015	0.58	0.001
1B.	108	40.6	-	6.0	
1C.	1000	160	0.40	5.0	
1D.	1800	135	0.24	3.3	
1E.	332		0.11-0.15		
	166		0.13-0.21		
	2.2		0.13-0.26		
1F.	293	150(1)	0.41	5.7	
1G.	24	186(1)	1.03	6.1	0.001
	1000	327(2)	0.23	3.0	0.001
2. Carbothermal Reduction					
2A.	120?	29.2	0.10	2.4	0.043
2B.	108	3.3	-	12.6	
2C.	1000	100	0.10	2.4	
3. Solar Wind Hydrogen Extraction					
3A.	?	18,600 mt/mt H_2			
3B.	?	13,600 mt/mt H_2			
3C.	NA	1,670 mt/mt H_2			
		210 mt/mt O_2			
3D.	83 mt/yr H_2	21,100 mt/mt H_2	6.7 mt-yr/mt H_2	1,340 kw-yr/mt H_2(3)	
3E.	24 mt/yr O_2	14,700 mt/mt O_2	2.5 mt-yr/mt O_2	72 kw-yr/mt O_2(4)	
	14 mt/yr H_2	25,000 mt/mt H_2	4.3 mt-yr/mt H_2	124 kw-yr/mt H_2	
4. H_2S Reduction					
4A.	108	18	-	11.5	
5. Carbochlorination					
5A.	120?	23.8	0.10	1.4	0.48
5B.	120?	23.8	0.11	1.9	0.22
6. Fluorine Exchange					
6A.	108	2.5	-	9.7	
6B.	332		0.10-0.15		
	166		0.13-0.21		
	2.2		0.09-0.19		
7. HF Acid Leach					
7A.	120?	2.4	0.024	0.8	0.23
7B.	120?	8.7	0.10	2.9	0.14
7C.	120?	6.0	0.13	2.3	0.13
7D.	10,570	2.8	0.021	2.8	0.003
7E.	293	4.9	0.30	1.8	
8. Magma (Direct) Electrolysis					
8A.	120?	132.5	0.008	1.8	
9. Electrolytic Reduction of Caustic Solution					
9A.	108	2.4	-	7.9	
10. Reduction with Lithium					
10A.	1000	31.6	-	3.0	

Notes:
(1) For pilot plant at 45% duty cycle, PV/RFC power.
(2) For production plant at 90% duty cycle, nuclear power.
(3) 3E power based on 50%+75% heat recovery, 500 kw-yr/mt O_2 without any heat recovery.
(4) 3E power based on 50%+75% heat recovery, 857 kw-yr/mt H_2 without any heat recovery.

Table 4-2 (Cont). Process Mass and Power Ratios (Derived from Data in Table 4-1)

Process	O_2 Prod. (mt/yr)	Feedstock per O_2 Prod.[2] (mt/mt O_2)	Plant Mass per O_2 Prod. (mt-yr/mt O_2)	Energy per O_2 Prod. (kW-yr/mt)	Annual Resupply Reactants per O_2 Prod. (mt/mt O_2)
11. Reduction with Aluminum					
11A.	1000	-	-	1.4	
12. Vapor Phase Reduction					
12A.	120?	2.4	0.13	0.4	
12B.	-	5		3.4	
13. Ion Separation					
13A.	120?	2.4	0.13	0.5	
13B.	120?	2.4	0.13	1.1	
13C.	-	2.6		3.9	

Table 4-3. Process Comparison

Process	Technoloy Readiness 1 = No Major Unknowns/ Tech. Requirements 2 = Some Unknowns 3 = Major Tech. Req.	Number of Major Processing Steps 1 = Few (1-2) 2 = Several (3-5) 3 = Many (>5)	Process Conditions (Hi-Temp. &/or Hi-Corrosion) 1 = Low 2 = Moderate 3 = Severe	Comments
1. H_2 Redn of Ilm.	1	1	2	Chemistry well known, high-temperature electrolysis subject of much current research. Reduction and water electrolysis only steps. Moderate thermal conditions (900-1000°C)
2. Carbothermal	1	2	3	Chemistry relatively well known, process units extension of Earth technology. Carbon recovery requires several steps. Proposed processes involve molten oxides.
3. H_2 Extraction	1	2	2	Hydrogen release well studied. Unknowns on extent of mechanically released H_2 works in favor of process. Same number of process units as #1, but 2 rating given since reactors are large and energy requirements are high.
4. H_2S Reduction	3	2	2	Research required into thermal decomposition of metal sulfides (a major process step). 3 steps: Red'n, water electrolysis, and sulfide decomposition. Reduction is low temperature, but decomposition is likely to require high temps.
5. Carbochlorination	2	3	3	More research, especially for aluminum electrolysis step, is required. 6 major steps: reactor, (3) staged condensers, Al electrolysis, centrifuges, hydrolysis and calcining. C-Cl_2 reactor and Al electrolysis cell environment particularly corrosive.
6. F_2 Exchange	2	3	3	Several process steps require additional research. Process complex (8 steps). One step may require temperatures in excess of 1200°C. Most steps in hot fluoride corrosive environment.
7. HF Leach	2	3	3	Although major process chemistry has been investigated, additional research for steps to recover of fluorine/HF is required. This is the most complex of those surveyed in terms of the number and variety of different chemical process units required. Although the leach step is at low temperature, several separation steps require high-temperature (>1000°C) hydrolysis steps. Hot acid environment.
8. Magma Electrolysis	3	1	3	Anode and cathode materials problems require resolution. Molten silicates pose severe corrosion problems.
9. Caustic Electrolysis	2	2	2	Caustic recovery methods require further investigation. Dendritic growth of metals deposited at electrodes could eventually short cell. Inert electrode material alternatives are needed.

Table 4-3 (Cont). Process Comparison

Process	Technoloy Readiness 1 = No Major Unknowns/ Tech. Requirements 2 = Some Unknowns 3 = Major Tech. Req.	Number of Major Processing Steps 1 = Few (1-2) 2 = Several (3-5) 3 = Many (>5)	Process Conditions (Hi-Temp. &/or Hi-Corrosion) 1 = Low 2 = Moderate 3 = Severe	Comments
10. Redn by Li or Na	3	2	2	Additional research is required for Li_2O separation/recovery. Research on long-term performance of Li/O_2 electrolytic cell is needed. 3 Process steps: Li Redn., Li_2O separation, Li/O_2 electrolysis.
11. Redn w/ Al	3	3	2	Only 1 of 3-5 step process has been investigated. Additional separation steps will possibly be needed, particularly to recover cryolite flux.
12. Vapor Phase Redn	3	1	3	Only theoretical studies have been performed, the process exists as concept only. Very high temperatures will result in containment problems.
13. Ion Separation	3	2	3	Experimental work is lacking. Separation of oxygen from non-ionized silicon/metals is not clean and will require additional steps/potential yield losses. Extreme temperatures.

SUMMARY

Rank	Process	Total Pts.
1	H_2 Redn of Ilmenite (#1)	4
2	H_2 Extraction (#3)	5
3-4	Carbothermal (#2)	6
3-4	Caustic Electrolysis (#9)	6
5-8	H_2S Reduction (#4)	7
5-8	Magma Electrolysis (#8)	7
5-8	Li/Na Reduction (#10)	7
5-8	Vapor Phase Reduction (#12)	7
9-13	Carbochlorination (#5)	8
9-13	F_2 Exchange (#6)	8
9-13	HF Leach (#7)	8
9-13	Redn w/ Al (#11)	8
9-13	Ion Separation (#13)	8

5.0 Process Feedstocks

The abundance of minerals in typical lunar materials has been described in detail (2-5). However, because the concentration of ilmenite and hydrogen in the process feedstocks is an important parameter in sizing the two pilot plants described in this report, a brief description of sources and relative abundances for ilmenite and hydrogen follow.

5.1 Ilmenite

There are two main sources of ilmenite ($FeO{\cdot}TiO_2$): high-titanium mare basalts and mare soils (Table 5-1).

High-Ti Basalts

As presented in Table 5-2, the richest mare basalts from the Apollo samples contain about 25 volume percent ilmenite (2) which corresponds to approximately 33 weight percent ilmenite (given a specific gravity for basalt of 3.4 and ilmenite S.G. of 4.5). The element chemistry of the major minerals in high-Ti basalts, as given in Table 5-3, shows that lunar ilmenites are mixtures of primarily ilmenite ($FeTiO_3$) with small amounts of geikielite ($MgTiO_3$) and traces of minor elements.

Crushing and grinding of the basalt will be necessary to release ilmenite grains for the reaction step. The extent of grinding depends on the grain size of the basalt minerals. The texture of the basalts vary with the cooling rate of the lava flow from coarse grained with average crystal grain size of 1.0-5.0 mm (formed deeper in an extrusive flow where cooling rates are slower), to medium grained with grains 0.5-1.0 mm, or fine grained with grains 0.1-0.5 mm (75-77). The coarser grained rocks are generally more friable (easier to break up). Ilmenite grain sizes of 2-3 mm have been reported (75, 78), but these are generally elongated lath- or plate-like structures (79). Typically, 0.5 mm is the maximum length in three-dimensions of equant ilmenite grains (80).

High-titanium basaltic bedrock can be found in quantity 2-5 m below the regolith in mare regions (see Figure 5-1). Regions of the Moon containing high-Ti basalt have been mapped from Earth-based spectral studies to 1 km resolution (3, p.3-18). Basalt blocks fill impact craters that penetrate through the regolith and were ejected from the crater to litter the surrounding landscape. Basalt mines could be located in or near craters to collect the broken rock in these areas.

Mare Soils

Lunar regolith is also a potential ilmenite source since it is already pulverized and easy to mine. However, two thirds of the ilmenite in mare soils is incorporated in glassy agglutinates and basaltic rock fragments, and can not be separated cleanly from other minerals without additional grinding (2, p.249). The amount of ilmenite in bulk lunar soil available for immediate separation by magnetic or electrostatic means (without grinding) consists of relatively pure ilmenite mineral fragments liberated from lithic fragments. As given in Table 5-4, the richest mare soil in Apollo samples contains about 9 volume percent ilmenite mineral fragments (2, p.250), or ~12.7 weight percent (based on a 3.2 S.G. of soil from Ref. 6, p.26). Ilmenite contents in mare soil of 5 volume percent (7 wt.%), suggested as typical high values (3, p.2-16 and p.4-2; 2, p.249), are used for design purposes in this study. There tends to be a greater portion of ilmenite fragments at

finer soil size fractions (see Table 5-5) because more ilmenite grains are liberated as the soil particle size approaches the grain size of the mineral (2).

The average particle size of most lunar soils is quite fine, ranging between 45 and 100 μm (3, p.3-6). Table 5-6 lists the weight percents of a typical mature mare soil (Soil 10084). More than a quarter of the soil is less than 20 μm. Table 5-7 gives the chemical composition of the major components for this soil. Note that ilmenite does not account for all 16 wt.% FeO reported. Significant FeO is contained in pyroxenes, a mineral group consisting of varying amounts of enstatite ($MgSiO_3$), wollastonite ($CaSiO_3$), and ferrosilite ($FeSiO_3$), and in olivine which is a solid solution of forsterite (Mg_2SiO_4) and fayalite (Fe_2SiO_4).

5.2 Hydrogen

Hydrogen abundance in mature lunar soils typically ranges from 50-100 μg H/g soil as given in Tables 5-8 and 5-9. A cubic meter of mature lunar soil contains 100-200 grams of hydrogen (for bulk soil density of 2 mt/m^3). Mature lunar soils dominate most flatter areas where a lunar base will likely be located. Mining sites should be located away from young sharp rimmed craters.

Soil maturity influences hydrogen content because: 1) mature soil has been exposed to the solar wind for a longer period of time, and 2) the average soil particle size becomes finer in mature soils due to the longer period exposed to the comminutive effects of micrometeoroid impacts, thus increasing the surface to volume ratio and hydrogen content of the soil. Formation of agglutinates, which increases with soil maturity and which tends to increase the mean grain size of the soil, traps hydrogen containing particles within the agglutinate assemblage. However, soil maturity and hydrogen content does not smoothly increase at shallower depths into the regolith because local cratering can throw out immature ejecta that covers a mature soil layer. Thus, the lunar soil shows definite layering in hydrogen content depending on the nearby cratering record. For instance, an Apollo 17 deep core, taken 400 m SE of Camelot crater (~500 m diameter), contained soil with 60 μg H/g at 280 cm deep while the surface concentration was less than 30 μg H/g (40). Over 80 percent of the hydrogen is contained in soil particles less than 45μm (40).

For this study, due to mixing of regolith materials from meteorite impacts, an average 50 ppm of solar derived hydrogen in bulk lunar soil is assumed to extend to a depth of several meters (3). Figure 5-2 summarizes data from JSC laboratories (39) for gas release from soil samples heated at 6°C/minute. The average of this release data was used in this study, although it may be conservative. Gibson, et al. (40) and Blanford, et al. (47) suggest that for practical purposes complete release can be achieved by 900°C, and Carter (41) reports that about 80 percent of the hydrogen is released below 600°C (41). The released gases contain water vapor formed by reduction of ilmenite with hydrogen, the extent of which is temperature dependant as given in Figure 5-3.

Table 5-1. Ilmenite Abundance in Lunar Materials (From Ref. 3, p.2-16)

Lunar Material	Vol.% Ilmenite	Comments
Mare Basalt	0-25	High-Ti basaltic rocks typically contain over 15% ilmenite while low-Ti basalts contain less than 10%.
Soil	0.5-5	Higher ilmenite contents occur in regions with high ilmenite contents in local rocks and low where local rocks are low.
Fragmental Breccias	2-12	In high-Ti mare regions, breccias contain about 10% ilmenite, in low-Ti mare regions about 4%, and in highland regions about 1%.
Crystalline Breccias	1-2	These rocks limited to highland regions.
Anorthositic Rocks	trace	Contains almost no ilmenite.

Table 5-2. Modal (Microscopically Identified) Ilmenite in Mare Basalts (Ref.2, p.248)

Sample	Modal Ilmenite Content Vol. Percent	Sample	Modal Ilmenite Content Vol. Percent
10003	14-18	12202	8-11
10017	14-24	12021	5-12
10044	6-12	12022	9-23
10045	7-11	12039	8-10
10049	16-17	12051	8-11
10072	13-22	12063	8-10
Apollo 11 Mean	14.5	Apollo 12 Mean	10
15016	6	75055	12-20
15076	0.5	70215	13-37
15475	1.0	70035	15-24
15555	1-5	70017	19-23
15556	2		
Apollo 15 Mean	2.6	Apollo 17 Mean	20.4

Table 5-3. Element Chemistry Ranges for the Major Minerals in High-Ti Basalts (Ref.3, p.3-23 & 3-24)

	Pyroxene	Olivine	Plagioclase	Opaques (Mostly Ilmenite)
Vol.%	42-60	0-10	15-33	10-34
Chemical Composition (wt.%)				
SiO_2	44.1 - 53.8	29.2 - 38.6	46.9 - 53.3	<1.0
Al_2O_3	0.6 - 7.7	-	28.9 - 34.5	0 - 2.0
TiO_2	0.7 - 6.0	-	-	52.1 - 74.0
Cr_2O_3	0 - 1.0	0.1 - 0.2	-	0.4 - 2.2
FeO	8.1 - 45.8	25.4 - 28.8	0.3 - 1.4	14.9 - 45.7
MnO	0 - 0.7	0.2 - 0.3	-	<1.0
MgO	1.7 - 22.8	33.5 - 36.5	0 - 0.3	0.7 - 8.6
CaO	3.7 - 20.7	0.2 - 0.3	14.3 - 18.6	<1.0
Na_2O	0 - 0.2	-	0.7 - 2.7	-
K_2O	-	-	0 - 0.4	-

Table 5-4. Ilmenite in the 90-150 μm Grain Size for Apollo 11 and 17 Mare Soils (Ref.2) (Microscopically Identified Free Mineral Grains)

Sample	Modal Ilmenite Volume Percent
10084	2.2
79221	1.3
78501	3.7
75081	7.6
75061	5.3
71501	9.0
71061	4.6
71041	5.6
70181	2.3
70161	5.0
Apollo 17 Mean	4.9

Table 5-5. Modal Ilmenite Abundance as a Function of Grain Size (Ref.2)

Mare Soil 71061

Grain Size μm	Ilmenite Vol. %
45-75	6.0
75-90	3.3
90-150	4.6
150-250	3.3
250-500	2.3

Table 5-6. Grain Size Distribution for a Mature Mare Soil (10084) (Ref.3)

Grain Size	Weight Percent	Cumulative Weight Percent
4 - 10 mm	1.67	1.67
2 - 4 mm	2.39	4.06
1 - 2 mm	3.20	7.26
0.5 - 1 mm	4.01	11.27
0.25 - 0.5 mm	7.72	18.99
150 - 250 μm	8.23	27.22
90 - 150 μm	11.51	38.72
75 - 90 μm	4.01	42.73
45 - 75 μm	12.40	55.14
20 - 45 μm	18.02	73.15
<20 μm	26.85	100.00

Table 5-7. Chemical Composition of Mare Soil 10084 (Ref.4)

	Wt. %
SiO_2	41.0
TiO_2	7.3
Al_2O_3	12.8
Cr_2O_3	0.305
FeO	16.2
MnO	0.220
MgO	9.2
CaO	12.4
Na_2O	0.38
K_2O	0.15
Total	99.955

Figure 5-1. Depth of the Lunar Regolith at the Apollo Landing Sites (Ref. 81)
For Apollo 14, 16, 17 sites, seismic velocities of the upper units were measured and are shown at the side of the columns.

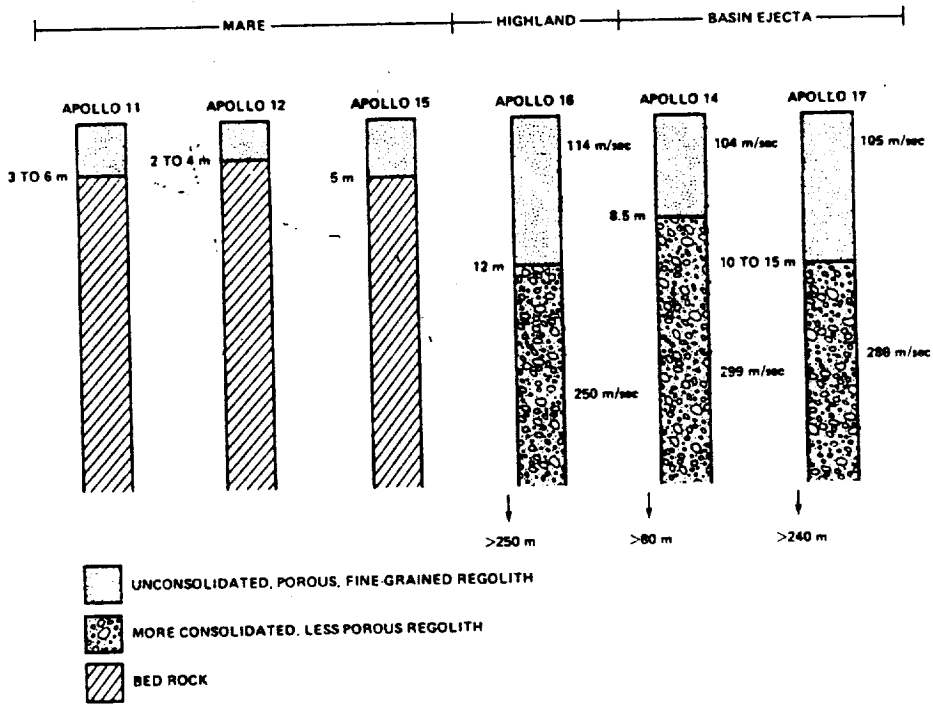

Table 5-8. Hydrogen Abundance Dependence on Grain Size (from Ref. 40)

	10084,149			12070,127			15021,2		
Size Fraction (μm)	Hydrogen Content (μg/g)	Weight Percent	Hydrogen Calculated in Bulk Soil (μg/g)	Hyd. Cont. (μg/g)	Wt. %	H Calc. in Bulk Soil (μg/g)	Hyd. Cont. (μg/g)	Wt. %	H Calc. in Bulk Soil (μg/g)
<20	146.7	25.78	37.8	107.4	22.35	24.0	128.5	23.02	29.6
20-45	29.7	18.33	7.3	30.1	17.34	5.2	51.1	22.96	11.7
45-75	24.4	15.01	3.7	16.2	14.82	2.4	22.4	15.61	3.5
75-90	20.1	5.01	1.0	9.0	5.09	0.5	20.8	4.37	1.1
90-150	20.2	12.24	2.5	8.7	13.37	1.2	15.5	13.26	2.1
150-250	11.3	9.06	1.0	7.5	10.60	0.8	8.4	9.25	0.8
250-500	15.7	8.73	1.4	9.4	8.80	0.8	8.2	7.23	0.6
500-1000	7.2	5.82	0.4	8.5	7.63	0.6	11.0	3.31	0.4
Total Hydrogen Calc. in Bulk (μg/g)			55.1			35.5			49.8
Total Hydrogen Found Experimentally in Bulk (μg/g)			54.2			39.2			49.6

	60501,1			71501,138		
Size Fraction (μm)	Hydrogen Content (μg/g)	Weight Percent	Hydrogen Calculated in Bulk Soil (μg/g)	Hyd. Cont. (μg/g)	Wt. %	H Calc in Bulk Soil (μg/g)
<20	124.1	24.12	29.9	126.4	17.62	22.3
20-45	43.0	17.76	7.6	47.2	17.67	8.3
45-75	16.1	13.48	2.2	18.5	15.60	2.9
75-90	12.8	4.40	0.6	9.4	4.42	0.5
90-150	9.6	11.54	1.1	7.7	14.75	1.1
150-250	5.2	9.72	0.5	2.0	11.51	0.2
250-500	4.4	10.75	0.5	2.4	10.69	0.3
500-1000	2.6	8.22	0.2	1.7	6.64	0.1
Total Hydrogen Calc. in Bulk (μg/g)			42.6			35.7
Total Hydrogen Found Experimentally in Bulk (μg/g)			35.8			25.7

Table 5-9. Bulk Thermal Release of Hydrogen (as H_2 and H_2O) From Lunar Soil

Sample Number	Maturity	H_2 (ppm)	Ref.	Sample Number	Maturity	H_2 (ppm)	Ref.
10084	Mature	46	51	74220,22	Immature	0.4	55
12070	Submature	38	52	60006,230	Core, top	36	55
12033	Immature	2	52	60006,227	Core, next down	30	55
12042	Mature	40	52	60004,407	Core, next down	36	55
14240	Submature	36	53	60004,366	Core, next down	58	55
14422	?	50	53	60002,311	Core, near bottom	36	55
15301	Submature	52	53				
15021,4	Mature	62	54				
64421,21	Mature	46	54				
61221,8	Immature	8	54				
74220,22	Immature	0.2	54				
73121,28	Mature	46	55				
15006,141	Core, top	40	55				
15004,183	Core, next down	30	55				
15001,213	Core, bottom	28	55				

Figure 5-2. Fraction Total Hydrogen (As H_2 + H_2O) Released From Lunar Soil

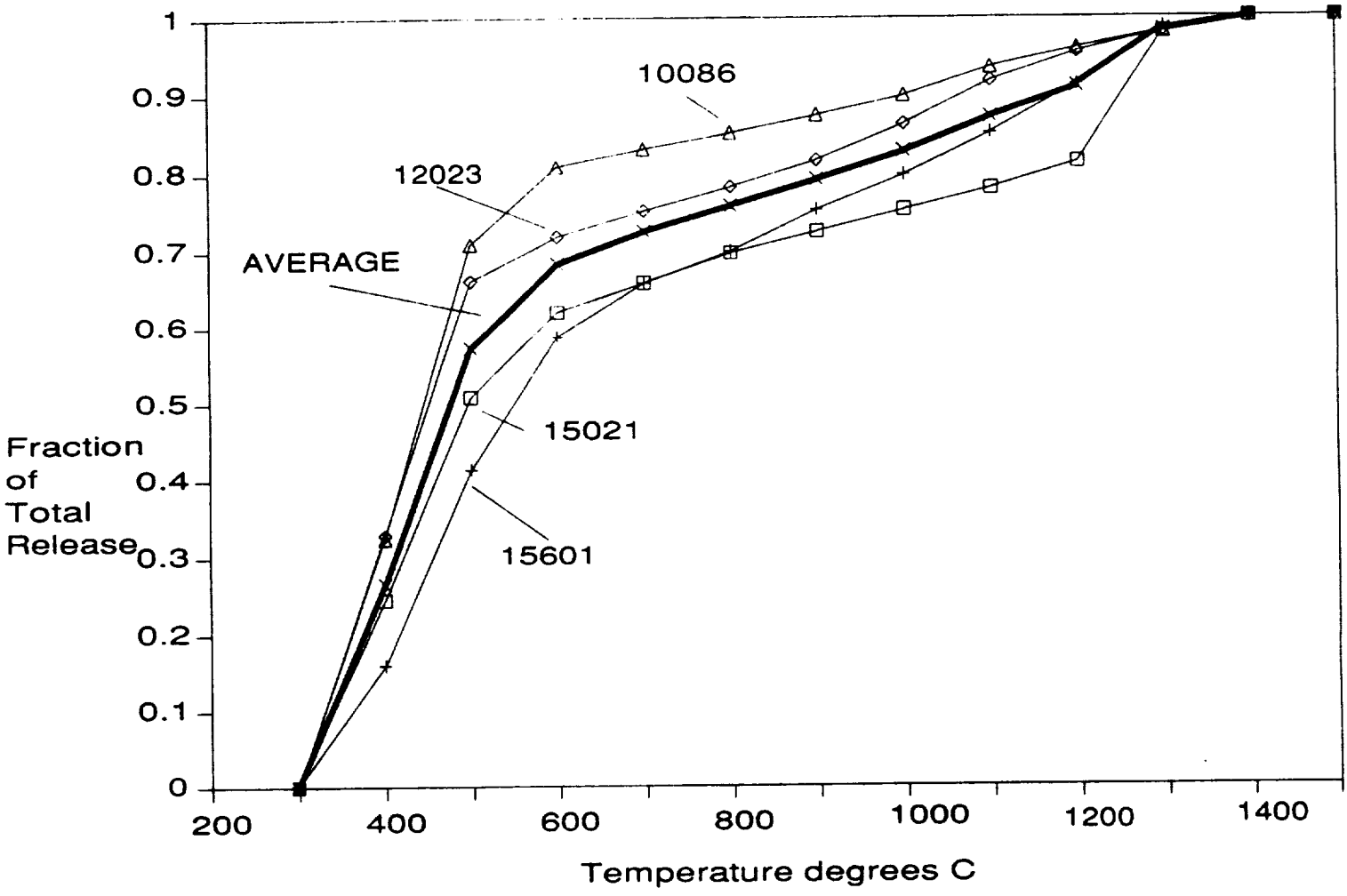

Figure 5-3. Gas Composition Released From Lunar Soil
(μg gas/g soil vs. temperature)

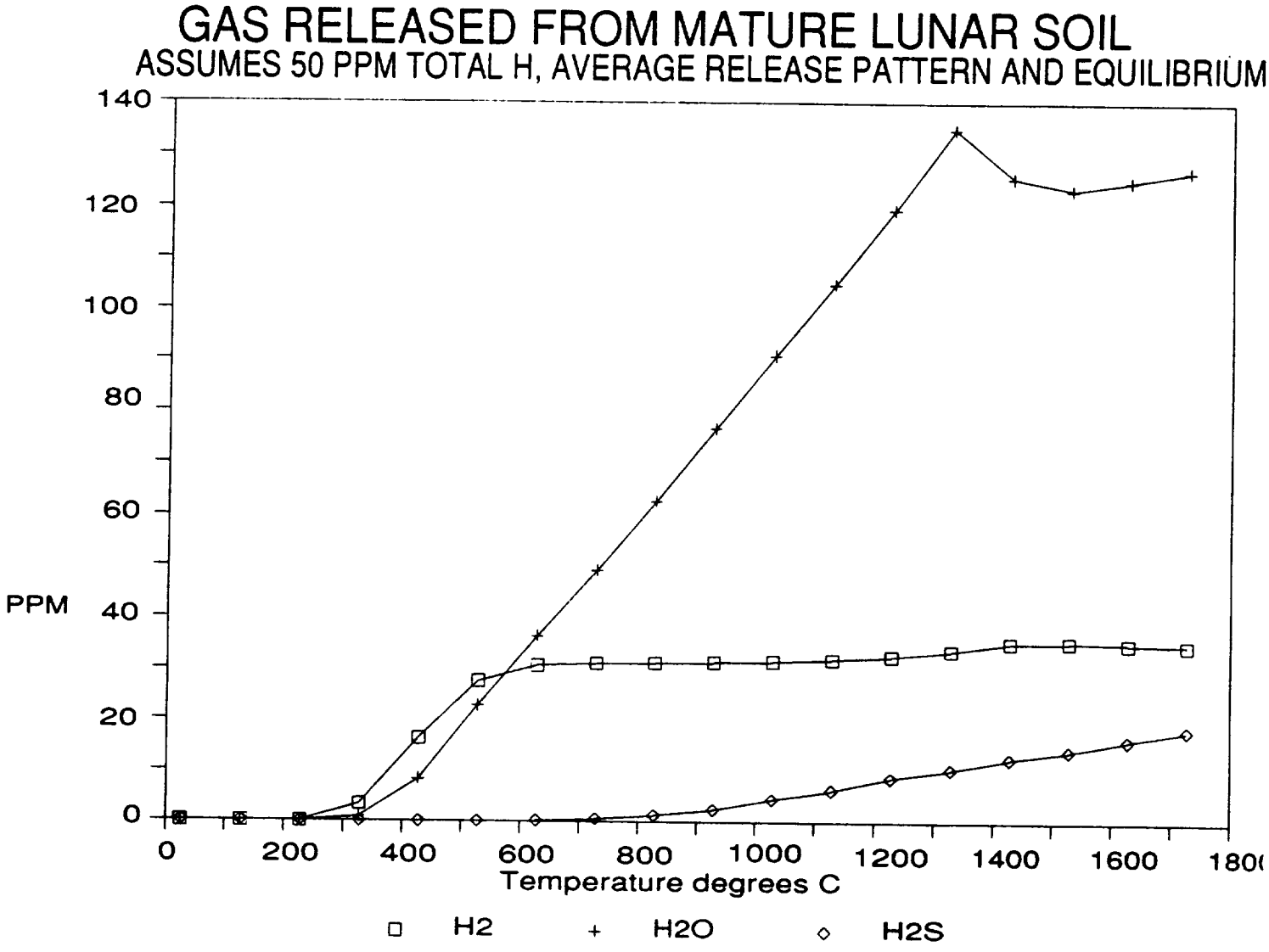

6.0 Oxygen from H_2 Reduction of Ilmenite

As described in Section 4.2, a process employing reduction of ilmenite by hydrogen was selected for further study. The following sections describe:

1. Steps leading to full-scale oxygen production including establishing a pilot plant on the lunar surface.
2. A conceptual design for a lunar pilot plant.
3. Trade studies completed as a part of the analyses.
4. Scaleup of the plant to higher production rates.
5. Plant impacts on base operations.

6.1 Steps to Full-Scale Oxygen Production

A program to develop a process that produces large quantities of propellant-grade and life-support grade oxygen from lunar materials is envisioned to evolve through the same three phase approach proposed for a Lunar Base program in the Civil Needs Database (CNDB) (83). The lunar base phases and timing are described in detail elsewhere (1, 84). Phase I activities take place prior to a human return to the Moon. Oxygen process development steps in Phase I include:

- Laboratory scale feasibility studies. Chemical reaction kinetics and yields determined. Basic principles of process chemistry demonstrated.

- Hardware (mining and process units) conceptual designs formulated and demonstrated in bench scale tests. Investigations made into component/breadboard response to input and process changes, measurement and control of impurity levels in feedstock/product streams, interactions in integrated systems, effects of process unit scale-up, and materials susceptibility to corrosion/erosion in long-term process operation. Computer models of process developed and predictions compared to experimental data. Process optimization studies by computer models and tests. Process control rules formulated and tested. Improved estimates of process mass and power requirements.

- Development/testing of automatic and telerobotic techniques and hardware for both mining and process plant equipment. Operation, monitoring/inspection, and maintenance of equipment should be carried out automatically and telerobotically to the greatest extent possible to reduce direct human involvement.

- Environmental testing of hardware components and breadboards in vacuum chambers, in vacuum/thermal cycling chambers, in 1/6-gravity field (i.e. with KC-135), and other environmental simulators. This data is essential to properly design the process equipment for the lunar environment, and to produce realistic performance and lifetime estimates.

- Earth-based pilot plant investigations to verify equipment scaleup laws and to optimize process conditions. For instance, the optimum configuration of fluidized bed internals could be studied. Quantities of simulated lunar feedstock materials would be required.

- Unmanned lunar orbiter and sample return missions conducted to select lunar base and oxygen production plant sites.

A human-tended lunar base is established in Phase II which is assumed to encompass a 6 year period from 2000-2005 (83-85). Phase II base objectives include:

- Establishing a pilot oxygen production plant on the lunar surface. The pilot plant is conceived as a fully-integrated plant that serves to validate lunar oxygen production from mining through chemical processing and product storage. Engineering data collected during pilot plant operation would support the design of a full-scale production plant optimized for 1/6 g. In addition, and especially if operated continuously during periods without on-site human involvement, the lunar pilot plant would serve to verify system automation, teleoperation/telerobotic, and remote maintenance approaches in the lunar environment (and with a 3 second communication time-lag) prior to implementation in a full-scale plant. The pilot plant would also be useful to evaluate equipment lifetime under actual operating conditions and to certify product quality (thus demonstrating the effectiveness of process steps to remove impurities).

  After establishing a larger liquid oxygen (LOX) plant to produce propellant, the pilot plant could still be used as a research tool to test new process conditions or equipment prior to implementation in the full-scale plant. Pilot plants are often used for such purposes in terrestrial operations. Alternatively, the pilot plant could be used to manufacture a high-purity, special grade product such as oxygen for life-support, especially if the penalty is large in equipment mass and energy to remove impurities or contaminants.

  The real need for a lunar pilot plant to accomplish these objectives versus use of Earth test facilities and small-scale lunar demonstration projects of key processing steps deserves additional study. For this study, a complete pilot plant was assumed required. Given that a pilot plant is necessary, it should be delivered early in the Phase II period to allow as much time as possible to reflect the results of pilot plant operation in the design of the production plant. Assuming that 1-2 years of operation is needed to develop a sufficient data base and another 2 years is required to apply pilot plant results and lessons-learned in production plant design changes (and still allow time for Earth testing, fabrication, and delivery to the launch site), a minimum of 3-4 years would elapse from lunar delivery of the pilot plant to delivery of the production plant. If no design changes are necessary, a shorter delay may result, but it also means that the pilot plant may not have been needed in the first place.

- Installation of necessary refueling facilities and demonstration of reusable lander refueling. At a pilot plant production rate of 2 mt/month LOX (1), 13 months of full-rate pilot plant production would be needed to provide the lunar lander's round-trip requirement of 25.7 mt LOX (based on 30 mt LOX/LH_2 at 6:1 mixture ratio) (50).

- Installation of a larger LOX production plant to provide oxygen for 6-7 reusable lander flights per year, or ~180 mt/year LOX production. Operation of the plant marks the transition to Phase III lunar base (84).

The lunar base is permanently occupied in Phase III. Oxygen production activities include:

- Operation of the 180 mt LOX production plant and lander refueling facilities. Remote operation, pioneered during pilot plant operation, would still be the operating

mode of choice to reduce demands on base personnel. However, the permanently occupied base would provide access to a nearby human maintenance crew for plant equipment repair or replacement.

- Later plant construction to increase production rates as market conditions indicate for supplying LOX to orbital transfer vehicles (OTV's) and interplanetary missions.

6.2 Conceptual Design of Pilot Plant

A conceptual design of a pilot plant to produce 2 mt/month of liquid oxygen (LOX) by reducing ilmenite with hydrogen is described in the following sections. A flowsheet of the process shows all major process units and streams, compositions, temperatures and pressures. Section 6.2.2 lists process equipment mass, power requirements, and volume. The pilot plant layout and important features are described in Section 6.2.3.

6.2.1 Flowsheet

A schematic of the oxygen production process using basaltic rock feedstock is illustrated in Figure 6-1. Approximately 88 metric tons of basalt is required for each metric ton of oxygen produced, given 25 vol.% ilmenite in basalt and other parameters defined in Table 6-1. The actual mining rate depends on assumptions of the basalt quality of mined material. Given the baselines used for this study (50 percent basalt in the mined material and 5 percent oversized basalt as mined), 186 mt is mined per metric ton oxygen. In addition, overburden must be removed from the basalt layer, although removal of the overburden should be more energy efficient and less time intensive than basalt mining. The amount of overburden removal depends on the thickness of the overburden layer and the depth of the basalt mine. A thin overburden is likely if basalt were mined from the bottom of a mare crater. However, given 2 m deep overburden and basalt layers, 1.1 mt of overburden would be removed per metric ton basalt layer mined (a larger area of overburden must be removed per unit area mined due to angle of repose and to allow clearance). If soil feedstock is used, 327 mt of soil at 5 vol.% ilmenite must be mined and processed per metric ton oxygen produced as given in Table 6-1.

Table 6-1. Mining Rates for LOX Plants Using Either Basalt or Soil Feedstock

Basalt Feedstock

Basis: 25 vol.% ilmenite or 33 wt.% ilmenite (see Section 5.1)

10.5% available oxygen in ilmenite	= 9.484 mt ilmenite/mt LOX
90% reactor conversion	= 10.54 mt ilmenite in reactor feed/mt LOX
98% ilmenite recovery in mag. sep.	= 10.75 mt ilmenite in mag. sep. feed/mt LOX
43.1% < minimum reactor input size	= 18.88 mt ilmenite in fine screen feed/mt LOX
64.7% ilmenite liberated by grinder	= 29.19 mt ilmenite in ball mill feed/mt LOX
33% ilmenite in basalt	= 88.23 mt basalt fed to process plant/mt LOX
5% basalt > crusher inlet size	= 92.87 mt basalt/mt LOX
50% basalt in mined material	= 185.74 mt mined material/mt LOX

Soil Feedstock

Basis: 5 vol.% ilmenite or 7.5 wt.% ilmenite (see Section 5.1)

10.5% available oxygen in ilmenite	= 9.484 mt ilmenite/mt LOX
90% reactor conversion	= 10.54 mt ilmenite in reactor feed/mt LOX
98% ilmenite recovery in mag. sep.	= 10.75 mt ilmenite in mag. sep. feed/mt LOX
7.5% ilmenite in soil	= 143.38 mt soil/mt LOX
44.9% of soil < minimum reactor input size & 11.3% of soil > maximum input size	= 326.82 mt soil mined/mt LOX

Figure 6-1. Pilot Plant Process Schematic (For Basaltic Rock Feedstock)

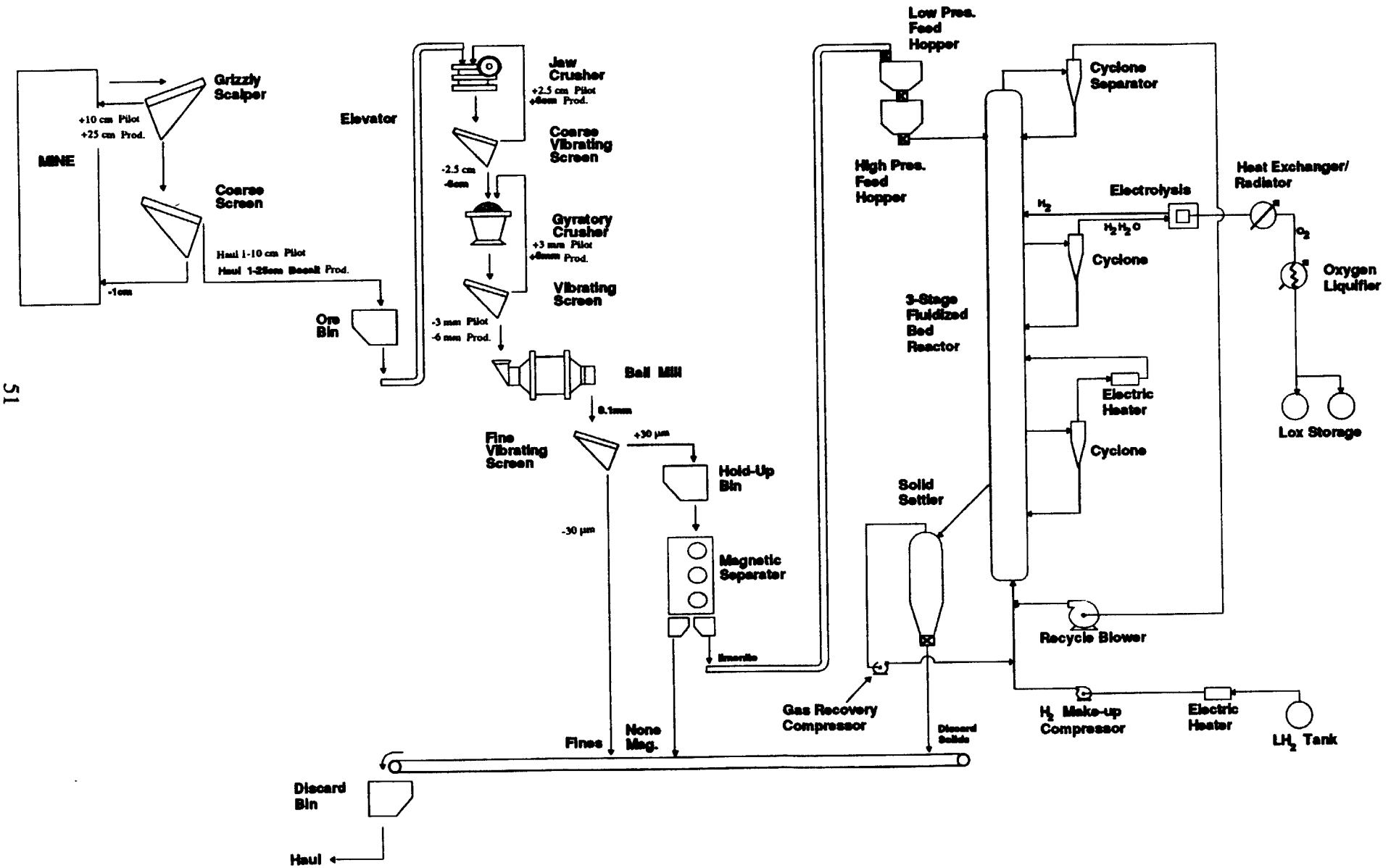

The schematic (Figure 6-1) can be divided into four main areas: 1) mining, 2) beneficiation, 3) process, and 4) power.

Mining

The mining area consists of excavators, oversize and undersize sorters, and haulers. Excavators, such as front-end loaders, deposit loads of basaltic rock in the input bin of a grizzly scalper. The grizzly contains heavy-duty spaced-bars positioned at an angle to remove materials too large for the feed openings of downstream equipment. The rock sizes removed were allowed to float with production rate. For the 2 mt LOX/month pilot plant, the grizzly was sized to remove rocks larger than 10 cm, while for 83 mt LOX/month, 25 cm was the cut size. This kept the size of the primary crusher in reasonable balance with the required capacity. Another sorter removes particles less than 1 cm from the grizzly's undersize material. This step was designed to remove the small particles and soils in the mined material containing glassy agglutinate constituents which would complicate downstream equipment and calculations. A hauler transports the sized basalt feedstock to the feed bin of the crushers. Overburden removal is not illustrated in the schematic.

The major changes in the mining area for a process using soil feedstock would be to combine the grizzly scalper and secondary coarse screen into a single oversize separator. Overburden removal would, of course, not be necessary for a soil feedstock operation.

Beneficiation

A continuous conveyor transports the sized basalt from the feed bin to a three-stage crushing and grinding circuit which reduces the size of the rock to less than the average ilmenite grain size (<0.5 mm, as described in Section 5.1). Fines generated in the milling operation are removed by vibratory screens to avoid excessive carryover/entrainment of these small particles in the reduction reactor. Particles greater than the minimum allowable reduction reactor feed size are fed into a holdup bin and then into a magnetic separator. This separator subjects the feed to several stages of high-intensity magnetic fields to remove the slightly magnetic ilmenite particles from non-magnetic gangue (mixed particles of pyroxene, plagioclase, and olivine minerals from the basalt). The recovered ilmenite is conveyed to a low-pressure feed hopper of the reduction reactor.

A soil feedstock process would not need the crushing/grinding circuit but would require additional screening units (or other fines separators such gas classifiers) and larger ilmenite magnetic separators.

Process

Ilmenite is fed through low and high pressure feed hoppers into a three-stage fluidized bed reactor. The feed is preheated in the top bed of the reactor by gases from the middle bed and electrolysis cell. Reduction of ilmenite by hydrogen takes place primarily in the middle bed. Residual solids are cooled by preheating the gas stream in the bottom bed before being discharged through a gas/solid separator. The water product of reaction from the middle bed is dissociated into oxygen and hydrogen in a solid-state electrolytic cell operated at reaction temperature. The oxygen is cooled, liquefied, and stored while the hydrogen is used to preheat the incoming solids. Sensible and endothermic reaction heat requirements of the reactor are provided by electrically heating the gas stream to the middle bed. Cyclone separators are used to separate dust from gas, necessary to protect downstream equipment from erosion damage and fouling. Liquid hydrogen is

vaporized to provide makeup for process H_2 losses. Active cooling loops, not shown in the schematic, transfer waste heat from the beneficiation equipment, motors/pumps and other rotating equipment, and the oxygen product stream to a central radiator system.

Power

Solar-electric sources provide power requirements during the lunar day for the process and for regenerating reactants used in fuel cell power storage systems. During the lunar night, fuel cells maintain high temperature portions of the process (reactor, electrolysis cell, electric heater, and gas recycle compressor) on hot-standby to reduce thermal cycling of refractory linings, which might otherwise reduce equipment lifetime. Alternatively, a nuclear-electric power source would allow the process to operate day and night, thus decreasing the size of the plant for a given oxygen production requirement.

Flowsheet Conditions

The compositions and flowrates of the various process streams are given in Table 6-2, where the stream numbers for the flowsheet are defined in Figure 6-2. This flowsheet is for a 2 mt/month LOX pilot plant using basalt feedstock. The pilot plant is assumed to be powered by solar photovoltaic arrays during the 2-week lunar day, and kept on hot-standby during the 2-week lunar night using a regenerative fuel cell to provide power for reactor/electrolysis system heat losses and miscellaneous requirements. Overall plant duty cycle is 45% (based on 90% utility for 50% of the time), while the duty cycles of mining area units are 35% (70% utility for 50% of the time) due to the greater likelihood of higher maintenance requirements for mining equipment. The flowsheet conditions have been adjusted for 45% duty cycle throughout to allow comparisons.

Figure 6-2. Process Stream Numbers for Flowsheet Conditions (Table 6-2)

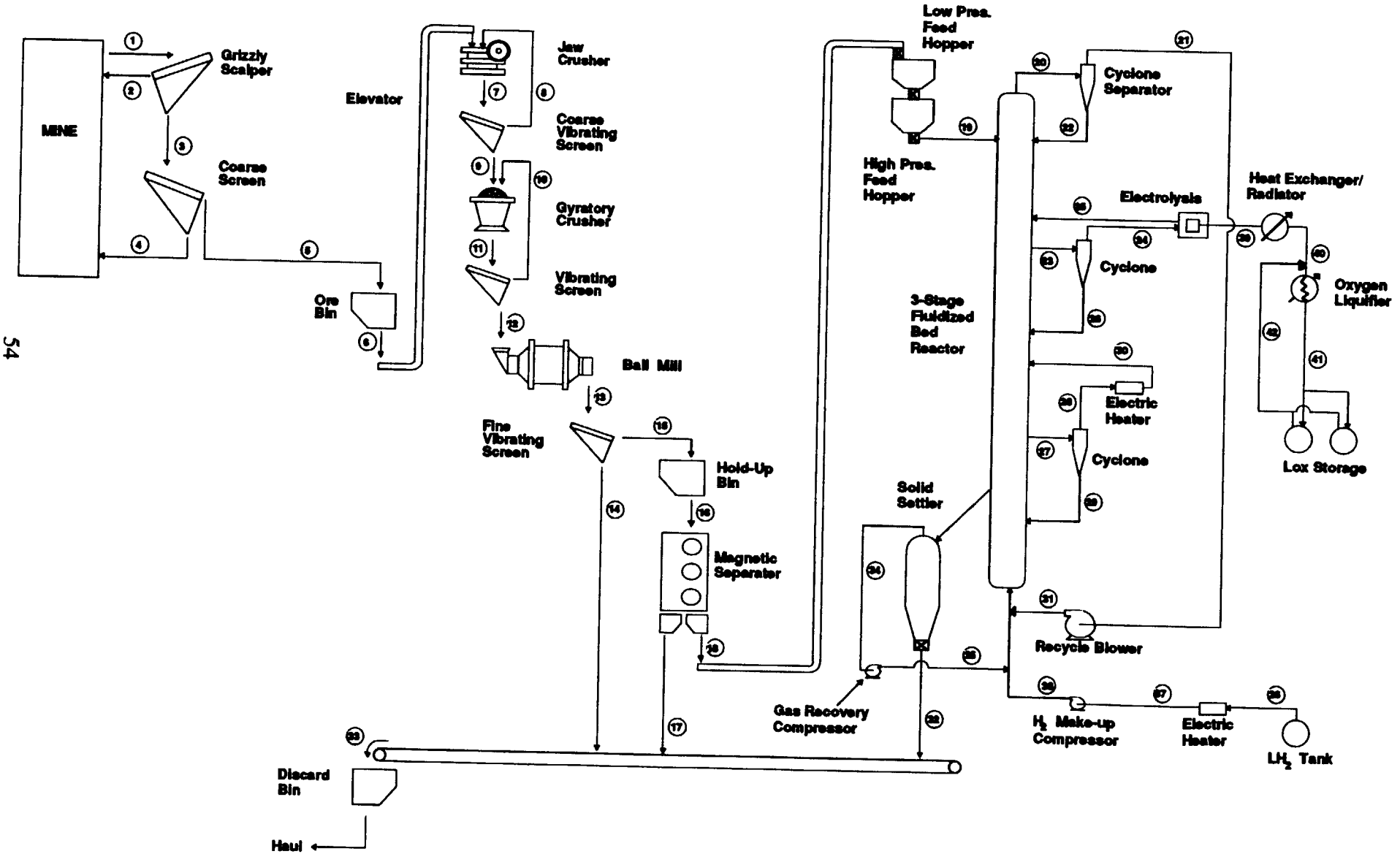

Table 6-2. Pilot Plant Process Flowsheet Conditions
(2 mt LOX/month, basalt feedstock, PV/RFC power system, 45% duty cycle)

Stream No.	Phase	Flow Rate (kg/day)	Stream Constituents (kg/day)	Temp. (°C)	Pressure (atm)	Description
None - Overburden	Solid	30,941	Soil	-20	-	Overburden removal.
1	Solid	27,141	Basalt: 13,571 Soil: 13,571	-20	-	Mining basalt layer. Subsurface temperature nearly constant (86).
2	Solid	679	Basalt	-20	-	Oversize basalt rocks, >10 cm.
3	Solid	26,463	Basalt: 12,892 Soil: 13,571	-20	-	Undersize from grizzly, <10 cm.
4	Solid	13,571	Soil	-20	-	Small particles < 1 cm.
5	Solid	12,892	Basalt	-20	-	Sized basalt fragments, > 1 cm, < 10 cm. Stream #5 flow actually 16,576 kg/day @ 35% mining duty cylce. Bin provides holdup volume.
6	Solid	12,892	Basalt	-20	-	Feed of sized basalt fragments to crusher.
7	Solid	14,181	Basalt		-	1,289 kg/day fragments > desired output, 12,892 kg/day < or = desired output (2.5 cm).
8	Solid	1,289	Basalt		-	Oversize (>2.5 cm) from jaw crusher screen.
9	Solid	12,892	Basalt		-	Sized < 2.5 cm feed to secondary crusher.
10	Solid	1,289	Basalt		-	Oversize (>3 mm) from secondary screen.
11	Solid	14,181	Basalt		-	1,289 kg/day > desired output size (3 mm). 12,892 kg/day < or = desired 3 mm size.
12	Solid	12,892	Basalt		-	Sized < 3 mm feed to ball mill.
13	Solid	12,892	Basalt Gangue: 10,133 Ilmenite: 2,759		-	5,550 kg/day < minimum allowable size (0.03 mm) to avoid excessive carryover in reactor. 7,342 kg/day > 0.03 mm. Feed fine screen.
14	Solid	5,550	Gangue: 4,362 Ilmenite: 1,188		-	Fines (<0.03 mm) discarded.
15	Solid	7,342	Gangue: 5,771 Ilmenite: 1,571		-	Oversize (>0.03 mm) from screens.
16	Solid	7,342	Gangue: 5,771 Ilmenite: 1,571		-	Duty cycle (45%) same before and after hold-up bin. Therefore, feed magnetic separator at same flow rate as feed bin.
17	Solid	5,631	Gangue: 5,599.4 Ilmenite: 31.4		-	Non-magnetic discharge from magnetic separator.
18	Solid	1,711	Gangue: 171.1 Ilmenite: 1,539.9		-	Ilmenite to low-pressure feed hopper.
19	Solid	1,711	Gangue: 171.1 Ilmenite: 1,539.9		9.9	Feed-hoppers cycle in sequence, same duty cycle. Same flow as stream #18.
20	Gas	284.5	H_2: 275.88 H_2O: 8.66 Dust/fines < 0.03 mm	732	9.9	Offgas from top bed routed to cyclone to remove entrained fines.
21	Gas	284.5	H_2: 275.88 H_2O: 8.66	732	9.8	Pressure drop through cyclone small (<0.5 psi), pressure drop through pipe < 1 psi.

Table 6-2 (Cont). Pilot Plant Process Flowsheet Conditions
(2 mt LOX/month, basalt feedstock, PV/RFC power system, 45% duty cycle)

Stream No.	Phase	Flow Rate (kg/day)	Stream Constituents (kg/day)	Temp. (°C)	Pressure (atm)	Description
22	Solid		Dust/fines < 0.03 mm			Cyclone calculated to remove 98% of 10μm or larger particles, 69% of 2μm particles, and 36% of 1 μm particles.
23	Gas	430.7	H_2: 257.47 H_2O: 173.18 Dust/fines	1000	9.95	Product gas from reduction reaction.
24	Gas	430.7	H_2: 257.47 H_2O: 173.18	1000	9.9	Pressure drop through cyclone small.
25	Gas	284.5	H_2: 275.88 H_2O: 8.66	1000	9.9	Electrolysis hydrogen-rich exit stream.
26	Solid		Dust/fines < 0.03 mm			Cyclone removes most >10μm particles as in stream #22.
27	Gas	284.5	H_2: 275.88 H_2O: 8.66 Dust/fines	771	10	Gas in bottom bed heated by descending solids.
28	Gas	284.5	H_2: 275.88 H_2O: 8.66	771	10	Inlet gas to electric heater.
29	Solid		Dust/fines < 0.03 mm			Cyclone removes most >10μm particles as in stream #22.
30	Gas	284.5	H_2: 275.88 H_2O: 8.66	1228	10	Gas heated to provide heat of reaction.
31	Gas	284.5	H_2: 275.88 H_2O: 8.66	732	10.0	Gas from top bed compressed, injected into bottom bed.
32	Solid	1,565	Gangue: 171.1 Ilmenite: 154.0 TiO_2: 729.7 Fe: 510.1	<771	-	Residual solids from reactor w/ some interstitial gases (97 wt.% hydrogen) which are lost when exposed to vacuum.
	Gas	0.14	H_2: 0.144		-	
33	Solid	12,746	Fines: 5550 Non-magnetics: 5631 Residual Reactor Solids: 1565		-	Total processing tailings rate.
34	Gas		H_2 H_2O			Hydrogen (97 wt.%) and water recovered from reactor discharge hopper. (Flow not calc)
35	Gas		H_2, H_2O		10.0	Recovered gas recompressed.
36	Liq.	0.14	H_2: 0.144	-252.7	1	Liquid hydrogen pumped to electric heater/ vaporizer for process makeup.
37	Gas	0.14	H_2	771	1	Hydrogen vapor to makeup process losses.
38	Gas	0.14	H_2	771	10	Compressed hydrogen injected into reactor.
39	Gas	146.12	O_2	1000	9.8	Product oxygen from electrolysis.
40	Gas	146.12	O_2	27		Oxygen cooled by active thermal control system prior to liquefaction (1.8 kwt rejected).
41	Liq.	239.48	O_2	-183	1	Includes 146.12 kg/hr oxygen from process and a maximum of 93.36 kg/hr oxygen boiloff.
42	Gas	93.36	O_2	-183	1	

6.2.2 Mass Statement

A list of mass, power, and dimensions for the equipment required in a 2 mt/month LOX pilot plant is given in Table 6-3. Total plant mass is 24,700 kg, including a power system generating 146 kwe during the lunar day and 9.6 kwe during the lunar night. Plant equipment was sized using the equations and scaling relations described in Appendix A. Basalt feedstock was used. Power was provided by photovoltaic (PV) arrays and regenerative fuel cells (RFC). Given these power sources, plant duty cycle was baselined as 45% and mining equipment duty cycle was 35%.

Table 6-3. Lunar Oxygen Pilot Plant Equipment List (2 mt LOX/month, basalt feedstock, PV/RFC power system)

Item	Mass (kg)	Nominal Power (kw)	Dimensions W/D (m)	L (m)	H (m)	V (m^3)	Comments
Front End Loader	1968	2.99	2.1	3.9	2.3	18.6	Same front loader and hauler used for both overburden removal and mining.
Hauler	1015	0.29	2.5	4	2.5	25	
Pit Scalper	380	1.18	2.1	4.2	3.6	31	Spaced, parallel bars to remove oversize and vibratory screen to remove fragments < ~1 cm.
Mining Total	3363	4.45				74.6	
Feed Bin	215		3.9	3.9	1.5	22.7	
Primary Jaw Crusher	724	0.38	0.4	1.4	0.7	0.4	
Coarse Screen	3	0.08	0.3	0.4	0.4	0.04	
Secondary Crusher	239	1.50	0.5		1.0	0.24	
Secondary Screen	3	0.09	0.3	0.4	0.4	0.04	
Ball Mill	1914	16.4	0.8	1.0		0.4	
Fine Vibratory Screen	500	15	2.5	4.0	0.9	9.0	
Storage Hopper	32		2.7		2	11.6	
Magnetic Separator	248	0.3	0.5	0.6	0.9	0.2	
Beneficiation Total	3879	33.8				44.7	
Lo-Pressure Feed Hopper	12		1.3		2	2.7	
Hi-Pressure Feed Hopper	77		1.3		2	2.7	
Reactor	1963		0.9		6.6	4.4	
Electric Heater	134	24.0	0.9	1.1		0.7	
Electrolysis Cell	213	33.5	0.6	0.6	1	0.4	
Blower	29	0.3	0.2		0.3	0.01	
Cyclone Separators (3)	3		0.1		0.4	0.01	
Discharge Hopper	102		1		2	1.6	
Tailings Conveyor	23	0.01	0.2	15	1	0.3	Volume based on stowed 0.1 m thickness.
Oxygen Liquefier	199	4.6	0.4	1.3		0.2	
LOX Storage Tanks (2)	219		1.7			5.1	Mass & volume of both tanks. 4 mt LOX capacity.
Radiator/TCS	1362		3	22.7	0.01	0.7	136 m^2 radiator area, 24.4 kwt heat rejection.
Hydrogen Makeup System:							
Liq. Hydrogen Tank	12		1.0			0.6	Empty weight.
Liq. Hydrogen (Max.)	12						180 days supply for expected loss of 2 kg/month.
H_2 Heater	0.1	0.03	0.1	0.1		-	
H_2 Blower	3	0.03	0.1		0.1	-	
Process Piping:							
3 cm ID Pipe	302		0.03	89		0.06	
0.25 cm Pipe	151			120		-	
Process Total	4817	62.5				18.8	
Process + Beneficiation			4.3	13.7		199	Major equipment in the beneficiation/process areas can be manifested into Shuttle payload pallet (~14' diameter x 45' long) leaving room for access/maintenance.
Margin	3618	30.2					Contingency for structure & misc., spares, redundancy.
Total Mining & Plant	15677	131.0				274	
Photovoltaic Power Sys.	5721					13.2	Generates 145.9 kwe (131.0 for process and 14.9 for recharging regenerative fuel cell). 7 space station size panels (8.74 m x 29.1 m) required @ 86 W/m^2. Volume of solar wing boxes and mast canister 1.9 m^3/panel.
Regenerative Fuel Cell	3285		4.3	7		102	Includes (2) 2.7 m GH_2 tanks, (2) 2.2 m GO_2 tanks, (1) 1.3 m H_2O tank, and regenerative fuel cell. Generates 9.6 kwe to maintain process on hot standby during lunar night (336 hrs). RFC units individual total volume is 33.6 m^3, but manifested into Shuttle payload pallet (w/ water tank full, other tanks empty) requires 102 m^3.
Power Total	9005					115	Total power generation = 156.3 kwe, 57.8 kg/kwe.
Plant & Power Total	24682	145.9				389	

6.2.3 Equipment Description

A depiction of the lunar oxygen pilot plant conceptual design is presented in Figure 6-3. Principal features are illustrated in the callout given in Figure 6-4. A brief description of the plant's major equipment is given in this section. Physical parameters of the equipment are listed in Table 6-3 while Appendix A presents additional supporting data in many cases for the equipment sizing equations.

Front-End Loader

A front-end loader (FEL) is shown in Figure 6-4 excavating basalt from the bottom of a conveniently located nearby crater. A number of excavator alternatives are possible including dragline excavator, bucket-wheel excavator, bulldozer, backhoe, and three-drum slusher (87). The FEL depicted in this concept, as described in a previous study (84), is conceived as a multifunctional, teleoperated vehicle. The FEL was capable of using various implements (such as front loader bucket, backhoe, and winch/cable system) to perform a variety of jobs. Thus, this vehicle has the flexibility to be applied in other areas besides mining/resource utilization. Especially for an early base, this is an important option. In recognition of this potential, a minimum FEL size constraint was established based on a 0.5 m^3 bucket (approximately triangular 1.6 m wide x 0.8 m deep x 0.8 m high) which, when applying scaling equations (88) defined in more detail in Appendix A, results in a vehicle mass of 2 mt. As given in the following table, the FEL can complete both overburden and basalt mining with sufficient time resources remaining to perform additional surface base operations.

Basis: 35% duty cycle, 255.5 hrs/month, 2 mt/month LOX pilot, Basalt Feedstock

	Percent of Available Time used to: Remove Overburden	Mine Feed	Total	TimeAvail. ForOther Tasks(hr)
Front-End Loader	6.5%	5.0%	11.5%	226
Hauler	7.6%	7.7%	15.3%	217

Basis: 35% duty cycle, 255.5 hrs/month, 2 mt/month LOX pilot, Soil Feedstock

Front-End Loader	0%	10.0%	10.0%	230
Hauler	0%	20.0%	20.0%	205

A dozer would be more efficient than the FEL for overburden removal (87). For a larger LOX plant, dedicated mining equipment will probably be necessary. Low mass equipment specifically designed for collecting large quantities of feedstock (but having few other applications), such as the three-drum slusher (89), may be favored for a dedicated application.

The FEL dumps its load into the receiving bin of the grizzly scalper/coarse screen which is located in the pit as shown in Figure 6-4 (the receiver bin containing the grizzly is near ground-level behind the two elevated bins).

Pit Scalper

The pit scalper contains a grizzly to remove large oversize rock, and a coarse screen to remove fines (< 1 cm). The grizzly is a simple device of spaced bars that are aligned

at an angle to permit oversize rock to roll off. In the pilot plant concept, rock greater than 10 cm in diameter is rejected. The remaining undersize material is conveyed to the top of the pit scalper where it enters a coarse vibratory screen which separates soil/rock particles finer than 1 cm. The oversize (> 1 cm) is discharged to the right-hand bin in Figure 6-4, while the undersize drops into the bin on the left side. Power for the pit scalper is provided from the power system via electricial cables laid on the surface (with bridges over them) as indicated in Figure 6-3.

Hauler

The hauler is envisioned as a self-propelled, telerobotic materials transporter. It acquires a load of sized basalt feedstock from the pit scalper, transports it to the process feed bin (the bottom opens to dump the material into the bin), collects a load of tailings from the tails discharge bin (#17 in Figure 6-4), dumps the tails at a discharge area (#18), returns to the pit to take a load of undersize material to the discharge area, then returns to the pit to repeat the cycle. One hauler with a 4.5 m^3 bed (selected as a minimum size) can accomplish these tasks for the pilot plant with sufficient time remaining to perform additional soil transport duties around the base. If a dedicated FEL and hauler for mining was required, significantly smaller vehicles than those given in the equipment list (Table 6-3) could be substituted. However, given the range of surface operations anticipated (84), multifunctional vehicles performing a variety of jobs seem more likely for an early base. These vehicles may also require more maintenance than other lunar base systems.

Both the FEL and hauler are teleoperated/robotic devices that will require control from Earth if the pilot plant is to operate during non-manned periods of the Phase II base. Significant on-board computational capability, combined with strategically located navigational markers/beacons around the plant and mine area, will be required for teleoperated control of these vehicles with the 3 second delay in Earth teleoperated mode (84, 90). Human supervisory control of a nearly autonomously operating vehicle is indicated. This will require automation and robotic (A&R) research and technology development. Teleoperations from the lunar base is also possible when the base is manned.

Fuel cell power systems were baselined for both the FEL and hauler (with a penalty added to the PV array power load for regenerating the FC reactants). Dedicated machines could probably use extension cords plugged into the plant's power system. It would be advantageous to permit dual-power mode vehicles, capable of receiving power requirements from either on-board fuel cells or the power network via electric cables.

The mine in Figure 6-3 is approximately 30 m from the process plant. Although a distance of 1 km was used in the sizing calculations, the only requirement is to minimize the effects of dust generated from the mining and processing requirements on optical and thermal properties of sensitive components, such as solar arrays and radiators. Since small particles follow ballistic trajectories, and the forces exerted by the mining operations will not be great (unless explosives are used), the illustrated distance may be more realistic than the 1 km used in sizing calculations. Shorter distances will reduce required hauling time, and thus reduce hauler size and mass (for the production plant). Figure 6-3 also illustrates the mine after a single year of operation. The size of the mine after several years operation is given in Table 6-4.

Figure 6-3. Conceptual Design of a Lunar Oxygen Pilot Plant

Figure 6-4. Conceptual Design Call-Out

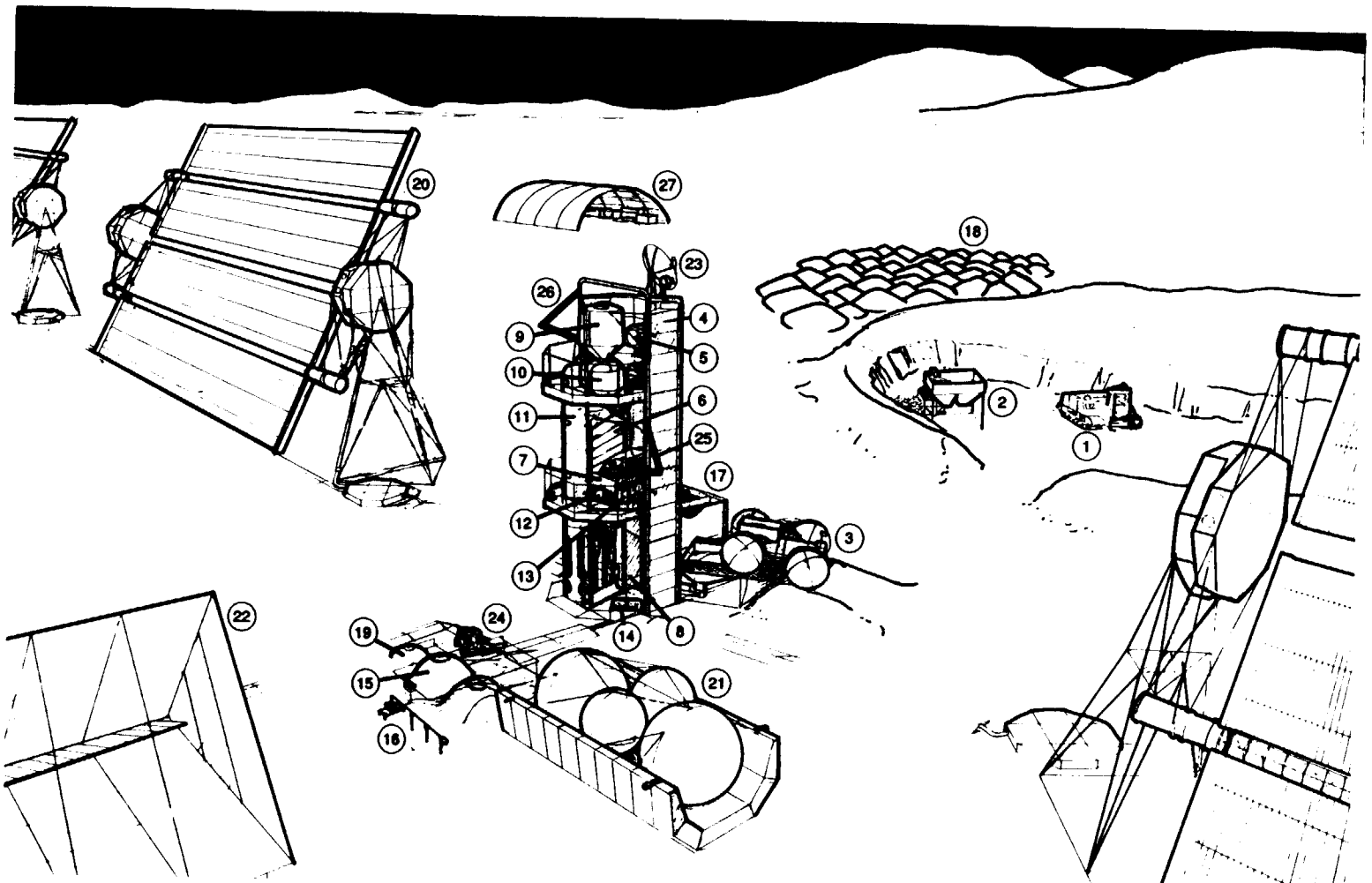

Location: Lacus Veris (87.5°W, 13°S)
View Facing North-East

1. Excavator (Front-End Loader)
2. Pit Scalper
3. Hauler
4. Support Structure (Payload Bay Pallet)
5. 3-Stage Crushing/Grinding Circuit
6. Vibratory Screen (Fines Removal)
7. Hold-up Bin
8. High-Intensity Magnetic Separator
9. Low-Pressure Reactor Feed Hopper
10. High-Pressure Reactor Feed Hopper
11. 3-Stage Fluidized Bed Reactor
12. Electric Gas Heater
13. Solid-State Electrolysis Cell
14. Oxygen Liquefier
15. Buried Oxygen Storage Tanks
16. Liquid Oxygen Loading Station
17. Tails Discharge Bin
18. Tailings Piles
19. Makeup Hydrogen Storage Tank
20. Photovoltaic Power System (Sun-Tracking)
21. Regenerative Fuel-Cell Gaseous-Reactant Storage Tanks
22. Radiator with Fixed Sun-Screen
23. Communications: High- and Low-Gain Antennas
24. Telerobotic Servicer on Lunar Surface Mobile Platform
25. Telerobotic Servicer on Remote Manipulator Arm
26. Spare Remote Manipulator Arm
27. Equipment Repair and Spares Storage Shed

Table 6-4. Extent of Mine (Basis: 2 mt LOX/month, basalt feedstock, 2 m deep overburden and 2 m deep basalt layer, other parameters given in Table 6-1)

Year =	1	2	3
Sq. Side of Overburden Removed (m)	38	53	65
Mass Overburden Removed (mt)	5,088	10,177	15,265
Square Side of Basalt Mine (m)	33	47	57
Mass of Basalt Layer Mined (mt)	4,458	8,915	13,373

Support Structure

After a hauler load of basalt feedstock is dumped into the process feed bin, the basalt is conveyed by continuous conveyor to the top of the process support structure. A Shuttle payload bay pallet (14' outside diameter x 45' long) was used as the pilot plant structure, both to provide a reference size scale and to convey the point that the major plant units are delivered fully-integrated to the lunar surface. Besides emplacing the process pallet itself, the only required assembly and connections are for utility interfaces and large, flexible structures such as the solar arrays and central thermal control system radiator. The pallet will need to be stablized in the vertical position by securing it to pilings that have been drilled into the bedrock (2-5 m below the surface) or by using guy-wires. The process support structure is mounted in the vertical direction because this orientation is required for the long fluidized-bed reactor and to take advantage of gravity for solids processing. After they are conveyed to the top of the process stack, the solids drop through all subsequent unit operations.

The plant is operated nearly autonomously with remote monitoring and supervision, however, direct human access to the plant must be accommodated. For this purpose, the structure has floor gratings at ground level, 15' level, and 30' level with connecting ladders and guard rails to allow human inspection/maintenance of the process vessels. The plant was also arranged to provide access room around the process units.

Although effort was expended on arranging the process units in the support structure to optimize plant operations and allow access by on-site crew, no effort was made in checking the center-of-gravity location with Shuttle payload allowables and other launch criteria. It should be noted that payload manifesting could significantly impact plant design and should be considered in early design studies.

Crushing/Grinding Circuit

A 3-stage crushing and grinding circuit reduces the size of feedstock rock from 1000 to 2500 times to release ilmenite grains in relatively pure form from the basalt groundmass. Ideally, the rock would break along interfaces between mineral grains, thus releasing pure ilmenite with a minimum of crushing. However, random breakage across grains is more typical in actual practice (91, p.8-15; 92). Therefore, grinding to a size substantially smaller than that of the grains is necessary to separate mineral particles. Figure 6-5 shows that for an ore with 25 vol.% ilmenite and 0.5 mm grains (see Section 5.1), approximately 65 percent of the ilmenite will be released as essentially pure ilmenite particles by grinding to an average size of 0.1 mm. The rest of the ilmenite will be contained in particles with various amounts of gangue minerals.

Figure 6-5. Fraction of Ilmenite Released as a Function of Abundance and Reduction Ratio (Reduction Ratio is the ratio of original ilmenite grain size in basalt rock to the final particle size of the rock fragments after crushing and grinding)

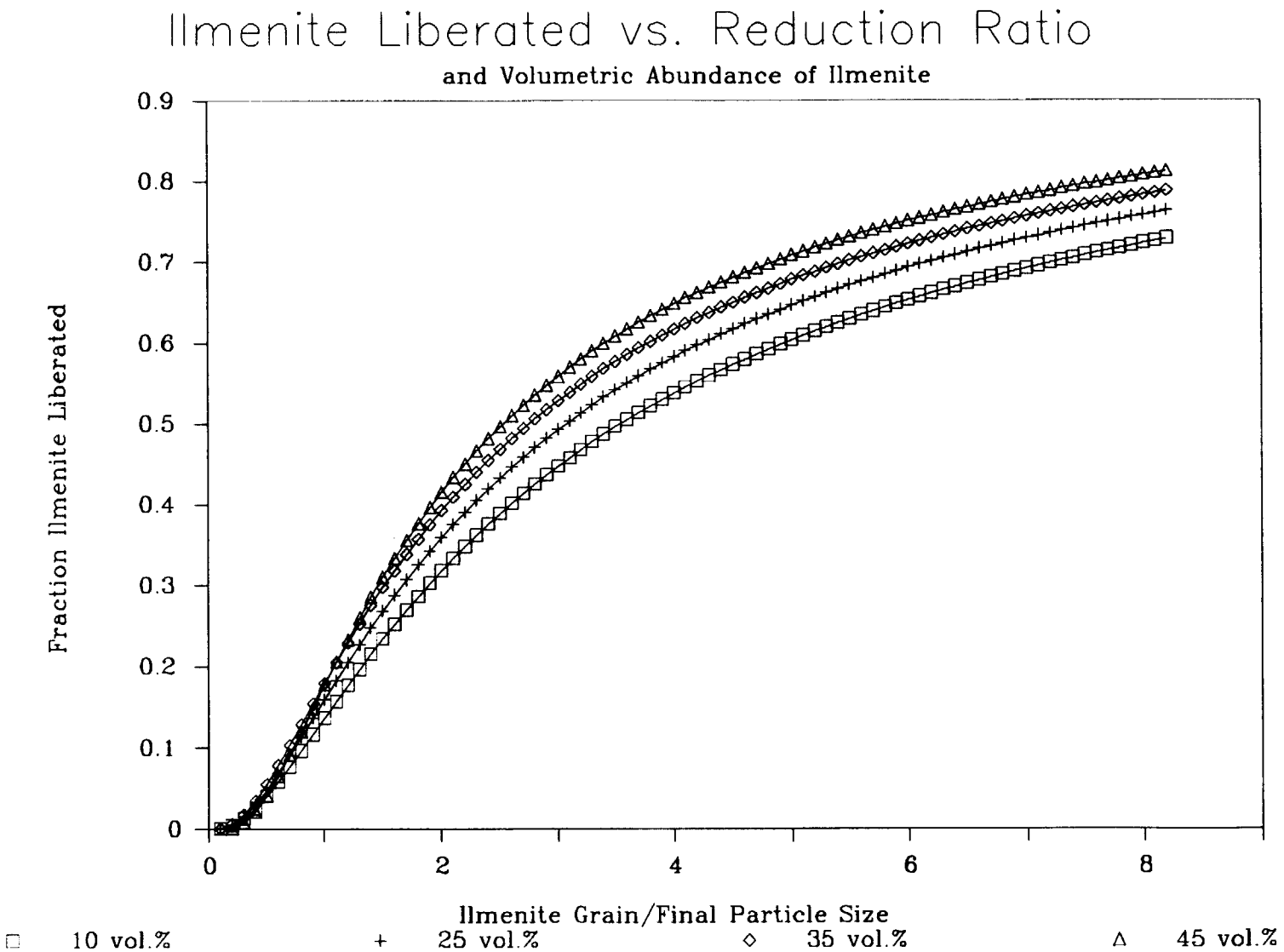

Figure 6-6. Schematics of Crushers/Grinders (Ref. 92)

Jaw Crusher - Primary Crusher

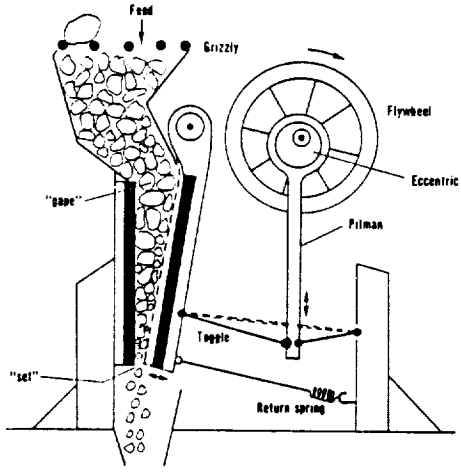

Secondary Crusher: Gyratory or Cone

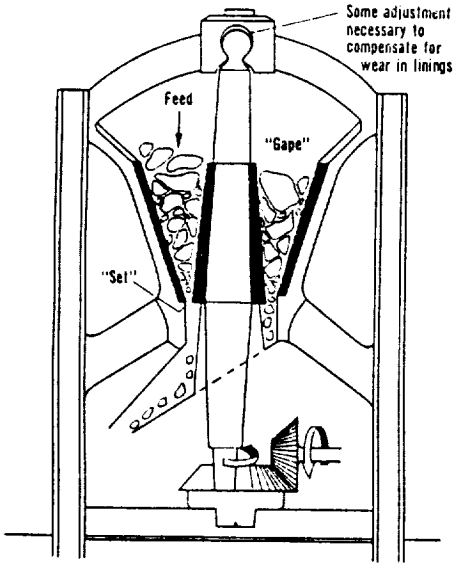

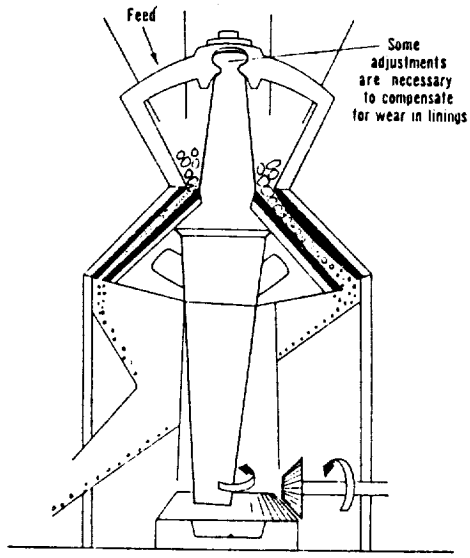

Grinder: Ball Mill

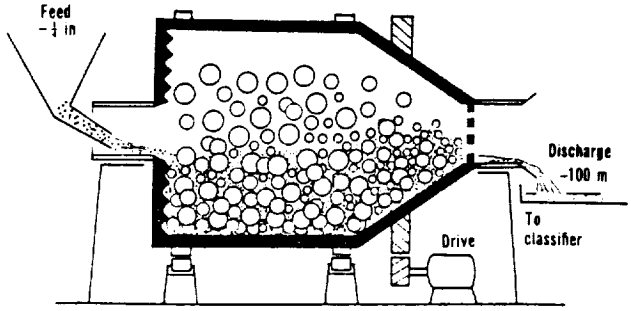

The first stage of the crushing/grinding circuit is a jaw crusher that operates at a 4:1 reduction ratio of input to output particle sizes. This crusher works by squeezing the rock between fixed and movable jaws until it breaks (Figure 6-6). The jaws cycle several hundred times per minute as the fragments fall down to a narrower part of the wedge to be squeezed again, until they can escape through the minimum gap at the bottom. A jaw crusher is more efficient than other types for reducing large, blocky feed (93, 94). Jaws feature easy adjustment for wear and simple maintenance/repair (92, 94).

Secondary crushing by cone or gyratory crusher reduces the sized output from the jaw crusher by 10:1. As given in the schematic of Figure 6-6, the crushing faces in a cone or gyratory are between a eccentrically mounted rotating cone and a fixed bowl. These crushers are known for high throughput and lower power consumption for a given size reduction (93, 94).

A ball mill is used to reduce sized materials from the secondary crusher to a target size of 0.1 mm. This mill utilizes steel or ceramic balls or rods as a grinding medium. An alternative to reduce mass by eliminating the heavy steel/ceramic grinding media is an autogenous grinder that uses larger fragments of the material to be ground itself as the grinding agent, however, adequate characterization testing must be performed and productivity may be lower.

The sizing/scaling relationships were developed on conservative assumptions as to the degree of ilmenite liberation, fines generation, and power requirements. Actual crushing tests on the proposed ore feedstock are always recommended to ascertain what can be achieved (91-95).

Fines Removal

Ball mill product will contain small particles or fines that will need to be removed since they will be swept out of the fluidized bed reactor by the gas stream. At conditions existing in the reactor, 0.03 mm particles are the minimum allowable feed size to avoid excessive entrainment in the gas stream (calculations in Appendix A). At an average target size of 0.1 mm, the ball mill product will contain 43 wt.% particles less than 0.03 mm. A vibratory screen was selected to remove these fines and is shown in Figure 6-4. However, screens with apertures less than about 100 microns are inefficient (91), thus, this application of screening results in relatively large screen areas and high power consumption. Alternatives to screening include cyclones and mechanical gas classifiers, that could possibly be combined with the reactor system to remove fines from the top bed of the fluidized bed reactor. Electrostatic sizers have also been proposed (46) and some industrial/laboratory experience with this concept exists (91, p.21-44).

Hold-up Bin

A bin was inserted between the fine screen product-stream and ilmenite separation stage to allow for hold-up time in the event of mechanical problems with either upstream or downstream equipment. Hold-up tanks or bins are useful in continuously operating terrestrial plants to maintain productivity in the event of unexpected problems and to balance feed and product flow rates between different areas of the plant. If a problem occurs in the crushing/grinding circuit of the lunar pilot plant, inventory in the hold-up bin can be worked off to keep downstream equipment operating while the problem is corrected. If a problem occurs in the magnetic separator, the hold-up bin can be filled while making

the necessary repairs. The bin was sized to contain up to 3 days of storage capacity at maximum production rates.

Magnetic Separator

Ilmenite in the material from the hold-up bin is extracted by a magnetic separator. Because ilmenite is slightly magnetic, a high intensity magnetic field is required to affect efficient separation. An induced magnetic roll (IMR) machine was selected for the pilot plant process. In this machine, a series of revolving laminated rolls in the IMR are energized by induction from a stationary electromagnet. The poles of the electromagnet are in close proximity to the rolls creating an intense magnetic field where the magnetic flux converges on the roll surface. A carefully controlled thin stream of material is fed to the top of the first roll. As the roll revolves, the material passes in the narrow gap between the pole of the magnet and the roll. Non-magnetic particles follow a trajectory unaffected by the field as they are discharged from the roll while magnetic ilmenite particles are attracted to the roll and are discharged into a separate chute. Non-magnetic particles from the first roll are passed by gravity to successive lower rolls, each at a greater magnetic field strength, where additional ilmenite is removed. Of the ilmenite released as essentially pure mineral particles by the grinding steps, it is expected that these successive magnetic separation stages will recover approximately 98% of the ilmenite. However, the purity of this stream was assumed to be only 90 percent by weight ilmenite.

High-intensity permanent magnetic roll separators (permrolls) using rare-earth materials in the rolls are presently available (96, 97). These machines can produce similar magnetic field intensities as IMR equipment but at significant savings in equipment mass and power. A permroll installation would typically require only 10 percent of the electric energy, 10-20 percent of the mass, and 60 percent of the volume compared to an IMR machine for identical applications (98, p.145). However, an IMR provides flexibility unavailable from a permroll, which would be especially important for a lunar pilot plant application. For instance, to produce the most efficient separation, the magnetic field strength of an IMR can be adjusted by changing the magnet/roll gap spacing, roll speed, and flow rate. An adjustable splitter can also be used to regulate the amount/purity of ilmenite removed. However, only roll speed and splitters can be adjusted to affect separation efficiency in a permroll installation. It is possible, though, that the in-situ optimization experience provided by a pilot plant operation could provide the data necessary to design permrolls with confidence for the full-scale production plant.

Electrostatic separation based on the difference in electrical conductivity between ilmenite and other gangue minerals is another alternative for beneficiation of the ilmenite particles (46, 74, 99). Although mass and power requirements for an electrostatic unit itself may be less than an equivalent IMR application (46), the feed to the electrostatic separator has to be heated to 150-200°C and precharged for best results (99, 100). This requires large amounts of electrical energy or mass penalties for solar-thermal concentrators (70). Besides a thermal energy penalty, preheating lunar dust fines would probably require a heat transfer agent (gas or liquid) for efficient heating, thus introducing additional process complications. Magnetic separation methods were preferred for these reasons.

Reactor Feed Hoppers

A continuous-flow conveyor transfers the ilmenite recovered from the magnetic separator to the reactor feed hoppers at the top of the support structure. A series of two hoppers is used to minimize gas losses from charging the reactor. Feedstock is fed into the

low-pressure feed hopper while a screw conveyor feeds the reactor from the high-pressure feed hopper. A valve (star valve, slide gate, or other solids handling valve capable of holding pressure and multiple operations) between the hoppers is kept closed. When inventory in the high pressure feed hopper is at an appropriate low point, feed to the reactor is momentarily shut-off, a valve between high-pressure feed hopper and reactor closes, and pressure in the high-pressure feed hopper is bled-off (either to vacuum or into a gas collection system). Then the valve between feed hoppers is opened to rapidly reinventory the high-pressure feed hopper. After the valve between hoppers is closed, feed from the high-pressure hopper is re-established into the reactor. Maximum capacity of each hopper is three days of feedstock. Therefore, cycling of the feed hoppers would take place every 2-2.5 days, with small gas losses, even if gas is bled to vacuum.

Alternatives are possible to this feed system. Both hoppers could have direct access to the reactor, one being on-line while the other is being filled. However, both would be sized to contain the high pressures associated with reactor operation, requiring thicker skins and more mass than the stacked system proposed. Modified designs of systems used to charge modern (pressurized) iron-blast furnaces, such as a dual lock-hopper system with rotating distributor chute (called a Paul-Wurth bell-less top) or standard multiple-bell systems (101, p.27; 15, p.397) could be used. In any case, gas losses while feeding the reactor should not be a problem.

Fluidized Bed Reactor and Reactor Auxiliaries

Ilmenite reduction takes place in a three-stage fluidized bed reactor (see Figure 4-1b) operating for this conceptual design at a maximum of 1,000°C and 10 atm. Assumptions in sizing the reactor were solids residence time of 4 hrs, a 5.5 m inside reactor length (1.8 m of which is actually occupied by solids in all three beds), per-pass hydrogen conversion of 2/3 of the equilibrium value (14), and 90% conversion of the ilmenite to iron/rutile. Given these assumptions, a 0.31 m (1.02') interior diameter of the reactor was determined. Superficial gas velocity in the fluid beds of this reactor can be expected to be 1'/sec (14). Reactor input material sizes under these conditions should be greater than 0.03 mm to avoid excessive carryover of fines and less than 0.9 mm to allow fluidization to occur (calculations in Appendix A). The steel shell of the reactor is protected from the high temperatures by a refractory lining. For sizing purposes and thermal balances, the central 0.31 m core of the reactor was surrounded by 7.5 cm of high-density (S.G. 2.24) superduty firebrick that has the toughness to withstand the erosional nature of the high temperature gas/particles in the fluidized beds. Surrounding this is 23 cm of low-density (S.G. 0.14), low thermal conductivity insulation used for the Shuttle thermal protection tiles. The Shuttle tile ceramics can withstand repeated thermal cycling without cracking, but are susceptible to impact damage. Thermal cycling should be avoided in the reactor and other high temperature systems to protect high-density insulation, reduce the chances of process leaks, and extend lifetimes of metallic equipment. For this reason, the reactor and associated high temperature equipment will not be shutdown cold, but will be left on hot standby (no production) during the 2-week lunar night.

Handways are shown on the exterior of the reactor in Figure 6-3. They are 12 cm diameter penetrations into the interior with bolted covers that allow access for visual inspections of the fluidized bed internals and refractory lining (after the reactor is shutdown). If repairs or configuration changes to internals are necessary, the reactor heads must be pulled (by unbolting and using a winch/cable system) to allow sufficient maintenance access.

Calculated reactor radiative heat losses (7.5 kw), sensible heat requirements (10.8 kw), and endothermic reaction heat requirements (4.7 kw) are provide by heating the gas stream entering the middle bed of the reactor in an electric resistance heater.

Dust in the exit gas streams is removed in cyclone separators containing no rotating parts. The cyclones will remove 98% of the 10 micron particles and 36% of the 1 micron particles. Several cyclones in series may be required to reduce total particulates in the gas stream to acceptable levels for downstream equipment.

A screw conveyor transports reactor residual solids from the bottom bed of the reactor to a discharge hopper. This unit may require a double lock hopper system such as the feed system. A single, long unit was sized for the pilot plant to allow a maximum of 2 days residence time for the solids to settle and separate trapped gases. A gas recycle loop recovers expelled gases. A maximum hydrogen loss rate of 2 kg/month was calculated by assuming that interstitial gas is trapped in pores of the solids bed (60% porosity assumed).

A solid-state electrolysis cell operating at 1,000°C will separate the water product of reaction into oxygen and hydrogen. The hot hydrogen is recycled to the reactor's top stage to pre-heat the solids feed which reduces reactor thermal requirements.

Oxygen Liquefaction and Storage

Oxygen from the electrolysis cell is actively cooled by jacketed pipe to 25°C prior to entering the oxygen liquefier. A Stirling cycle refrigerator operating at a 38% Carnot efficiency, or 23% overall efficiency over theoretical minimum cooling load of 0.106 kw-hr/kg O_2 (101), was used as the basis for mass/power estimates. The liquefied oxygen is stored in two buried tanks (to minimize boiloff) with a total capacity of 4 mt oxygen (2 months production at full rates). Boiloff from the tanks is recycled through the liquefier. Maximum boiloff rates based on unburied tanks, protected only by 3" of multi-layer insulation, were assumed for calculating worst case boiloff for liquefier sizing purposes.

An oxygen loading station is shown in Figure 6-4 consisting of a pump, piping and valves to allow withdrawal of oxygen from either tank, and a flexible hose (metallic wire or fabric overwrap with suitable liner for cryogenic service, and specialized end fittings). A loading station might be necessary as a demonstration. Pilot plant oxygen would also be useful for suppling oxygen reductant requirements for surface vehicle fuel cells.

Tailings Disposal

Of the 88.23 mt basalt/mt oxygen that is delivered by hauler into the feed bin of the process plant (see Table 6-1), 87.23 mt/mt oxygen will be discarded. Tailings from the fine vibratory screen (undersize), magnetic separator (non-magnetics), and reactor residuals (ilmenite, rutile, and iron) are collected on a V-belt conveyor and transported to the discharge bin shown in Figure 6-4. A hauler collects the tails and deposits them in the tailings discharge area. Lighter tailings piles would result from the vibratory screen and magnetic separator tails because they would turn light or white after being crushed and ground. The tails from the mine pit itself (and from the reactor) would be darker reflecting basalt colors (and the dark iron/unreacted ilmenite in the reactor tails).

Makeup Hydrogen System

A buried tank contains 6 months supply of liquid hydrogen (12 kg) to makeup process losses. A vaporizer is included that supplements boiloff from the tank to provide hydrogen vapor for the system.

Photovoltaic Power System

A sun-tracking photovoltaic solar power system provides process power requirements during the 2-week lunar day and regenerates the reactants for fuel cells to be used during the lunar night. Because the Lacus Veris base site is near the equator (87.5°W, 13°S), the solar arrays are oriented on a north-south line to maximize sun viewing, and minimize self-shadowing.

Regenerative Fuel Cell Power System

3,200 kw-hr (2 weeks at 10 kw) of electrical energy is provided by oxygen/hydrogen fuel cells for keeping the process in hot standby during the lunar night. Basically, the recycle gas compressor is left on continuously, and heat losses from the reactor and other high temperature systems are made up by the electric heater. 1,103 kg of gaseous oxygen and hydrogen reactants are required and stored at 100 atm pressure in the 4 large tanks shown in Figure 6-4 on a Shuttle payload pallet. Graphite/epoxy overwrapped tanks are used to reduce mass.

Thermal Control System

A central thermal control system (TCS) and radiator were sized to reject waste heat from various process units (principally crushing/grinding, beneficiation, and oxygen liquefaction equipment). The TCS uses heat exchangers and an appropriate cooling medium (i.e., ammonia, water, etc.) to transfer waste heat from the users to the radiator. Dedicated thermal control loops for the mining vehicles, photovoltaic arrays, and regenerative fuel cells are assumed. The radiator is positioned in an East-West orientation, with a fixed sun-screen to keep the radiator permanently shaded from the slightly northernly track of the sun (for Lacus Veris). Sun-screen surfaces would be coated with special (low α/ϵ) thermal coatings.

Communications

Data return requirements for the pilot plant were not studied in detail. The high and low gain antennas shown in Figure 6-4 are to indicate: 1) a communications system is required to allow transmission of several simultaneous video channels and many data channels, 2) that communications with both Earth and the lunar base are required, and 3) process monitoring and supervisory control initially resides in a control room on Earth.

Video channels: 2-3 each for the front-end loader, hauler, and each telerobotic servicer. Additional cameras pointed at particular solids handling areas would also be useful, such at feed and discharge points (where solids can bridge and hangup), through access ports on the vibrating screens (to visually assess screening efficiency, aperture blinding, etc.), and at the flow from each crusher/grinder. General panoramic cameras would be useful to spot process or radiator fluid/gas leaks.

Data channels: Each plant unit should be heavily instrumented to detect faults or problems. All data would not necessarily be transmitted to Earth. On-board computer systems could monitor conditions of the various data streams, and report only anomalous situations to Earth. In addition, sampling rates could vary since certain process conditions (i.e., tank levels) vary slowly. Typical data measurements might include: temperature, pressure, flow rate, fluid or solids level, valve loadings (indicator of valve position), strain gauges, lubricant level, gas/liquid composition from automatic samplers/gas chromatographs, motor amps, revolution speed, voltage, local controller output signals, etc.

Telerobotic Servicing

The pilot plant is envisioned to operate without continuous on-site human presence. This is not a problem for the beneficiation and processing part of the pilot plant, since it is standard operating procedure for most modern terrestrial chemical plants which often run automatically under computer control with an operator required only to monitor the process and respond when the control authority of the computer is exceeded or something breaks. The mining equipment will require advancement of state-of-the-art to allow teleoperated control from Earth. Mining, process, and power equipment will require periodic maintenance and repair. This requirement will occur more frequently than the anticipated periods the base will be manned during the Phase II man-tended period.

Thus, telerobotic servicers for the lunar surface were proposed (84) to provide remote maintenance and servicing capability. They would be teleoperated from Earth, although they would contain enough on-board logic and memory to perform many tasks autonomously with only supervisory control required of the human operator. Similar concepts for telerobotic servicers are currently proposed for Space Station as well. For the lunar base, they could be applied in many more areas than resource utilization (84). The lunar surface servicers are envisioned to be in two parts. The servicer part contains the computational capability, stereo vision, and at least a pair of dexterous manipulators, and is assumed to be generic. The second part is the mobility base which can be either general or specialized, and can be exchanged as a job requires. In Figure 6-4, a telerobotic servicer on a general surface mobility platform is shown inspecting a repair made to stop a process leak near the stem packing of a valve (#24). Another servicer is attached to a remote manipulator arm and is shown viewing the solids flow through a view port in a section of the fines screen. The remote manipulator arm is attached to a mobile translator that travels on rails around the periphery of the support structure of the process plant. A spare manipulator arm/mobile translator is also on the rails in case a particularly delicate job requires both telerobotic servicers, or if one fails and needs to be repaired.

Success of remote maintenance via telerobotic servicers will require design of the LOX plant equipment and interfaces to match the capabilities of the telerobot support system. This approach has been successfully demonstrated in the terrestrial undersea oil production industry. A large (200' x 150' x 40') oil production platform, resting on the sea bed at 1,500', is operated and maintained almost exclusively by telerobots (115). The key to the success of this operation was the modification of subsea equipment to allow telerobotic operation. Specific equipment design areas addressed by the oil industry (115) in this teleoperated undersea activity that have equal importance for teleoperated lunar processing include providing: physical accessibility to equipment, visual accessiblity, modularity, standardized manipulator interfaces, compatibility between telerobotics and manned EVA, location referencing for navigation and worksite identification, built-in test equipment, and work fixtures. Space station is also advancing aerospace applications of telerobotics,

such as for telescience (116). Thus, although requiring much specific development work, current technology trends support the concept of teleoperated lunar processing facilities.

Lunar telerobotic servicers will require access to tools and equipment spares. Spares for the plant are stored in an unpressurized storage shed shown in Figure 6-4. Placing critical electronic components in replaceable unit elements or boxes is preferred for quick changeout. Certain low reliability components or equipment, particularly rotating equipment such as pumps, compressors, and motors, will require redundant in-place spares. As practiced in terrestrial chemical plants, if a pump fails, the spare pump can be immediately started while the failed pump is removed and repaired. It would be inefficient to provide in-place redundancy for large process vessels such as the reactor. Further study is required to quantify the optimum split between on-site spares and in-place redundant elements.

Lunar Gravity Effects on Equipment Design

The lunar thermal, vacuum, and dust environment will have significant effects on the design of reliable pilot plant equipment and components, especially rotating equipment, seals, and lubricants. In addition to these factors, the 1/6-gravity field will offer some advantages in terms of mass savings for materials transport equipment and support structures, but will reduce the effectiveness of many chemical processes that rely on density differences to perform the operation. The areas of the plant believed to be relatively insensitive to 1/6-g are:

- Front-end loader. The mass of a front-end loader is independent of the gravity field (88). This is because the vehicle mass acts as a counter-balance to prevent the vehicle from tipping over when the bucket is loaded and extended. However, it may be possible to load lunar soil or rocks on the vehicle to stabilize it, if other factors (vehicle geometry, manueuverability) allow it.

- Rock crushers (some reduction in capacity is possible because the rocks will fall through the machine at a lower rate).

- Water electrolysis.

- Blowers, compressors.

- LOX Liquefier.

- LOX Storage.

Plant areas that are affected by the gravity difference are:

- Haulers. Lower structural mass for the hauler is possible in a 1/6-g field because most of the mass of the hauler is devoted to structural support of the payload (88). An equivalent mass payload on the Moon will impose 1/6th as much structural load as on Earth.

- Screens. Lower capacity will result because particles will fall at a slower rate through the screen apertures.

- Conveyors. Lower conveyor mass and energy will be required because the payload weight decreases (46).

- Ball mill grinders. The drums will be limited to lower rotational speeds in a 1/6-g field before the balls start to ride up the sides of the mill from centrifugal acceleration. Ball mill capacity will decrease.

- Magnetic separators. Separation performance will improve because the low gravity will cause the arc of non-magnetic particles to deviate more than in Earth gravity. Separations between ilmenite and non-magnetic particles will be cleaner. The same is true for electrostatic separators, although charging of the feed will probably be more difficult in vacuum (air ionization improves charging in terrestrial applications) (99).

- Liquid pumps. Energy requirements to pump liquid upward will decrease.

- Fluidized bed reactors. Lunar performance may decrease because lower gas velocities or larger particle sizes are required since the bed fluidizes easier in lunar gravity (14). Lower gas velocities reduce reaction and production rates. Larger particles may decrease reaction kinetics (because of lower surface to volume ratios) and thus decrease production rates. Bed expansion is greater in lunar gravity (14) requiring longer fluidized bed sections (taller reactors, more mass) for a given production rate. Lower lunar gravity will also require taller reactors for sufficient freeboard (freeboard is the space above a fluidized bed where gas/solids disengage or separate; freeboard that is too short leads to excessive fines carryover).

- Structural support for plant, individual equipment, and solar arrays will be less than on Earth.

Generally, the quantitative effect of 1/6-g on equipment design is not completely understood. However, a correction factor has been used to decrease performance, where appropriate, to compensate for the effect (Appendix A contains details of correction factors).

6.3 Trade Studies

A computer model of the plant was developed using scaling equations documented in Appendix A, thermodynamic relationships, and mass and energy balances to estimate the mass, power, and volume of major plant equipment. The model was applied to assess several trades and sensitivities of interest:

- The effect of alternative feedstock materials: high-titanium mare soil vs. basalt.

- The effect of power source: solar or nuclear-electric.

- Potential mass/power savings in the pilot plant to vent instead of cool, liquefy, and store product oxygen.

- Trades associated with growth of plant capacity by landing self-contained, modular production units, instead of constructing a single large plant.

- The effect of processing unconcentrated feedstock in the reactor instead of concentrating ilmenite in a magnetic or electrostatic separator prior to the reaction step.

- Sensitivity of plant mass and power to LOX capacity.
- Sensitivity of a basalt fed plant to ilmenite grain size.
- Sensitivity of a soil fed plant to ilmenite abundance.

The results of the trade and sensitivity studies are given in this and the following section. Many other trades are possible, the results of which could indicate significant reductions in plant mass. Some additional studies are described in Section 6.5.

A summary is given in Table 6-5 of the calculated mass and power for mining, beneficiation, process, and power areas of the plant as determined for the different cases assessed in the trade studies. The equipment contained in each area is defined in Section 6.2.1. A 30% contingency factor was applied to plant mass and power estimates to account for factors such as automation, general structure, in-place redundancy, on-site spares, and other considerations not included.

Table 6-5. Summary of Trade Study Calculations

LOX (mt/month):	2	2	2	2	2	2	2	2
Feed:	Soil	Soil	Soil	Soil	Basalt	Basalt	Basalt	Basalt
Power:	PV/RFC	Nuclear	PV/RFC	PV/RFC	PV/RFC	Nuclear	PV/RFC	PV/RFC
Duty Cycle:	45%	90%	90%	45%	45%	90%	90%	45%
O_2 Liquefaction?:	Y	Y	Y	N	Y	Y	Y	N
Mass (mt)								
Mining	2.7	2.7	2.7	2.7	3.4	3.4	3.4	3.4
Beneficiation	3.4	3.0	3.0	3.4	3.9	2.6	2.6	3.9
Process	5.2	3.7	3.7	4.4	4.8	3.5	3.5	4.0
PV	6.4		7.6	6.2	5.7		7.4	5.5
RFC	3.3		24.7	3.3	3.3		24.7	3.3
Nuclear Power		5.2				5.1		
Margin	3.4	2.8	2.8	3.1	3.6	2.9	2.9	3.4
Total	24.4	17.3	44.4	23.1	24.7	17.5	44.4	23.4
Power (kwe)								
Mining	3	3	3	3	4	4	4	4
Beneficiation	49	24	24	49	34	19	19	34
Process	63	35	35	58	63	35	35	58
RFC	15		114	15	15		114	15
Margin	34	19	19	33	30	17	17	29
Total	164	81	194	158	146	75	189	140

LOX (mt/yr):	144	144	144	1000	144	144	1000
Modules:	6x24 mt/yr	(1)	(1)	(1)	6x24 mt/yr	(1)	(1)
Feed:	Soil	Soil	Soil	Soil	Basalt	Basalt	Basalt
Power:	Nuclear	Nuclear	Nuclear	Nuclear	Nuclear	Nuclear	Nuclear
Duty Cycle:	90%	90%	90%	90%	90%	90%	90%
Ilmenite Sep.?:	Y	Y	N	Y	Y	Y	Y
Mass (mt)							
Mining	3.7	3.7	3.7	14.3	3.4	3.4	17.6
Beneficiation	17.7	15.0	11.8	93.6	15.8	11.6	73.4
Process	21.9	12.4	18.1	65.1	21.0	10.6	51.8
Power	7.4	6.9	7.6	18.9	7.8	6.5	16.0
Margin	13.0	9.3	10.1	51.9	12.1	7.7	42.8
Total	63.7	47.2	51.1	243.8	60.0	39.7	201.7
Power (kwe)							
Mining	19	19	19	137	21	21	144
Beneficiation	146	152	143	1002	112	89	526
Process	208	177	290	1160	208	177	1160
Margin	112	104	136	690	102	86	549
Total	485	452	587	2988	443	372	2380

6.3.1 Soil vs. Basalt Feedstock

The basis of this assessment was:

- 25 vol.% ilmenite in basalt, 0.5 mm equant ilmenite grains. Mining rate is 327 mt/mt oxygen produced (see Table 6-1).
- 5 vol.% (7.5 wt.%) ilmenite in soil, 11% of soil greater than maximum allowable and 45% less than minimum allowable reactor input sizes (0.9 mm maximum and 0.03 mm minimum calculated, but selected 0.5 mm and 0.045 mm for margin and because data available from soil 10084).

Two production cases were compared: basalt and soil fed, pilot and production LOX plants. Pilot plant conditions were:

- 2 mt/month LOX pilot plant.
- Plant beneficiation and processing areas operating at 45% duty cycle (90% utility during lunar day and on hot standby, but with feed shutdown and no oxygen production, during lunar night). Mining equipment operating at 35% duty cycle (70% during lunar day and shutdown during lunar night).
- Photovoltaic solar array to power process and regenerate fuel cell reactants during 2-week lunar day, oxygen/hydrogen fuel cell power to makeup process heat losses during night.

Pilot plant results are:

	Basalt	Soil	Difference (Delta/Soil)
Total Plant & Power Mass (mt)	24.7	24.4	+ 1.3%
Power (kw)	146	164	-10.9%

Mass/power breakdowns are shown in Figures 6-7 and 6-8. Pilot plant masses were nearly identical. The reduction in solids handling and loads on screening and magnetic separation provided for a basalt fed plant due to the richer-ilmenite content of the feedstock were offset by the relatively large sizes of crushing/grinding equipment at low production rates. Benefits for using basalt feedstock are more apparent at high production rates where grinding/crushing equipment become more efficient (on a capacity to equipment mass/power basis). The LOX production plant conditions were:

- 1,000 mt/year LOX production.
- Nuclear-electric power. Plant duty cycle 90%, mining 35%.

Results, as given in Figures 6-9 and 6-10, are:

	Basalt	Soil	Difference (Delta/Soil)
Total Plant & Power Mass (mt)	186	225	-17.5%
Power (kw)	2,379	2,988	-20.4%

Because mass and power savings are significant for a large production plant, basalt was selected as the feedstock for the pilot plant. However, other considerations may reduce this advantage:

- The basalt crushing/grinding circuit will add complexity to the pilot plant. Maintenance requirements will increase, reliability will decrease. It will be more difficult to remotely operate the plant. The crushing/grinding equipment are subject to wear that limits the lifetime of certain high wear surfaces. Although wear in the ball mill may be somewhat less in the 1/6-g lunar environment than on Earth, thicker liners or tougher liner materials may be required in the interior of the grinder to extend lifetimes (ball mill liners typically last 2 yrs or less).

- Alternatives to the vibratory screens used in the soil-fed plant to separate fines prior to the reactor could reduce soil plant mass/power as described in Section 6.5.1.

Figure 6-7. Effect of Feedstock (Soil vs. Basalt) on LOX Pilot Plant Mass

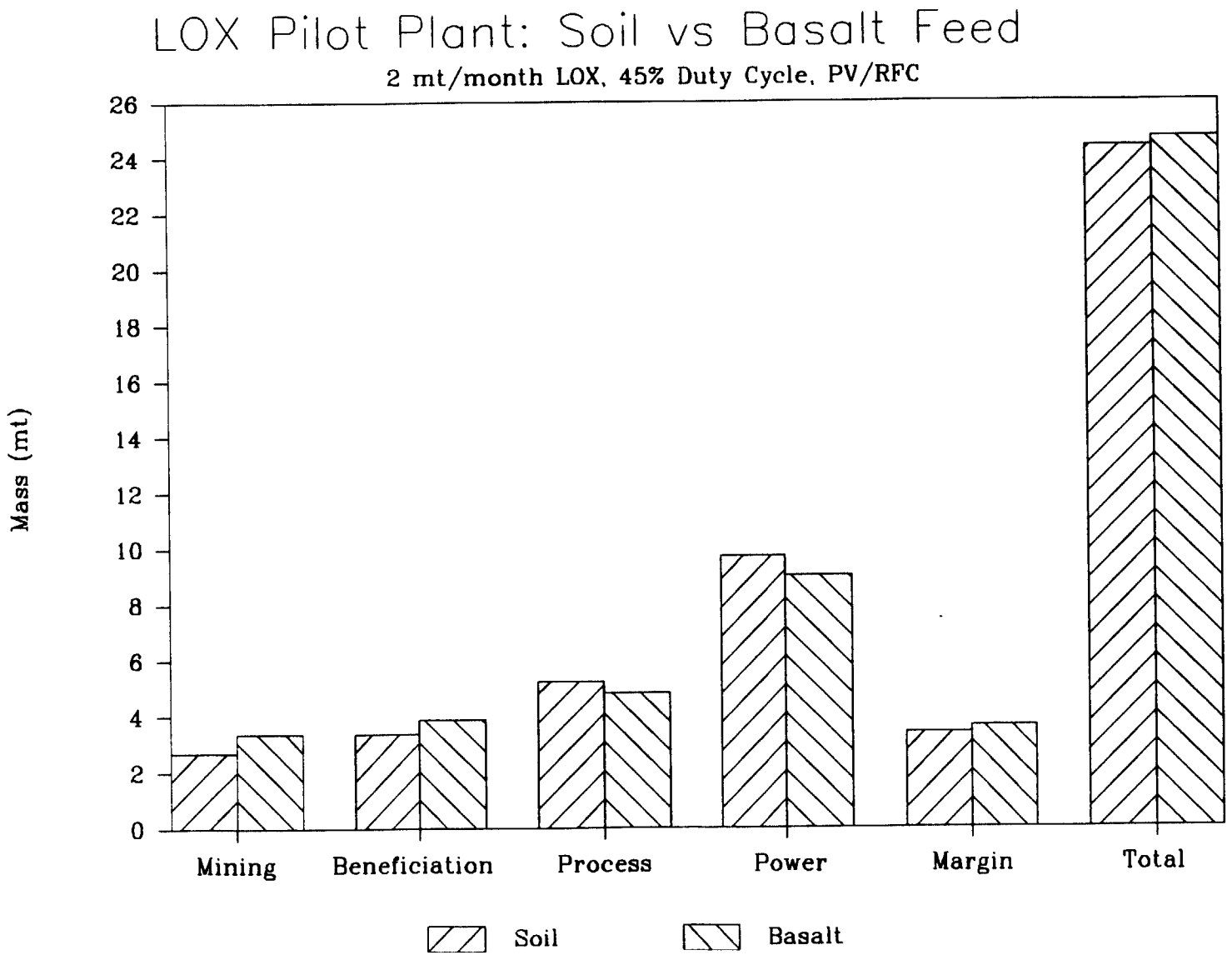

Figure 6-8. Effect of Feedstock (Soil vs. Basalt) on LOX Pilot Plant Power

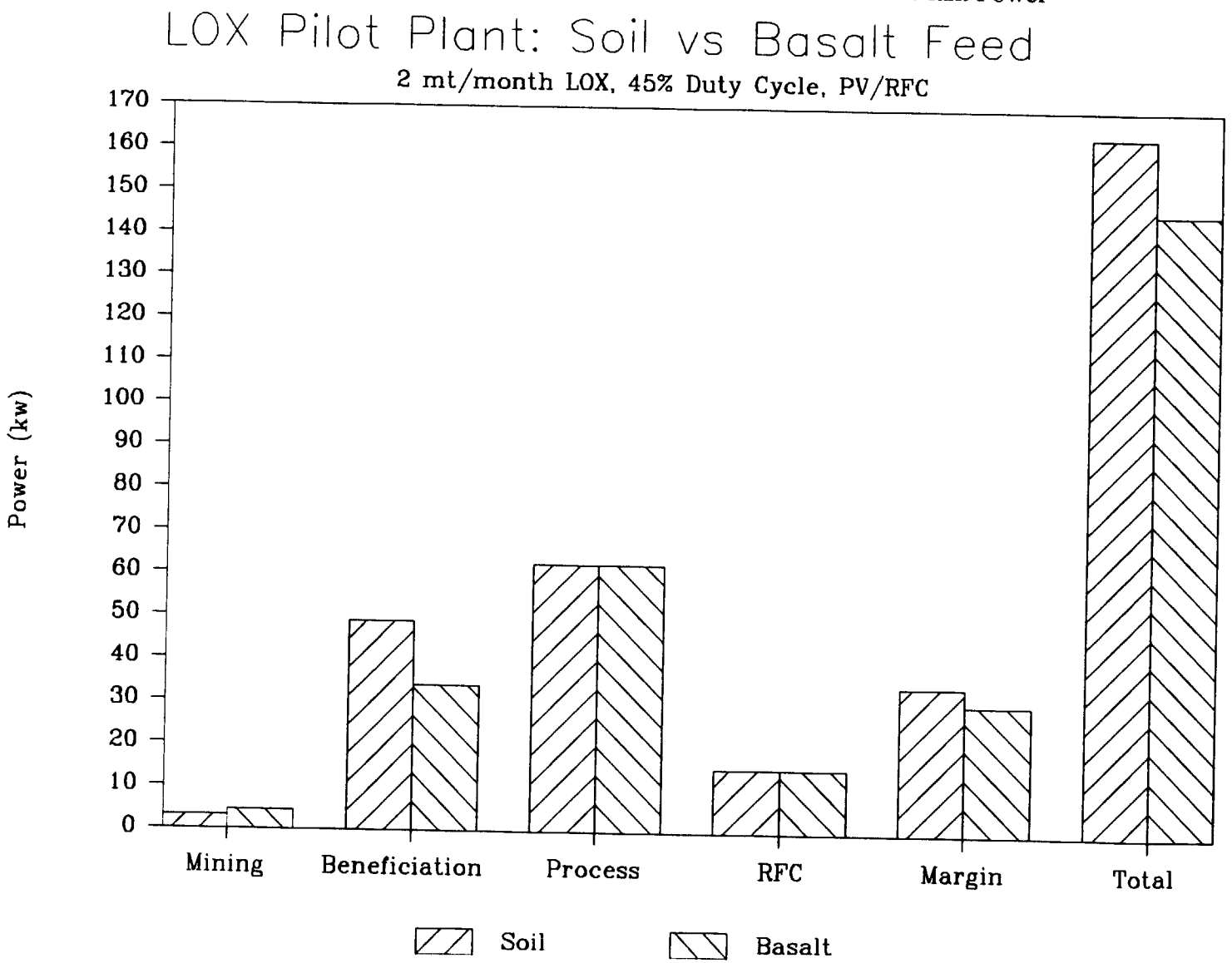

Figure 6-9. Effect of Feedstock (Soil vs. Basalt) on LOX Production Plant Mass

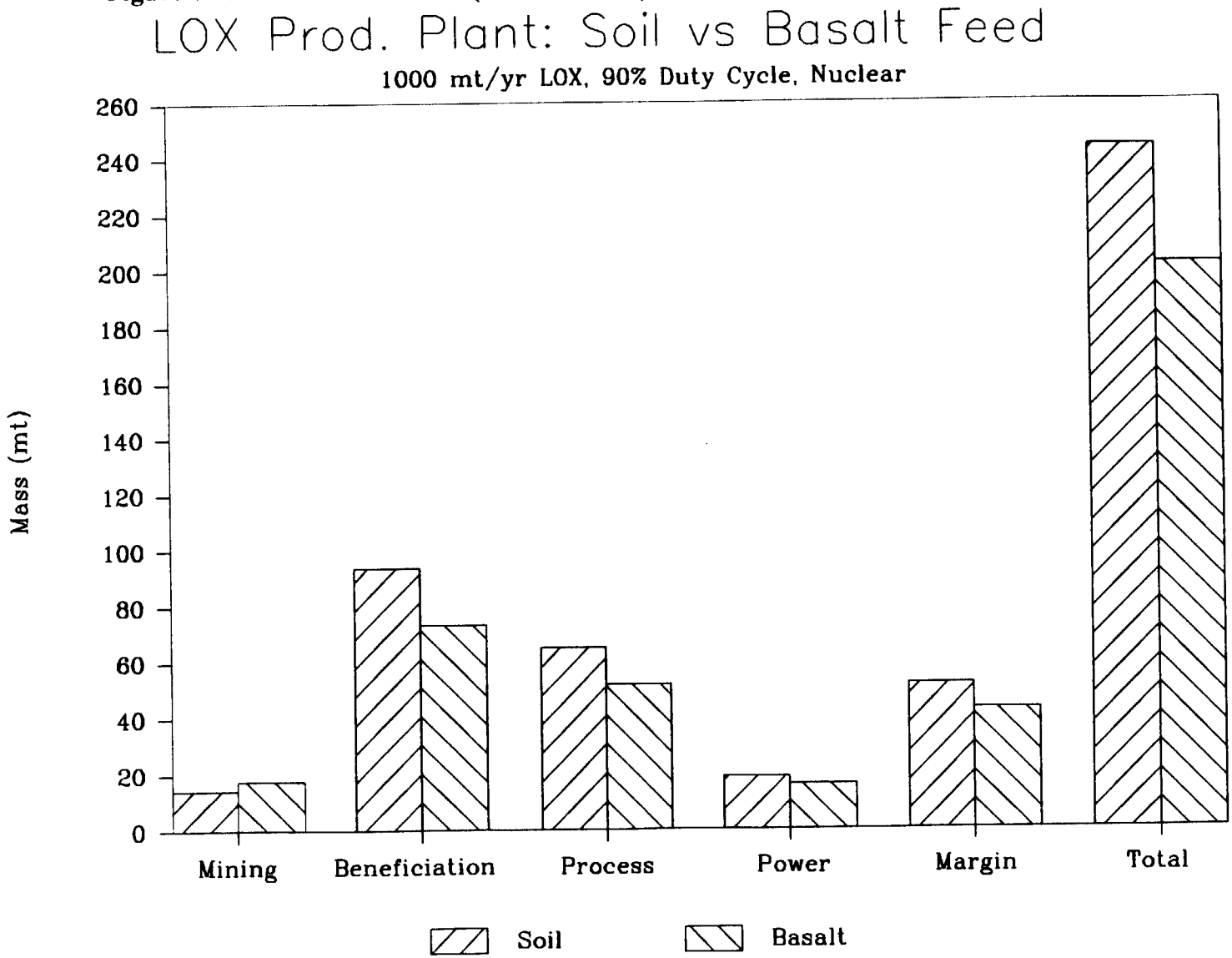

Figure 6-10. Effect of Feedstock (Soil vs. Basalt) on LOX Production Plant Power

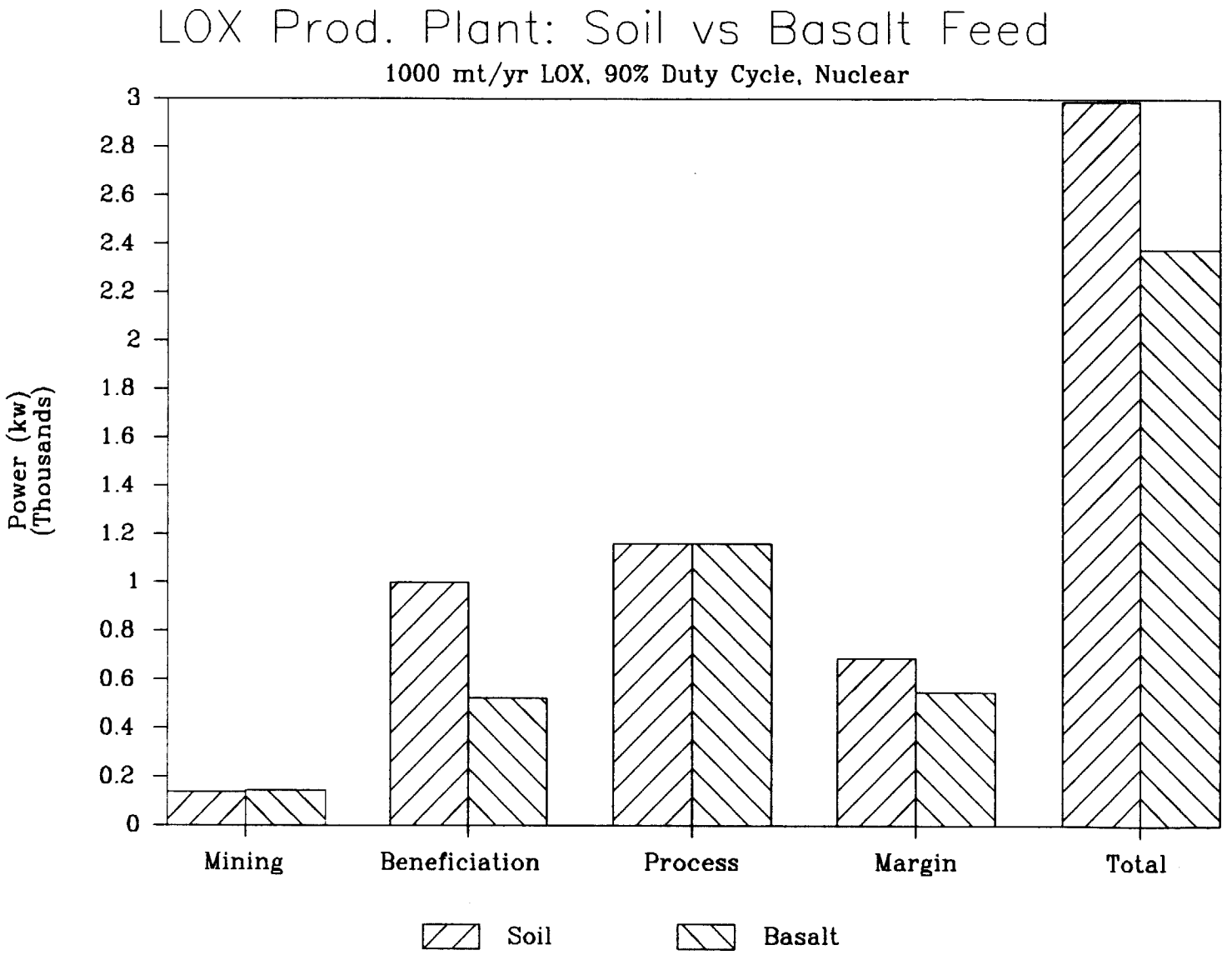

6.3.2 Nuclear vs. Solar Power

The choice of power source has an important impact on plant operational strategy. A nuclear-electric power plant will allow continuous day/night operation of the process plant while solar power plants will require energy storage in regenerative fuel cells or rechargeable batteries to allow night process operation. This trade study was performed for both a basalt and soil fed pilot plant producing 2 mt/month LOX (soil/basalt conditions given in Section 6.3.1) with similar results. Three cases were examined:

1. Power provided by solar photovoltaic (PV) arrays and regenerative fuel cells (RFC) with a 45% plant duty cycle.

2. Power provided by nuclear-electric source with 90% plant duty cycle.

3. Power provided by PV/RFC with 90% plant duty cycle.

Breakdown of the mass and power requirements are given in Figures 6-11 and 6-12 for the basalt-fed pilot plant, and in Figures 6-13 and 6-14 for the soil-fed pilot plant. Nuclear power not only reduces the size of beneficiation and process equipment because the plant operates at a higher duty cycle over case 1, but also the power plant does not have to generate as much power and so is itself less massive. Total plant and power mass reductions of 45-50 percent appear possible using nuclear power at a 90% plant duty cycle instead of a PV/RFC system at 45% duty cycle. Operating a PV/RFC system at 90% duty cycle produces the same mass/power savings in the plant as nuclear power, but because RFC systems are very inefficient compared to nuclear power, total plant and power system mass is much higher than even a PV/RFC operating a plant at 45% duty cycle.

For the three cases, total pilot plant and power system mass (mt) are:

	Basalt Feedstock	Soil Feedstock
Case 1 (PV/RFC, 45% DC)	24.7	24.4
Case 2 (Nuclear, 90% DC)	17.5	17.3
Case 3 (PV/RFC, 90% DC)	44.4	44.4

and power (kw):

	Basalt Feedstock	Soil Feedstock
Case 1 (PV/RFC, 45% DC)	146	164
Case 2 (Nuclear, 90% DC)	75	81
Case 3 (PV/RFC, 90% DC)	189	194

A specific performance ratio of 39 kg/kw for a PV power system was used based on typical values for oriented solar array systems for spacecraft (102-104). Nuclear power scaling included reactor, radiator, power conversion systems, and instrument-rated shielding masses based on a Los Alamos study (105). The same data was used in another LBSS report on spacecraft mass scaling (106). Performance ratios varied from 64-75 kg/kw for the soil and basalt 2 mt/month pilot plants to 13 kg/kw for a 144 mt/yr production plant. Man-rated shielding was not included because it was assumed that the nuclear plant would be located in a local crater or use of other in-situ shielding concepts would be

possible. The mass of electric transmission cable from a remote nuclear power site to the plant was not estimated. The 30% mass contingency factor was assumed to provide sufficient margin. The RFC power system provides thermal energy lost from the process during the 2-week night. The mass of this system is dominated by the mass of oxygen/-hydrogen reactants required, and the mass of reactant storage tanks. Since the fuel cell reactants are regenerated, they are stored as high-pressure gases requiring large, massive tanks. Graphite overwrapped tanks were used to reduce mass estimates. However, 340 kg/kwe was calculated for a system providing pilot plant requirements (averaging 10 kwe for 2 weeks). Additional details and documentation are given in Appendix A.

Figure 6-11. Effect of Power Source on Basalt Fed Pilot Plant Mass

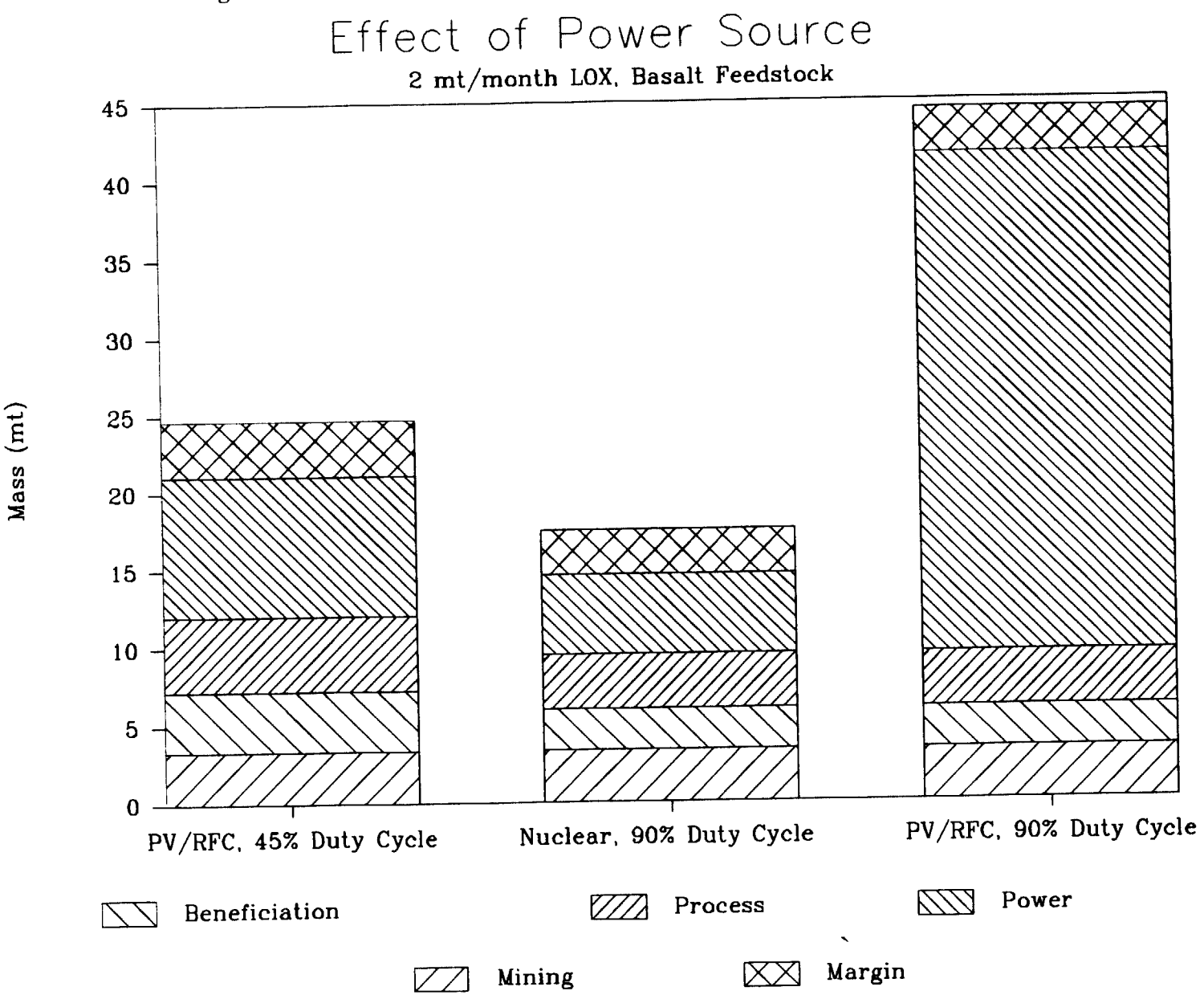

Figure 6-12. Effect of Power Source on Basalt Fed Pilot Plant Power Requirements

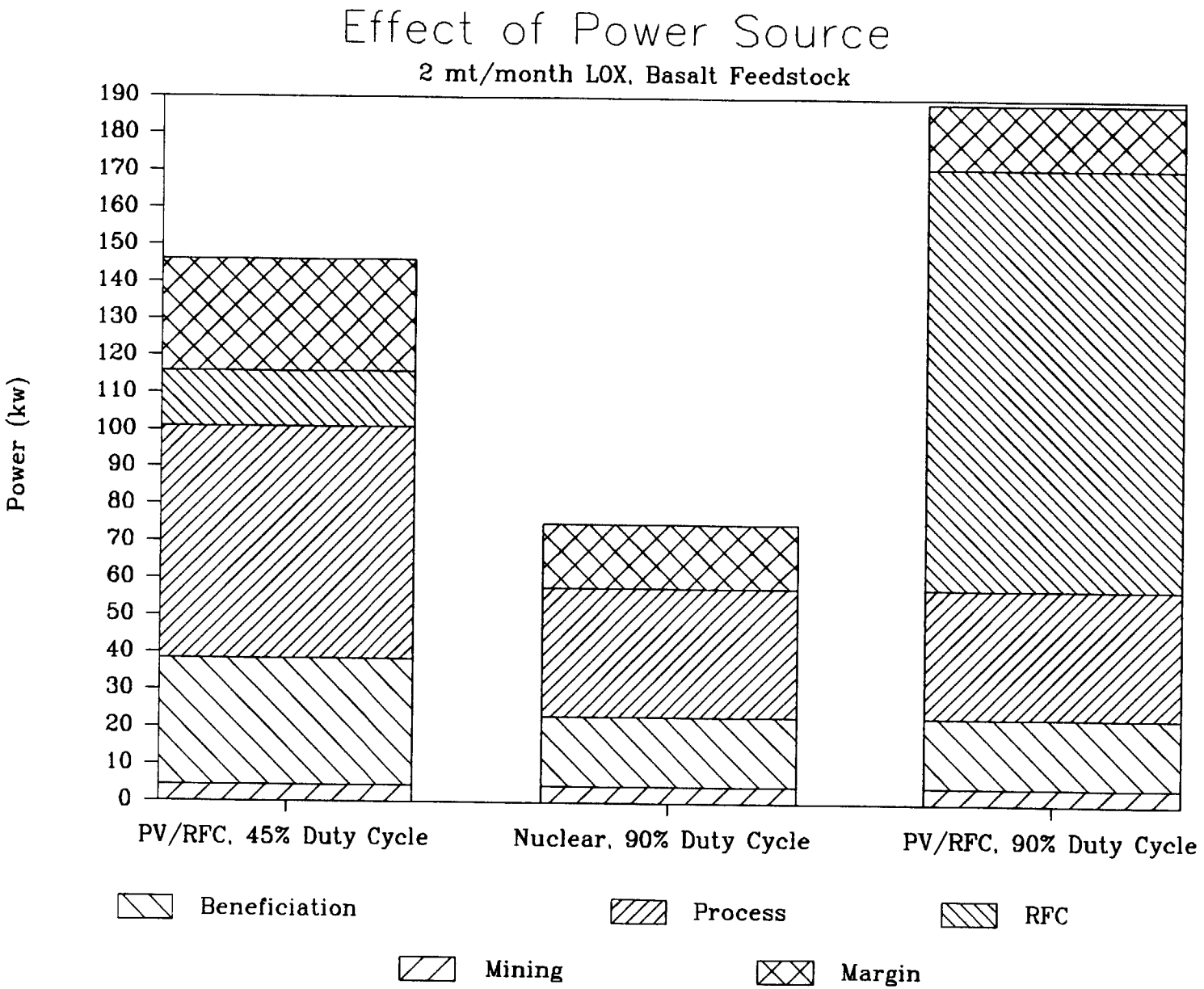

Figure 6-13. Effect of Power Source on Soil Fed Pilot Plant Mass

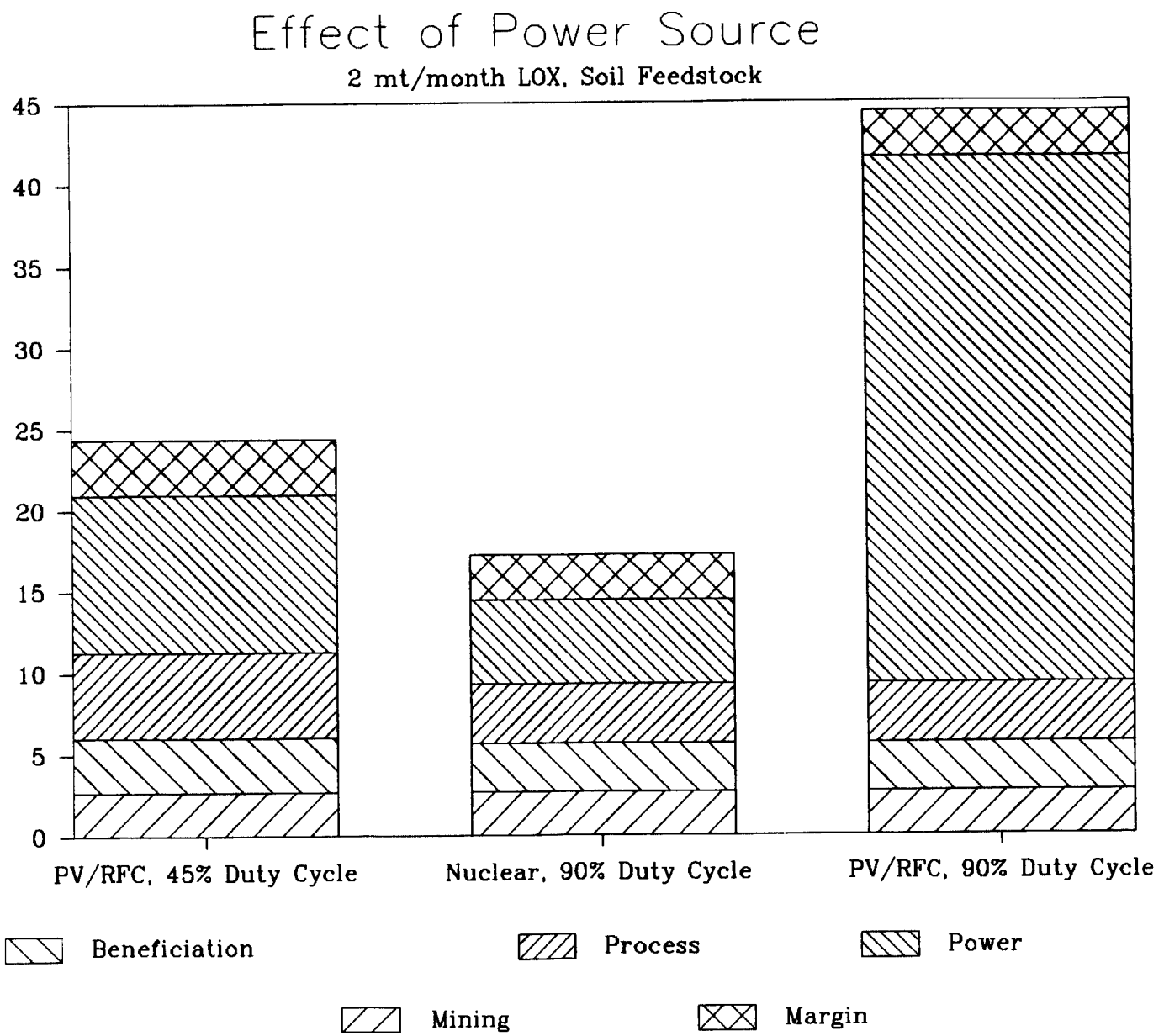

Figure 6-14. Effect of Power Source on Soil Fed Pilot Plant Power Requirements

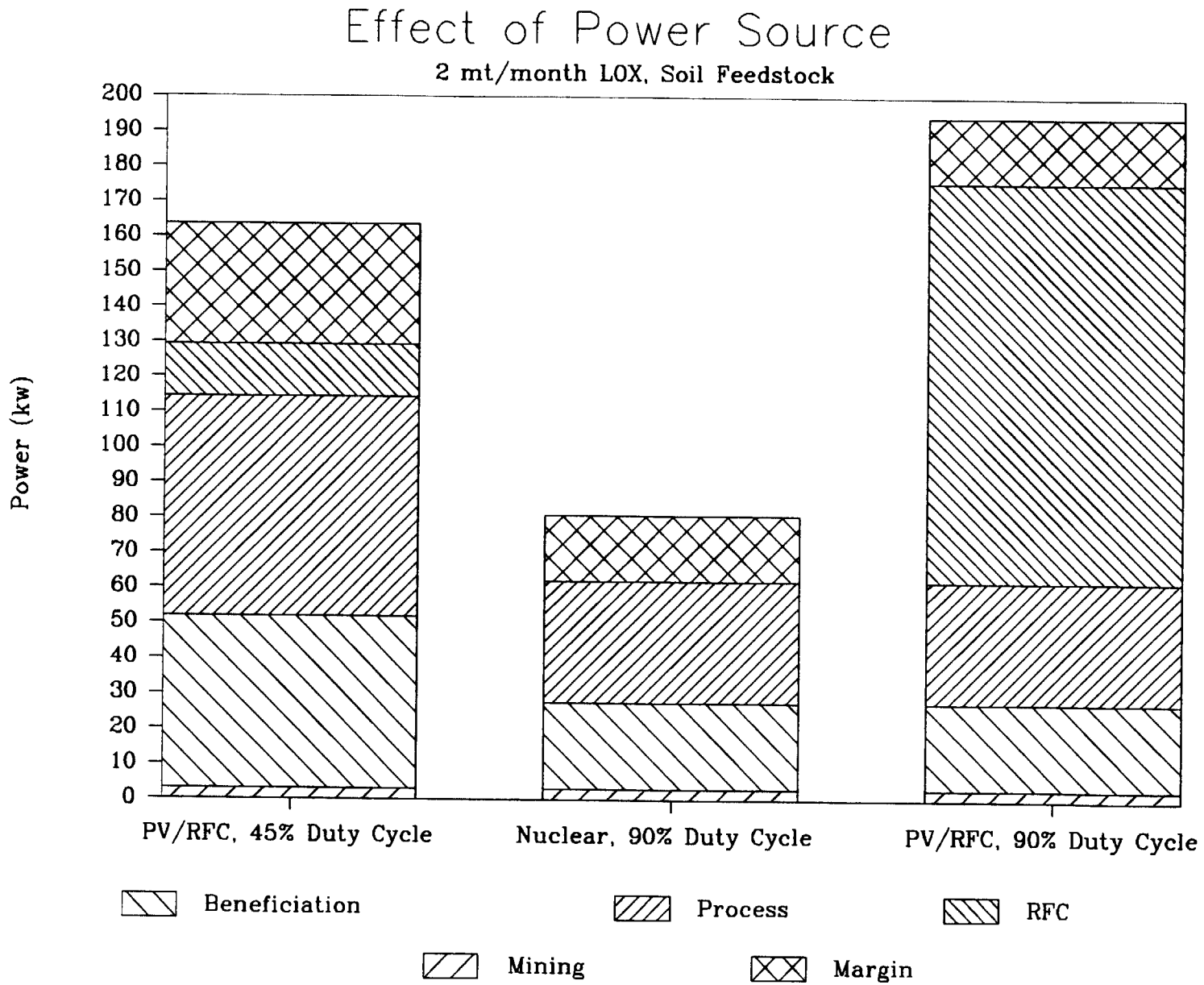

6.3.3 Effect of Eliminating Oxygen Liquefaction and Storage Systems

Mass and energy savings are possible for the pilot plant by eliminating the oxygen refrigerator, LOX storage tanks, LOX loading station, and the thermal load to cool oxygen prior to liquefaction by simply venting the plant's product oxygen stream after the water electrolysis step. This was investigated for both basalt and soil fed pilot plants. Basis for the analysis was: 2 mt/month oxygen production rate, PV/RFC power system, 45% duty cycle, and feedstock properties given in Section 6.3.1. Pilot plant mass and power breakdowns with and without oxygen liquefaction are given in Figures 6-15 and 6-16.

For a basalt fed pilot plant:	w/ Liq.	w/out Liq.	Diff.(delta/with)
Total plant & power mass (mt)	24.7	23.4	- 5.4%
Power (kw)	146	140	- 4.1%

For a soil fed pilot plant:	w/ Liq.	w/out Liq.	Diff.(delta/with)
Total plant & power mass (mt)	24.4	23.1	- 5.4%
Power (kw)	164	158	- 3.6%

Thus, significant mass and power savings are not available by eliminating oxygen liquefaction, and downstream equipment. Other considerations dictated that liquefaction remain in the conceptual design.

Oxygen liquefaction, storage, and loading/refueling in the lunar environment are an important set of process demonstrations. Performance of long-term LOX storage in the unique thermal environment of the Moon should be assessed. Operational capability for withdrawing LOX from the storage tanks and loading it into a user should be demonstrated prior to delivery of full-scale production units.

Liquefaction of the pilot plant product may also be required to certify liquid oxygen quality to propellant grade (and possibly ECLSS) standards. Various impurities will be present in the gas stream to the electrolysis cell, including carbon dioxide (slowly building from accumulated extraction of solar wind carbon) and hydrogen sulfide. CO_2 will dissociate during electrolysis to produce carbon monoxide at the cathode (where hydrogen forms) and oxygen at the anode. The CO will be recycled with hydrogen back to the reactor. The effect, then, of carbon impurities is to increase the quantity of reducing gases, which is a beneficial outcome. H_2S in the electrolysis cell feed gas on the other hand, might likely create sulphur dioxide, SO_2, at the anode, which will need to be removed before oxygen liquefaction since it solidifies at -83°C and could foul heat exchange surfaces as it condenses. The separation equipment to remove SO_2 should not be too complicated, but its operation would require demonstration. The pilot plant conceptual design studies did not include a detailed analysis of possible impurities or purifying techniques, and no equipment baseline was established.

In addition, the effect of venting 146 kg/day of oxygen vapor may require the pilot plant be located far enough away to prevent interfering with scientific experiments and optics. This may require a pilot plant location remote from the base, increasing plant setup and servicing time requirements. The effect of possible oxygen deposition on pilot

plant radiator surfaces (which may remain permanently in shadow from sun-screen) would require investigation if the option to not liquefy is pursued.

Figure 6-15. Effect of Eliminating Oxygen Liquefaction on Pilot Plant Mass

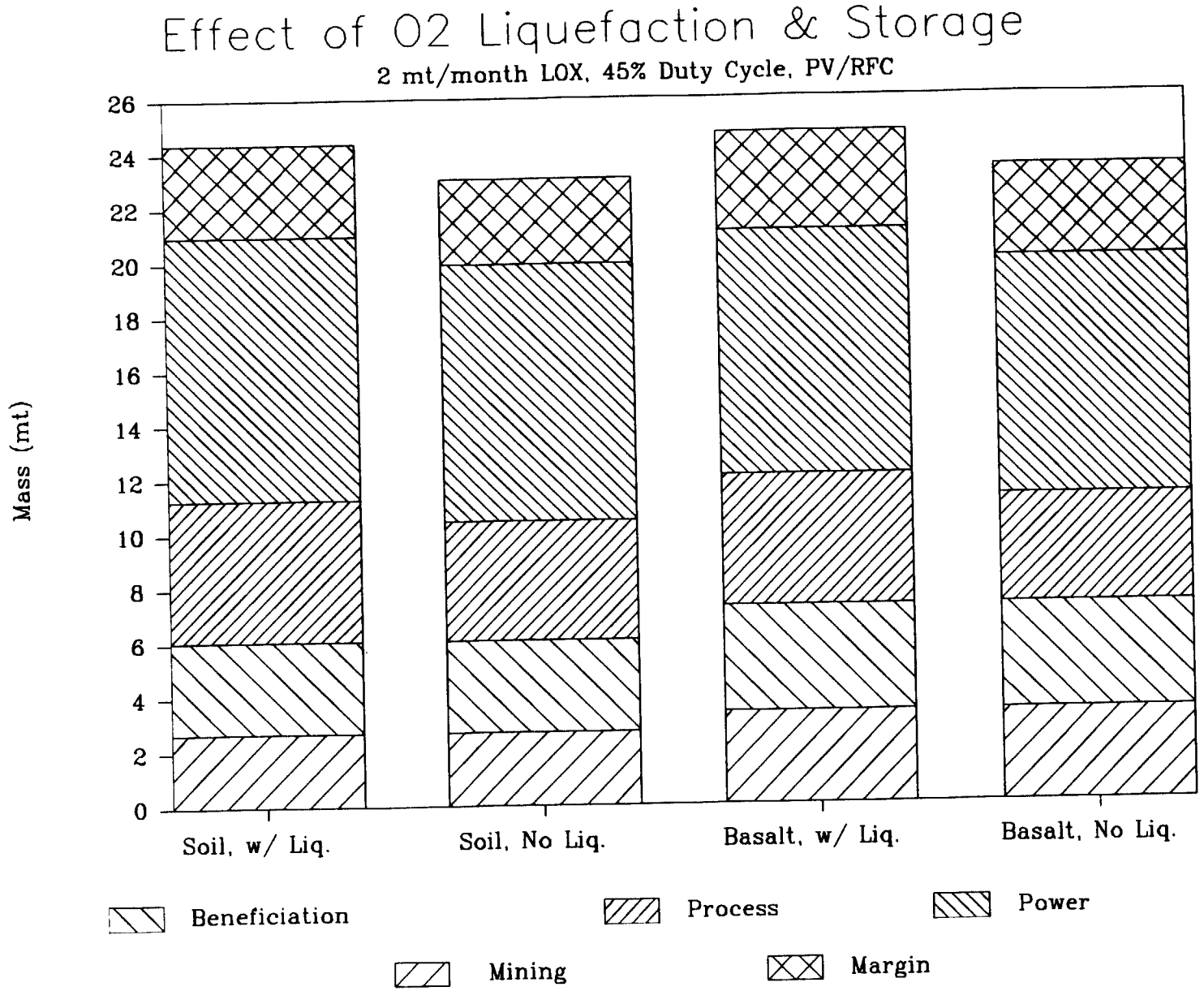

Figure 6-16. Effect of Eliminating Oxygen Liquefaction on Pilot Plant Power

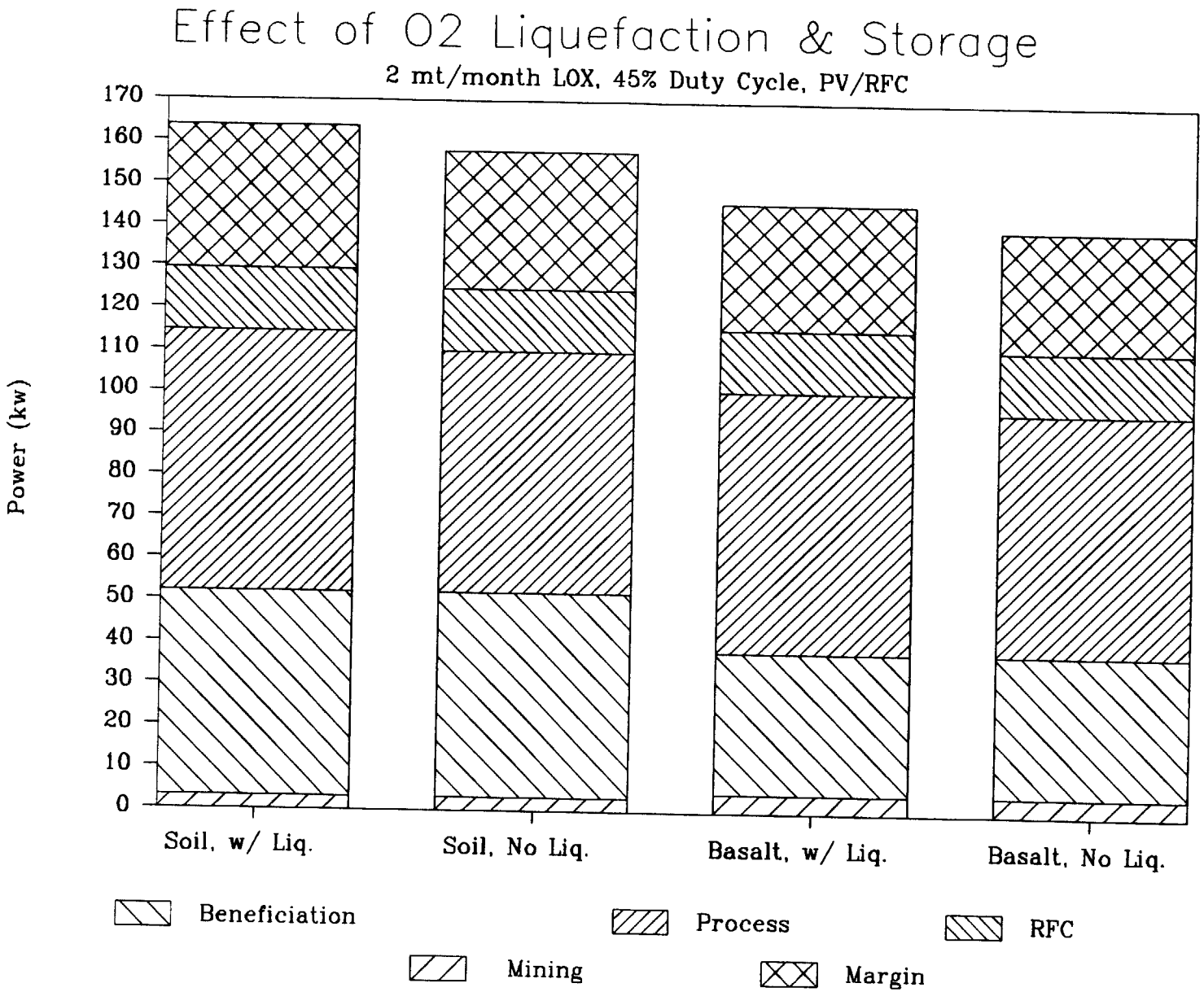

6.3.4 Effect of Modular Construction

Since a LOX production plant will typically mass more than the maximum 25 mt payload capacity of a reusable lander under consideration (50), it can not be delivered in a single integrated unit as envisioned for the pilot plant. Thus, a LOX production plant can be delivered in two ways: 1) delivering two or more units that, when assembled together into one large production plant, is capable of producing the required LOX rate, or 2) delivering several self-contained production modules, that operate either independently or are cross-tied at key locations to increase operating flexibility and redundancy, but which together produce the required LOX. This trade study was designed to investigate the consequences of achieving a given LOX capacity by delivering separate modular production units. Both basalt and soil fed plants were examined (with feedstock properties the same as in Section 6.3.1), although results were similar. The basis of the trade was a comparison between:

- A 144 mt/year LOX production plant, nuclear power, 90% duty cycle.
- Six 24 mt/year LOX pilot plants, also nuclear powered, with 90% duty cycle. The mining area mass and power for the six 24 mt/yr plants was set equal to the 144 mt/year plant, since the minimum excavator/hauler size constraint in the model is an artifact that is not relevant for this trade.

Results for the basalt fed plant are given in Figures 6-17 and 6-18, and for the soil fed plant in Figures 6-19 and 6-20.

Basalt Feedstock:	144 mt/year	Six x 24 mt/year	Diff. (Del/144)
Total Plant and Power Mass (mt)	39.7	60.0	+51.1%
Power (kw)	372	443	+18.9%

Soil Feedstock:	144 mt/year	Six x 24 mt/year	Diff. (Del/144)
Total Plant and Power Mass (mt)	47.2	63.7	+34.9%
Power (kw)	452	485	+ 7.2%

These results show that a significant mass penalty would result from delivery of low-rate modular production plants over a single higher rate production plant. However, other factors to consider are:

- A single larger plant can not begin LOX production until all units have been delivered and assembled. For the 144 mt/year plant, massing 40 mt, this is only 2 flights or perhaps a year delay (if 6 lunar flights per year are performed, with 2 for crew rotation, 2 for science experiments, and 2 for resource utilization). However, a 1000 mt/year LOX plant masses 200-240 mt for a basalt or soil fed plants. This means a delay of 4-5 years from first unit delivery to final unit delivery based on the same manifest assumption (2 resource flights/year). Modular units, on the other hand, have an advantage that they can be delivered and begin LOX production as soon as they are setup and function checked.
- The total number of equipment parts for X number of modular units will be approximately X times as many as a single large production plant. This means that overall

system reliability will be lower and maintenance higher for the modular production case. However, if something breaks on a modular unit, only the production from that one unit suffers. Thus, total modular plant LOX output is subject to degradation, but because the modular units are redundant, the likelihood of total LOX production stopage due to maintenance problems is remote. A problem in a single large plant, however, could result in shutdown of the entire plant, with no LOX production until the problem is corrected.

In other words, a modular plant approach to emplacing a certain LOX capacity will probably result in higher maintenance manpower requirements. However, although maintenance requirements for a single large plant will be lower, if something does go wrong in the plant, it can have a greater adverse effect on LOX production.

Figure 6-17. Effect of Modular Construction on Basalt-Fed Plant Mass

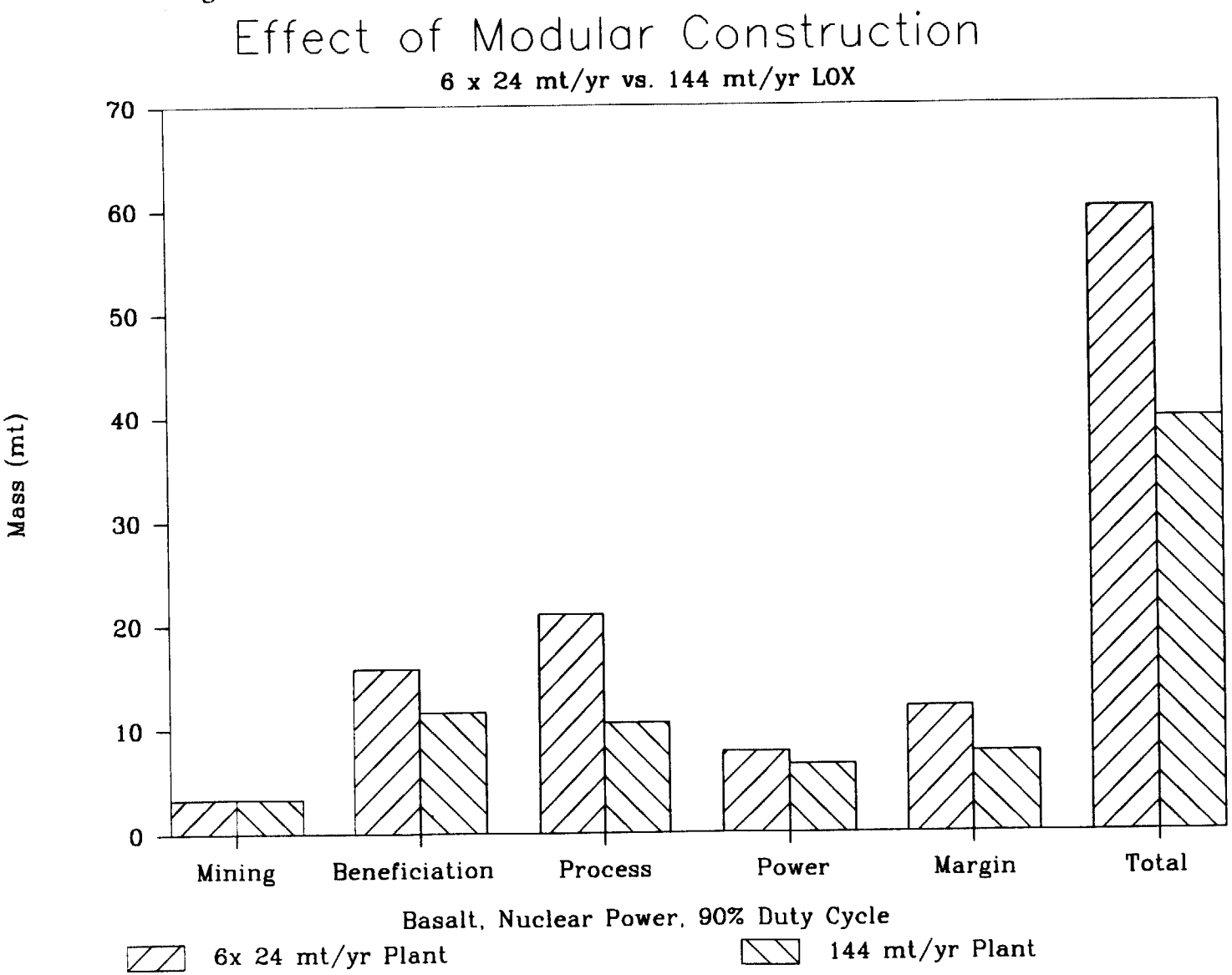

Figure 6-18. Effect of Modular Construction on Basalt-Fed Plant Power

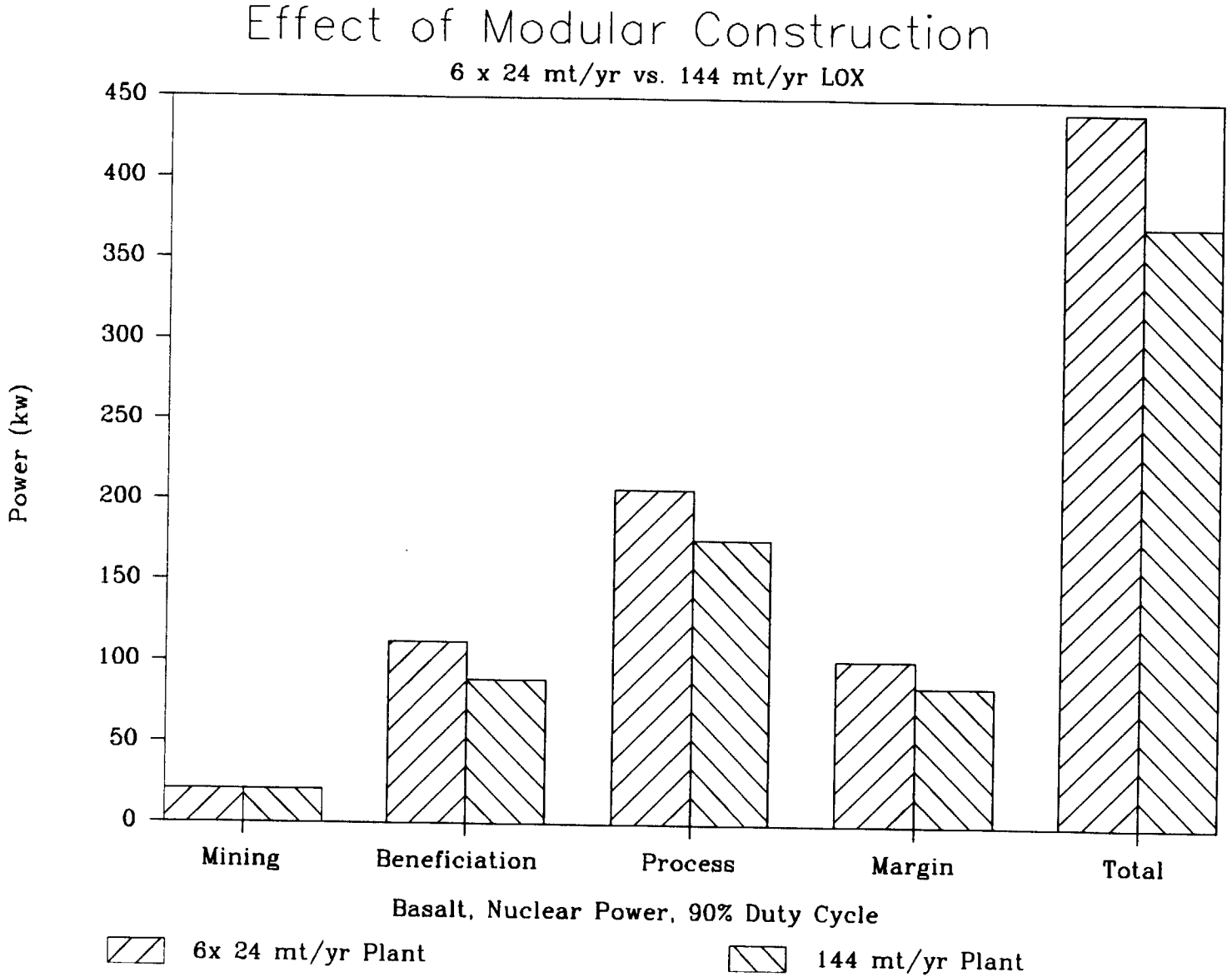

Figure 6-19. Effect of Modular Construction on Soil-Fed Plant Mass

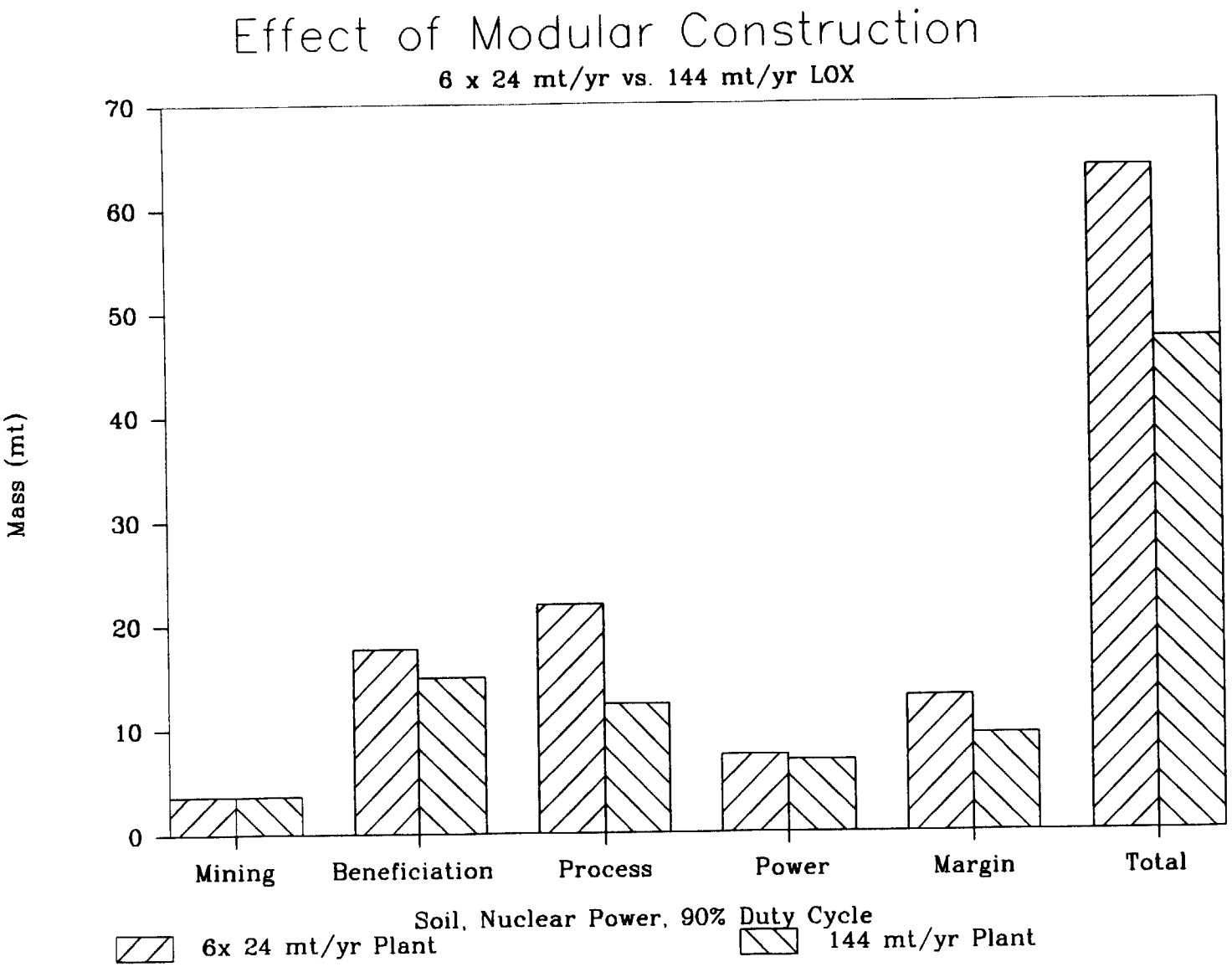

Figure 6-20. Effect of Modular Construction on Soil-Fed Plant Power

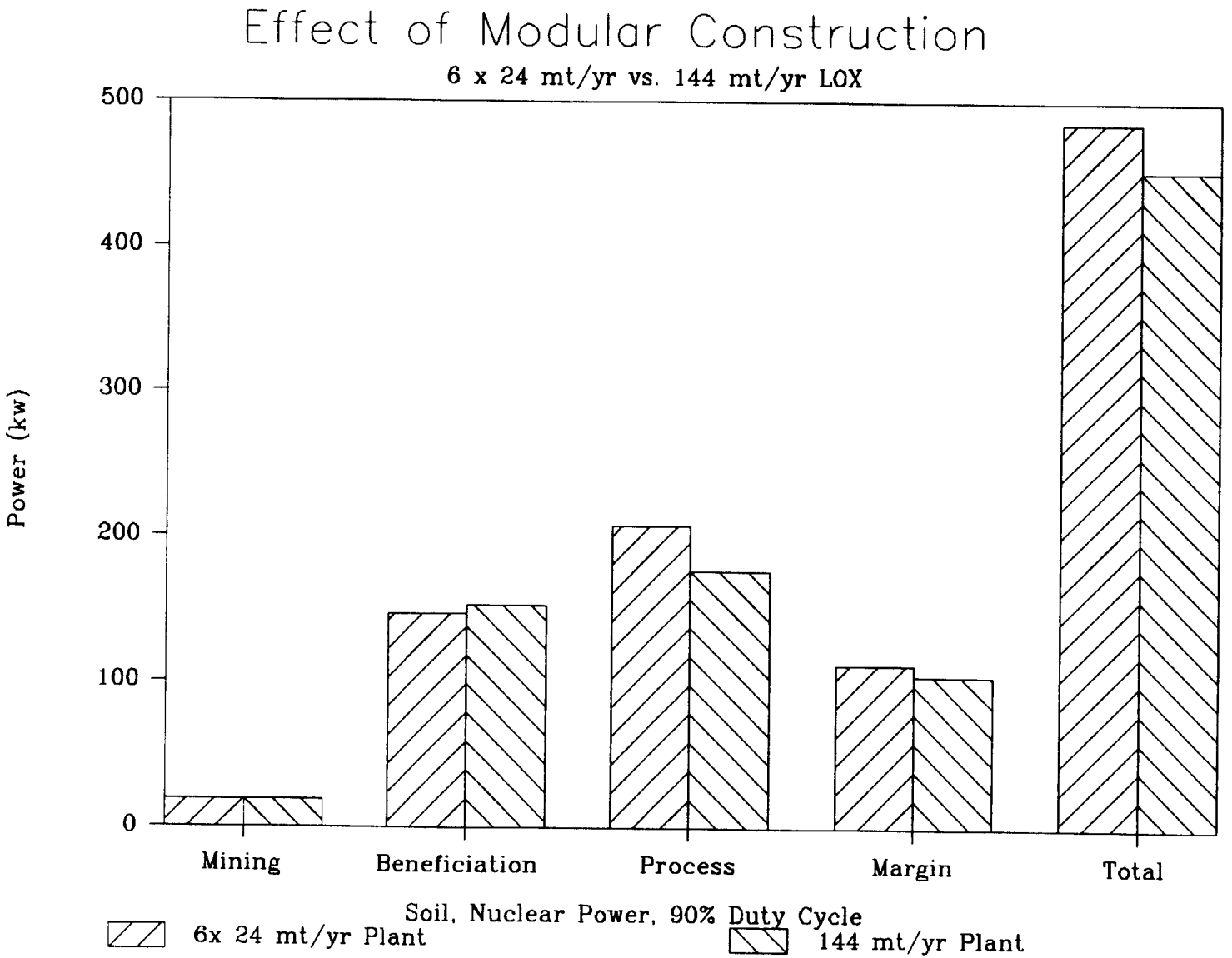

6.3.5 Effect of Eliminating Ilmenite Beneficiation

This trade was setup to show the benefits of separating ilmenite prior to reduction versus feeding unbeneficiated material. The results, however, were somewhat surprising because the benefit was not as great as expected. The comparison was made for a soil fed plant producing 144 mt/year LOX with nuclear power (90% plant duty cycle). The baseline case was with a magnetic separator to concentrate ilmenite (electrostatic separators resulted in higher power consumption, and thus greater plant masses in all cases) after screening, which removes feed sizes that are too large or too small for the fluidized bed reactor. The alternative case still had the screening, but eliminated the magnetic separator. Results are given in Figures 6-21 and 6-22.

	With Separation	Without Separation	Diff.(Delta/with)
Plant + Power Mass (mt)	47.2	51.1	+ 8.2%
Power (kw)	452	587	+29.8%

As expected, eliminating the magnetic separator reduced the mass of the beneficiation area (see Figure 6-21) and increased the mass of the process area because the feed rate to the reactor is higher which requires a wider, more massive reactor. Also as expected, the small decrease in beneficiation power requirement was more than offset by higher power demands of the reactor to heat up all the extra non-ilmenite material. However, total plant and power mass only increased slightly, due primarily to the efficiency of the nuclear power system. The large power increase resulted in only a slight rise in nuclear power plant mass.

A basalt-fed plant case was not examined, but probably should be. Eliminating ilmenite separation becomes more advantageous as the natural ilmenite concentration in the feedstock increases, which is the case with basalt.

Figure 6-21. Effect of Ilmenite Separation on Soil-Fed Plant Mass

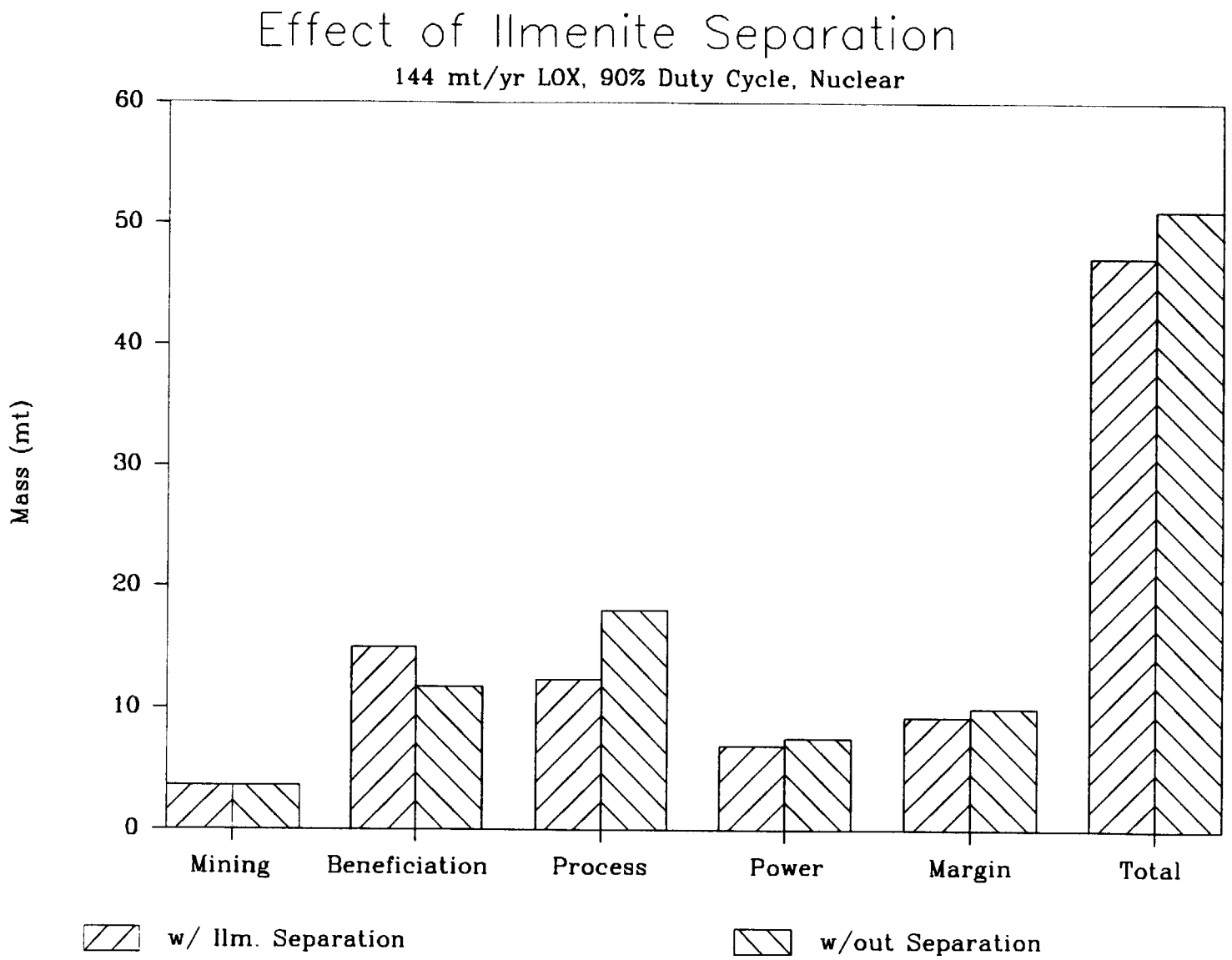

Figure 6-22. Effect of Ilmenite Separation on Soil-Fed Plant Power

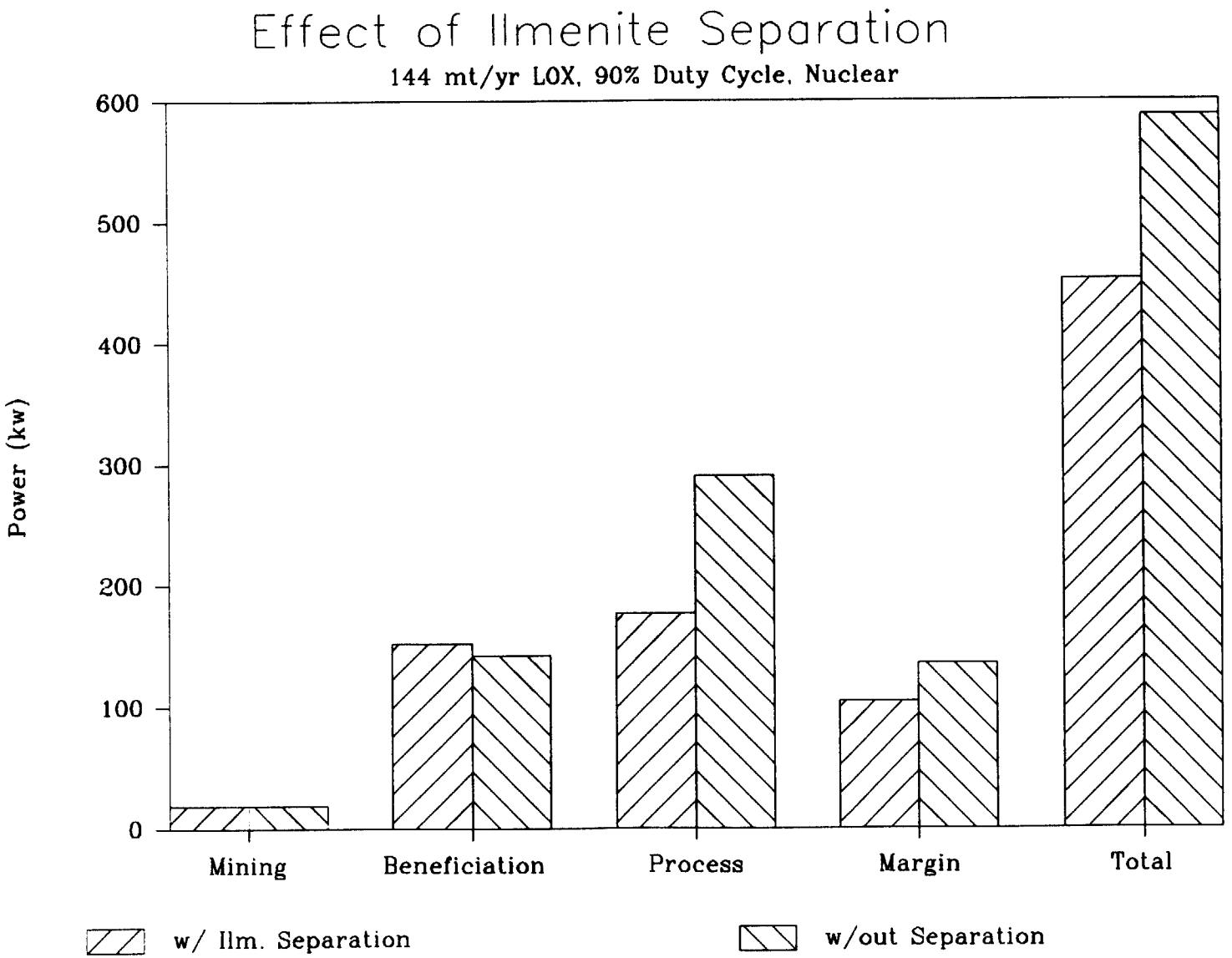

6.4 Sensitivity Studies

The effect of LOX production rate, ilmenite grain size in basalt, and ilmenite abundance in soil on production and pilot plant mass and power was determined.

6.4.1 Sensitivity of Plant Mass and Power to Production Rate

Analyses of the sensitivity of plant mass and power to production rate were made to develop more convenient scaling relationships for program analysis. Separate relationships were developed for basalt and soil fed plants, and for pilot and production plants.

Basalt-Feedstock, Pilot Plant

The basis for this case is 1-5 mt/month LOX pilot plants, basalt feedstock with properties described in Section 6.3.1, PV/RFC power system, 45% plant duty cycle. Mass and power as a function of production rate is shown in Figures 6-23 and 6-24. Plant mass (sum of mining, beneficiation, process areas, and margin) was found to be a nearly linear function of production rate in the 1-5 mt/month LOX range:

Plant mass (mt) = 3.85 * LOX (mt/month) + 8.1 Error = ± 0.2 mt

The error is equal to one standard deviation of the plant mass derived by these correlation equations to the plant mass calculated from the computer program. Total plant and power system (photovoltaic and regenerative fuel cell power system) is given by:

Total Plant + Power mass (mt) = 6.50 * LOX (mt/month) + 11.8 Error = ± 0.3 mt

Plant and RFC power requirements supplied by the PV system are:

Power (kw) = 58.2 * LOX (mt/month) + 30.5 Error = ± 3.0 kw

Soil-Feedstock, Pilot Plant

The basis for this case is 1-5 mt/month LOX pilot plants, soil feedstock with properties described in Section 6.3.1, PV/RFC power system, 45% plant duty cylce. Mass and power sensitivity to production rate is illustrated in Figures 6-25 and 6-26. Plant mass is given by:

Plant mass (mt) = 4.05 * LOX (mt/month) + 6.6 Error = ± 0.2 mt

Total plant and power system mass is:

Total Plant + Power mass (mt) = 7.21 * LOX (mt/month) + 10.0 Error = ± 0.4 mt

Plant and RFC power requirements supplied by the PV system is given by:

Power (kw) = 71.1 * LOX (mt/month) + 22.8 Error = ± 2.7 kw

Note that the slopes of the mass and power curves will cause these curves to intersect, at lower rates the soil-fed pilot plant has the smaller mass and power while the reverse is true of the basalt-fed pilot plant at higher production rates. (The intersections were not found).

Basalt-Feedstock, Production Plant

The basis for this case is 144-1500 mt/year LOX production plants, nuclear power, 90% plant duty cycle. Figures 6-27 and 6-28 show mass and power for the different plant areas. Derived correlations for the curves are:

Plant mass (mt) = 0.176 * LOX (mt/yr) + 11.4 Error = ± 2.8 mt

Plant & Power mass (mt) = 0.187 * LOX (mt/yr) + 16.4 Error = ± 2.8 mt

Power (kw) = 2.35 * LOX (mt/yr) + 34.4 Error = ± 5.0 kw

Soil-Feedstock, Production Plant

The basis for this case is 144-1500 mt/year LOX production plants, nuclear power, 90% plant duty cycle. Mass and power as a function of production rate is given in Figures 6-29 and 6-30. Correlations are:

Plant mass (mt) = 0.217 * LOX (mt/yr) + 8.73 Error = ± 0.6 mt

Plant & Power mass (mt) = 0.231 * LOX (mt/yr) + 13.6 Error = ± 0.6 mt

Power (kw) = 2.95 * LOX (mt/yr) + 27.7 Error = ± 4.0 kw

As with the pilot plants, the soil and basalt production plant mass and power curves will intersect. Basalt-fed plants are more efficient at high rates, soil at low rates.

A summary of the results is given in Table 6-6.

Table 6-6. Summary of Production Rate Sensitivity Results

(Nuclear Power, 90% process duty cycle, 35% mining duty cycle)

BASALT FEEDSTOCK

LOX Prod. (mt/yr)	Plant Area Mass (mt) Mining	Beneficiation	Process	Margin	Plant	Nuclear Power	Total
144	3.4	11.6	10.6	7.7	33.2	6.5	39.7
180	6.1	14.2	12.4	9.8	42.6	6.9	49.5
300	9.4	23.5	18.5	15.4	66.9	8.3	75.2
500	12.3	38.2	28.1	23.6	102.1	10.5	112.6
1000	17.6	73.4	51.8	42.8	185.7	16.0	201.7
1500	26.7	109.0	75.7	63.4	274.7	21.6	296.3

LOX Prod. (mt/yr)	Plant Area Power (kwe) Mining	Beneficiation	Process	Margin	Plant
144	20.8	89.1	176.5	85.9	372.3
180	28.1	105.2	218.5	105.5	457.3
300	45.6	170.5	357.5	172.1	745.7
500	75.2	267.5	587.8	279.1	1209.6
1000	144.4	525.7	1160.4	549.2	2379.7
1500	216.8	796.5	1730.7	823.2	3567.2

SOIL FEEDSTOCK

LOX Prod. (mt/yr)	Plant Area Mass (mt) Mining	Beneficiation	Process	Margin	Plant	Nuclear Power	Total
144	3.7	15.0	12.4	9.3	40.3	6.9	47.2
180	3.7	18.5	14.8	11.1	48.0	7.4	55.4
300	5.0	29.5	22.3	17.1	73.9	9.1	83.0
500	7.4	47.9	34.6	27.0	117.0	11.9	128.9
1000	14.3	93.6	65.1	51.9	225.0	18.9	243.8
1500	24.1	138.7	95.0	77.3	335.1	25.8	360.9

LOX Prod. (mt/yr)	Plant Area Power (kwe) Mining	Beneficiation	Process	Margin	Plant
144	19.1	152.3	176.5	104.4	452.3
180	23.9	190.2	218.5	129.8	562.4
300	39.9	304.0	357.5	210.4	911.8
500	66.5	501.2	587.8	346.6	1502.1
1000	136.5	1001.6	1160.4	689.5	2988.0
1500	210.5	1487.1	1730.7	1028.5	4456.8

Figure 6-23. Basalt-Fed Pilot Plant Mass

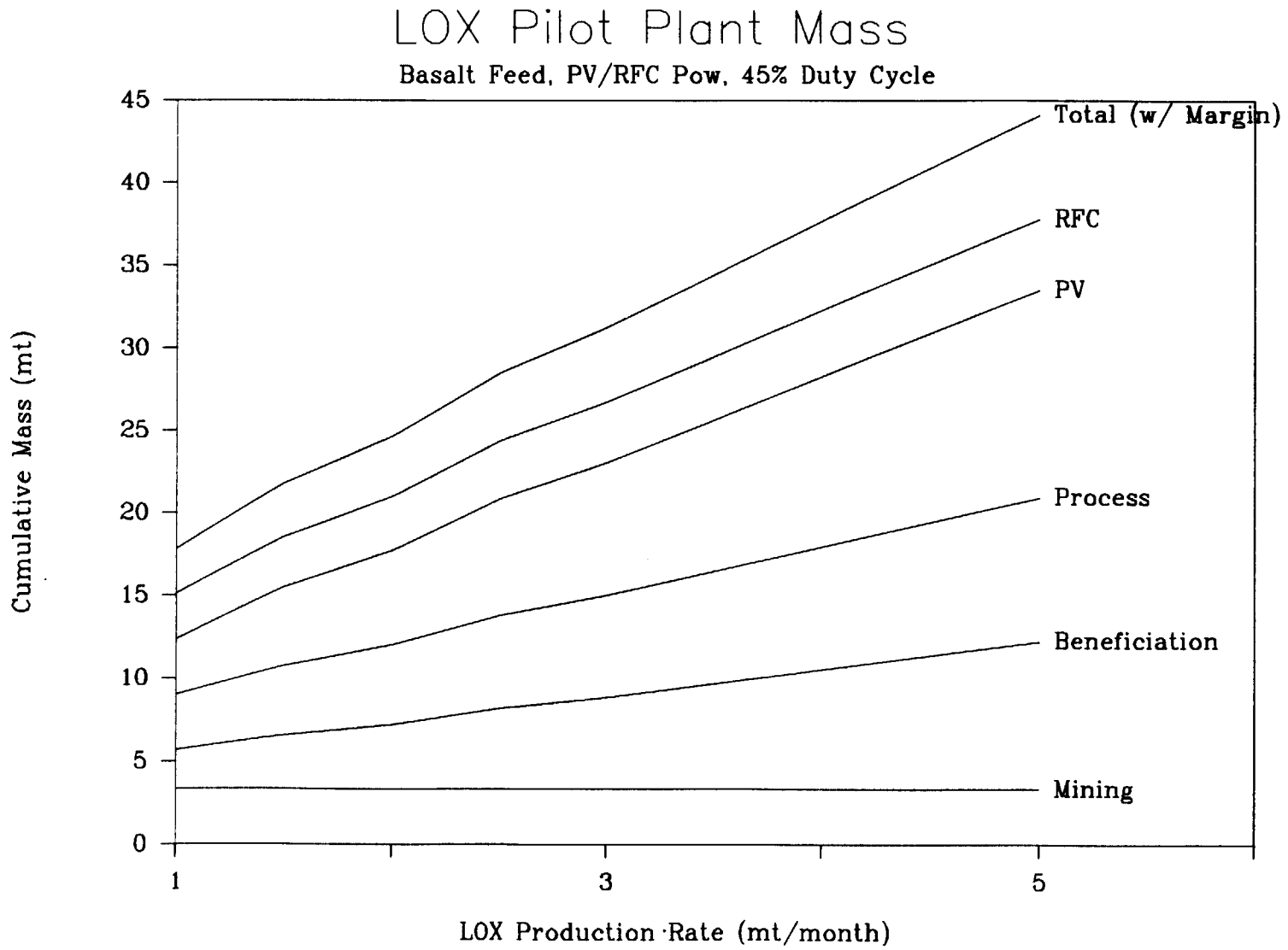

Figure 6-24. Basalt-Fed Pilot Plant Power

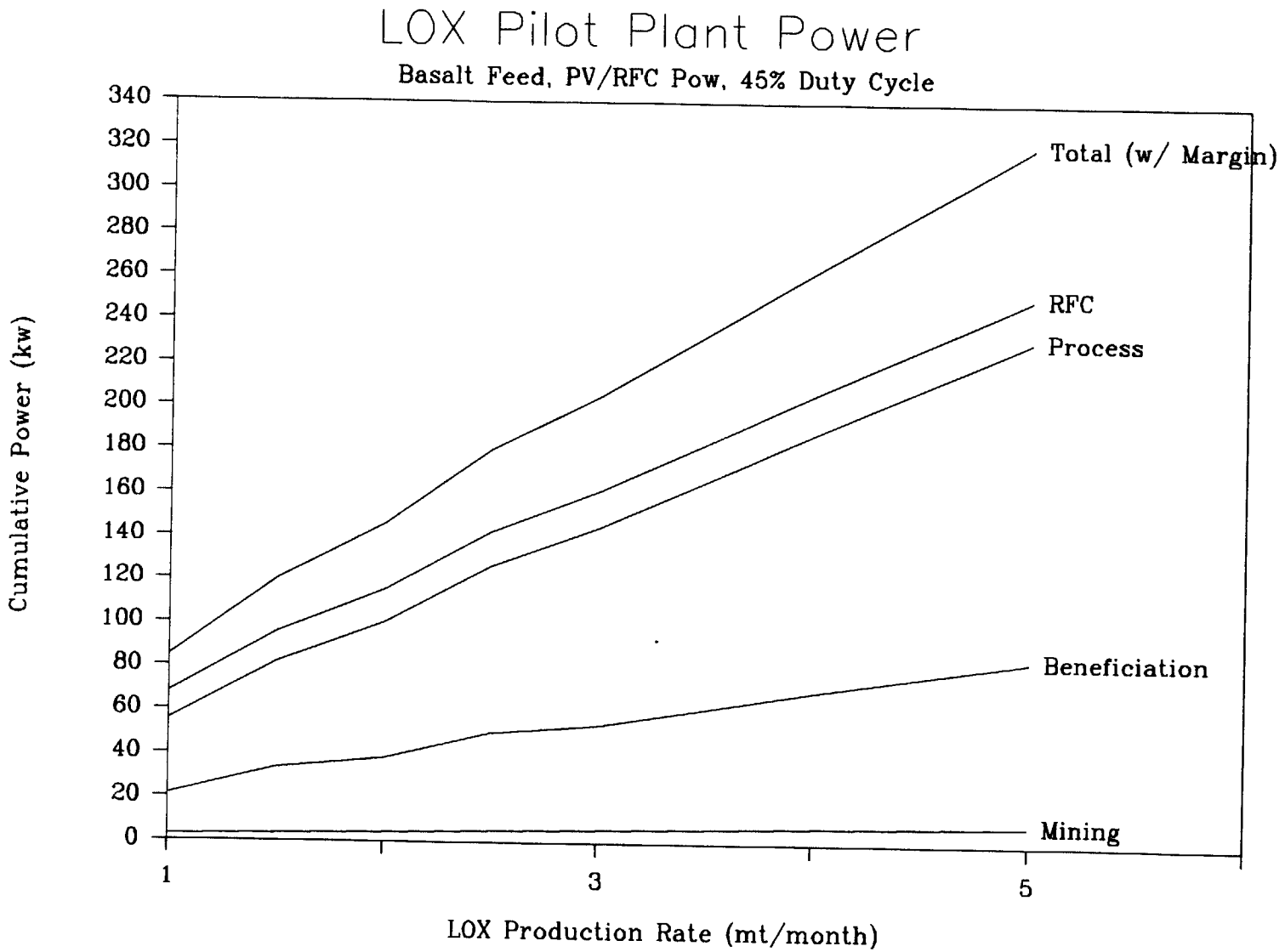

Figure 6-25. Soil-Fed Pilot Plant Mass

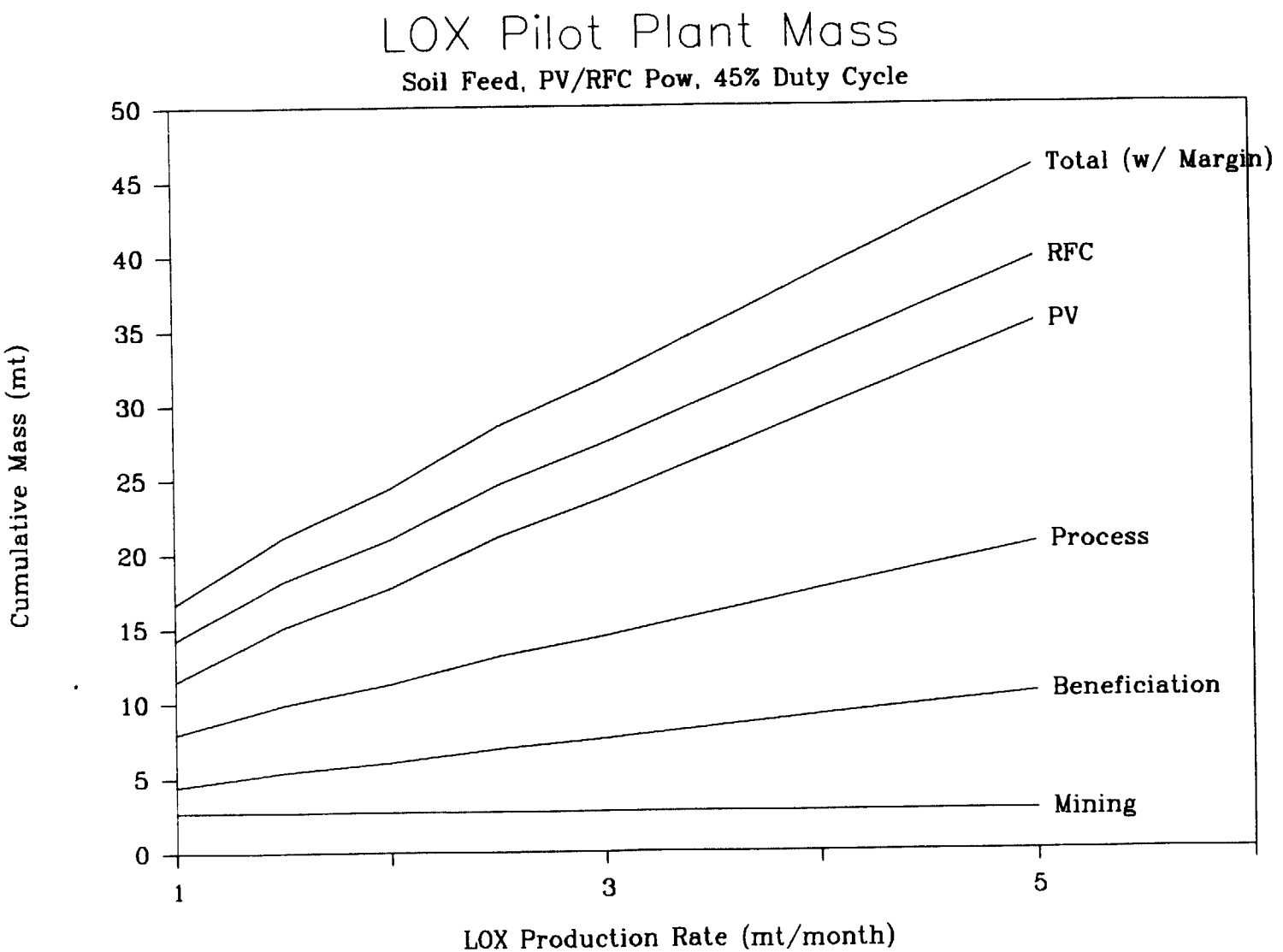

Figure 6-26. Soil-Fed Pilot Plant Power

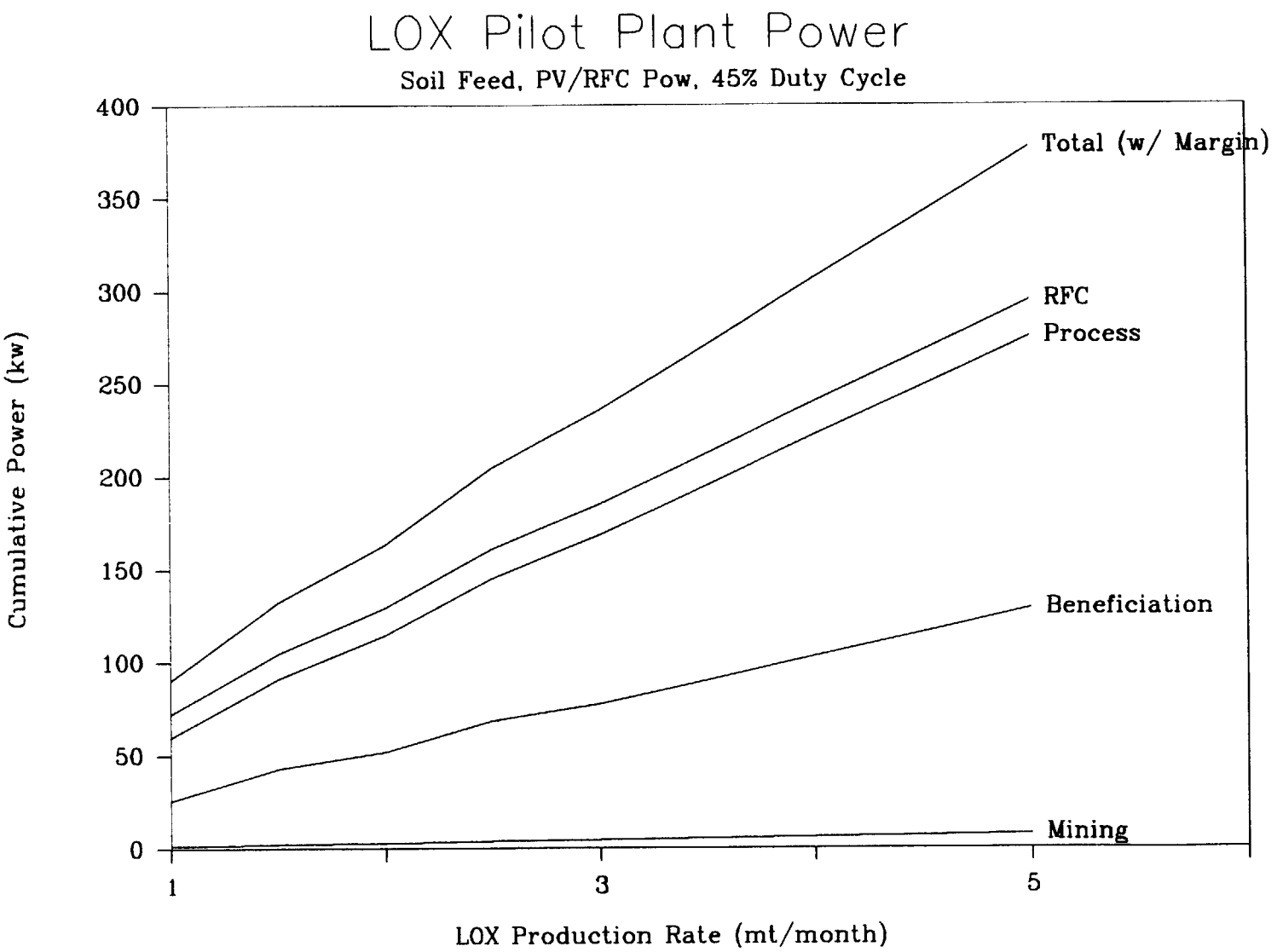

Figure 6-27. Basalt-Fed Production Plant Mass

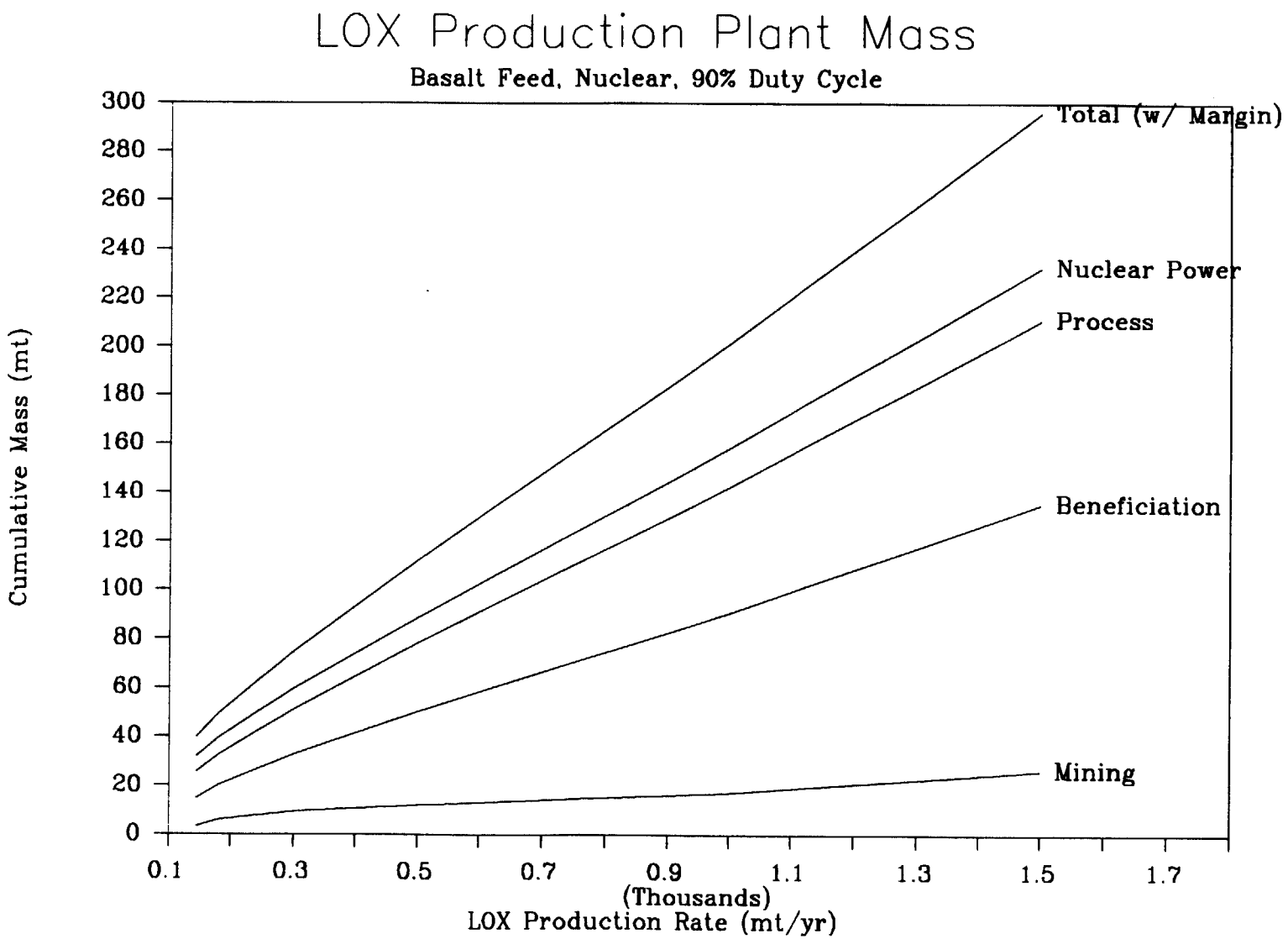

Figure 6-28. Basalt-Fed Production Plant Power

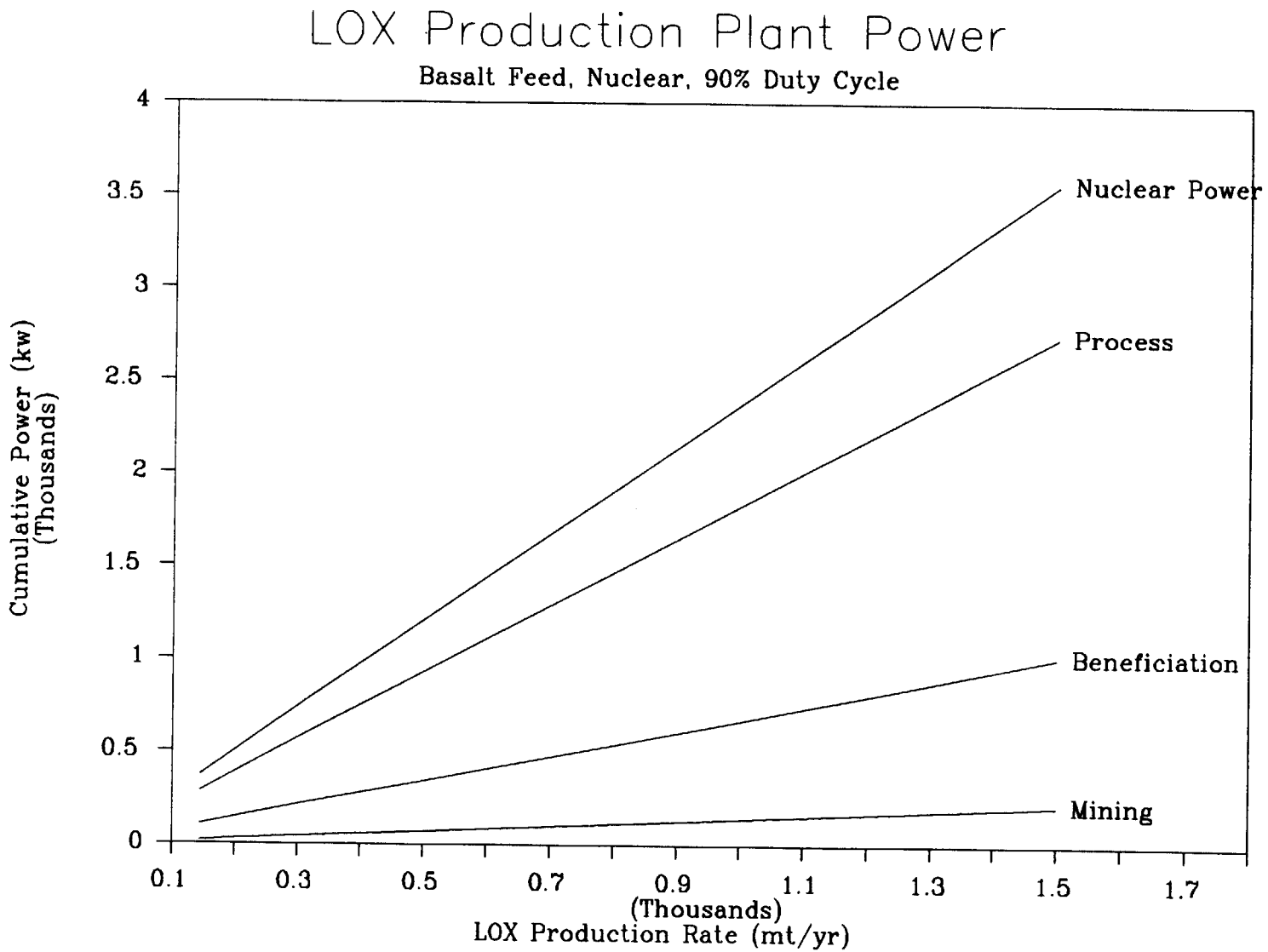

Figure 6-29. Soil-Fed Production Plant Mass

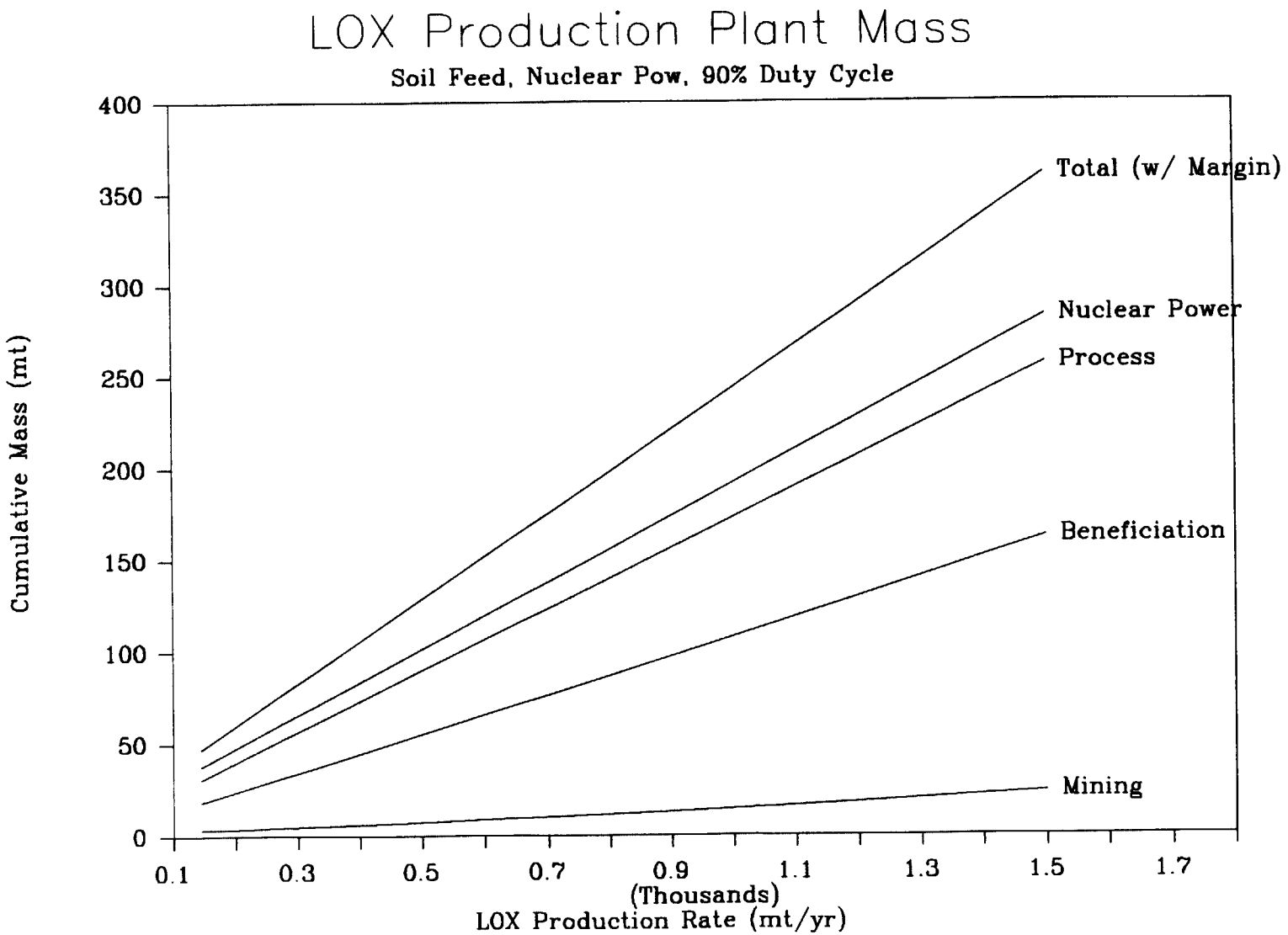

Figure 6-30. Soil-Fed Production Plant Power

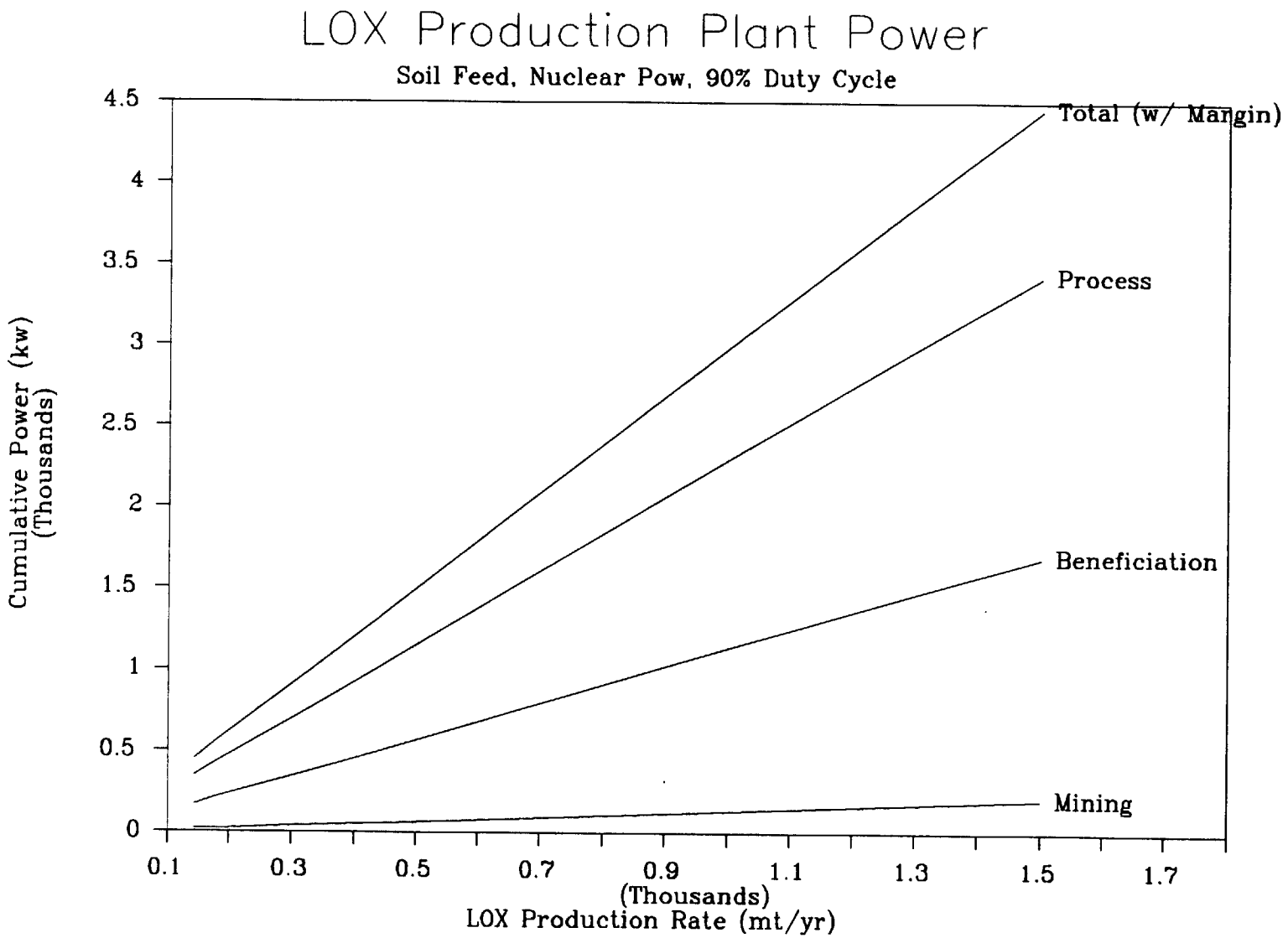

6.4.2 Sensitivity of Basalt-Fed Plant to Ilmenite Grain Size

If basalt of a larger grain size is available, less grinding will be necessary to liberate the same amount of ilmenite (see Figure 6-5), thus decreasing the size and power of necessary grinding equipment (e.g. ball mill). In addition, if target grind size increases, fewer fines are produced, which results in less screening (saving screen power and mass), but also decreasing mining requirements since less fines are produced and discarded. This effect is shown below:

Basalt Grain Size, mm	Percent Fines	Mining Req. mt/mt O_2
0.5	43	186
0.75	32	157
1.0	27	144
1.5	20	132
2.0	16	126

Pilot Plant

The combined effect of these improvements is given in Figures 6-31 and 6-32. For a 2 mt/month LOX plant, operating with basalt feed, PV/RFC power, and 45% plant duty cycle, total plant & power mass decreases from 24.7 mt with a 0.5 mm ilmenite grain size, to 23.1 mt (-6.5%) with a 1.0 mm grain size, and to 22.6 mt (-8.3%) with a 1.5 mm grain size. Power requirements decrease from 146 kw at 0.5 mm grains to 138 kw (-5.7%) and 135 kw (-7.3%) for 1.0 mm and 1.5 mm grains, respectively.

Production Plant

A case was run for a 144 mt/yr LOX plant, basalt feed, nuclear power, 90% plant duty cycle. Total plant and power mass decreases from 39.7 mt with 0.5 mm ilmenite grains to 34.7 mt (-12.6%) and 32.9 mt (-17.3%) for 1.0 mm and 1.5 mm grains, respectively. Power decreased from 372 kw @ 0.5 mm grains, to 339 kw (-9.0%) and 322 kw (-13.4%) for 1.0 mm and 1.5 mm grains, respectively. Figures 6-33 and 6-34 illustrate the results.

Figure 6-31. Effect of Basalt Grain Size on Pilot Plant Mass

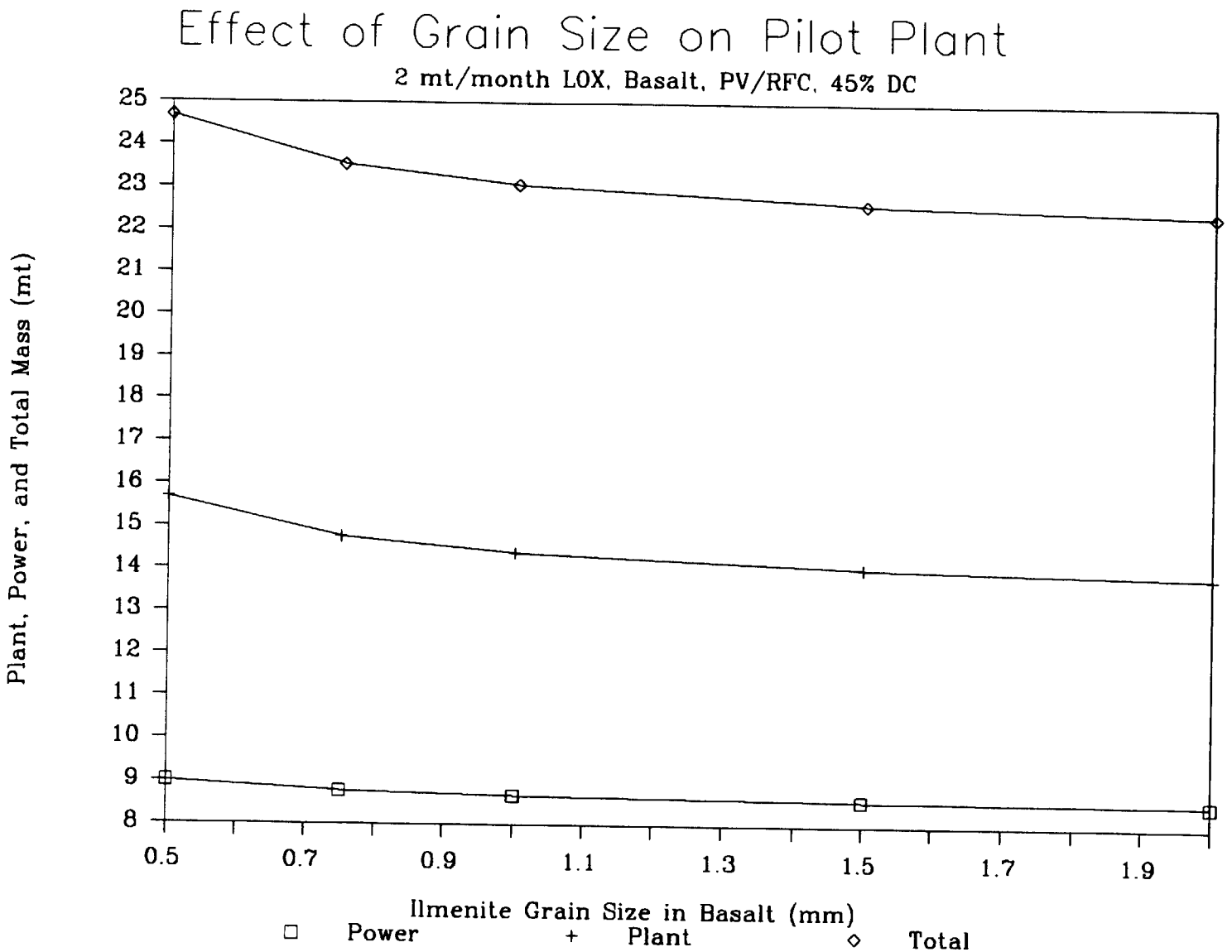

Figure 6-32. Effect of Basalt Grain Size on Pilot Plant Power

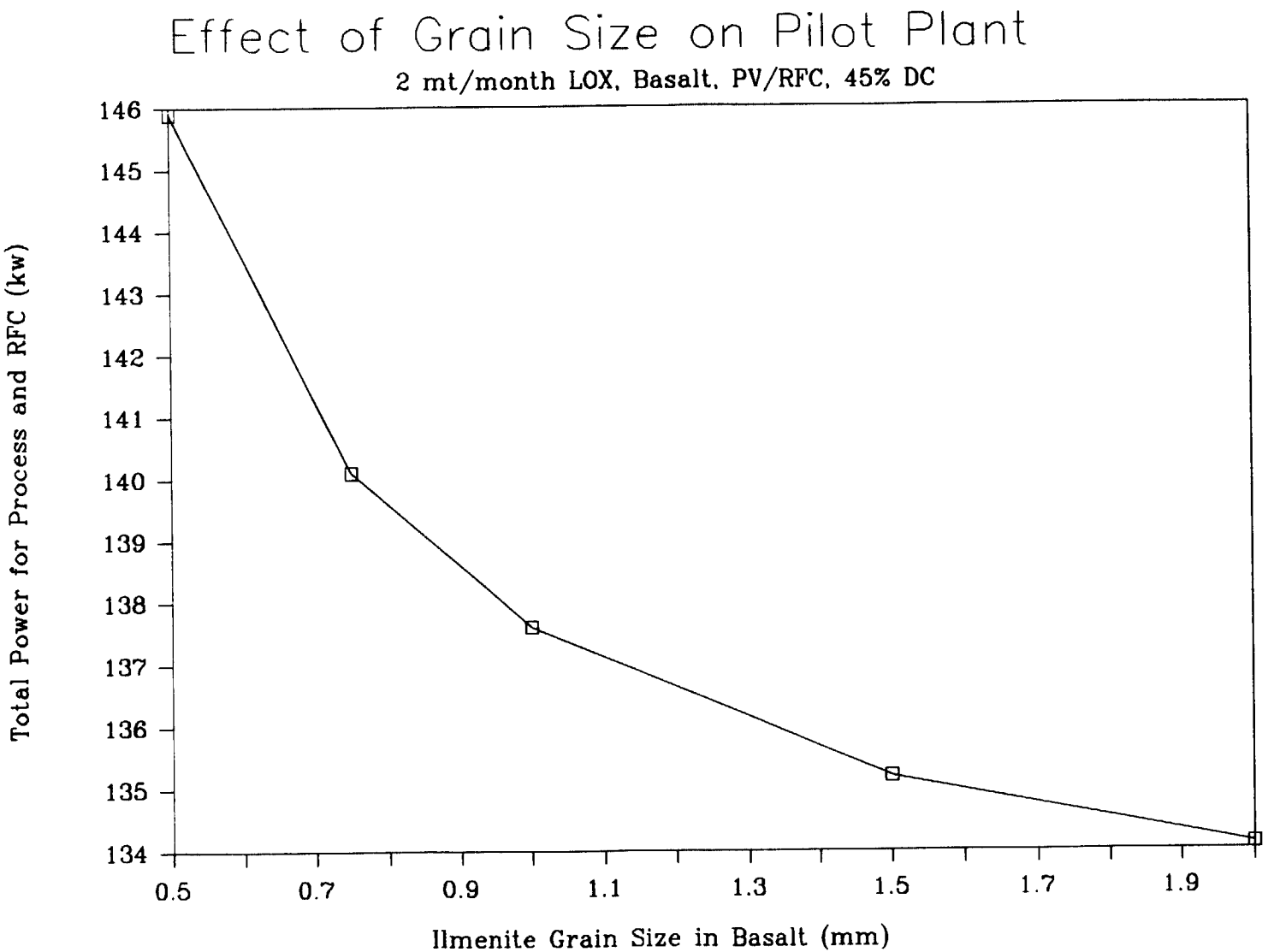

Figure 6-33. Effect of Basalt Grain Size on Production Plant Mass

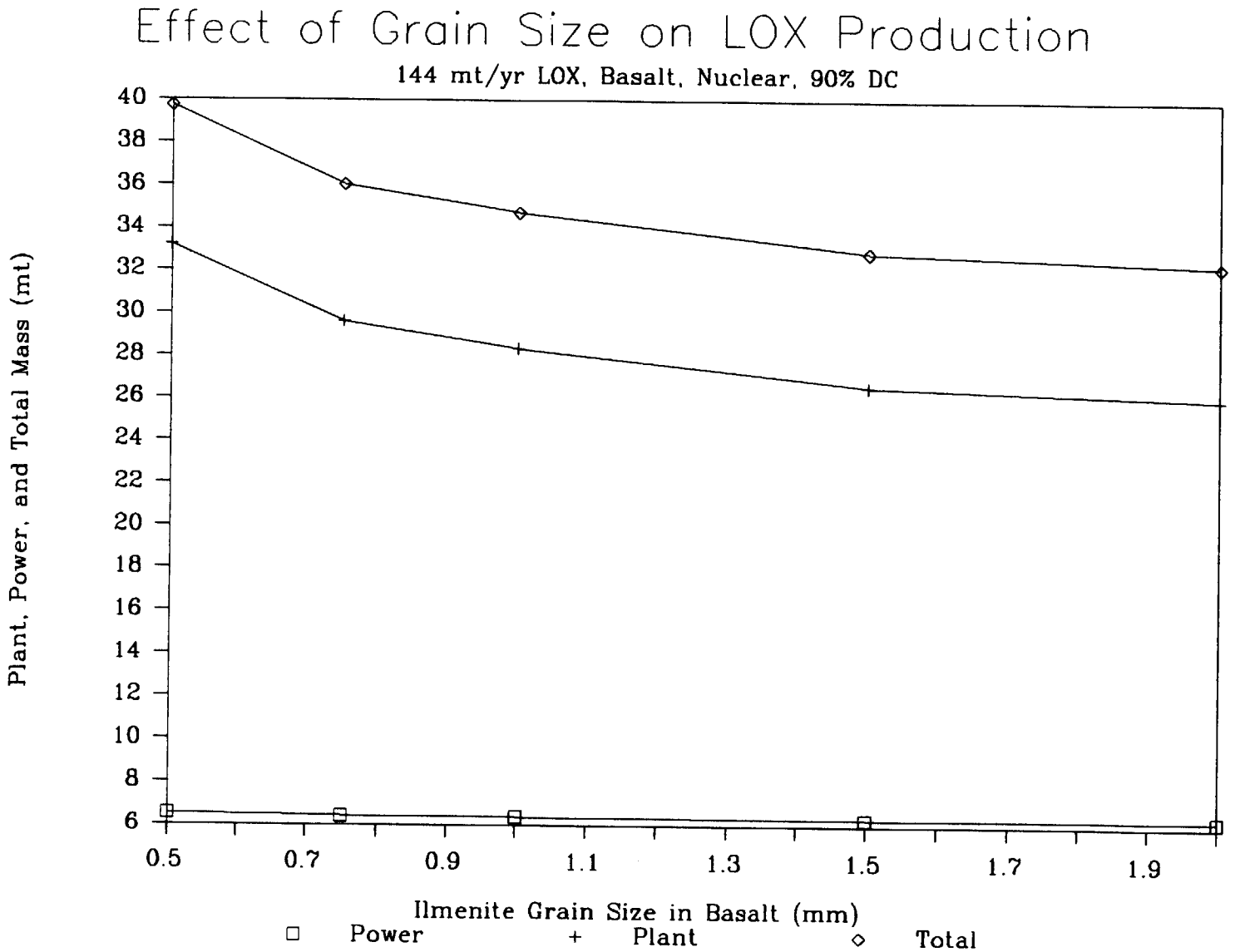

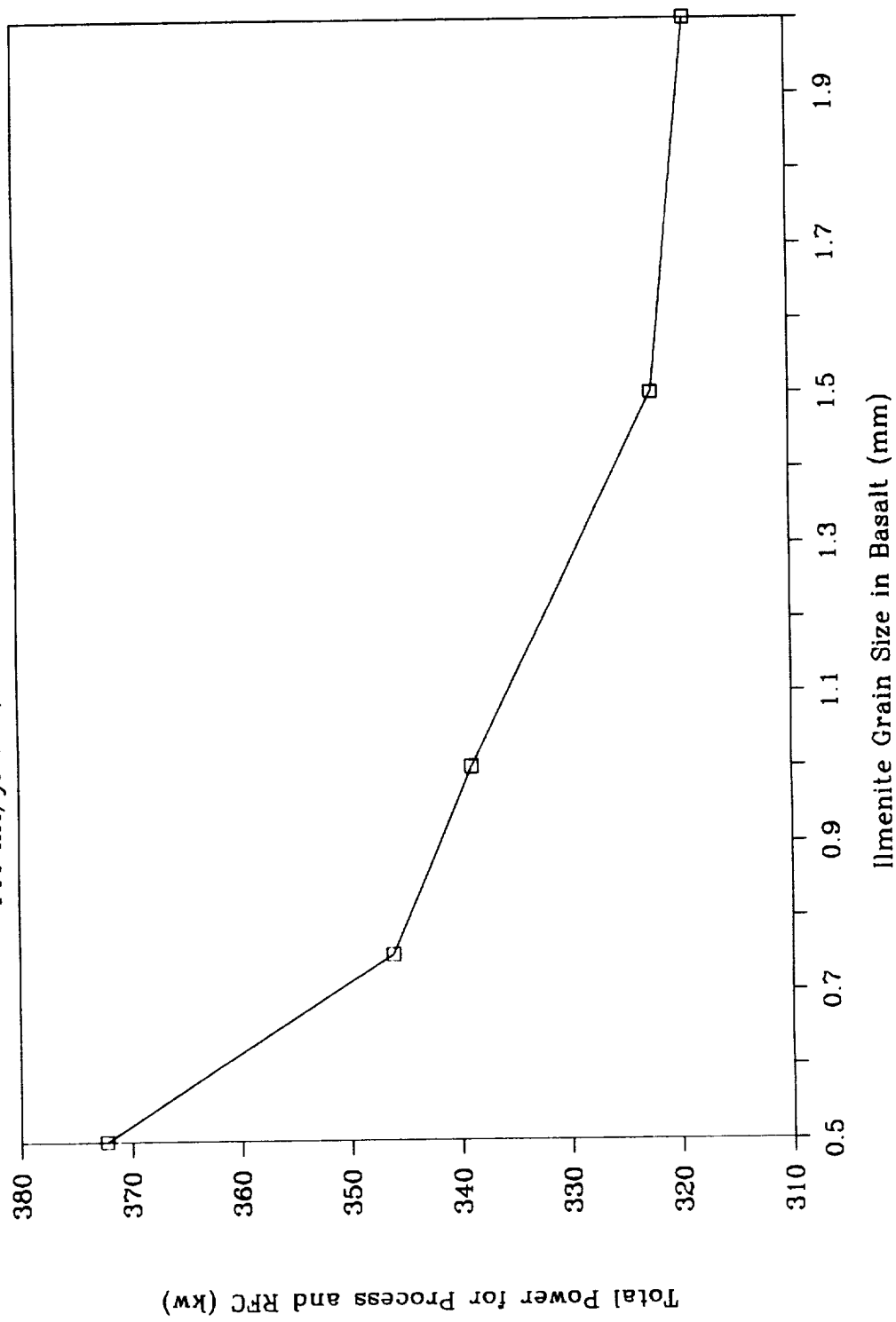

Figure 6-34. Effect of Basalt Grain Size on Production Plant Power

6.4.3 Sensitivity of Soil-Fed Plant to Soil Ilmenite Abundance

The mass and power of a soil-fed production plant (144 mt/yr LOX, nuclear power, 90% duty cycle) is given as a function of soil ilmenite abundance in Figures 6-35 and 6-36. Soil ilmenite abundance is given in weight percent in the figures. Weight percent ranges from 7.5%-15% ilmenite as shown in the figures corresponds to volume percent ilmenite ranges from 5%-10% (based on 4.5 S.G. for ilmenite and 3.0 S.G. for soil). For soil ilmenite abundance increase of 5 vol.% to 8 vol.% (7.5-12 wt.%), total plant and power system mass decreases from 47.2 mt to 36.3 mt (-23%). Thus, a significant mass savings can be realized if an extensive ilmenite-rich region on the Moon were located for the mine site (several hundred meters on a side).

Figure 6-35. Effect of Soil Ilmenite Abundance on Production Plant Mass

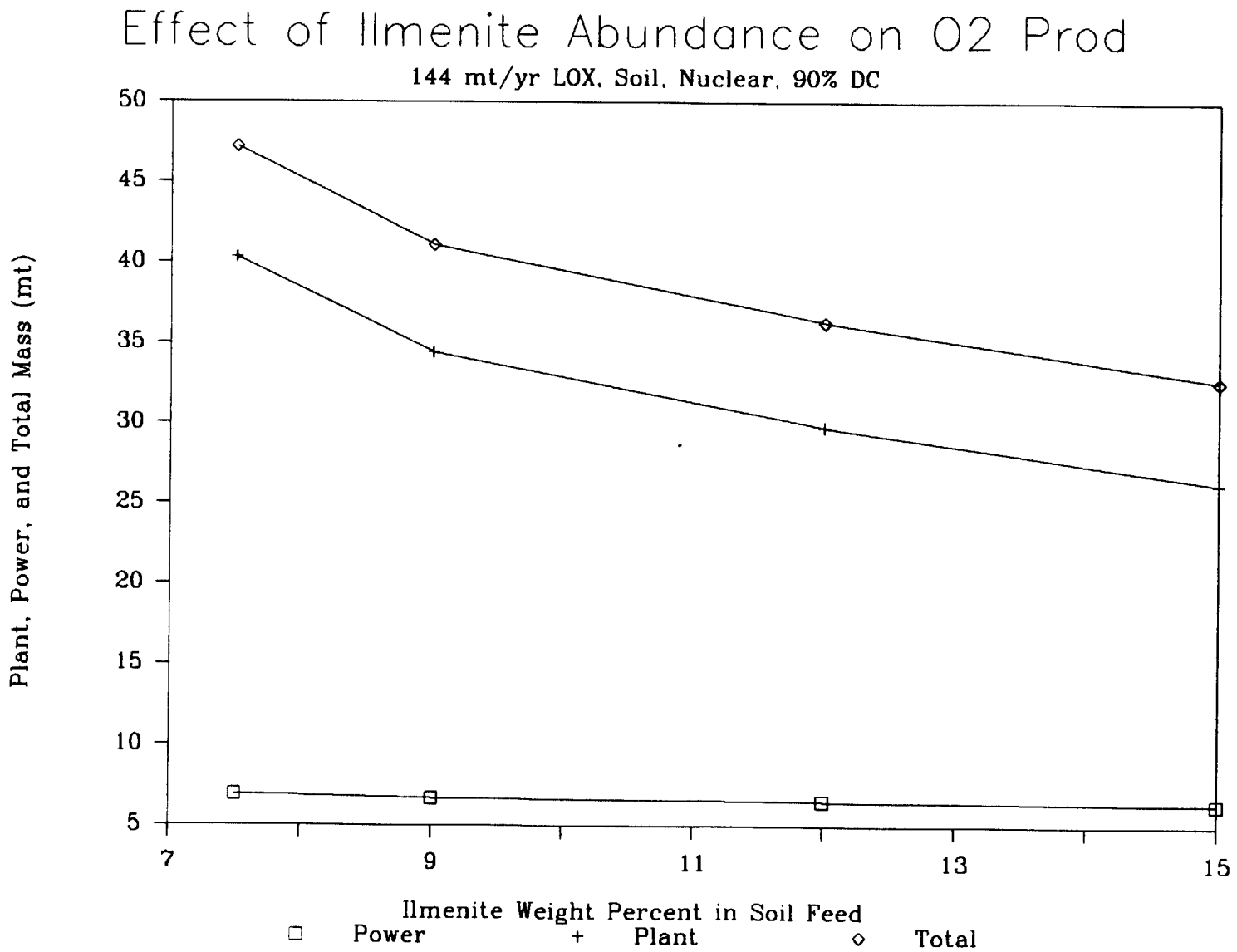

Figure 6-36. Effect of Soil Ilmenite Abundance on Production Plant Power

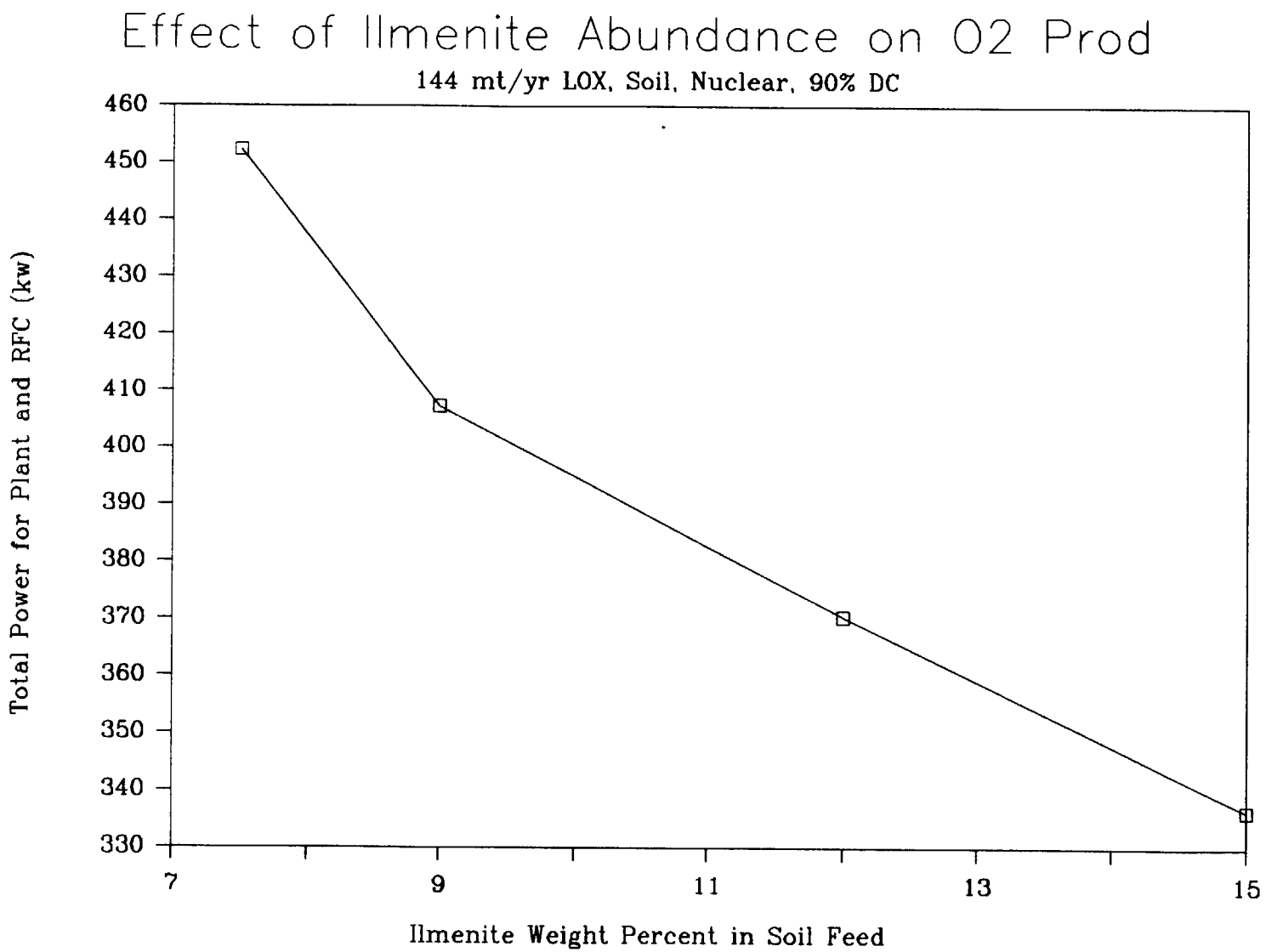

6.5 Process Alternatives and Potential Payoff

More process alternatives and trades are possible than those described in Sections 6.3 and 6.4. Some are described in this section although study resources prevented detailed analysis.

6.5.1 Alternative Fines Removal Concepts

Vibratory screens become inefficient below about 0.1 mm aperture size. Soil-fed plants in particular would benefit from a more efficient way to remove fines. Although electrostatic sizing methods have been proposed by some (22, 46), this suffers from the large thermal energy penalty associated with pre-heating the soil to 150-200°C prior to feeding the electrostatic unit (this is a requirement with ilmenite separation, it may not be for size separation). Cyclone separators or mechanical gas classifiers are alternatives to removing fines (<0.03-0.045 mm). Schematics of these units are shown in Figure 6-37. They rely on a gas stream to carry the fines into the units, where centrifugal and drag forces act to separate out the fines. Cyclones contain no moving parts and are the preferred alternative. Probably the easiest way to incorporate one or the other of these units into the process is to put it at the top the reactor. The fines would be allowed to enter the reactor in the feed, the ascending gas would entrain them and carry them into the cyclone or gas classifier where they would be removed. The principal difference between a cyclone in this application and the cyclone normally installed at the top of the reactor is its size which must be large enough to handle large volumes of fines (also the solids return line would not re-enter the reactor but would descend to a gas/solid separator and discharge conveyor). This concept would eliminate the vibratory screens to remove fines, but would require a larger magnetic separator to handle the increased flow. The top bed of the reactor might also require a larger diameter.

The vibratory screen for a 2 mt/month LOX soil-fed pilot plant (at 45% duty cycle) masses 1500 kg (6% of 24.4 mt total) and requires 45 kw (27% of 164 kw total). The additional load on the magnetic separator would approximately double its mass and power (adds 910 kg and 1.2 kw). Even if the cyclones or mechanical classifier scales at 25% of the vibratory screen, savings of 215 kg (1% of total mass) due to equipment mass decrease, and 1200 kg (5% of total mass) in solar array mass savings due to a decrease in power of 33 kw (20% of total power) are possible.

Figure 6-37. Mechanical Gas Classifier and Cyclone Separator (Ref.91)

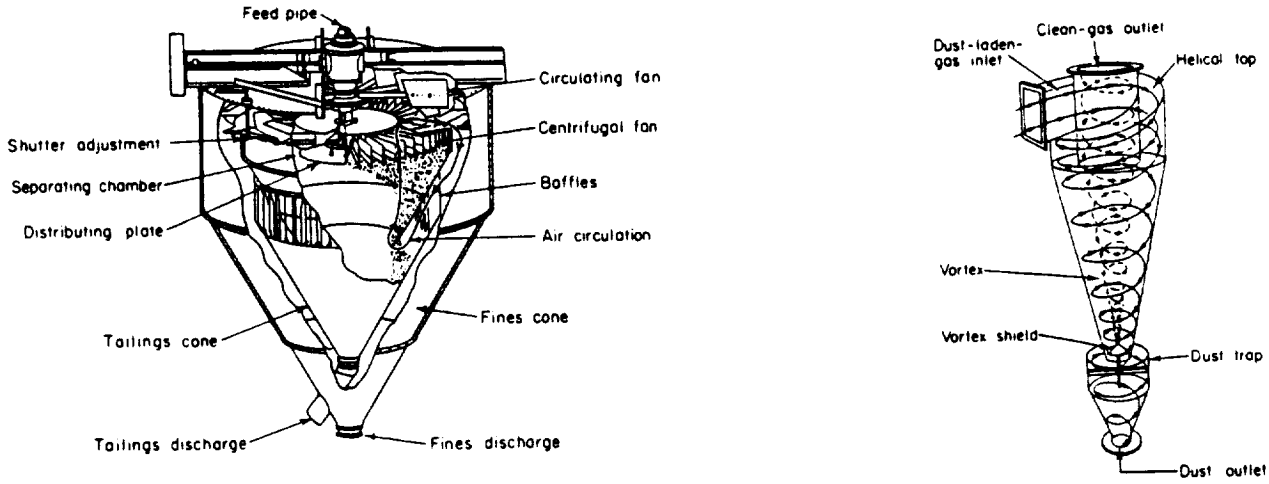

Another possibility is to use a fast-fluidized bed reactor with large cyclone and not remove the fines at all. There is no well-defined bed in a fast-fluidized reactor since the gas rate through the bed is maintained sufficiently high to entrain a majority of the particles. Cyclones are used to separate the fines and gas. The fines would return to the reactor while the water in the gas would be electrolyzed. Since a greater quantity of gas is required, mass penalties for gas handling would have to be traded with the lower mining and solids handling requirements (since fines are not discarded).

6.5.2 Alternative Reactor Insulation Concepts

The reactor shell/insulation concept baselined for this study included (from outside to inside): a steel external shell (for pressure containment), a 23 cm thick middle layer made of low-density (S.G. 0.14) Shuttle tile insulation, and a 7.5 cm thick inner core layer made of high-density (S.G. 2.24) tough refractory firebrick to protect the low-density insulation. Total mass of insulation for the basalt-fed pilot plant (2 mt/month LOX, RFC/PV, 45% duty cycle) was calculated as 1.82 mt (7% of total mass of 24.7 mt plant & power mass). Another option could be to use a refractory metal structure, such as a molybdenum based alloy or cermets (ceramic/metallic composites), around the interior core to contain pressure, with low-density insulation on the exterior to reduce heat losses and no high-density insulation. If shell weight remains about the same (low strength of Mo-alloy will tend to increase skin thickness and mass, higher density of Mo-alloy will also tend to increase mass, but smaller shell radius will tend to decrease skin thickness and mass), potential savings in insulation mass are estimated as 1.2 mt (5% of total mass) and heat losses are expected to be less.

Another option is to use multilayer insulation (MLI) made of thin metallic foils separated by spaces that are open to vacuum. Inconel 600 metal MLI (that has been coated with zirconium oxide) has been tested as a light-weight alternative to ceramic fiber insulations for high-temperature (850-1,150°C) carbon dioxide removal subsystems in advanced environmental control systems (117).

Other Reactor Thermal Issues

Additional trades are possible between the bed heights of the fluidized bed reactor and gas-solid heat transfer/recovery.

6.5.3 Alternative Reactants

Carbon monoxide reductant should be studied for ilmenite reduction. Products of reaction, carbon dioxide, can be reduced in a similar high-temperature, solid-state electrolysis cell as proposed for water vapor in hydrogen reduction of ilmenite.

Another option is to pre-oxidize iron oxides in ilmenite prior to reduction. Pre-oxidation of divalent-iron containing ilmenite (divalent iron oxide, FeO, contains somewhat reduced iron which is more typical of lunar conditions than the more oxidized trivalent-iron mineral) has been experimental shown to increase ilmenite reduction reaction rates by 3-4 times (9). Preoxidation could be incorporated into the process by using a 4-stage fluidized bed reactor, instead of 3-stages. Ilmenite oxidation would take place in the top bed between incoming solids and a measured stream of oxygen from the electrolysis oxygen product stream. The exothermic oxidation reaction would tend to help preheat the solids. Bed lengths of the other stages could likely be reduced (at least for the middle reaction stage) because of the high reaction rates after oxidization, resulting in possible

reactor mass savings. Alternatively, bed lengths could remain constant while reaction takes place at lower temperatures, thus saving thermal energy requirements.

6.5.4 Iron From Reactor Residual

The reduced soil product from the ilmenite reduction process is rutile, TiO_2, in solid solution with iron. Iron may be useful later in lunar base development for manufacturing structural elements from lunar sources. One way to remove the iron from the residual solids would be to first grind to liberate relatively pure iron particles, which could then be removed easily from groundmass materials with magnets. Perhaps a better way is to heat the rutile/iron mixture to 1,535°C or higher. Iron would melt, forming a metal pool (S.G. 7.86) that could then be easily separated from solid rutile floating on its surface (S.G. 4.26).

6.6 Base Operations Impacts

Oxygen production impacts on base operations and manpower requirements are described in the following sections.

6.6.1 Pilot Plant

Pilot plant operations are divided into setup and operational tasks.

Setup

The sequence of tasks to be performed in setting up the pilot plant are:

1. Select and survey pilot plant and mine sites.

2. Site preparation.
a) Prepare surface for processing unit (7 m diameter) and power systems.
b) Dig holes for (2) LOX storage tanks and (1) LH_2 tank. Tanks are half-sunk, half-buried. Prepare cleared or marked way to mine site from pilot plant site.

3. Sink deadman, pilings, or other anchoring hardware/method into bedrock (2-5 m deep). These will be used as stablizing attach points for process structure and power systems.

4. Offload pilot plant payloads from lander (mining vehicles, process payload pallet structure, photovoltaic power systems and regenerative fuel cell power systems). Load all but mining vehicles on transporters.

5. Offload from lander, function check and activate lunar surface telerobotic servicers.

6. Transport payloads to site.

7. Set-up mining site equipment.
a) Function check mining vehicles and transport to pilot plant site.
b) Begin mine site preparation, overburden removal, roadways, etc.
c) Offload transport, position, and place mine site pit scalper.

8. Set-up process plant structure.
a) Offload transporter, position, and place process structure (Shuttle payload pallet) in vertical position, attach to anchoring hardware (perhaps deploy guy-wires as well).
b) Deploy equipment outside payload bay envelope (feed and disposal bins, communications antennas, remote manipulator arms and transporters, handrails and walkways.

9. Set-up photovoltaic power system.
a) Offload transporter, position, and place all photovoltaic power modules and systems (4 of the sun-tracking, double panel arrays shown in Figure 6-3 are required).
b) Deploy electrical cabling.
c) Make electrical connections between panel power converters and process plant.
d) Make electrical function checks of power and process equipment.
e) Make communications/data links function checks.

10. Set-up central thermal control system.
a) Offload transporter, position, and place central thermal control system and sun-screen.
b) Make interface connections with process structure.

11. Set-up liquid oxygen and liquid hydrogen storage systems.
a) Offload transporter, position, and place LOX storage tanks and LH_2 tank.
b) Make piping connections.
c) Bury tanks.

12. Set-up regenerative fuel cell system.
a) Offload transporter, position, and place regenerative fuel cell system.
b) Make connections to PV power and process electrical systems.
c) Function check systems.

13. Set-up LOX loading systems.
a) Offload transporter.
b) Construct LOX loading station equipment.

14. Startup operations.
a) Startup mining and processing operation.
b) Work out and repair startup problems.

15. Set-up spares/miscellaneous support facilities.
a) Offload spares shed and construct.
b) Offload spares, tools, lighting, etc. and place in shed.

The following is a rough estimate of manhours required to complete these tasks. Some task times are extracted from a previous operations study (84).

Task No.	Task Time (hr)	Telop Time (hr)	EVA Time (hr)	Number of EVA Personnel	Total EVA (man-hrs)	Comments
1	3		3	2	6	From (84).
2a	2		2	2	4	Assumed 100 m^2 area. From (84).
2b	4	2	2	2	4	Assume use teleoperated excavation equipment controlled from lunar lander.
3	6	4	2	2	4	Assume 1 anchor drilled/placed every 30 minutes, assume 4 anchors for process equipment, 2 anchors/PV array, 4 PV modules.
4	18		18	2	36	Assume 7 major payloads (process, RFC, PVs, 1 Thermal, 2 Mining vehicles, 1 Tank Set). 2.6 hrs/offload (84)
5	2		2	2	4	
6	5		5	2	10	7 major payloads, 40 min/transport (84).
7a	6	4	2	2	4	Teleop veh.: Function chk 2 hr/veh IVA, 1 hr/veh EVA.
7b	8	8				
7c	5		5	2	10	Teleop veh.: 2 hr/100 m^2, 400 m^2
8a	5		5	2	10	Offload 3 hrs, Position 1 hr, Place 1 hr
8b	4		4	2	8	Offload 3 hrs, Position 1 hr, Place 1 hr Assume 16 pcs, 30 min/pcs
9a	5		5	2	10	Offload 3 hrs, Position 1 hr, Place 1 hr
9b	2		2	2	4	
9c	12		12	2	24	6 connections, 2 hr/connection
9d	10	8	2	2	4	Function chk, teleop most from base/Earth
10a	5		5	2	10	Offload 3 hrs, Position 1 hr, Place 1 hr
10b	4		4	2	8	2 connections, 2 hr/connection
11a	5		5	2	10	Offload 3 hrs, Position 1 hr, Place 1 hr
11b	2		2	2	4	1 connection, 2 hr/connection.
11c	2	2				Bury assume teleop
12a	5		5	2	10	Offload 3 hrs, Position 1 hr, Place 1 hr
12b	2		2	2	4	1 connection, 2 hr/con.
12c	2	2				Function chk, teleop from base/Earth
13a	5		5	2	10	Offload 3 hrs, Position 1 hr, Place 1 hr
13b	2		2	2	4	1 connection, 2 hr/con
14a	8	8				Startup Mining, process, all teleop
14b	104	96	8	2	16	Continue Startup cycle 4 days straight, teleop from Earth, fix problems via lunar EVA.
15a	5		5	2	10	Offload 3 hrs, Position 1 hr, Place 1 hr
15b	4	4				Unload spares remotely.
Total	252	138	114	2	228	

The total EVA time estimate of 228 person-hrs corresponds to 19 two-person 6-hr EVA's. Assuming that a 4-person crew is capable of supporting a 6-hr two-person EVA every 24 hrs (84), a 4-person mission that devotes almost 3 weeks exclusively to pilot plant setup and startup support is required. Assuming 2 days for landing day and launch day checks (84) and 6 days in transit, a minimum of a month long mission is indicated.

Operation

Pilot plant operation is performed by teleoperation control from Earth during the man-tended base phase. The alternative to teleoperation is to operate the pilot plant only when humans are at the base. However, expected data requirements for supporting the optimum design of a production plant (see Section 6.1) can not be acquired in short pilot plant campaigns. Therefore, operation of the pilot plant without continuous on-site human involvement was baselined. Advancement of the state-of-the-art in automation, robotics, and teleoperation is required, particularly for the mining vehicles. To compensate for the 3-second communications delay, these vehicles need extensive on-board computation capability to perform many functions nearly autonomously, with only supervisory control exercised by Earth teleoperators (90). Maintenance functions are performed by telerobotic lunar surface servicers (84). Design of the plant and power equipment will require special consideration to allow remote maintenance.

Shortly before crews return to the lunar base, the pilot plant will be commanded to go through a shutdown cycle in preparation for intensive on-site inspection and maintenance by the crew. A budget of 84 EVA-hrs (or 7 two-person 6-hr EVAs) would allow ample time for these inspections and maintenance chores. Upon completion of the human inspection/maintenance tasks, the pilot plant should (via Earth teleoperations) commence its startup cycle so that crew are available to perform EVA support of the startup. As with tasks 14a and 14b above, budgeting 16 EVA-hrs should be sufficient to support a 4 day (96 hr) Earth controlled startup cycle.

6.6.2 Production Plant

The production plant basis is 180 mt/year LOX using basalt feedstock and powered by a nuclear-electric source (460 kwe). The mass of this plant (including power) is 50 mt.

Setup

A setup time of 460 EVA-hrs is estimated for this production plant based on the estimated pilot plant setup requirements from the previous section, scaled with the ratio of plant masses (pilot plant mass is 24.7 mt).

Operation

The operation philosophy of the production plant remains nearly the same as the pilot plant. Since techniques for remote operation should have been perfected during pilot plant operation, Earth teleops control of the day-to-day operation of the plant should be possible. However, since the plant operates during the permanently occupied base period, maintenance provided by telerobotic servicers can be backed up by ready access to human support. Therefore, a 2-man maintenance crew is baselined for this support. The crew would work standard 5-day weeks, 8-hr/day. Crew relief would occur every 180 days (83). The crew would be equipped for possible EVA although direct teleoperated

control of the surface servicers and repair tasks in a pressurized maintenance shop may be their normal operating mode.

Consumables and Hardware Resupply

Makeup for hydrogen losses will require resupply from Earth. A correlation of computer program predictions was made to relate LH_2 resupply requirements and LOX production rate:

$$LH_2 \text{ Required (kg/yr)} = 0.97 * \text{LOX Production (mt/yr)} + 0.5$$

Hardware resupply and equipment spares will also be required. Spares for high maintenance items such as for rotating equipment components, mining and solids handling equipment components, and electronics will mainly be needed. Although total mass of these items is not expected to be greater than 1-2% of plant mass per year (based on 5%/yr replacement of equipment mass for mining, crushing/grinding, screens, magnetic separator, electric heater, electrolysis cell, compressors, conveyors, and radiator/thermal control system), additional study is needed to better quantify the expected amount of hardware resupply.

6.7 Preliminary Assessment of Lunar Oxygen Production

A previous analysis (48) of lunar oxygen production for a 1,400 mt/yr low Earth orbit (LEO) LOX market concluded that LOX delivery to a LEO market from the Moon cannot compete with a low-cost Earth heavy-lift launch system. Many assumptions were made in the analysis, including the mass and manpower requirements of the lunar LOX and LH_2 production plants. The model developed for the original analysis has been updated with the production plant mass and power sizing relationships developed in this study. The LEO market case was repeated, and results are given in the Tables in Appendix E. It should be noted that the payback period and lifetime program savings for using lunar oxygen for reusable lunar landers was not analyzed in this study; but it is highly recommended that it should be analyzed using the concept of fully-integrated process modules and plant mass correlations developed in this study.

A LEO market of 1,400 mt/yr LOX was used in the analysis (Table 1 in Appendix E gives a breakdown of LEO LOX users). Several cases were examined with various propulsion technologies (including conventional LOX/LH_2 propulsion and advanced: solar sail, electric, and mass driver) and lunar LOX and LH_2 production. Table 2 in Appendix E describes parameters of the production plant while Tables 3-6 characterize the Earth launch, orbital transfer vehicles (OTV's), and lunar landers. Only the LOX/LH_2 production plant parameters were adjusted for this analysis. In particular, the number of personnel required for LOX/LH_2 production was decreased substantially (from 20-50 to 2-4 depending on production rate) to reflect assumed Earth teleoperations mode of the plants with only lunar on-site maintenance support.

The results of the analysis did not change significantly from the previous study. Basically, the reasons for this are due to lunar surface to LEO transportation efficiency, not LOX/LH_2 production efficiency. A brief discussion of the results is included here, but additional information can be attained in the previous report (48). The first major comparison of each case is the steady-state mass payback ratio (Table 7, Appendix E) which is the ratio of lunar LOX delivered to LEO to the hydrogen (and tankage) sent from LEO. The reason for calculating this ratio is to determine if the mass of lunar oxygen delivered to LEO is greater than the LH_2 needed to operate the system. It is fixed by the characteristics of the spacecraft used in the transportation system. The steady-state mass payback ratio is infinite for the case of both lunar oxygen and hydrogen production because no LH_2 from Earth is needed for servicing the OTV's and lunar landers. For the case of only lunar LOX production and conventional LOX/LH_2 propulsion systems, a mass payback ratio of 1.63 was calculated, meaning that 63% more oxygen is delivered to LEO than hydrogen used in the OTV's and lunar landers needed to deliver that oxygen. This ratio depends on the size of the transportation vehicles used. In this case, an OTV that delivers 50 mt LOX to LEO requires 12.5 mt LH_2 for each roundtrip. The lunar landers that deliver the 50 mt LOX to a LLO rendezvous with this OTV require 12.6 mt LH_2 (which is contained in 5.4 mt of tankage).

Lifetime mass payback is another ratio calculated by the model (Table 8, Appendix E). This ratio includes the mass of the lunar production plants, resupply, and crew and base support to determine if the total mass of lunar LOX produced is greater than the total mass required over the lifetime of the propellant plants. A 20 year lifetime was selected for this analysis, over which 27,000 mt LOX is delivered to LEO (20 yrs for a 1,357 mt/yr LEO market). The lunar surface propellant plant is sized to produce additional oxygen for the propellant carrier OTV's and landers. The amount of lander and OTV oxygen required depends on whether lunar hydrogen is available. If lunar hydrogen is not

available, more lander/OTV trips and more oxygen are needed to deliver LH_2 to the lunar surface (LS) for the lunar landers. If both lunar oxygen and hydrogen are produced, 1.17 mt of oxygen is needed for the transportation system per metric ton of oxygen delivered to the LEO market. For lunar oxygen only production, more OTV/lander flights are required to deliver the same amount of LEO propellant, which translates into the need for 3.52 mt of oxygen per metric ton of oxygen delivered. Thus, for the lunar oxygen only case, a 6,140 mt/yr lunar LOX plant is needed. Lunar LOX production of 2,940 mt/yr is needed if both lunar oxygen and hydrogen are produced. The lifetime LOX market is 123,000 mt for the lunar oxygen only case and 58,800 for the lunar oxygen and hydrogen case.

With the correlations developed in this report, a 1,150 mt LOX plant (assuming a basalt-fed plant) is needed to supply the 6,150 mt/yr LOX requirement for the oxygen only case. For lunar oxygen and hydrogen, both a 430 mt LOX plant (producing 2,300 mt LOX/yr) and a 1,120 mt LH_2 plant (producing 375 mt LH_2/yr and 640 mt LOX/yr) are required. In both cases, an additional 35 mt of base elements was assumed required to support the plant maintenance crew. To deliver the base and plant components to the lunar surface, 5.8 mt of propellant is required in LEO for OTV/lander spacecraft per metric ton of base/plant. Thus, the LOX only case requires 8,040 mt in LEO for delivery of plant and support base, while 10,810 mt is needed for the LOX/LH_2 case. Plant resupply mass was estimated as 12 mt/yr and 16 mt/yr for the LOX only and the LOX/LH_2 plants, respectively. The maintenance crew of four was assumed to require 1.1 mt/yr per person (for both plants). Over the 20 year lifetime, a total of 325 mt (for the LOX only case) and 410 mt tons (for the LOX & LH_2 case) are needed on the lunar surface for crew support. A total lifetime requirement of 16,610 mt LH_2 (and tankage) is needed in LEO for OTV's and landers if only lunar oxygen is available (of course, no LH_2 is needed in LEO if both lunar oxygen and hydrogen are available). To summarize the lifetime mass results:

Lifetime propellant production (20 yrs) on Moon vs. LEO outbound mass requirements (from Earth):

	Lunar LOX only	Lunar LOX and LH_2
LOX Production (mt)	122,800	58,800
LH_2 Production (mt)	0	7,500
Total Propellant (mt)	122,800	66,300
Plant/Base (mt)	1,180	1,590
LEO Propellant to transport Plant/Base to LS (mt)	6,860	9,220
Crew/Hardware Support (mt)	330	410
LEO LH_2 (mt)	16,610	0
Total LEO (mt)	24,980	11,220
Lifetime Propellant Production /LEO Outbound Mass	4.9	5.9

Lifetime LEO outbound mass vs. LOX market in LEO (Lifetime Mass Payback Ratio):

	Lunar LOX only	Lunar LOX and LH_2
LOX Market (mt)	27,100	27,100

	Lunar LOX only	Lunar LOX and LH_2
Plant/Base (mt)	1,180	1,590
LEO Propellant to transport Plant/Base to LS (mt)	6,860	9,220
Crew/Hardware Support (mt)	330	410
LEO LH_2 (mt)	16,610	0
Total LEO (mt)	24,980	11,220
Lifetime Mass Payback Ratio	1.09	2.4

This analysis does not include the inert mass of the extra OTV's and landers needed for propellant carriers. Even so, it shows that it is not viable (over a 20 year period) to produce lunar oxygen for a LEO market if only lunar oxygen is produced, since the lifetime mass payback ratio is just over one (saving only 2,000 mt or 100 mt/yr in LEO). It also shows that the results are much more dependant on transportation efficiencies (propellant requirements) than the mass of the propellant plants and crew support.

There are possible alternatives to improve the results. This analysis has assumed that the entire propellant plant is delivered to the lunar surface before oxygen production starts. A phased approach to oxygen production may yield significant savings for the lunar oxygen only case; i.e. first delivering a small oxygen plant producing oxygen for the lunar landers, then using that oxygen to reduce the costs of transporting a larger plant to produce oxygen for the OTV's, then delivering a third production increment to supply the LEO market. This approach was not treated but probably should be.

At the next level of the analysis, transportation costs are calculated (Tables 9-11, Appendix E), which include the operations costs for Earth launch vehicles, OTV's, and lunar landers that support propellant production. The purpose is to see if the steady-state operations costs for the LS to LEO LOX delivery system are less than anticipated costs for providing the LEO LOX market from Earth with advanced launch vehicles. Total system lifetime costs are determined at the next level, which include development, plant/base placement, and resupply costs (Tables 12 and 13, Appendix E). Summarizing:

Cost ($/kg LOX delivered to LEO)	Lunar LOX only	Lunar LOX and LH_2
Transportation Cost	2,370	960
Lifetime Cost	4,080	3,130
Estimated Earth Launch Costs to LEO:		
Shuttle	4,800	4,800
Large Shuttle Derived Vehicle	1,410	1,410

Many assumptions are made in the cost numbers, however, the results tend to indicate that given the assumptions made in the study (non-phased approach to supplying LOX

market, etc.) it is difficult to supply LOX to a LEO market at less than competing Earth launch systems.

Based on the above analysis, it is recommended that two additional cases be studied: 1) To determine if lunar oxygen for the reusable landers alone has a reasonable payback period and overall program mass and cost savings, and 2) If a phased approach to lunar oxygen production can be shown to be economical for supplying a LEO oxygen market. Current transportation cost estimates would be used in these additional analyses (especially to incorporate new studies of Earth launch costs), since costs were not updated in this preliminary analysis.

In the first study of lunar LOX for the landers, the LOX plant would be sized to supply an annual schedule of 5-7 lunar lander flights, requiring 130-180 mt LOX/yr (50). At 180 mt LOX/year, a 50 mt plant would produce its own mass in oxygen within 4 months. Costs of operating/supporting the plant over its lifetime will be a key number that determines whether the payback is sufficient to justify proceeding with lunar oxygen. A sensitivity analysis on operating costs could be used to determine the maximum operating cost that would still achieve the desired result. This might indicate whether minimizing the number of operating personnel by automation, robotics, and teleoperation as proposed in this report is really necessary and by how much.

It should also be noted that there are other benefits, less easily evaluated in an economic sense, for lunar oxygen production, including:

1. Lunar oxygen production is a first step toward self-sufficiency and independence. This should be encourage in a scenario that results in a permanent lunar base.

2. To test and demonstrate propellant extraction techniques for later application at other extraterrestrial locations. A major part of a Martian atmospheric oxygen plant could be verified in a lunar application. Various pieces of lunar oxygen production and Mars in-situ oxygen production equipment are similar, including solid-state electrolysis cells, oxygen liquefaction, oxygen storage, oxygen loading, and power system components (PV arrays, regenerative fuel cells, and/or nuclear power). Hardware for purifying the oxygen product stream and measuring composition may be similar. Operations techniques would also be developed in a lunar setting.

3. A lunar soil transportation system (excavators/haulers) will probably be developed for other tasks at the lunar base (eg. to provide radiation protection for modules). A great deal of synergism is anticipated in the designs for these vehicles and a version to mine feedstock for a lunar oxygen plant. Development costs could be split between these design efforts, and costs will be lower for each project. Such vehicles would have uses at a Mars base as well.

4. Lunar oxygen has potential commercial application. Chemical and mining companies could get involved in commercial development if NASA is willing to buy oxygen at a fixed price and quantity.

7.0 Hydrogen Extraction

This section presents the major results of sizing a plant to extract both oxygen and hydrogen from lunar materials. The basis of the plant is thermal extraction of solar wind hydrogen from bulk lunar materials. Simultaneous reaction of a portion of the released hydrogen with ilmenite forms water, which is subsequently electrolyzed to form hydrogen and oxygen.

7.1 Pilot Plant Conceptual Design

7.1.1 Process Flowsheet

Figure 7-1 illustrates a block diagram of the process. Lunar material is mined and loaded into a reactor after large (>1 cm) particles are removed. Soil is heated in the reactor to 900°C to release hydrogen and produce water from reaction with ilmenite. Because of the minuscule hydrogen content in bulk lunar soil (50 ppm), approximately 25,000 kg soil is required per kg of hydrogen recovered. Thermal energy requirements are large. Therefore, a long, multi-stage, insulated reactor vessel, similar to the proposed ilmenite reactor (Section 4.1.1), is used to recover thermal energy by preheating the solid charge in the upper stages with the hot evolved gases from the reaction zone, and by cooling the spent residual solids in lower stages by preheating the incoming gas stream.

Product gases from the reactor contain H_2O, H_2, and H_2S. The water is electrolytically separated into oxygen and hydrogen. A portion of the hydrogen is heated and returned to the reactor. Oxygen and the remainder of the hydrogen is cooled, liquefied, and stored. Sulfide impurities can be removed either prior to or after the electrolyis step.

Sintered ceramic products can be manufactured as a byproduct of the process since the temperatures for soil sintering fall within the range for hydrogen extraction. Sintered products could be useful as structural and thermal/radiation shielding materials. The sintering process has been demonstrated at the laboratory scale.

Figure 7-1. Hydrogen Extraction Process Block Diagram

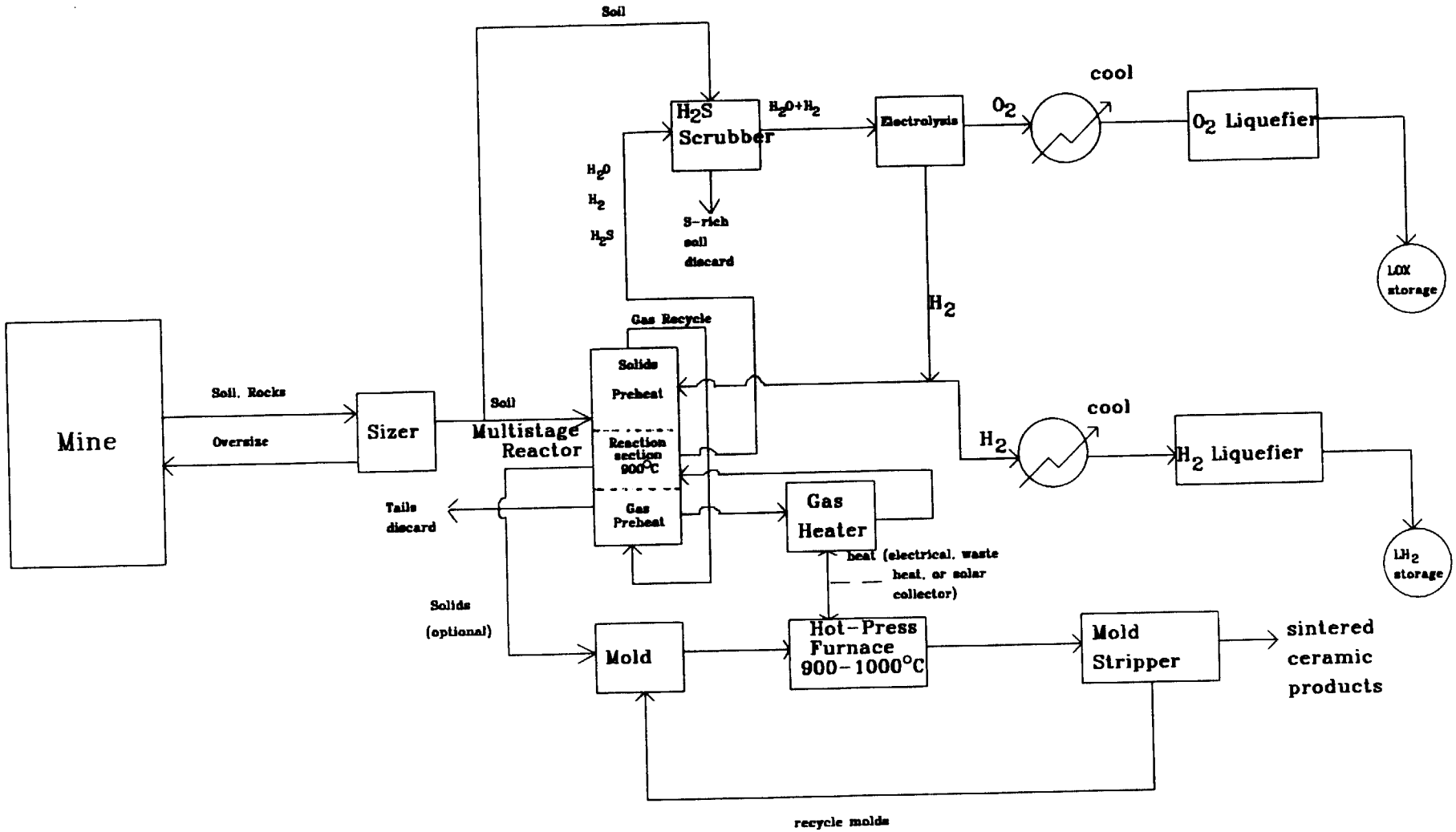

7.1.2 Pilot Plant Equipment

The equipment necessary to produce 14 metric tons LH_2/year and 24 metric tons LOX/year (2 metric tons LOX/month) is listed in Table 7-1. Total pilot plant mass is 60 metric tons, including a nuclear power plant producing 1.7 MW_e. Appendix C and D provides details of the calculations for the various units. The plant is divided into three major areas: mining, process, and power. An additional mass and power margin is added to account for miscellaneous equipment and structure.

Mining

Large amounts of mature (hydrogen-rich) lunar soil must be processed. At the 900°C temperature selected for the pilot plant hydrogen extraction reactors, 25,000 metric tons of lunar soil is required per metric ton hydrogen produced, given the basis of 50 ppm H in bulk soil and the hydrogen/water release curves shown in Figures 5-2 and 5-3. This requires processing the soil in a 300 m x 300 m x 2 m deep pit to produce 14 metric tons LH_2 over a year of pilot plant operation. Due to their flexibility, front-end loaders and self-propelled haulers were selected for this operation since they could potentially be applied to other lunar base surface operations. Other surface mining alternatives, such as three-drum drag scrapers (89), offer the possibility of mass/power savings but at the cost of flexibility. Another alternative is to process the soil in place (in-situ) using a mobile processing plant. However, providing the power supply for an in-situ processing plant would be challenging.

Process

As given in Table 7-1, the hydrogen extraction units are the largest individual contributor to the process mass. The calculation was based on splitting the feed to two reactors operating in parallel, since the required wall thicknesses/reactor mass decreases with reactor diameter and feed rate. For purposes of the conceptual design, reactor temperature was limited to 927°C (1700°F). This approximates the upper limit for uncooled pressure vessels made of aerospace qualified super alloys such as Inconel 600 or X-750 (107, 108). About 80% of the hydrogen is released at this temperature (Figure 5-2). The temperature is sufficiently high such that hydrogen reacts with ilmenite in the soil to form H_2O (Figure 5-3). Although the proposed process requires the presence of ilmenite, all lunar soils will typically contain sufficient ilmenite to react with the available hydrogen. For a maximum plausible hydrogen content of 120 ppm, only 0.9 weight percent or 0.6 volume percent ilmenite is required for complete reaction. Typical ilmenite-poor Apollo 14-17 highland rocks, from which highland soils are produced, contain at least 1 percent by volume ilmenite. The ferrous oxides contained in other minerals (pyroxenes, olivines) may also be reduced by hydrogen.

A multistage gas/solid counter-current flow reactor is required for energy efficiency. Even for this conceptual design, where 50% of the thermal energy required to heat the incoming soil (0.3 kw-hr/mt soil-°C) is recovered in the multistaged-reactor, over 6 MW of thermal and electrical power is needed just for the extraction step of the pilot plant.

Water of reaction is electrolyzed in a ceramic-electrolyte cell operating at reaction temperature (900°C). The majority of the hot hydrogen gas from the cell is returned to the reactor to preheat the soil feed. Additional energy is added in a heater to supply reactor heat requirements and makeup radiation losses. An inert gas may be required to reduce the gas temperature exit this heater.

Sulfide impurities are removed prior to the electrolysis step by passing the product gas through a bed of raw (cold) soil where hydrogen sulfide reacts with free iron to form troilite (FeS) and hydrogen. An alternative is to remove sulfur after the electrolysis step by selectively condensing out SO_2 from the oxygen stream.

Power

Because of the large power requirements, a nuclear power source was selected for the pilot plant. This allows a 90% plant duty cycle for both lunar day and night processing. Soil mining and transport was limited to day only with a 35% duty cycle. Since the nuclear power source is 5-10% efficient, large amounts (22 MWt in this case) of high quality waste heat (900°K) is generated during power generation (105). The pilot plant conceptual design assumes that 75 percent of the process reactors' 6 MW power requirement is supplied by a suitable heat transfer system from the nuclear power generator's waste heat, while the remainder is supplied by electric heater.

Table 7-1. Hydrogen Extraction Pilot Plant Equipment List
Basis: 14 mt/yr LH_2, 24 mt/yr LOX, 90% process duty cycle, 35% mining duty cycle.

Item	Total Mass (kg)	Total Elect. Power (kwe)	Dimensions (each unit) W/D (m)	L (m)	H (m)	V (m^3)	Comments
Front End Loaders (3)	7,743	65.8	2.3	3.3	2.3	17.2	0.7 m^3 bucket.
Haulers (5)	5,080	18.6	2.5	4	2.5	25	4.5 m^3 bed.
Mining Total	12,823	84.4				177	Mine/transport 29,364 mt/month soil at 35% duty cycle.
Feed Bin	370		6.1	6.1	1.2	45	Stores 4 hrs of reactor feed.
Discharge Bin	370		6.1	6.1	1.2	45	
H_2 Extract Reactors (2)	16,620		2.9		9.2	60	Includes 0.3 m insulation all around. 927°C operational temperature. Total 177 kwt heat loss.
Heat Transfer Equip.	831	1,557					Provides electrical heat requirements for extraction reactor. 4,670 kw thermal also provided by heat exchange with power system.
Gas Purification Equip.	267						Removes hydrogen sulfide.
Electrolysis Cell	107	16.8	0.5	0.5	0.8	0.2	High-temperature solid-state electrolysis.
Oxygen Liquefier	73	1.7	0.3	0.9		0.1	2.9 kw total heat rejection required.
Hydrogen Liquefier	86	36.3	0.3	1.0		0.1	45.3 kw heat rejection.
LOX Storage Tanks (2)	299		1.9			3.5	3 months LOX storage (6 mt LOX).
LH_2 Storage Tanks (2)	1,311		3.4			20	2 month LH_2 storage (2.3 mt LH_2).
Thermal Control System	3,002		6	25			Radiator rejects 48.2 kwt at 290°K.
Process Total	23,336	1,611					Also requires 4,670 kw thermal power from nuclear reactor waste heat.
Margin	10,848	41.7					Contingency factor (30% of process+mining mass, and 30% of power net the extraction reactor power req.) redundancy, spares, process structural components, A&R, and other miscellaneous factors.
Total Mining & Plant	47,007	1,737					
Nuclear Power	12,970						Generates 1,737 kwe, rejects 22,427 kwt (of which 4,670 kwt contributed to reactor thermal requirement). Includes mass of reactor, radiator, power converter, and instrument-rated shielding.
Total Plant & Power	59,977	1,737					

7.1.3 Optional Process to Produce Sintered Ceramic Products

A process to mold sintered products can be integrated into the hydrogen extraction equipment since sintering temperatures are nearly the same as extraction temperatures. In sintering, granular materials are bonded into solids at temperatures below their melting point without the addition of binding agents such as cement, plastics, or fluxes. Thermal bonding occurs naturally on the lunar surface. Several meter thick breccia layers have formed from lunar soil components as a result of the heat generated by meteorite impacts. Petrographic studies by McKay and Morrison (109) demonstrated that bonding occurs by the welding together or sintering of fine glass particles in the soil. Studies of returned lunar material and vitreous simulates by Simonds (110) and Uhlmann et al. (111) quantified the process.

The principal requirement for a sinterable lunar soil is that it contain a substantial amount of glass. This is true of most lunar soils which typically contain at least 30% glass, occuring both as glassy fragments and as glass-bonded aggregates called agglutinates. Glass fragments range in size from 5 microns to several millimeters with an average approximately the same as the bulk soil or 0.08 mm. Average agglutinate size also approximates the soil average, although particle size ranges from 0.01 mm to several centimeters (4).

Depending on glass composition, temperatures must be controlled in a range spanning approximately ±100°C that will allow rapidly sintering but be below the glass crystallization temperature. The process of sintering comes to a halt once the glass is crystallized (111, 113). Figure 7-2 shows the time and temperature required for sintering a variety of lunar soil compositions. Low titanium mare basaltic soil compositions characteristic of the Apollo 12 and 15 landing sites have the lowest sintering temperature (810°C for 1000 sec). High titanium mare soils found at the Apollo 11 and 17 landing sites have the next most sinterable compositions (910°C for 1,000 sec), while the aluminous soils of the highlands observed at Apollo 14 and 16 require the highest sintering temperatures (930°C for 1000 sec). The curves in Figure 7-2 were derived from an equation describing sintering (112):

$$X/r = (3 \tau t / 2 \pi n r)^{1/2}$$

where X is the radius of the neck between coalescing grains, r is the grain radius, τ is the surface tension (~300 erg/cm^2 for typical silicate glasses), t is time in seconds, and n is viscosity in poise. Viscosity data for lunar glasses are summarized in Figure 7-3 (114). Typical compositions for these glasses are given in Table 7-2.

Design Concept

A small flow of solids that is withdrawn from the high-temperature (900°C) region of the multistaged fluidized-bed reactor can be used as the feedstock for the ceramic making equipment. The solids would be loaded into a mold and transferred to a furnace where they would be maintained within the sintering temperature range. A low-porosity part can be formed by hot-pressing, applying either mechanical or gas pressure, during sintering. After formation, the part is removed from the mold and the mold recycled. The mass penalty for sintering equipment is not expected to be large. A sinter plant consisting of the molds, furnace, and other equipment to produce 5 mt/day of ceramic products was estimated to mass under 500 kg (49). Hot-pressed blocks could be used as high-density radiation protection for pressurized modules. Other uses for sintered products include mounts, supports, and road-building materials.

Figure 7-2. Time/Temperature to Sinter Lunar Soils

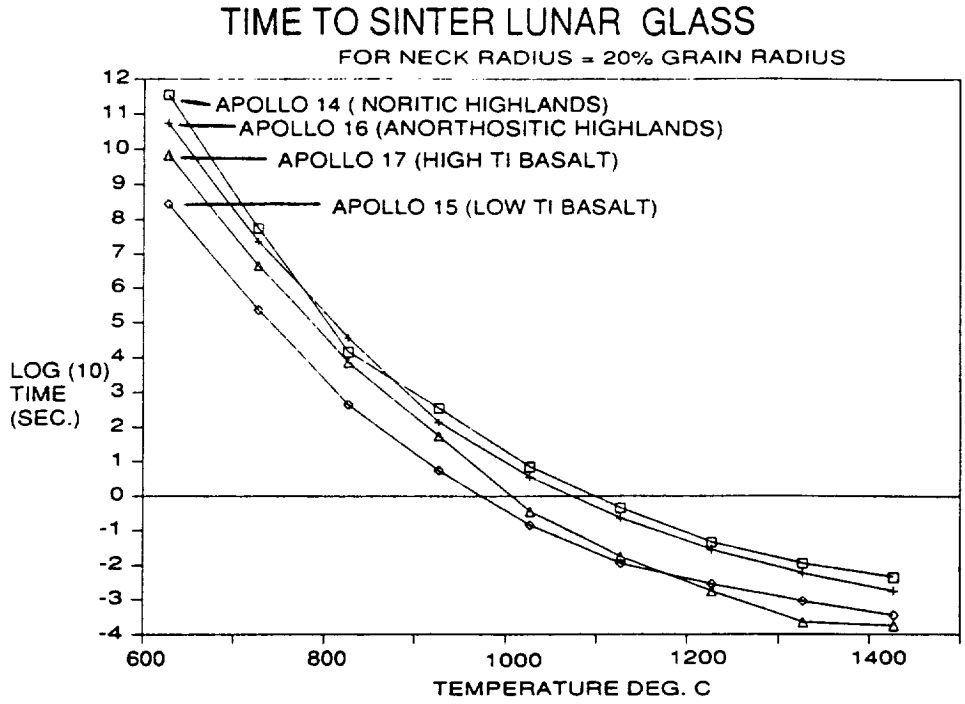

Figure 7-3. Viscosity of Lunar Glass as a function of Temperature (Ref. 114)

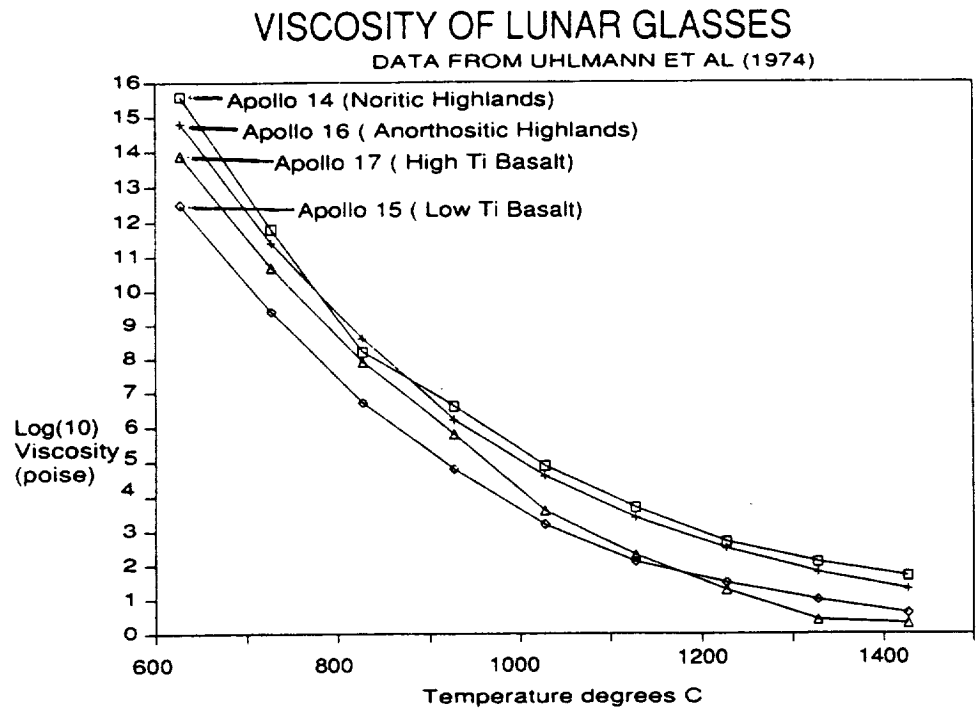

Table 7-2. Composition of Lunar Soils (Ref. 4)

	Mare		Highlands	
	Hi-Ti	Lo-Ti	Noritic	Anorthositic
	10084	12041	14003	61160
Chemical Comp. (Wt.%):				
SiO_2	41.0	46.8	48.1	44.7
TiO_2	7.3	2.7	1.8	0.6
Al_2O_3	12.8	15.4	17.6	26.3
Cr_2O_3	0.3	2	0.3	1.0
FeO	16.2	14.2	10.5	5.3
MnO	0.2	0.2	0.1	0.7
MgO	9.2	9.1	9.3	6.4
CaO	12.4	10.9	11.1	16.2
Na_2O	0.4	0.4	0.7	0.4
K_2O	0.2	0.3	0.5	0.1
Total	100	102	100	101.7
Modal Comp. (Vol.%):				
Lithic Fragments				
Mare Basalt	24.0		1.3	0.3
Highland Rocks	2.3		20.5	10.1
Dark Breccia	7.5		3.0	28.6
Agglutinates	52	58	60.3	37.0
Mineral Fragments				
Pyrox.& Olivine	4.2	15	3.6	2.6
Plagioclase	1.9	1	2.3	14.7
Opaques	1.1			
Glass				
Orange/Black	2.7			
Yellow/Green	0.8			
Brown		23	4.8	3.1
Clear	1.3		4.3	0.7
Devitrified	1.8			
Others	0.3			
Total	99.9	97	100.1	97.1

7.2 Trade Studies

The effect on plant mass and power of extraction temperature, solar vs. nuclear power source, and heat recovery options are described in the following sections.

7.2.1 Extraction Temperature

The amount of hydrogen evolved depends on temperature as given in Figure 5-2. More hydrogen is generated at higher extraction temperatures, which means less soil processing and reduced equipment volumes/mass for a given hydrogen production rate goal. However, energy requirements increase with extraction temperature. The trade-offs in soil and power requirements with extraction temperature are described in this section.

Table 7-3 shows the amount of soil required and the ratio of oxygen/hydrogen produced as a function of extraction temperature based on gas release curves given in Figure 5-2 and Figure 5-3. Total plant and power system mass for producing 1 mt/month LH_2 is minimized with a 600-700°C extraction temperature as given in Figure 7-4. The basis of this trade was:

- Nuclear power.
- 90% process duty cycle, 35% mining duty cycle.
- 50 ppm H in bulk soil.
- 50% of thermal requirements to heat soil feed is recovered in the multistage reactor.
- 75% of remaining reactor heat requirements supplied by nuclear power waste heat.

Figure 7-4 shows that the mass of mining equipment decreases with increasing extraction temperature since less mining is required. However, even though the size of the extraction reactors decreases as the extraction temperature increases, the reactor shell mass tends to increase because yield strength of containment materials declines at higher temperatures and denser reactor shell materials must be used (see Table 7-4).

As temperature increases, more oxygen is produced from the water product of hydrogen reduction of ilmenite. Figure 7-5 represents the expected oxygen to hydrogen recovery ratio based on several passes of hydrogen through the reaction bed and simultaneous water removal by electrolysis. More oxygen can be removed given enough ilmenite and additional hydrogen passes. However, it is obvious that higher temperatures are preferred for oxygen extraction. As shown in Figure 7-6, total mass of plant and power system for a 2 mt/month LOX pilot plant is minimized for extraction temperatures above 1000°C.

As a compromise between efficient hydrogen and oxygen recovery, a maximum temperature of 927°C (1,700°F) was selected for the H_2 pilot plant extraction reactors.

Another option not examined in this study is to extract hydrogen from bulk soil at a lower, more H_2-efficient, temperature (600°C), then react the recovered hydrogen with concentrated ilmenite at higher, O_2-efficient, temperatures (900-1100°C). Ilmenite beneficiation equipment and more reactors would be required, but total system mass savings, especially for high capacity plants, may justify the added complexity (and potentially lower reliability).

Table 7-3. Soil-Mining Requirements for Hydrogen Extraction Plant (Basis: 50 ppm H in bulk soil, Figures 5-2 and 5-3 gas release, water separated into O_2 and H_2, and H_2S discarded)

Extraction Temperature (°C)	Oxygen/ Hydrogen Ratio (mt O_2/mt H_2)	Soil/ Hydrogen Ratio (mt soil/mt H_2)	Soil/ Oxygen Ratio (mt soil/mt O_2)
427 (800°F)	0.43	57,512	134,124
527 (980°F)	0.67	33,181	49,299
627 (1160°F)	0.93	28,801	30,902
727 (1340°F)	1.19	27,269	22,895
827 (1520°F)	1.45	26,110	17,971
927 (1700°F)	1.70	25,012	14,682
1027 (1880°F)	1.93	23,943	12,397
1127 (2060°F)	2.13	22,845	10,723
1227 (2240°F)	2.30	21,716	9,421
1327 (2420°F)	2.45	20,471	8,354

Table 7-4. Reactor Shell Materials' Yield Strength (Ref.107,108)

Extraction Temperature (°C)	Shell Material	Room Temperature Yield Stress (MPa)	Ratio of Yield Stress @ Temp. and R.T. Yield Stress
227 (440°F)	Aluminum (2219-T87)	352	0.54
327 (620°F)	Inconel (600 or X-750)	1034	1.0
427 (800°F)	Inconel	1034	0.91
527 (980°F)	Inconel	1034	0.89
627 (1160°F)	Inconel	1034	0.81
727 (1340°F)	Inconel	1034	0.48
827 (1520°F)	Inconel	1034	0.33
927 (1700°F)	Inconel	1034	0.18
1027 (1880°F)	Mo-.5% Ti or TZM alloy	517	0.45
1127 (2060°F)	Molybdenum alloy	517	0.21
1227 (2240°F)	Molybdenum alloy	517	0.15
1327 (2420°F)	Molybdenum alloy	517	0.1

Figure 7-4. Effect of Extraction Temperature for Constant LH_2 Production

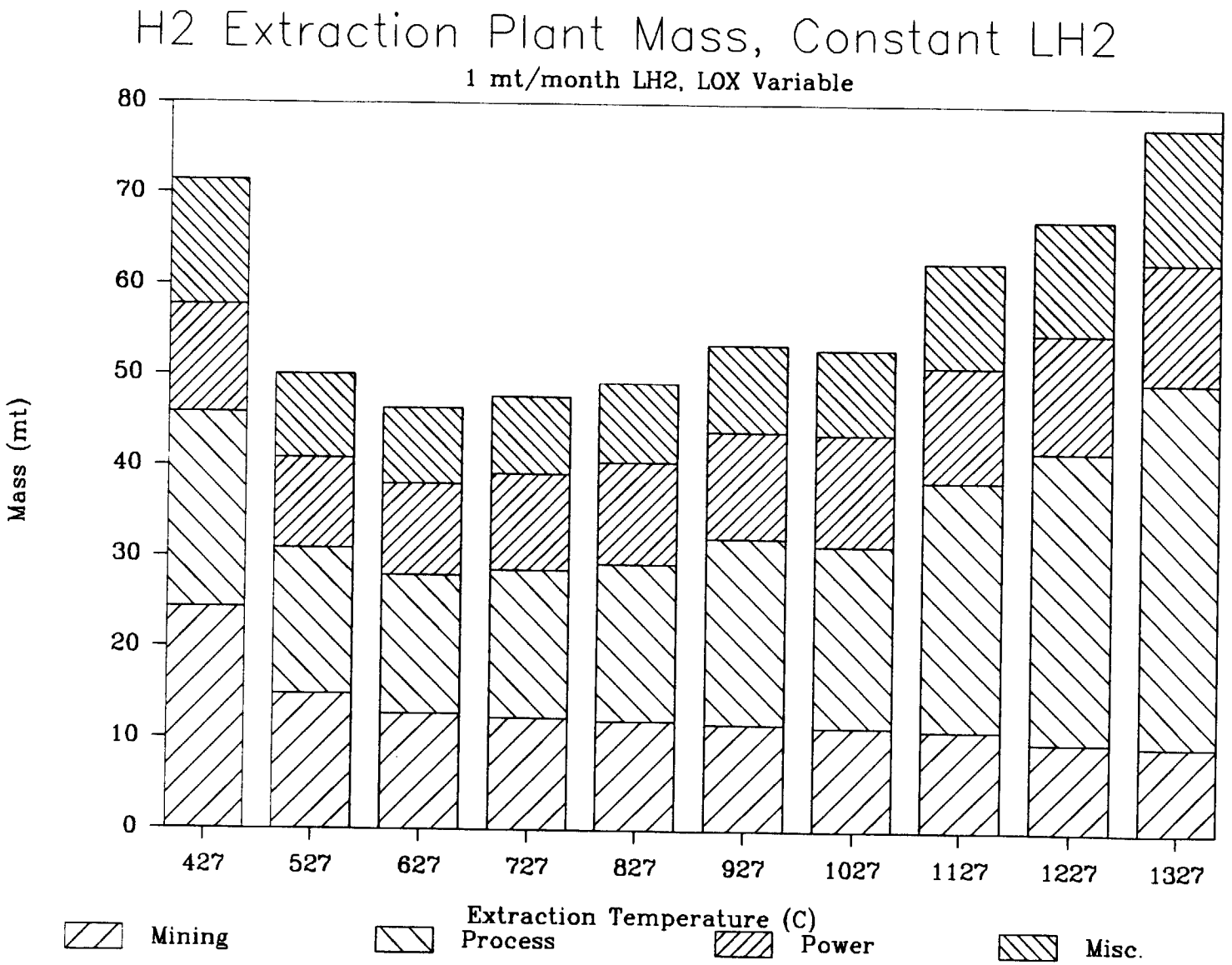

Figure 7-5. Oxygen to Hydrogen Extraction Ratio

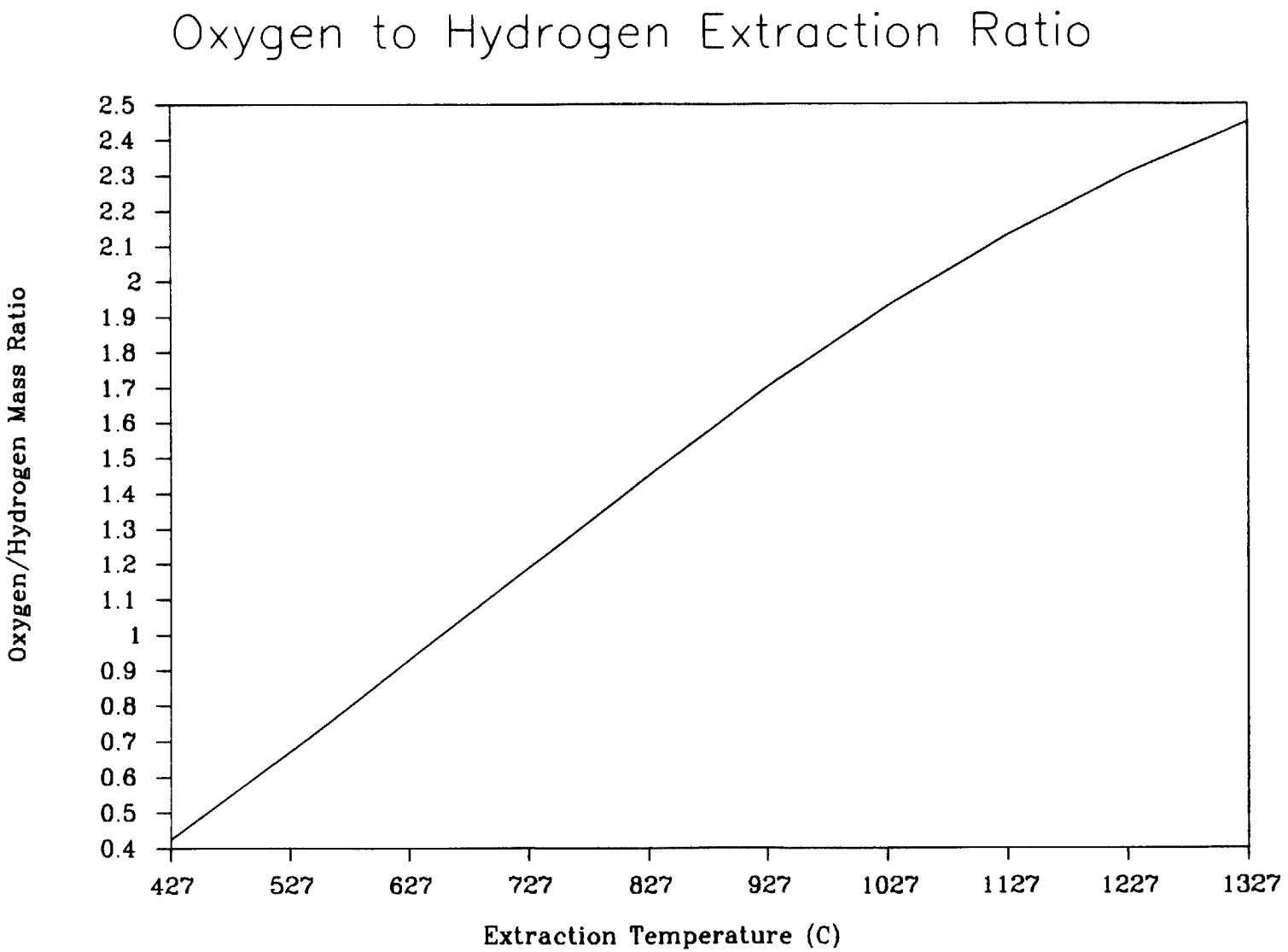

Figure 7-6. Effect of Extraction Temperature for Constant LOX Production

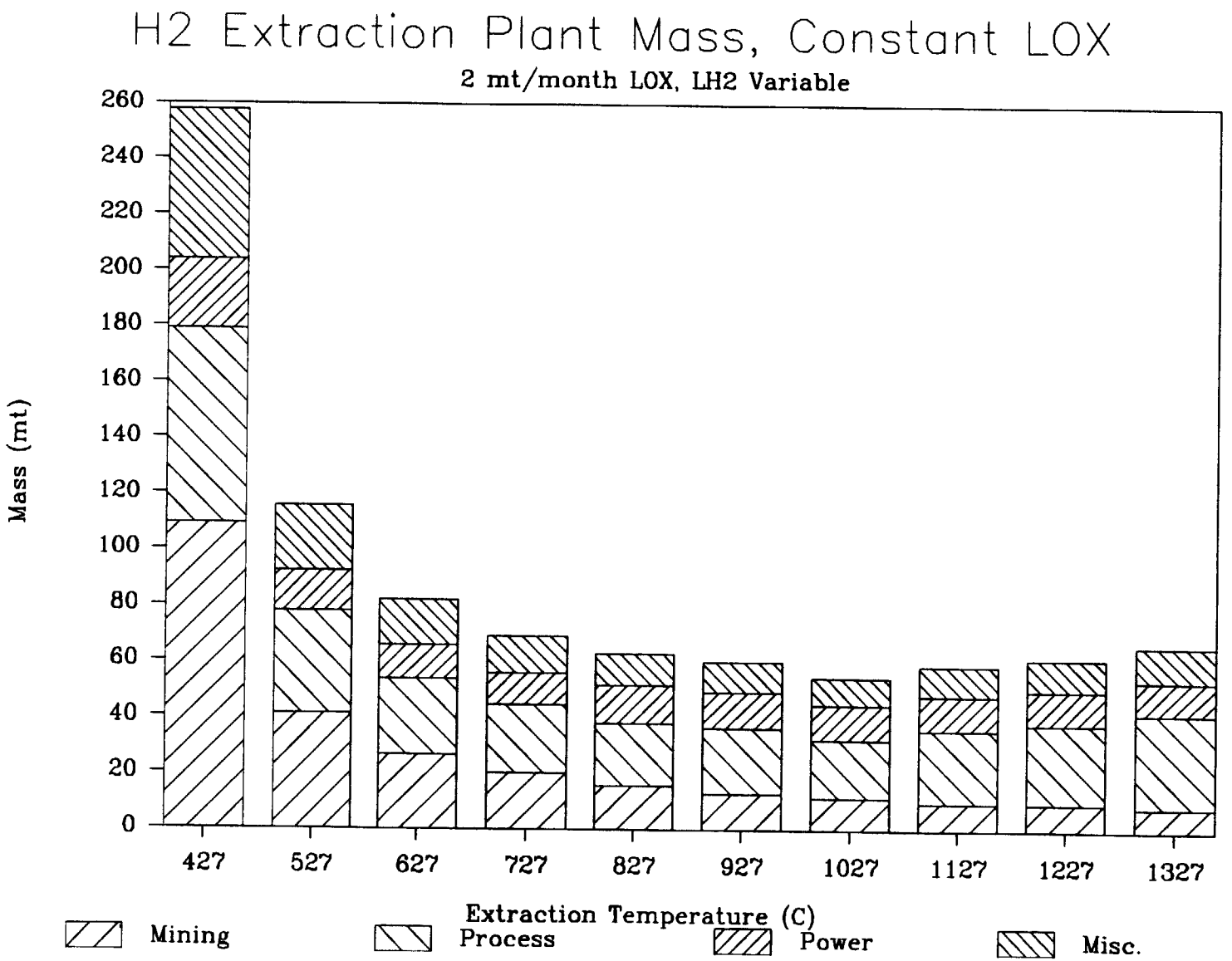

7.2.2 Power Source

This trade was comparing the use of solar and nuclear power sources. Basis of the study is a pilot plant producing 2 mt/month LOX and 1.2 mt/month LH_2 at 927°C extraction temperature. Characteristics of the cases compared are:

Case 1 - Nuclear Power:

- 90% process duty cycle, 35% mining duty cycle.
- 50% recovery of soil heat requirements in multi-stage reactor.
- 75% of remaining reactor heat requirements supplied by nuclear power waste heat, 25% by nuclear-electric. Nuclear power performance ratios range from 24 kg/kwe for a 250 kwe system to 7.5 kg/kwe for a 1.7 MWe system.

Case 2 - Solar Concentrator and Nuclear-Electric Power:

- 45% process duty cycle (daylight processing only), 35% mining duty cycle.
- 50% recovery of soil heat requirements in multi-stage reactor.
- All remaining reactor heat requirements supplied by solar concentrator. Solar concentrator sized at 1 kg/m^2, including mirror and support structure, rotating equipment, etc. Concentrator assumed 70% efficient, solar intensity 1.352 kw/m^2.
- Nuclear power provides all electrical power requirements and makes-up reactor heat loss during the lunar night.

Case 3 - Solar Concentrator, Photovoltaic (PV) Solar Arrays, and Regenerative Fuel Cells (RFC):

- 45% process duty cycle (daylight only), 35% mining duty cycle.
- 50% recovery of soil heat requirements in multi-stage reactor.
- All remaining reactor heat requirements supplied by solar concentrator.
- Electrical power provided by PV system during lunar day, RFC system provides heat loss makeup during lunar night. PV array performance ratio of 25.5 kg/kwe was used, and RFC typically > 300 kg/kwe.

Mass and power breakdowns for each of these cases are given in Figures 7-7 and 7-8. A summary is:

	Mass (mt)	Percent Difference From Case 1	Total Electric & Thermal Power (MW)	Percent Difference From Case 1
Case 1 - Nuclear	60.0		6.4	
Case 2 - Solar Conc.	92.3	+ 54%	12.6	+ 97%
Case 3 - Conc./PV/RFC	225.6	+276%	13.7	+106%

The ability to operate day and night (90% duty cycle) and efficient power generation at high-power levels made the nuclear powered case the preferred option. This trade shows that use of solar energy is not "free" for two reasons: 1) solar concentrators limit operation of the plant to the lunar day, thus requiring larger process vessels for a given production rate, and 2) solar concentrators are less efficient than nuclear sources at higher power levels (megawatt range), given that nuclear waste heat can also be used for some of the process thermal requirements.

Figure 7-7. Effect of Power Source on H_2 Extraction Plant Mass

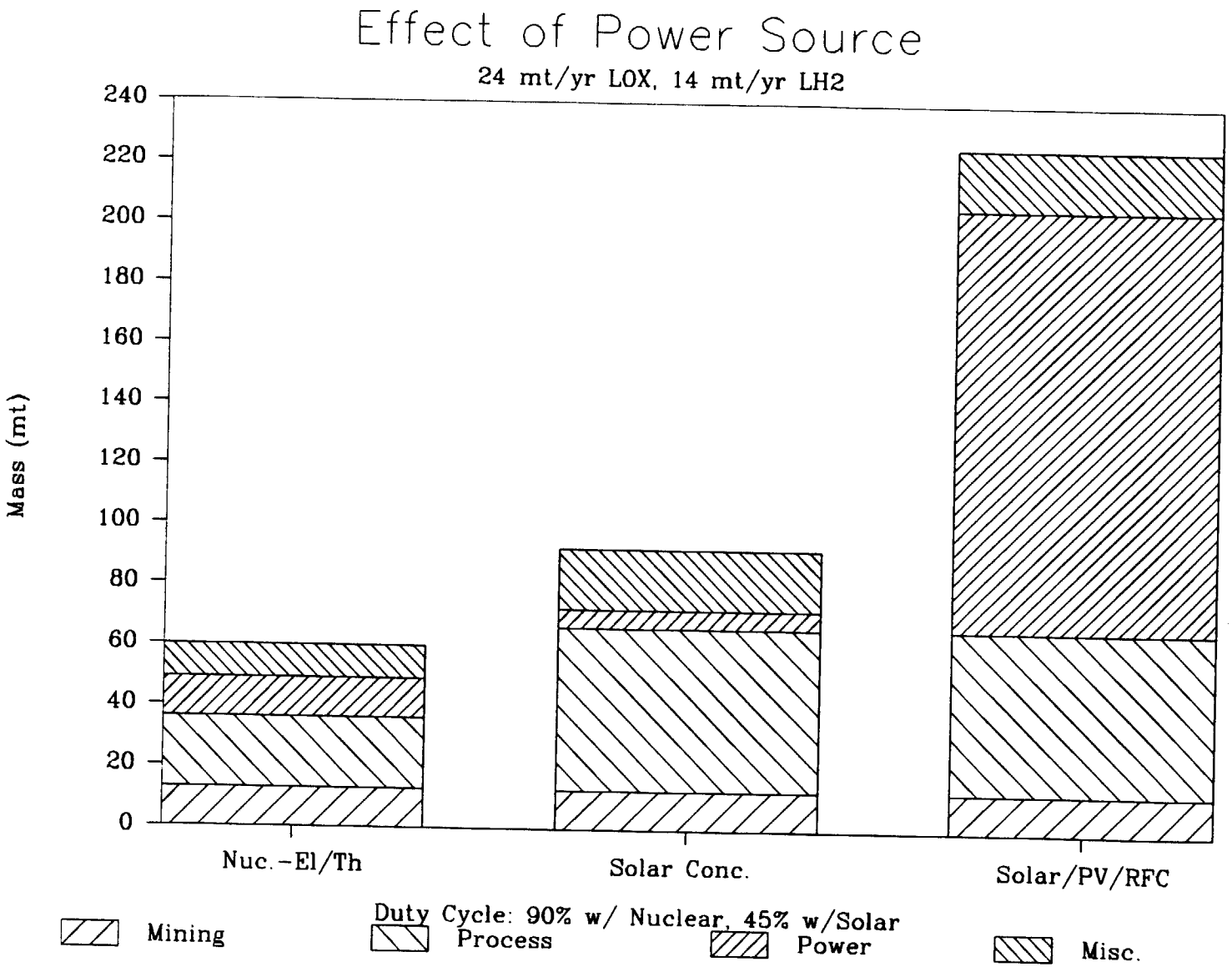

Figure 7-8. Effect of Power Source on H_2 Extraction Plant Power

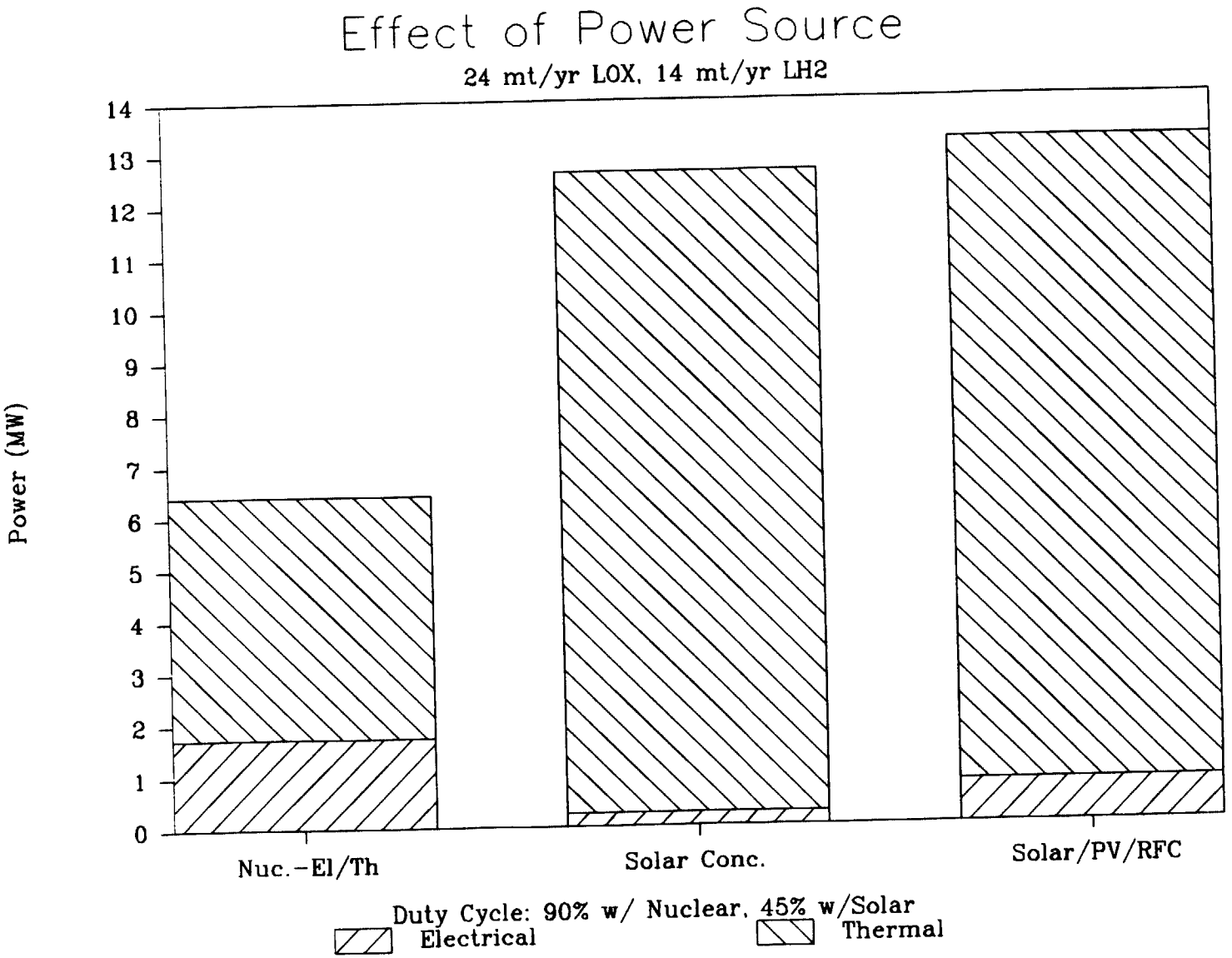

7.2.3 Heat Recovery Options

A trade was performed to determine the effect of using nuclear power waste heat, and of recovering significant amounts of energy in a multi-stage fluidized bed reactor. A 2 mt/month LOX, 1.2 mt/month LH_2 pilot plant was the basis of the study. Case 1 was the same as in the previous section, i.e.:

Case 1 - Nuclear power using nuclear reactor waste heat:

- 90% process duty cycle, 35% mining duty cycle.
- 50% recovery of thermal requirements in multi-stage reactor.
- 75% of remaining reactor heat requirements supplied by nuclear power waste heat, 25% by nuclear-electric.
- 3 hours total solids residence time in each reactor.

In Case 2, the effect of recovering more thermal energy in the reactor was assessed.

Case 2 - Nuclear power using nuclear reactor waste heat and recovering more thermal energy in the extraction step:

- 90% process duty cycle, 35% mining duty cycle.
- 80% recovery of thermal requirements in multi-stage reactor.
- 75% of remaining reactor heat requirements supplied by nuclear power waste heat, 25% by nuclear-electric.
- 3 hours total solids residence time in each reactor.

Case 3 assesses the effect of supplying all hydrogen extraction reactor heat requirements with electrical power instead of a combination of electric and waste heat from the nuclear power source. As given in Figure 7-9, the total thermal/electrical power requirements for Cases 1 and 3 are the same, however, Case 3 requires significantly greater electrical power (4.7 MW).

Case 3 - Nuclear power without using reactor waste heat:

- 90% process duty cycle, 35% mining duty cycle.
- 50% recovery of thermal requirements in multi-stage reactor.
- All reactor heat requirements supplied by nuclear-electric power.
- 3 hours total solids residence time in each reactor.

Case 4 illustrates the effect of not recovering any heat in the extraction step, nor using nuclear reactor waste heat. The extraction reactors are conceived as single-stage with no heat recovery. The reactors can be made smaller but power requirements are the maximum possible for a 90% duty cycle.

Case 4 - Nuclear power, no waste heat utilization or heat recovery:

- 90% process duty cycle, 35% mining duty cycle.
- No recovery of thermal requirements in process reactor.
- All reactor heat requirements supplied by nuclear-electric power.
- 1 hour total solids residence time in each reactor.

A comparison of these cases is given in Figure 7-10 and summarized by:

	Mass (mt)	Percent Difference From Case 1	Total Electric & Thermal Power (MW)	Percent Difference From Case 1
Case 1 - Nuc., 50% rec	60.0		6.4	
Case 2 - 80% recovery	55.6	- 7%	2.7	-58%
Case 3 - Nuc-El. Only	70.4	+17%	6.4	0
Case 4 - No Heat Rec.	73.1	+22%	12.0	+88%

The comparison shows that energy recovery schemes are not as effective in reducing total plant and power system mass as is improved process duty cycle (effectively examined in the previous section where it was shown that the lower the duty cycle, the larger the plant must be to produce a given quantity of product). This is because nuclear power is relatively efficient in the megawatt range. However, a 20% reduction in plant mass is significant, and thermal recovery steps will play an important role in reducing total process mass.

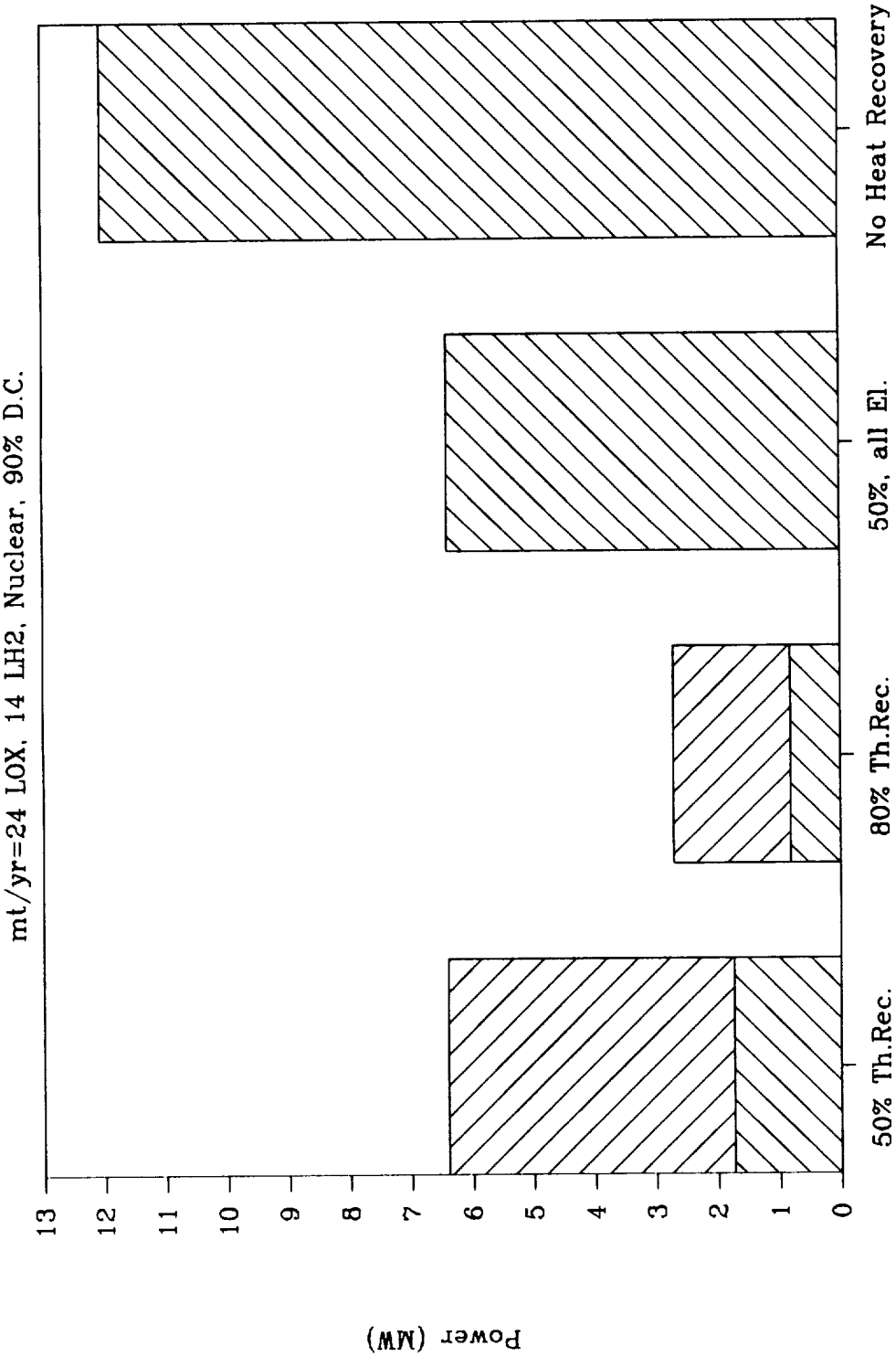

Figure 7-9. Effect of Heat Recovery Options on H_2 Extraction Power

Figure 7-10. Effect of Heat Recovery Options on H_2 Extraction Plant Mass

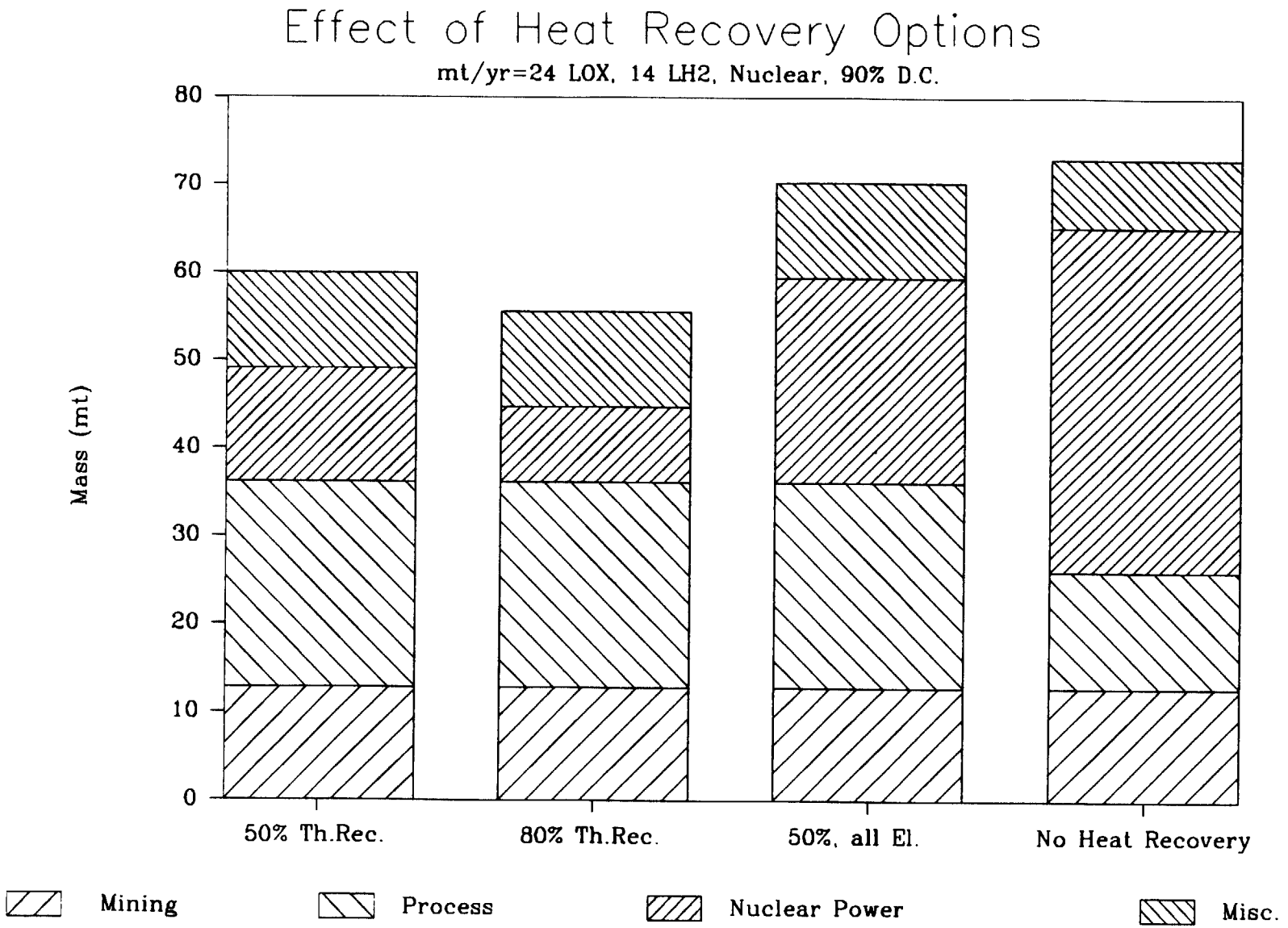

7.2.4 Other Trades

Other trades are possible, including:

Mining Options

- Alternative mining vehicles could be evaluated, such as bucket wheel excavators, bulldozers, scrapers, draglines, and three-drum slushers (or three-drum drag-scraper). Although offering a light-weight mining alternative (89), the three-drum slusher is not suitable for other lunar surface tasks, and may not be preferred for pilot plant operations. However, it would be particularly effective for a large mining operation since dedicated mining machines would be necessary. At least two slushers would be required, one for collecting raw soil and another for disposing spent fines.

- Mobile mining/processing plants could also be evaluated. A mobile plant would heat soil in-place (without using a reactor) by microwave or other technique (19, 42) and the evolved gases would be recovered, thus eliminating the need for soil mining and transport, as well as the reactor vessels. Gas losses will probably be much higher, however.

Beneficiation

- Since the majority of solar wind gases are concentrated in fine soil particles (in one sample, 95% of the hydrogen is in the sub-45 micron fraction, Ref.40), a hydrogen-rich concentrate of fine particles could be used to reduce extraction thermal requirements. Mechanically agitated screens are inefficient for size separations on feeds with average size of 0.1 mm or less. Over 80 mt of screens was calculated for separating 45 micron particles in the 14 mt/year LH_2 pilot plant, which is more than the entire plant and power system masses without screens. Thus, an alternative fines separation system is needed. Possiblities include cyclone separators or mechanical gas classifiers (Figure 6-37).

Process

- It may be more efficient to extract hydrogen from bulk soil at lower temperatures (600°C), then using the recovered hydrogen to extract oxygen from a concentrated ilmenite feedstock at higher temperatures (900-1000°C).

- Evaluation of alternative low-density and refractory reactor shell materials. Cermets (ceramic/metallic composites) are a possiblility. Use of multilayer Inconel metal/zirconia vacuum-insulation and other insulation concepts could also be evaluated.

- The optimum oxygen/hydrogen production split needs additional analysis.

- Trades between the number and total mass of the gas extraction reactors.

7.3 Sensitivity to Production Rate

Scaling relationships were developed that relate plant mass and power to production rate. Basis for the production rate sensitivity analysis is:

- Nuclear power.

- 50 ppm H in bulk soil feedstock.
- 927°C extraction temperature. 1.7 mt O_2 produced per mt H_2.
- 90% process duty cycle, 35% mining duty cycle.
- 50% of thermal requirements for heating soil feed are recovered in multi-stage reactor.
- 75% of remaining reactor heat requirements supplied by nuclear power waste heat, 25% by nuclear-electric.

Figure 7-11 shows plant and power system mass as a function of liquid hydrogen production rates ranging from 6-140 mt/yr. Plant mass (the sum of the mining and process areas, and margin) is correlated by:

Plant Mass (mt) = 2.64 * LH_2 Prod. (mt/yr) + 10.8 Error = ± 2.5 mt

Total plant and nuclear power mass is given by:

Plant and Power Mass (mt) = 2.97 * LH_2 Prod. (mt/yr) + 17.7 Error = ± 2.2 mt

Process power requirements are shown in Figure 7-12. The electric power requirements are:

Electric Power (MWe) = 0.122 * LH_2 Prod. (mt/yr) + 0.021 Error = ± 0.007 MWe

Thermal requirements for the process reactor that are provided by nuclear reactor waste heat are:

Thermal Power (MWt) = 0.326 * LH_2 Prod. (mt/yr) + 0.079 Error = ± 0.023 MWt

Total electric and thermal power is:

Power (MW) = 0.448 * LH_2 Prod. (mt/yr) + 0.100 Error = ± 0.030 MW

Figure 7-11. Sensitivity of H_2 Plant Mass with LH_2 Production

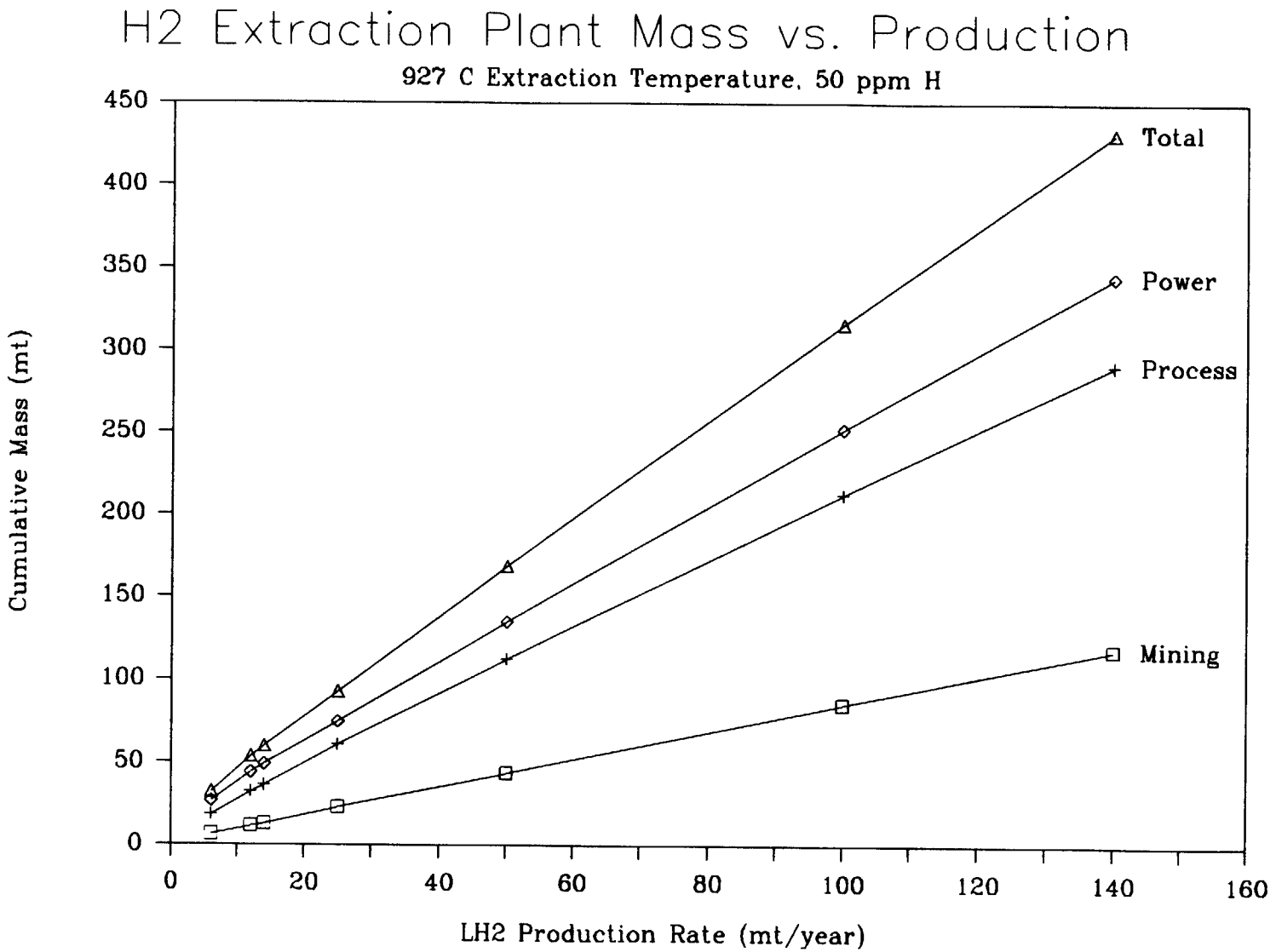

Figure 7-12. Sensitivity of H_2 Plant Power with LH_2 Production

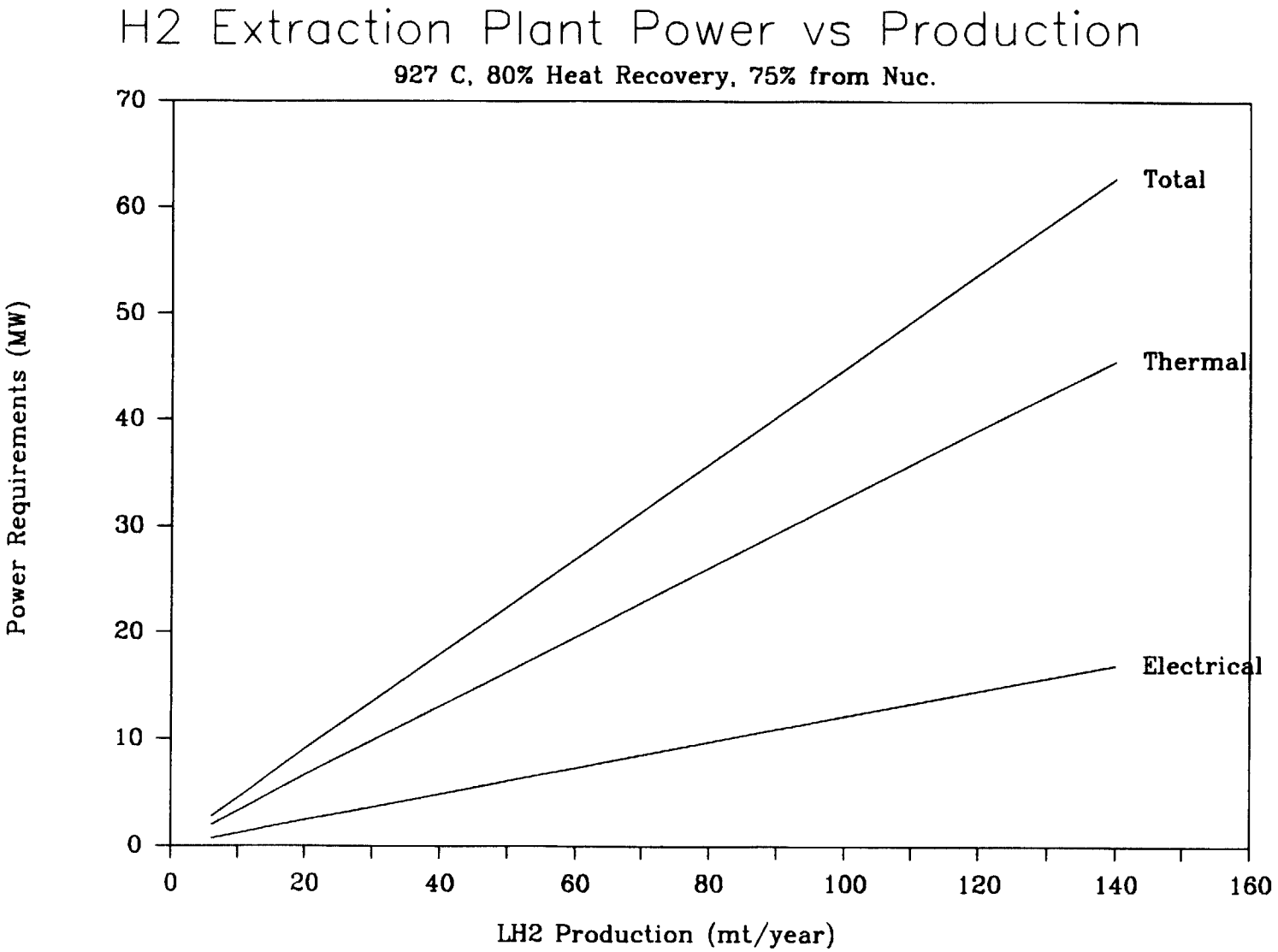

8.0 Conclusions

8.1 Summary of Findings

- Numerous chemical pathways to lunar oxygen production have been proposed. However, realistic comparisons are difficult because: 1) reported process mass and power estimates lack a consistent basis to allow comparison, 2) many process alternatives exist which can significantly effect process power and mass, and 3) many processes produce a range of byproducts besides oxygen.

- A conceptual design of a 2 mt/month LOX pilot plant was produced. The process extracts oxygen by reducing ilmenite with hydrogen. For a plant at 45% duty cycle, using basalt rock as feedstock, and powered by photovoltaic (PV) solar arrays and regenerative fuel cells (RFC), the mass of plant and power was estimated as 24.7 metric tons (mt) and the PV system was sized to deliver 146 kwe to plant and RFC. The major units of the process are delivered to the lunar surface in a fully-integrated Shuttle payload bay pallet, with external dimensions of 14' diameter x 45' long.

- From trade studies of the hydrogen reduction process, it was concluded:

  - Ilmenite rich, high-titanium mare basalt is a feedstock offering potential plant and power mass reductions of over 15% from a mare soil-fed 1000 mt LOX/year production plant. There is an insignificant difference in total mass between pilot plants using basalt and soil feedstocks.

  - Nuclear power offers the greatest potential for significant plant mass reductions. Total pilot plant and power mass reductions of 45-50 percent are possible using nuclear power at a 90% plant duty cylce instead of a PV/RFC system at 45% duty cycle.

  - Eliminating oxygen liquefaction and storage systems from the pilot plant saves 5% in total mass. This reduction is gained at the expense of significantly degraded capability to demonstrate key oxygen production technologies such as long term LOX storage in the lunar thermal environment, LOX refueling, and LOX quality certification and impurity control demonstration.

  - Delivery of small, self-contained, modular oxygen production units is inefficient in terms of total mass compared to delivery of units that are assembled into a single large production plant. The total mass of a single large oxygen plant and nuclear power system that produces 144 mt/year LOX was, at 40 mt, 50% less than six 24 mt/year pilot plant units operating under the same conditions.

- Scaling equations were developed for total plant and power system mass and process power requirements as a function of production rate.

  - For a basalt-fed pilot plant (1-5 mt LOX/month), PV/RFC power, 45% duty cycle:

    Mass (mt) = 6.50 * LOX (mt/month) + 11.8
    Power (kw) = 58.2 * LOX (mt/month) + 30.8

- For a soil-fed pilot plant (1-5 mt LOX/month), PV/RFC power, 45% duty cycle:

  Mass (mt) = 7.21 * LOX (mt/month) + 10.0
  Power (kw) = 71.1 * LOX (mt/month) + 22.8

- For a basalt-fed production plant (144-1500 mt/yr), Nuclear power, 90% duty cycle:

  Mass (mt) = 0.187 * LOX (mt/yr) + 16.4
  Power (kw) = 2.35 * LOX (mt/yr) + 34.4

- For a soil-fed production plant (144-1500 mt/yr), Nuclear power, 90% duty cycle:

  Mass (mt) = 0.231 * LOX (mt/yr) + 13.6
  Power (kw) = 2.95 * LOX (mt/yr) + 27.7

- A second conceptual design was produced of plant that extracts solar wind hydrogen from bulk lunar soil. The mass of a 2 mt/month LOX, 1.2 mt/month LH_2 pilot plant was estimated as 60 mt, including a nuclear power plant providing 1.7 MWe and 4.7 MWt to the process. Scaling equations were also developed for plant mass and power:

  Mass (mt) = 2.97 * LH_2 (mt/yr) + 17.7
  Electric Power (MWe) = 0.122 * LH_2 (mt/yr) + 0.021

- Progress in applying automation and robotics technology to remote mining operations, and to remote servicing/maintenance of complex process equipment is needed to offset high man-power requirements which are typical of terrestrial mining/chemical processing.

8.2 Recommendations

- A thorough cost/benefit analysis is needed of lunar oxygen production strategies of interest, including: 1) oxygen production for reusable lunar landers, 2) both lunar oxygen and hydrogen production for the landers, and 3) an incremental approach to placing LOX production capacity for supplying a LEO market. Sensitivity to operations costs and annual rate of lander missions should be assessed.

  A re-analysis of the payback period and lifetime program savings for a scenario that uses lunar oxygen for reusable landers is the top priority. The study should incorporate the LOX plant sizing equations given in this report. It should also recognize that a teleoperated LOX plant module can be delivered in an integrated package, allowing LOX production to begin soon after interfaces to utilities are provided.

- A consistent comparison of extraterrestrial resource utilization processing methods and alternatives is needed. Mass, power, and volume estimates reported in the literature for various process alternatives differ fundamentally in what is and is not included in the estimates. Researchers now involved in assessments of new initiatives will require a consistent set of data for comparison purposes.

  A study to produce a set of process mass, power, and volume requirements on a consistent basis is recommended. Values given in the literature for these process

requirements will be used as possible, but where values for certain parameters are not included (e.g. mining equipment, or oxygen liquefaction), a consistent estimating scheme will be applied to generate the additional numbers. Some trades to generate a more optimized process will be conducted as appropriate.

This study would incorporate all the latest results publicly available from on-going Small Business Innovation Research (SBIR), University space research, and other relevant investigations of Lunar/Mars/Phobos propellant production processes.

- A general trade study is needed between the Moon, Mars surface, or Phobos/Deimos to determine which are the most favorable sources for propellant manufacture for each of a given set of scenarios from the proposed New Initiatives. Propellant production impacts on program/lifetime LEO launch mass will be used as a first-order discriminator between sources and process alternatives.

- An analysis of likely oxygen product impurities and possible remedies is suggested for the hydrogen reduction of oxygen process.

- Additional analytical study of processing alternatives to optimize hydrogen reduction plant mass and power were indicated in this report. Certain alternatives hold particular promise in reducing plant mass and power requirements such as improved methods to separate soil fines and application of permanent magnetic roll ilmenite separators.

- Additional experimental data is needed in a number of areas to produce a more realistic design, such as:

  - Magnetic separation efficiency with typical mixed lunar minerals is desirable to develop a better estimate of beneficiation mass/power requirements and efficiencies. Particular care in terms of selecting lunar materials simulants with the proper ferrous (divalent) iron contents in ilmenite. The response in magnetic or electrostatic mineral separation equipment of iron oxide constituents in pyroxenes and olivines should also be determined.

  - Testing of lunar soil sizing schemes is needed to determine efficiencies, mass and power requirements.

  - Crushing and grinding characterization tests of appropriate lunar basalt rock simulants are needed for a more detailed assessment of using basalt as an ilmenite feedstock.

  - Research to determine the optimum hydrogen reduction reactor configuration.

- Testing and analysis should continue to determine the extent of lunar gravity and environment effects on process equipment.

9.0 References

1. Alred, J.W.: "Lunar Base Activities: An Overview," NASA JSC Advanced Programs Office, September 21, 1987.

2. McKay, D.S. and Williams, R.J.: "A Geologic Assessment of Potential Lunar Ores," pp. 243-256, Space Resources and Space Settlements, Billingham, J. and Gilbreath, W. (eds), NASA SP-428, 1979.

3. NASA: "Handbook of Lunar Materials," NASA, Johnson Space Center, Lunar and Planetary Sciences Division, May 1978.

4. Morris, R.V., Score, R., Dardano, C., and Heiken, G.: "Handbook of Lunar Soils, Part I: Apollo 11-15, Part II: Apollo 16-17," NASA Johnson Space Center, Planetary Materials Branch, JSC-19069, July 1983.

5. Williams, R.J. and Hubbard, N.: "Report of Workshop on Methodology for Evaluating Potential Lunar Resource Sites," NASA TM 58235, 1981.

6. Waldron, R.D. and Criswell, D.R.: "Lunar Utilization," Ch.1, pp.1-54, Space Industrialization, Volume II, O'Leary, B. (ed), CRC Press, 1982.

7. Kelley, J.H. and Laumann, E.A.: "Hydrogen Tomorrow - Demands and Technology Requirements," Report of the NASA Hydrogen Energy Systems Technology Study, Jet Propulsion Laboratory, December 1975.

8. Jones, J.H.: Industrial Chemistry, Pennsylvania State University, Unpublished Book Pre-Print, 1980.

9. Briggs, R.A. and Sacco, A.: "Oxidation and Reduction of Ilmenite: Application to Oxygen Production on the Moon," Preprint, 2nd Symposium on Lunar Bases and Space Activities in the 21st Century, Paper No. LBS-88-170, April 5-7, 1988.

10. Gibson, M.A. and Knudsen, C.W.: "Lunar Oxygen Production from Ilmenite," Preprint, 2nd Symposium on Lunar Bases and Space Activities in the 21st Century, Paper No. LBS-88-056, April 5-7, 1988.

11. Williams, R.J.: "Oxygen Extraction from Lunar Materials: An Experimental Test of an Ilmenite Reduction Process," pp. 551-558, Lunar Bases and Space Activities of the 21st Century, Mendell, W.W. (ed), Lunar and Planetary Institute, Houston, 1985.

12. Williams, R.J. and Mullins, O.: "Enhanced Production of Water from Ilmenite: An Experimental Test of a Concept for Producing Lunar Oxygen," Abstract, 14th Lunar and Planetary Science Conference, Special Sessions Abstracts, pp.34-35, March 16-17, 1983.

13. Volk, W. and Stotler, H.H.: "Hydrogen Reduction of Ilmenite Ores in a Fluid Bed," Journal of Metals, pp.50-53, January 1970.

14. Gibson, M.A. and Knudsen, C.W.: "Lunar Oxygen Production from Ilmenite," pp. 543-550, Lunar Bases and Space Activities of the 21st Century, Mendell, W.W. (ed), Lunar and Planetary Institute, Houston, 1985.

15. McGannon, H. (Ed.): The Making, Shaping, and Treating of Steel, 8th Ed., United States Steel Corporation, Pittsburgh, PA, 1964.

16. Dalton, C. and Hohmann, E. (eds): Conceptual Design of a Lunar Colony, 1972 NASA/ASEE Systems Design Institute, NASA Grant NGT 44-005-114, September 1972.

17. NASA: "Lunar Surface Return," NASA Johnson Space Center, In-House Study 84-00657, 1984.

18. Waldron, R.D. and Criswell, D.R.: "Materials Processing in Space," Ch.5, pp. 97-130, Space Industrialization, Volume I, O'Leary, B. (ed), CRC Press, 1982.

19. Sanders, A.P.: "Extraterrestrial Consumables Production and Utilization," MSC-06816, NASA TM X-58087, May 1972.

20. Systems Development Corporation: "Lunar Power Systems," Final Report, Contract NAS9-17359, December 12, 1986.

21. Agosto, W.N.: "An Assessment of Nine Paths to Lunar Oxygen Production," LEMSCO, Houston Texas, November 1983.

22. Astronautics Corporation of America: "Lunar Surface Base Propulsion System Study," Final Report, Astronautics Corporation of America, NAS9-17468, February, 1987.

23. Bock, E.H.: "Lunar Resources Utilization for Space Construction," Volume I - Executive Summary, Volume II - Study Results, Volume III - Appendices, NAS9-15560, General Dynamics Convair Division, April 30, 1979.

24. Lawton, E.A.: "Risk Factors in the Development of Zirconia Cell Technology for the Production of Oxygen from the Martian Atmosphere," Jet Propulsion Laboratory, JPL-D-3546, August 1986.

25. Bents, D.J.: "High Temperature Solid Oxide Regenerative Fuel Cell for Solar Photovoltaic Energy Storage," NASA-TM-89872, AIAA-87-9203, August 1987.

26. Maskalick, N.J.: "High-Temperature Electrolysis Cell Performance Characterization," Hydrogen Energy Progress V, T.N. Veziroglu and J.B. Taylor (eds), Pergamon Press, New York, 1984, pp. 801-812.

27. Weissbart, J., Smart, W.H., and Wydenen, T.: "Oxygen Reclamation from Carbon Dioxide using a Solid Oxide Electrolyte," Aerospace Medicine, Vol.40, No.136, 1969, pp.136-140.

28. Rosenberg, S.D., Guter, G.A., and Miller, F.E.: "The On-Site Manufacture of Propellant Oxygen from Lunar Resources," Aerospace Chemical Engineering, AIChE, Volume 62, Number 61, pp.228-234, 1966.

29. Phinney, W.C., Criswell, D., Drexler, E., and Garmirian, J.: "Lunar Resources and their Utilization," pp. 171-182, Space Manufacturing Facilities II, Proceedings of the Third Princeton/AIAA Conference, Grey, J. (ed), September 1, 1977.

30. Cutler, A.H. and Krag, P.: "A Carbothermal Scheme for Lunar Oxygen Production," pp. 559-569, Lunar Bases and Space Activities of the 21st Century, Mendell, W.W. (ed), Lunar and Planetary Institute, Houston, 1985.

31. Rosenberg, S.D.: "A Lunar-Based Propulsion System," pp. 169-176, Lunar Bases and Space Activities of the 21st Century, Mendell, W.W. (ed), Lunar and Planetary Institute, Houston, 1985.

32. Bhogeswara Rao, D., Choudary, U.V., Erstfeld, T.E., Williams, R.J., and Chang, Y.A.: "Extraction Processes for the Production of Aluminum, Titanium, Iron, Magnesium, and Oxygen from Nonterrestrial Sources," pp. 257-274, Space Resources and Space Settlements, Billingham, J. and Gilbreath, W. (eds), NASA SP-428, 1979.

33. Johnson, R.D. (ed): "Space Settlements - A Design Study," NASA SP-413, 1977, pp.55-77.

34. Frisbee, R.H.: "In-Situ Propellant Production Requirements and Benefits," Case for Mars III Conference, July 22, 1987.

35. Frisbee, R.H.: "Mass and Power Estimates for Martian In-Situ Propellant Production Systems," Jet Propulsion Laboratory, JPL D-3648, October 1986.

36. Lawton, E.A. and Frisbee, R.H.: "A New Look at Oxygen Production on Mars ISPP," Jet Propulsion Laboratory, JPL D-2661, September 1985.

37. NASA: "In-Situ Propellant Production (ISPP) Technology Enhancement Study," NASA-OAST Space Research and Technology, Summary Technical Report 1986, TM-89191, pp.86-87, March 1987.

38. Friedlander, H.N.: "An Analysis of Alternate Hydrogen Sources for Lunar Manufacture," pp. 611-618, Lunar Bases and Space Activities of the 21st Century, Mendell, W.W. (ed), Lunar and Planetary Institute, Houston, 1985.

39. Gibson, E.K., Moore, G.W., and Johnson, S.M.: "Summary of Analytical Data from Gas Release Investigations, Volatilization Experiments, Elemental Abundance Measurements on Lunar Samples, Meteorites, Minerals, Volcanic Ashes, and Basalts," NASA Johnson Space Center, July 1, 1974 (Reprinted July 1981).

40. Gibson, E.K., Bustin, R., and McKay, D.S.: "Lunar Hydrogen: A Resource for Future Use at Lunar Bases and Space Activities," Preprint, 2nd Symposium on Lunar Bases and Space Activities in the 21st Century, Paper No. LBS-88-158, April 5-7, 1988.

41. Carter, J.L.: "Lunar Regolith Fines: A Source of Hydrogen," pp. 571-581, Lunar Bases and Space Activities of the 21st Century, Mendell, W.W. (ed), Lunar and Planetary Institute, Houston, 1985.

42. Tucker, D.S., Vaniman, D.T., Anderson, J.L., Clinard, F.W., Feber, R.C., Frost, H.M., Meek, T.T., and Wallace, T.C.: "Hydrogen Recovery from Extraterrestrial Materials Using Microwave Energy," pp. 583-590, Lunar Bases and Space Activities of the 21st Century, Mendell, W.W. (ed), Lunar and Planetary Institute, Houston, 1985.

43. White, D.C. and Hirsch, P.: "Microbial Extraction of Hydrogen From Lunar Dust," pp. 591-602, Lunar Bases and Space Activities of the 21st Century, Mendell, W.W. (ed), Lunar and Planetary Institute, Houston, 1985.

44. Leich, D.A., Tombrello, T.A., and Burnett, D.S.: "The Depth Distribution of Hydrogen in Lunar Materials," Earth Planet. Science Letters, Vol.19, pp.305-314.

45. DesMarais, D.J., Hayes, J.M., and Meinschein, W.G.: "The Distribution in Lunar Soil of Hydrogen Released by Pyrolysis," Proceedings of the 5th Lunar Science Conference, Vol.2, pp. 1811-1822, 1974.

46. Williams, R.J., McKay, D.S., Giles, D., and Bunch, T.E.: "Mining and Beneficiation of Lunar Ores," pp.275-288, Space Resources and Space Settlements, Billingham, J. and Gilbreath, W. (eds), NASA SP-428, 1979.

47. Blanford, G.E., Borgesen, P., Maurette, M., Moller, W., and Monart, B.: "Hydrogen and Water Desorption on the Moon: Approximate, On-Line Simulations," pp. 603-609, Lunar Bases and Space Activities of the 21st Century, Mendell, W.W. (ed), Lunar and Planetary Institute, Houston, 1985.

48. Stump, W.R., Christiansen, E.L., Babb, G., Sullivan, D.: "Analysis of Lunar Propellant Production," Eagle Report No. 85-103B, Eagle Engineering, December 9, 1985.

49. Simonds, C.H.: "Hot Pressing of Lunar Soil and Qualification for Manned Applications," Eagle Engineering, Inc., Preprint of paper submitted to the Space 88: Engineering, Construction, and Operations in Space Conference, Albuquerque, NM, August 29-31, 1988.

50. Stump, W.R.: "Lunar Lander Conceptual Design," NAS9-17878, Eagle Engineering, Inc., EEI Report No. 88-181, March 30, 1988.

51. Epstein, S. and Taylor, H.P.: "The Concentration and Isotopic Composition of Hydrogen, Carbon, and Silicon in Apollo 11 Rocks and Minerals," Proceedings of the Apollo 11 Lunar Science Conference, Vol.2, pp. 1085-1096, 1970.

52. Epstein, S. and Taylor, H.P.: "O^{18}/O^{16}, Si^{30}/Si^{28}, D/H, and C^{13}/C^{12} Ratios in Lunar Samples," Proceedings of the 2nd Lunar Science Conference, Vol.2, pp. 1421-1442, 1971.

53. Epstein, S. and Taylor, H.P.: "O^{18}/O^{16}, Si^{30}/Si^{28}, C^{13}/C^{12}, and D/H Studies of Apollo 14 and 15 Samples," Proceedings of the 3rd Lunar Science Conference, Vol.2, pp. 1429-1455, 1972.

54. Epstein, S. and Taylor, H.P.: "The Isotopic Composition and Concentrations of Water, Hydrogne, and Carbon in some Apollo 15 and 16 Soils and the Apollo 17 Orange Soil," Proceedings of the 4th Lunar Science Conference, Vol.2, pp. 1559-1576, 1973.

55. Epstein, S. and Taylor, H.P.: "Investigation of the Carbon, Hydrogen, Oxygen, and Silicon Isotope and Concentration Relationships on the Grain Surfaces of a Variety of Lunar Soils and some Apollo 15 and 16 Core Samples," Proceedings of the 6th Lunar Science Conference, Vol.2, pp. 1771-1798, 1975.

56. Burt, D.M.: "Lunar Production of Oxygen and Metals Using Fluorine: Concepts Involving Fluorite, Lithium, and Acid-Base Theory," Abstract, 19th Lunar and Planetary Science Conference, Houston, Texas, March 14-18, 1988.

57. Burt, D.M.: "Phase Equilibria Involving Fluorine; Application to Recovery of Lunar Resources," Dept. of Geology, Arizona State University, Tempe, Arizona, Lunar and Planetary Institute, Houston, Texas, November 10, 1987.

58. Burt, D.M.: "Lunar Mining of Oxygen Using Fluorine," Preprint, 2nd Symposium on Lunar Bases and Space Activities in the 21st Century, LBS-88-072, April 5-7, 1988.

59. Criswell, D.R., Waldron, R.D., Meier, J., Goldberg, A., MacKenzie, J.D., and Selman, J.R.: "Extraterrestrial Materials Processing and Construction," Final Report, NSR 09-051-001, Mod. No. 24, LPI, AN#59186 & AN#59187, January 31, 1980.

60. Criswell, D.R.: "Extraterrestrial Materials Processing and Construction," Final Report, NSR 09-051-001, Mod. No. 24, Lunar & Planetary Institute, AN#56531, TL797-E96, September 30, 1978.

61. Carroll, W.F. (ed.): "Research on the Use of Space Resources," JPL Publication 83-36, March 1, 1983.

62. Cutler, A.H.: "An Alkali Hydroxide Based Scheme for Lunar Oxygen Production," Abstract for 1st Lunar Bases and Space Activities of the 21st Century Symposium, 1984.

63. Lindstrom, D.J. and Haskin, L.A.: "Direct Electrolysis as a Means of Altering Lunar Melt Compositions," Abstract, pp.197-199, in "Extraterrestrial Materials Processing and Construction," (Criswell, D.R., et al.), Final Report, NSR 09-051-001, Mod. No. 24, LPI, AN#59186 & AN#59187, January 31, 1980.

64. Sammells, A.F. and Semkow, K.W.: "Electrolytic Cell for Lunar Ore Refining and Electric Energy Storage," Preprint, 2nd Symposium on Lunar Bases and Space Activities in the 21st Century, Paper No. LBS-88-017, April 5-7, 1988.

65. Semkow, K.W. and Sammells, A.F.: "The Indirect Electrochemical Refining of Lunar Ores," Eltron Research, Inc., Journal of the Electrochemical Society, Vol.134, No.8, pp.2088-2089, 1987.

66. Anthony, D.L., Cochran, W.C., Haupin, W.E., Keller, R., and Larimer, K.T.: "Dry Extraction of Silicon and Aluminum from Lunar Ores," Preprint, 2nd Symposium on Lunar Bases and Space Activities in the 21st Century, Paper No. LBS-88-066, April 5-7, 1988.

67. Keller, R.: "Dry Extraction of Silicon and Aluminum from Lunar Ores," Final Report, SBIR Contract NAS9-17575 (Non-Proprietary Portions), EMEC Consultants, July 30, 1986.

68. Steurer, W.H. and Nerad, B.A.: "Vapor Phase Reduction," pp. 4.1-4.29 in "Research on the Use of Space Resources," (Carroll, W.F., ed.) JPL Publication 83-36, March 1, 1983.

69. Gibson, M.A. and Knudsen, C.W.: "Lunar Oxygen Production from Ilmenite," Summary of paper for presentation at Space 88 - Engineering, Construction, & Operations in Space Conference, Albuqerque, NM, August 1988.

70. Davis, H.P. and Stump, W.R.: "Lunar Oxygen Impact Upon STS Effectiveness," Eagle Report No.83-63, Eagle Engineering, May 1983.

71. Waldron, R.D., Erstfeld, T.E., and Criswell, D.R.: "The Role of Chemical Engineering In Space Manufacturing," Chemical Engineering, McGraw-Hill Publication, pp.80-94, February 12, 1979.

72. Christiansen, E.L., et al.: "Conceptual Design of a Lunar Oxygen Pilot Plant," NASA Contract No. NAS9-17878, Eagle Report No. 88-182, July 1, 1988.

73. Cutler, A.H.: "Lunar Hydrogen Extraction," unpublished.

74. Inculet, I.I.: "Beneficiation of Lunar Soils," pp. IV.1-IV.64, in "Extraterrestrial Materials Processing and Construction," (Criswell, D.R., et al.) Final Report, NSR 09-051-001, Mod. No. 24, Lunar & Planetary Institute, AN#56531, TL797-E96, September 30, 1978.

75. Schmitt, H.H., Lofgren, G., Swann, G.A., and Simmons, G.: "The Apollo 11 Samples: Introduction," Proceedings of the Apollo 11 Lunar Science Conference, Vol.1, pp.1-54, 1970.

76. Beaty, D.W. and Albee, A.L.: "Comparative Petrology and Possible Genetic Relations Among the Apollo 11 Basalts," Proceedings of the 9th Lunar and Planetary Science Conference, Vol.1, pp.359-463, 1978.

77. Warner, R.D., Keil, K., Prinz, M., Laul, J.C., Murali, A.V., Schmitt, R.A.: "Mineralogy, Petrology, and Chemistry of Mare Basalts from Apollo 17 Rake Samples," Proc. Lunar Sci. Conf. 6th, Vol.1, pp.193-220, 1975.

78. Longhi, J., Walker, D., Grove, T.L., Stolper, E.M., and Hays, J.F.: "The Petrology of the Apollo 17 Mare Basalts," Proceedings of the Fifth Lunar Science Conference, Vol.1, pp.447-469, 1974.

79. Papike, J.J., Bence, A.E., and Lindsley, D.H.: "Mare Basalts from the Taurus-Littrow Region of the Moon," Proceedings of the Fifth Lunar Science Conference, Vol.1, pp.471-504, 1974.

80. Usselman, T.M., Lofgren, G.E., Donaldson, C.H., Williams, R.J.: "Experimentally Reproduced Textures and Mineral Chemistries of High-Titanium Mare Basalts," Proc. Lunar Sci. Conf. 6th, Vol.1, pp.997-1020, 1975.

81. NASA: "Space-Based Manufacturing From Nonterrestrial Materials," The 1976 NASA-Ames Research Center Study, NASA TM-73265, August 1977.

82. Waldron, R.D.: "Lunar Manufacturing - A Survey of Products and Processes," Preprint, 2nd Symposium on Lunar Bases and Space Activities in the 21st Century, Paper No. LBS-88-134, April 5-7, 1988.

83. Reese, T.G., Hemmerly, R.A., and Taylor, D.A.: "Civil Needs Data Base, Version 3.0," General Research Corporation, NASA Contract Number NASW-3921, July 16, 1987.

84. Christiansen, E.L., Conley, C.L., Davidson, W.L., Hirasaki, J.K, Overton, J.D., and Simonds, C.H.: "Lunar Surface Operations Study," NASA Contract No. NAS9-17878, Eagle Engineering Report No. 87-172, December 1, 1987.

85. Alred, J.: "Development of a Lunar Outpost: Year 2000-2005," NASA JSC Advanced Programs Office, paper presented at the AIAA Technical Symposium, Houston TX, May 11, 1988.

86. Langseth, M.G., Keihm, S.J., and Peters, K.: "Revised Lunar Heat-Flow Values," Proc. Lunar Sci. Conf. 7th, pp.3143-3171, 1976.

87. Martin, J.W., Martin, T.J., Bennett, T.P., and Martin, K.M.: Surface Mining Equipment, Martin Consultants, Inc., Golden, Colorado, 1982.

88. Carrier, W.D.: "Excavation Costs for Lunar Materials," AIAA Paper 79-1376, May 14-17, 1979, Chapter X (G) in "Extraterrestrial Materials Processing and Construction," (Criswell, D.R., et al.), Final Report, NSR 09-051-001, Mod. No. 24, LPI, AN#59186 & AN#59187, January 31, 1980.

89. Gertsch, R.E.: "A Method For Mining Lunar Soil," AAS83-234, Space Manufacturing, 1983, Advances in the Astronautical Sciences, Volume 53, (Burke, J.D. and Whitt, A.S., eds.), pp.337-346, 1983.

90. Silwa, N.E., Harrison, F.W., Soloway, D.I., McKinney, W.S., Cornils, K., Doggett, W.R., Cooper, E.G., and Alberts, T.E.: "Automation and Robotics Considerations for a Lunar Base," Paper No. LBS-88-184, presented at the second Lunar Bases and Space Activities of the 21st Century symposium, April 5-7, 1988, Houston, Texas.

91. Perry, R.H. and Green, D.: Perry's Chemical Engineers' Handbook, 6th Edition, McGraw-Hill, Inc., 1984.

92. Gilchrist, J.D.: Extraction Metallurgy, Pergamon Press, 1967.

93. Taggart, A.F.: Handbook of Mineral Dressing, Ores and Industrial Minerals, John Wiley & Sons, 1954.

94. Cummins, A.B. and Given, I.A.: SME Mining Engineering Handbook, Vol. 1 and 2, The American Institute of Mining, Metallurgical, and Petroleum Engineers, Port City Press, Baltimore, Maryland, 1973.

95. Peele, R. and Church, J.A.: Mining Engineers' Handbook, Third Edition, Vol. I and II, John Wiley & Sons, 1945.

96. Eriez Magnetics: "High Intensity Rare Earth Roll Magnetic Separators," "Electrodynamic Separators," and "Hi-Intensity Electro IMR Magnetic Separators," Literature from Eriez Magnetics, Erie, Pennsylvania, 1988.

97. Carpco, Inc.: "High Intensity Lift-Type Magnetic Separators," and "High Intensity

Induced Roll Magnetic Separators," Literature from Carpco, Inc., Jacksonville, Florida, 1988.

98. Svoboda, J.: Magnetic Methods for the Treatment of Minerals, Developments in Mineral Processing 8, Elsevier Science Publishers, Amsterdam, 1987.

99. Agosto, W.N.: "Electrostatic Concentration of Lunar Soil Minerals," pp. 453-464, Lunar Bases and Space Activities of the 21st Century, Mendell, W.W. (ed), Lunar and Planetary Institute, Houston, 1985.

100. Agosto, W.N.: "Electrostatic Separation of Binary Comminuted Mineral Mixtures," AAS 83-231, in Space Manufacturing, 1983, Vol.53, Advances in the Astronautical Sciences, (Burke, J.D. and Whitt, A.S., Eds.), pp.315-334, 1983.

101. Haselden, G.G.: Cryogenic Fundamentals, Academic Press, 1971.

102. Reppucci, G.: "Spacecraft Power Systems," Federal Systems Division, TRW Space & Technology Group, Presentation at the AIAA Fundamentals of Spacecraft Design Lecture Series, Houston, Texas, April 15, 1986.

103. Baraona, C.R.: "The Space Station Power System," NASA LeRC, Proceedings of 5th European Symposium: 'Photovoltaic Generators in Space', Scheveningen, The Netherlands, September 30 - October 2, 1986, ESA SP-267, November 1986.

104. Brandhorst, H.W., Juhasz, A.J., and Jones, B.I.: "Alternative Power Generation Concepts for Space," N87-28961, NASA LeRC, Proceedings of 5th European Symposium: 'Photovoltaic Generators in Space', Scheveningen, The Netherlands, September 30-October 2, 1986, ESA SP-267, November 1986.

105. Keaton, P.W. and Carlson, D.: "Nuclear-Electric OTV," Los Alamos National Laboratory, Memorandum to B. Roberts, NASA JSC, September 18, 1985.

106. Varner, C.C.: "Spacecraft Mass Estimation, Relationships, and Engine Data," NASA Contract No. NAS9-17878, Eagle Engineering Report No.87-171, April 6, 1988.

107. U.S. Department of Defense: "Military Standardization Handbook: Metallic Materials and Elements for Aerospace Vehicle Structures," MIL-HDBK-5D, June 1, 1983.

108. Smith, J.W.: "Materials for Space Operations Center, Primary Structural Materials," NASA JSC, Materials Technology Report, 81-ES5-4, 1981.

109. McKay, D.M. and Morrison, D.A.: "Lunar Breccias," Journal of Geophysical Research, v.76, pp.5658-5669, 1971.

110. Simonds, C.H.: "Sintering and Hot Pressing of Fra Mauro Composition Glass and Formation of Lunar Breccias," American Journal of Science, v.273, pp.428-439, 1973.

111. Uhlmann, D.R., Klein, L., Onorato, P.I.K., and Hopper, R.W.: "The Formation of Lunar Breccias: Sintering and Recrystallization," Proceedings of the 6th Lunar Science Conference, pp.693-705, 1975.

112. Frenkel, J.: "Viscous Flow of Crystalline Bodies Under the Action of Surface Tension," Journal of Physics (USSR) v.9, pp.385-391, 1945.

113. Uhlmann, D.R., Onorato, P.I.K., and Scherer, G.W.: "A Simplified Model for Glass Formation," Proceedings of the 10th Lunar and Planetary Science Conference, pp.375-381, 1979.

114. Uhlmann, D.R., Klein, L., Kritchevsky, G., and Hopper, R.W.: "The Formation of Lunar Glasses," Proceedings of the 5th Lunar Science Conference, pp.2317-2331, 1974.

115. Gernhardt, M.L. and Frisbie, F.R.: "Designing For Long-Term Telerobotic Support Of A Subsea Completion Facility," Ocean Systems Engineering, Inc., SAE Paper No.881007, 18th Intersociety Conference on Environmental Systems, July 11-13, 1988.

116. Rasmussen, D., Johnson, V., and Mian, A.: "Telescience Concept for Habitat Monitoring and Control," SAE Paper No. 881121, 18th Intersociety Conference on Environmental Systems, July 11-13, 1988.

117. Noyes, G.P.: "Carbon Dioxide Reduction Processes for Spacecraft ECLSS: A Comprehensive Review," SAE Paper No. 881042, 18th Intersociety Conference on Environmental Systems, July 11-13, 1988.

118. Isenberg, A.O. and Cusick, R.J.: "Carbon Dioxide Electrolysis with Solid Oxide Electrolyte Cells for Oxygen Recovery in Life Support Systems," SAE Paper No. 881040, 18th Intersociety Conference on Environmental Systems, July 11-13, 1988.

119. Robie, R.A. and Waldbaum, D.R.: "Thermodynamic Properties of Minerals and Related Substances at 298.15°K (25.0°C) and One Atmosphere (1.013 Bars) Pressure and at Higher Temperatures," Geological Survey Bulletin 1259, 1968.

120. Caterpillar: Caterpillar Performance Handbook, Edition 18, Caterpillar, Inc. Peoria, IL, October 1987.

121. Dresser Industries: "The World's Most Complete Line of Construction and Mining Equipment," Dresser Industries, Inc., Libertyville, IL, February 1987.

122. Davidson, W.L.: "Lunar Surface Transportation Systems Conceptual Design," NASA Contract No.NAS9-17878, EEI Report 88-188, July 7, 1988.

123. Sturtevant: "Pilot Plant Equipment: Jaw Crusher and Rotary Crusher Data," Sturtevant, Inc., Boston, MA, March 1988.

124. McCabe, W.L. and Smith, J.C.: Unit Operations of Chemical Engineering, 3rd Edition, McGraw-Hill Chemical Engineering Series, 1976.

125. Prasher, C.L.: Crushing and Grinding Process Handbook, John Wiley & Sons Ltd., 1987.

126. Greenkorn, R.A. and Kessler, D.P.: Transfer Operations, McGraw-Hill, Inc., 1972.

127. Continental Conveyor: "Conveyor Systems," and "Belt Conveyor Systems for Mining and Construction Industries," Continental Conveyor & Equipment Company, Inc., Winfield, AL, December, 1987.

128. E&MJ: "Conveyors in Mining," Engineering and Mining Journal, pp.58-65, December, 1987.

129. Schwartz, M.M.: Composite Materials Handbook, McGraw-Hill Book Company, 1984.

130. Ho, D. and Sobon, L.E.: "Extraterrestrial Fiberglass Production Using Solar Energy," pp.225-232, Space Resources and Space Settlements, Billingham, J. and Gilbreath, W. (eds), NASA SP-428, 1979.

10.0 Bibliography

Lunar Oxygen Production Assessments

Agosto, W.N.: "An Assessment of Nine Paths to Lunar Oxygen Production," LEMSCO, Houston Texas, November 1983.

Astronautics Corporation of America: "Lunar Surface Base Propulsion System Study," Final Report, Astronautics Corporation of America, NAS9-17468, February, 1987.

Bock, E.H.: "Lunar Resources Utilization for Space Construction," Volume I - Executive Summary, Volume II - Study Results, Volume III - Appendices, NAS9-15560, General Dynamics Convair Division, April 30, 1979.

Dalton, C. and Hohmann, E. (eds): Conceptual Design of a Lunar Colony, 1972 NASA/ASEE Systems Design Institute, NASA Grant NGT 44-005-114, September 1972.

NASA: "Lunar Surface Return," NASA Johnson Space Center, In-House Study 84-00657, 1984.

Sanders, A.P.: "Extraterrestrial Consumables Production and Utilization," MSC-06816, NASA TM X-58087, May 1972.

Systems Development Corporation: "Lunar Power Systems," Final Report, Contract NAS9-17359, December 12, 1986.

Waldron, R.D. and Criswell, D.R.: "Overview of Methods for Extraterrestrial Materials Processing," AIAA Paper 79-1379, 4th Conference on Space Manufacturing Facilities, Princeton University, May 14-17, 1979.

Waldron, R.D.: "Lunar Manufacturing - A Survey of Products and Processes," IAF Paper No.86-508, 37th International Astronautical Congress, Innsbruck, Austria, October 4-11, 1986.

Waldron, R.D.: "Lunar Manufacturing - A Survey of Products and Processes," Preprint, 2nd Symposium on Lunar Bases and Space Activities in the 21st Century, Paper No. LBS-88-134, April 5-7, 1988.

Oxygen Production (Ilmenite Reduction)

Briggs, R.A. and Sacco, A.: "Oxidation and Reduction of Ilmenite: Application to Oxygen Production on the Moon," Preprint, 2nd Symposium on Lunar Bases and Space Activities in the 21st Century, Paper No. LBS-88-170, April 5-7, 1988.

Gibson, M.A. and Knudsen, C.W.: "Lunar Oxygen Production from Ilmenite," pp. 543-550, Lunar Bases and Space Activities of the 21st Century, Mendell, W.W. (ed), Lunar and Planetary Institute, Houston, 1985.

Gibson, M.A. and Knudsen, C.W.: "Lunar Oxygen Production from Ilmenite," Preprint, 2nd Symposium on Lunar Bases and Space Activities in the 21st Century, Paper No. LBS-88-056, April 5-7, 1988.

Williams, R.J.: "Oxygen Extraction from Lunar Materials: An Experimental Test of an Ilmenite Reduction Process," pp. 551-558, Lunar Bases and Space Activities of the 21st Century, Mendell, W.W. (ed), Lunar and Planetary Institute, Houston, 1985.

Williams, R.J. and Mullins, O.: "Enhanced Production of Water from Ilmenite: An Experimental Test of a Concept for Producing Lunar Oxygen," Abstract, 14th Lunar and Planetary Science Conference, Special Sessions Abstracts, pp.34-35, March 16-17, 1983.

Oxygen Production (Carbothermal Reduction of Oxides)

Cutler, A.H. and Krag, P.: "A Carbothermal Scheme for Lunar Oxygen Production," pp. 559-569, Lunar Bases and Space Activities of the 21st Century, Mendell, W.W. (ed), Lunar and Planetary Institute, Houston, 1985.

Driggers, G.W.: "A Factory Concept for Processing and Manufacturing with Lunar Material," pp. 183-186, Space Manufacturing Facilities II, Proceedings of the 3rd Princeton/AIAA Conference, Grey, J. (ed), September 1, 1977.

O'Neill, G.K. and Chambers, A.B.: "Space-Based Manufacturing From Nonterrestrial Materials," 1976 NASA-Ames Research Center Study, NASA TM-73265, August 1977.

Phinney, W.C., Criswell, D., Drexler, E., and Garmirian, J.: "Lunar Resources and their Utilization," pp. 171-182, Space Manufacturing Facilities II, Proceedings of the Third Princeton/AIAA Conference, Grey, J. (ed), September 1, 1977.

Rosenberg, S.D., Guter, G.A., and Miller, F.E.: "The On-Site Manufacture of Propellant Oxygen from Lunar Resources," Aerospace Chemical Engineering, AIChE, Volume 62, Number 61, pp.228-234, 1966.

Rosenberg, S.D.: "A Lunar-Based Propulsion System," pp. 169-176, Lunar Bases and Space Activities of the 21st Century, Mendell, W.W. (ed), Lunar and Planetary Institute, Houston, 1985.

Oxygen Production (Carbocholorination)

Bhogeswara Rao, D., Choudary, U.V., Erstfeld, T.E., Williams, R.J., and Chang, Y.A.: "Extraction Processes for the Production of Aluminum, Titanium, Iron, Magnesium, and Oxygen from Nonterrestrial Sources," pp. 257-274, Space Resources and Space Settlements, Billingham, J. and Gilbreath, W. (eds), NASA SP-428, 1979.

Johnson, R.D. (ed): "Space Settlements - A Design Study," NASA SP-413, 1977, pp.55-77.

Oxygen Production (Electrolytic Reduction)

Anthony, D.L., Cochran, W.C., Haupin, W.E., Keller, R., and Larimer, K.T.: "Dry Extraction of Silicon and Aluminum from Lunar Ores," Preprint, 2nd Symposium on Lunar Bases and Space Activities in the 21st Century, Paper No. LBS-88-066, April 5-7, 1988.

Cutler, A.H.: "An Alkali Hydroxide Based Scheme for Lunar Oxygen Production," Abstract for 1st Lunar Bases and Space Activities of the 21st Century Symposium, 1984.

Downs, W.R.: "Oxygen and Water from Lunar-Surface Material," NASA TM X-58061, NASA JSC, 1971.

Jarrett, N., Das, S.K., and Haupin, W.E.: "Extraction of Oxygen and Metals from Lunar Ores," Alcoa Technical Center, pp.255-267 in "Extraterrestrial Materials Processing and Construction," (Criswell, D.R., et al.) Final Report, NSR 09-051-001, Mod. No. 24, LPI, AN#59186 & AN#59187, January 31, 1980.

Keller, R.: "Dry Extraction of Silicon and Aluminum from Lunar Ores," Final Report, SBIR Contract NAS9-17575 (Non-Proprietary Portions), EMEC Consultants, July 30, 1986.

Kesterke, D.G.: "Electrowinning of Oxygen from Silicate Rocks," U.S. Bureau of Mines Report of Investigations 7587, Reno NV, 1971.

Lindstrom, D.J. and Haskin, L.A.: "Direct Electrolysis as a Means of Altering Lunar Melt Compositions," Abstract, pp.197-199, in "Extraterrestrial Materials Processing and Construction," (Criswell, D.R., et al.), Final Report, NSR 09-051-001, Mod. No. 24, LPI, AN#59186 & AN#59187, January 31, 1980.

Sammells, A.F. and Semkow, K.W.: "Electrolytic Cell for Lunar Ore Refining and Electric Energy Storage," Preprint, 2nd Symposium on Lunar Bases and Space Activities in the 21st Century, Paper No. LBS-88-017, April 5-7, 1988.

Semkow, K.W. and Sammells, A.F.: "The Indirect Electrochemical Refining of Lunar Ores," Eltron Research, Inc., Journal of the Electrochemical Society, Vol.134, No.8, pp.2088-2089, 1987.

Oxygen Production (Acid Leach)

Agosto, W.N. and Wickman, J.H.: "Lunar Fuels Derived from Aqueous Processing of Lunar Materials," Preprint, 2nd Symposium on Lunar Bases and Space Activities in the 21st Century, LBS-88-7090, April 5-7, 1988.

Waldron, R.D.: "HF Acid Leach Process (Detailed Analysis and Revisions)," pp. 87-124 in "Extraterrestrial Materials Processing and Construction," (Criswell, D.R., et al.), Final Report, NSR 09-051-001, Mod. No. 24, LPI, AN#59186 & AN#59187, January 31, 1980.

Waldron, R.D.: "Processing of Lunar & Asteroidal Materials," pp. II.1-II.176, in "Extra-terrestrial Materials Processing and Construction," (Criswell, D.R., et al.) Final Report, NSR 09-051-001, Mod. No. 24, Lunar & Planetary Institute, AN#56531, TL797-E96, September 30, 1978.

Waldron, R.D., Erstfeld, T.E., and Criswell, D.R.: "The Role of Chemical Engineering In Space Manufacturing," Chemical Engineering, McGraw-Hill Publication, pp.80-94, February 12, 1979.

Oxygen Production (Fluorine Exchange)

Burt, D.M.: "Lunar Production of Oxygen and Metals Using Fluorine: Concepts Involving Fluorite, Lithium, and Acid-Base Theory," Abstract, 19th Lunar and Planetary Science Conference, Houston, Texas, March 14-18, 1988.

Burt, D.M.: "Phase Equilibria Involving Fluorine; Application to Recovery of Lunar Resources," Dept. of Geology, Arizona State University, Tempe, Arizona, Lunar and Planetary Institute, Houston, Texas, November 10, 1987.

Burt, D.M.: "Lunar Mining of Oxygen Using Fluorine," Preprint, 2nd Symposium on Lunar Bases and Space Activities in the 21st Century, LBS-88-072, April 5-7, 1988.

Hydrogen Production

Blanford, G.E., Borgesen, P., Maurette, M., Moller, W., and Monart, B.: "Hydrogen and Water Desorption on the Moon: Approximate, On-Line Simulations," pp. 603-609, Lunar Bases and Space Activities of the 21st Century, Mendell, W.W. (ed), Lunar and Planetary Institute, Houston, 1985.

Carter, J.L.: "Lunar Regolith Fines: A Source of Hydrogen," pp. 571-581, Lunar Bases and Space Activities of the 21st Century, Mendell, W.W. (ed), Lunar and Planetary Institute, Houston, 1985.

Cutler, A.H.: "Lunar Hydrogen Extraction," unpublished.

Friedlander, H.N.: "An Analysis of Alternate Hydrogen Sources for Lunar Manufacture," pp. 611-618, Lunar Bases and Space Activities of the 21st Century, Mendell, W.W. (ed), Lunar and Planetary Institute, Houston, 1985.

Gibson, E.K., Bustin, R., and McKay, D.S.: "Lunar Hydrogen: A Resource for Future Use at Lunar Bases and Space Activities," Preprint, 2nd Symposium on Lunar Bases and Space Activities in the 21st Century, Paper No. LBS-88-158, April 5-7, 1988.

Tucker, D.S., Vaniman, D.T., Anderson, J.L., Clinard, F.W., Feber, R.C., Frost, H.M., Meek, T.T., and Wallace, T.C.: "Hydrogen Recovery from Extraterrestrial Materials Using Microwave Energy," pp. 583-590, Lunar Bases and Space Activities of the 21st Century, Mendell, W.W. (ed), Lunar and Planetary Institute, Houston, 1985.

White, D.C. and Hirsch, P.: "Microbial Extraction of Hydrogen From Lunar Dust," pp. 591-602, Lunar Bases and Space Activities of the 21st Century, Mendell, W.W. (ed), Lunar and Planetary Institute, Houston, 1985.

Lunar Resource Processing

Criswell, D.R.: "Extraterrestrial Materials Processing and Construction," Final Report, NSR 09-051-001, Mod. No. 24, Lunar & Planetary Institute, AN#56531, TL797-E96, September 30, 1978.

Criswell, D.R., Waldron, R.D., Meier, J., Goldberg, A., MacKenzie, J.D., and Selman, J.R.: "Extraterrestrial Materials Processing and Construction," Final Report, NSR 09-051-001, Mod. No. 24, LPI, AN#59186 & AN#59187, January 31, 1980.

Ho, D. and Sobon, L.E.: "Extraterrestrial Fiberglass Production Using Solar Energy," pp.225-232, Space Resources and Space Settlements, Billingham, J. and Gilbreath, W. (eds), NASA SP-428, 1979.

Waldron, R.D. and Criswell, D.R.: "Materials Processing in Space," Ch.5, pp. 97-130, Space Industrialization, Volume I, O'Leary, B. (ed), CRC Press, 1982.

Lunar Materials

McKay, D.S. and Williams, R.J.: "A Geologic Assessment of Potential Lunar Ores," pp. 243-256, Space Resources and Space Settlements, Billingham, J. and Gilbreath, W. (eds), NASA SP-428, 1979.

Morris, R.V., Score, R., Dardano, C., and Heiken, G.: "Handbook of Lunar Soils, Part I: Apollo 11-15, Part II: Apollo 16-17," NASA Johnson Space Center, Planetary Materials Branch, JSC-19069, July 1983.

NASA: "Handbook of Lunar Materials," NASA, Johnson Space Center, Lunar and Planetary Sciences Division, May 1978.

Waldron, R.D. and Criswell, D.R.: "Lunar Utilization," Ch.1, pp.1-54, Space Industrialization, Volume II, O'Leary, B. (ed), CRC Press, 1982.

Williams, R.J. and Hubbard, N.: "Report of Workshop on Methodology for Evaluating Potential Lunar Resource Sites," NASA TM 58235, 1981.

Mineral Beneficiation

Agosto, W.N.: "Electrostatic Concentration of Lunar Soil Minerals," pp. 453-464, Lunar Bases and Space Activities of the 21st Century, Mendell, W.W. (ed), Lunar and Planetary Institute, Houston, 1985.

Agosto, W.N.: "Electrostatic Separation of Binary Comminuted Mineral Mixtures," AAS 83-231, in Space Manufacturing, 1983, Vol.53, Advances in the Astronautical Sciences, (Burke, J.D. and Whitt, A.S., Eds.), pp.315-334, 1983.

Inculet, I.I.: "Beneficiation of Lunar Soils," pp. IV.1-IV.64, in "Extraterrestrial Materials Processing and Construction," (Criswell, D.R., et al.) Final Report, NSR 09-051-001, Mod. No. 24, Lunar & Planetary Institute, AN#56531, TL797-E96, September 30, 1978.

Inculet, I.I. and Criswell, D.R.: "Electrostatic Beneficiation of Ores on the Moon Surface," The Institute of Physics Conference Ser. No. 48, 1979, pp.45-53 in "Extraterrestrial Materials Processing and Construction," (Criswell, D.R., et al.) Final Report, NSR 09-051-001, Mod. No. 24, LPI, AN#59186 & AN#59187, January 31, 1980.

Williams, R.J., McKay, D.S., Giles, D., and Bunch, T.E.: "Mining and Beneficiation of Lunar Ores," pp.275-288, Space Resources and Space Settlements, Billingham, J. and Gilbreath, W. (eds), NASA SP-428, 1979.

Lunar Propellant Assessments

Davis, H.P. and Stump, W.R.: "Lunar Oxygen Impact Upon STS Effectiveness," Eagle Report No.83-63, Eagle Engineering, May 1983.

Eagle Engineering: "Lunar Silane Impact Upon Lunar Oxygen Production Logistics," Eagle Report No. 83-70, Eagle Engineering, Inc., Houston, Texas, October 1983.

Wickman, J.H., Oberth, A.E., and Mockenhaupt, J.D.: "Lunar Base Spacecraft Propulsion with Lunar Propellants," AIAA-86-1763, AIAA/ASME/SAE/ASEE 22nd Joint Propulsion Conference, Huntsville, Alabama, June 16-18, 1986.

Extraterrestrial Resource Utilization

Arnold, J.R. and Duke, M.B. (eds.): "Summer (1977) Workshop on Near-Earth Resources," NASA CP-2031, 1978.

Carroll, W.F., Steurer, W.H., Frisbee, R.H., and Jones, R.M.: "Extraterrestrial Materials - Their Role in Future Space Operations," Jet Propulsion Laboratory paper submitted to Astronautics and Aeronautics, January 11, 1983.

Carroll, W.F. (ed.): "Research on the Use of Space Resources," JPL Publication 83-36, March 1, 1983.

Koelle, H.H. and Johenning, B.: "Analysis of the Utilization of Lunar Resources for Space Power Systems," Institut Fur Luft Und Raumfahrt, Technische Universitat, Berlin, 1980.

NASA: "The Utilization of Nonterrestrial Materials," NASA TM 83106, Proceedings of a Workshop held at Palo Alto California in June 1977, 1981.

NASA: "Space-Based Manufacturing From Nonterrestrial Materials," The 1976 NASA-Ames Research Center Study, NASA TM-73265, August 1977.

NASA: "Proceedings of the Seventh Annual Working Group on Extraterrestrial Resources," Held at Denver, Colorado, June 17-18, 1969, 1970.

NASA: "Proceedings of the Sixth Annual Meeting of the Working Group on Extraterrestrial Resources," NASA SP-177, Aerospace Medical Division, Brooks Air Force Base, Texas, February 19-21, 1968.

Morrison, D. and Wells, W.C. (eds.): "Asteriods: An Exploration Assessment," NASA CP-2053, 1978.

Sparks, D.R.: "The Large-Scale Manufacturing of Electronic and Electrical Components in Space," Acta Astronautica, Vol.15, No.4, pp.239-244, 1987.

Resource Utilization Economics

Chapman, P.K., Glaser, P.E., Csigi, K.I., and Roberts, B.: "Space Transportation and Lunar Economics,".

Criswell, D.R. and Waldron, R.D.: "Utilization of Lunar Materials in Space," AAS Paper 78-198, American Astronautical Society, 25th Anniversary Conference, October 30-November 2, 1978.

Glaser, P.E.: "Return to the Moon: Space Transportation Economics," Presentation to Space Studies Institute, Princeton, New Jersey, January 11, 1988.

O'Neill, G.K., Driggers, G., and O'Leary, B.: "New Routes to Manufacturing in Space," Astronautics and Aeronautics, pp.46-51, 1980.

Salkeld, R.J.: "Economic Implications of Extracting Propellants from the Moon," J. Spacecraft, pp. 254-261, February 1966.

Simon, M.C.: "A Parametric Analysis of Lunar Oxygen Production," pp. 531-541, Lunar Bases and Space Activities of the 21st Century, Mendell, W.W. (ed), Lunar and Planetary Institute, Houston, 1985.

Stump, W.R., Christiansen, E.L., Babb, G., Sullivan, D.: "Analysis of Lunar Propellant Production," Eagle Report No. 85-103B, Eagle Engineering, December 9, 1985.

Woodcock, G.R.: "Economic Potentials for Extraterrestrial Resources Utilization," IAA-86-451, 37th Congress of the International Astronautical Federation, Innsbruck, Austria, October 4-11, 1986.

Appendix A - Scaling Equations for H_2 Reduction of Ilmenite Plant

A.1 Front-End Loader

Front-end loader (FL) mass and power requirements are determined by the following equations for both mining feedstock (for basalt-fed and soil-fed LOX plants) and for overburden removal (for basalt-fed plants only).

FL Mass

Mass, M (mt), of all front-end loaders (FL) is:

$$M = N * M_{fl} \qquad \text{Eqn.1}$$

where the number of FLs, N, is selected to produce a FL with dimensions of a reasonable size (for payload manifesting) and M_{fl} is the mass of an individual FL (mt) found from:

$$M_{fl} = F_t * FOS * M_b \qquad \text{Eqn.2}$$

The tipping factor, F_t, is the ratio of FL mass to tipping mass. This ratio is independent of the gravity field (Earth and lunar F_t factors are the same). Numerous F_t factors for terrestrial FLs reviewed by Carrier (88) and others (87, p.177), consistently average about F_t=1.6, independent of FL size. Note that using lunar soil as ballast could potentially reduce the F_t factor below 1.6, thus reducing Earth launch mass of the FL (stability of terrestrial FLs is improved by adding counterweights to the rear of the FL or by adding ballast into the FL tires). The factor of safety, FOS, is the ratio of safe tipping mass to bucket load. For terrestrial FLs, the FOS is usually about 2, but since lunar FLs are assumed to incorporate automatic sensing systems to prevent tipping over, a FOS of 1.2 should be adequate (88). The maximum bucket load, M_b (mt), is related to the FL bucket size, V_b (m^3), and bulk density of loaded materials, p_{av} (mt/m^3):

$$M_b = V_b * p_{av} \qquad \text{Eqn.3}$$

Bulk density of loaded materials is determined from an average of the basaltic rock and soil bulk densities, and fraction basalt:

$$p_{av} = f_b * p_b + (1-f_b) * p_s \qquad \text{Eqn.4}$$

where,

f_b is the fraction basalt in the mined material = 0.5 (assumed)
p_b is basalt bulk density = 2.6, assuming basalt density of 3.2 (79) and 80% packing factor.
p_s is soil bulk density in the FL bucket = 1.8.

A minimum constraint of 0.5 m^3 is assigned to FL bucket size, V_b (m^3), to allow sufficient flexibility in the FL so that it can be applied to other lunar base surface operations. For minimum bucket sizes, there is additional time available to complete other tasks. For bucket sizes greater than the minimum, bucket size is calculated by:

$$V_b = mdot * t_{fl} / (3600 * N * f_{bf} * p_{av}) \qquad \text{Eqn.5}$$

The mining rate, mdot (mt/hr), is determined by applying a 35% duty cycle for mining equipment and the required monthly mining rate. For a 2 mt LOX/month pilot plant,

371 mt of basalt (with 5% oversize & 50% soil rejects) is mined (see Section 6.2.1), or 1,454 kg/hr at 35% duty cycle. The number of FL's, N, was defined in Eqn.1 and the average density of mined material, p_{av}, was defined in Eqn.4. A bucket fill factor, f_{bf}, of 0.95 is used to compensate for spillage of materials during loading. The FL cycle time, t_{fl} (sec), is defined as 120 sec. A basic cycle time of 27-33 sec is considered reasonable for terrestrial loaders, including load, dump, four reversals of direction, and full cycle of hydraulics (120, p.378-379). For a lunar teleoperated FL, 120 sec may be too short, unless a high degree of on-board sensing/computational capability is provided.

FL Power

The peak power required by each FL, P_{fl} (kw/vehicle), is determined by:

$$P_{fl} = M_{fl} * f_p \qquad \text{Eqn.6}$$

where M_{fl} is given in Eqn.1 and the power factor, f_l, is defined as 8.5 kw/mt of FL empty mass, typical of low-capacity terrestrial wheeled FLs (87, p.177; 121). This power can be supplied directly by the power system if each FL is connected by extension cord. However for power sizing purposes, a fuel cell powered FL is assumed. A 64% efficiency factor is assumed in regenerating fuel cell oxygen/hydrogen reactants. Therefore, the power, P (kw), demanded from the photovoltaic (PV) power system for all FLs is:

$$P = N * P_{fl} * f_t/0.64 \qquad \text{Eqn.7}$$

Where the fractional use of available front loader time, f_t, is 1 for front loaders not on the minimum bucket size constraint. For the minimum size constrained FL, the fraction of available mining time actually used by the FL is determined from the sum of the time required to remove overburden (for basalt-fed LOX plants) and to mine feedstock, divided by the available mining time (255.5 hrs/month at 35% duty cycle).

FL Size

The FL bucket is modelled as a triangular prism with dimensions width, W_b (m), height, H_b (m), and depth, D_b (m), related to bucket size, V_b (m^3):

$$V_b = 0.5 * W_b * H_b * D_b \qquad \text{Eqn.8}$$

Given the ratios of bucket width to depth, $R_{w/d} = 2$, and bucket depth to height, $R_{d/h} = 1$, the bucket dimensions are:

$$W_b = R_{w/d} (2 * V_b/R_{w/d})^{1/3} \qquad \text{Eqn.9a}$$

$$H_b = D_b = W_b/R_{w/d} \qquad \text{Eqn.9b}$$

The bucket must extend across the full width of the machine to protect the front tires while excavating (87, p.192). For sizing purposes, the distance the bucket extends beyond the FL chassis, l_e (m), is defined as 0.5 m. The distance the wheels extend beyond both sides of the frame, l_w (m), is set at 1 m. The FL width, W_{fl} (m), is then:

$$W_{fl} = W_b - l_e + l_w \qquad \text{Eqn.10}$$

Given a ratio of FL frame length to heigth, $R_{l/h}$, of 3 and a FL specific gravity, SG, (based on overall chassis dimensions) of 1, the FL length without bucket is:

$$L_{fl} = [M_{fl}/SG * R_{l/h}/(W_b - l_e)]^{0.5} \quad \text{Eqn.11}$$

The length with bucket includes the length of the bucket and the distance the bucket rests from the front of the FL (defined as $2 * D_b$):

$$L_{fl} \text{ w/ bucket} = L_{fl} + 2 * D_b \quad \text{Eqn.12}$$

The FL height includes the distance of the FL above ground, l_g (m), (defined as 1.5 m):

$$H_{fl} = L_{fl}/R_{l/h} + l_g \quad \text{Eqn.13}$$

A.2 Hauler

Haulers are used to deliver feedstock to the LOX plant, remove residual solids from the LOX plant to a discharge area, transport discards (oversize and undersize) from the mining pit to a discharge area, and to transport overburden materials to a discharge area.

Mass

Hauler mass, M_h (mt), is determined from the hauler feedstock load, M_{hl} (mt), and the ratio of hauler load to hauler mass, R:

$$M_h = M_{hl}/R \quad \text{Eqn.14}$$

Low lunar gravity allows the hauler load to empty hauler mass ratio to be substantially higher than the 1.3 ratio typical of terrestrial self-propelled haulers (88) since most of the hauler mass is required for structural support of the payload. A ratio of 8 was suggested as a reasonable design goal for lunar haulers (88). It should be noted that, like the Apollo lunar rover, such a vehicle would collapse if tested in Earth-normal gravity at maximum payload. The hauler load is determined from the hauler bed volume, V_{hb} (m^3), bulk density of hauled materials, p (mt/m^3), and hauler fill factor, f_f:

$$M_{hl} = V_{hb} * p * f_f \quad \text{Eqn.15}$$

The hauler fill factor is set equal to 0.95. The bulk density of hauled materials is the mined material density, p_{av}, (given in Eqn.4) compensated for a swell factor, f_s, which is set to 1.2:

$$p = p_{av}/f_s \quad \text{Eqn.16}$$

A minimum constraint of 4.5 m^3 was defined for the hauler bed volume to allow sufficient margin in pilot plant applications for the hauler to be used in other base surface operations. Otherwise, the hauler bed volume was given by:

$$V_{hb} = 4 * V_b \quad \text{Eqn.17}$$

where the FL bucket volume, V_b, is given in Eqn.5. The number of haulers, N_h, is determined by feedstock transport and overburden removal requirements; essentially given by:

$$N_h = M_f * t_{sum}/(M_{hl} * t_m) \quad \text{(Rounded up to the nearest whole number)} \qquad \text{Eqn.18}$$

where,

M_f (mt) is the mass of feedstock required per month.

t_{sum} (hr) is an average hauler cycle time (for all activities) including the times required by the FL to fill a hauler, for an individual hauler to transport and discharge feedstock at the plant, for filling and transporting process tails to a discharge area, for discharging the tails, for overburden and mining tails handling. Assumptions made for these calculations include: roundtrip haul distance is 2 km, hauler speed is 10 km/hr, discharge time is 10 sec/m^3 of material, reloading tails at the process plant takes 1 min/m^3, roundtrip distance for overburden disposal is 400 m, and processing the mining site tails doubles the feedstock processing time.

t_m (hr) is the available mining time in a month; 255.5 hrs at 35% mining duty cycle.

M_{hl} (mt) is given in Eqn.15.

Total hauler mass, M_{ht} (mt), is:

$$M_{ht} = N_h * M_h \qquad \text{Eqn.19}$$

Power

Assuming that hauler power is provided by fuel cells with a 64% reactant recharging efficiency, total hauler power, P (kw), required of the power system (PV or nuclear) is:

$$P = P_t * t_{hp} * N_t/(t_m * 0.64) \qquad \text{Eqn.20}$$

where,

t_{hp} is the time per cycle that the haulers are actually consuming power. Since hauler power consumption during filling stages (feedstock at the mining site and tails at the process site) is considered zero, power time per cycle is essentially equal to $(t_{sum} - t_{fill})$.

N_t is the total number of hauler roundtrips per month. t_m (hr) is the available mining time per month as defined in Eqn.19.

P_t is the peak hauler power per roundtrip (kw) calculated from:

$$P_t = C_f * (M_h + M_{hl}) * g_m * d_t/t_t \qquad \text{Eqn.21}$$

where,

C_f is the coefficient of rolling resistance, equal to 0.2 in this study (typical values of 0.1-0.2 for rolling in loose sand to soft/rutted roads have been given, Ref. 120, p.641).

M_h (mt) and M_{hl} (mt) are given in Eqns.14 and 15.

g_m is the lunar gravity acceleration, 1.62 m/s^2.

d_t is the total roundtrip distance, assumed as 2000 m.

t_t is the total roundtrip time (sec) assuming 10 km/hr transport time.

As given in Appendix B, a calculated hauler energy ratio of 0.09 w-hr/kg-km was calculated using Eqn.21. This compares with 0.08 w-hr/kg-km specified in another study (122) and the transportation energy requirements for surface and ballastic transport given in Figure A-1.

Size

The following assumptions are made for calculating overall hauler dimensions:

- Ratio of hauler bed length to width, $r_1 = L_{hb}/W_{hb} = 2$.
- Ratio of hauler bed length to height, $r_2 = L_{hb}/H_{hb} = 3$.
- Distance wheels extend beyond sides of vehicle, $l_t = 1$ m.
- Height of hauler above ground, $l_h = 1.5$ m.
- Ratio of hauler bed length to length of hauler drive unit, $r_3 = L_{hb}/L_{hd} = 3$.
- Hauler bed volume, V_{bh} (m^3), from Eqn.17.

Hauler bed length, L_{hb} (m), is:

$$L_{hb} = (V_{bh} * r_1 * r_2)^{1/3} \qquad \text{Eqn.22a}$$

Hauler bed width, W^h_b (m), and height, H_{hb} (m), are:

$$W_{hb} = L_{hb}/r_1 \qquad \text{Eqn.22b}$$

$$H_{hb} = L^h_b/r_2 \qquad \text{Eqn.22c}$$

Overall hauler length, L_h (m), width, W_h (m), and height, H_h (m), are:

$$L_h = L_{hb} * (1 + 1/r_3) \qquad \text{Eqn.23a}$$

$$W_h = W_{hb} + l_t \qquad \text{Eqn.23b}$$

$$H_h = H_{hb} + l_h \qquad \text{Eqn.23c}$$

Figure A-1. Energy Requirements for Hauler and Ballistic Transport (Ref. 88)

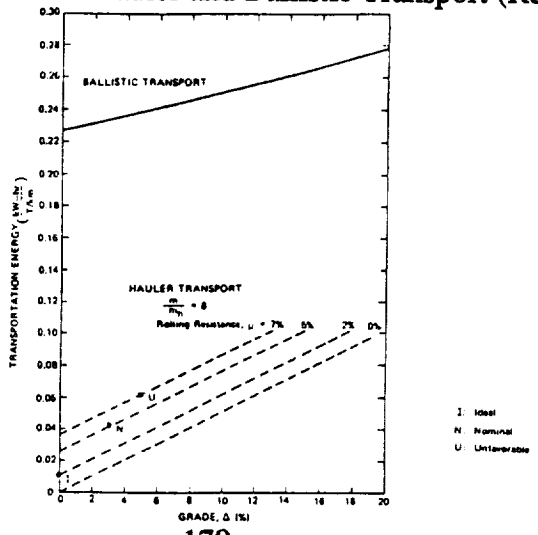

A.3 Pit Scalper

This machine sizes the feedstock (basaltic rock for the pilot plant conceptual design) to reject oversize (10-25 cm) and undersize (<1cm) prior to feeding downstream equipment. It mainly consists of a grizzly scalper to remove oversize, a vibrating screen to remove fine material (non-basalts), two bins (one to hold the sized feedstock, the other for undersize rejects), and the supporting structure.

Mass

Mass of each pit scalper, M_s (kg/unit), is the sum of the grizzly, M_g (kg), vibratory screen, M_v (kg), bins, M_b (kg), and supporting structure, M_{sp} (kg):

$$M_s = M_g + M_v + M_b + M_{sp} \qquad \text{Eqn.24}$$

The grizzly is assumed to consist of spaced, rectangular, steel bars. The length and width of the grizzly are set equal to the hauler bed width. The number of bars was determined from the required spacing between bars, which is set equal to the maximum allowed for the downstream crushing equipment. This maximum size, d^c (cm), was allowed to float with LOX production rate to balance the size of the primary (jaw) crusher (influenced by maximum inlet size) with crusher capacity:

$$d_c = 0.184 * \text{LOX (mt/yr)} + 9.63 \qquad \text{Eqn.25}$$

The mass of the grizzly was determined from the number, length and size (1 cm x 2.5 cm) of the grizzly bars, which were baselined as steel (with S.G. 7.8), multiplied by a 1.2 factor for structure.

The mass of the mechanically vibrated screen was determined by:

$$M_v = F_v * A \qquad \text{Eqn.26}$$

A factor, F_v (kg/m^2), relates vibratory screen mass to screen area; a value of 25 kg/m^2 was used. The screen area, A (m^2), is determined from a capacity relationship (91, p.21-17):

$$A = 0.4\, C_t\, e_m/(C_u\, F_o\, F_s) \qquad \text{Eqn.27}$$

where,

C_t is feed rate to the screen (mt/hr) which is the mining rate minus the oversize rejection rate from the grizzly (assumed to be 5% of the basalt or 2.5% of the mined material, see Section 6.2.1).

e_m is a factor (e_m = 1.5) to account for the expected inefficiencies of screening operation in the lunar low gravity conditions.

C_u is the unit capacity factor (mt/hr of feed per m^2 screen). The following unit capacity relations were derived from literature data (91, p.21-18, Figure 21-15), and using a 1 cm screen size (rejecting all material less than 1 cm as probable non-basalt soil components):
For screen sizes greater than 2.5 cm, $C_u = 43.7 * \text{Size (cm)} + 12$. Eqn.28a

For screen sizes less than 2.5 cm, $C_u = 14.88 * [\text{Size (cm)}]^{0.5}$. Eqn.28b

F_o is the open area factor for the screen (with a 10 mm opening in this case), which was also derived from literature (91, p.21-15, Table 21-6):
$F_o = 0.1079 * [\text{Opening (mm)}]^{0.5} + 0.3354$ Eqn.28c

F_s is the slotted opening factor, which is unity for the square mesh assumed in this study.

A minimum screen area equal to the grizzly area is assumed.

The basis of the mass calculation for the two bins, M_b in Eqn.24, is:

- Each bin's volume is capable of containing 2 hauler loads. Thus, the length of each side of the bin, $L\ (m) = (2 * V_{bh})^{1/3}$. Eqn.28d
- Bin walls are 5 mm thick and constructed of aluminum (S.G. = 2.8).

Structural support mass is:

$$M_{sp} = 0.5 * M_g * M_v \quad \text{Eqn.29}$$

The number of pit scalpers is set equal to the number of haulers required for feedstock and overburden transport, N_h (Eqn.18). Total pit scalper mass is therefore:

$$M_{st} = N_h * M_s \quad \text{Eqn.30}$$

Power

Power for the vibratory screen in the pit scalper is:

$$P_s = F_p * A \quad \text{Eqn.31}$$

where,

Screen area, A (m^2), is defined by Eqn.27 and the screen power factor, F_p (kw/m^2), is 0.75, which was derived from typical Earth industrial "hummer" vibratory screen data (93, p.7-42 and 7-45).

Power for all units is assumed to be provided by electric cabling from the power grid. Total power was determined by applying a mining utility factor (assuming for a 35% mining duty cycle, 70% of daylight time the unit is drawing power):

$$P_{st} = 0.7 * N_h * P_s \quad \text{Eqn.32}$$

Size

The width of the pit scalper is equal to the width of a bin (see Eqn.28d), $W_s = L$ (m), while the twin bin doubles the length of the scalper, $L_s = 2\ L$ (m). The deployed height of the scalper is found from the sum of the height of the hauler, H_h (m), the height of the screens, H_s (m) assumed to be at 30° with length of L (m), and the height of a bin, L (m).

A.4 Process Feed Bin

Mass

The mass of the feed bin is calculated based on:

- Aluminum structure.
- Bin capacity is sized for the maximum difference over a month in the input rate from the mining area (at 35% duty cycle) and the output rate to the process area operating at a different duty cycle (45-90%). The bin size for a 2 mt/month LOX pilot plant is large enough to store approximately 3 days of crusher feedstock.

Size

Size is based on a square-sided bin with a maximum height of 1.5 m. This maximum bin height constraint eases access for the hauler (bottom dump).

A.5 Primary Crusher (Jaw Crusher)

Mass

The following correlations were derived from data for Blake-type Jaw Crushers presented in Ref.91 (p.8-22, Table 8-6) and other sources (93, p.4.1-4.21; 95, p.28.01-28.03; 123).

$$\text{Mass (mt)} = 2 * \text{Width (m)} * \text{Length (m)} * \text{Height (m)} \qquad \text{Eqn.33}$$

where,

$$\text{Crusher Width (m)} = 2 * [\text{Width Receiver (m)}]^{0.5} \qquad \text{Eqn.34a}$$

$$\text{Width Receiver (m)} = \text{Receiver Area (m}^2\text{)/Gap (m)} \qquad \text{Eqn.34b}$$

$$\text{Minimum Rec. Width Constraint (m)} = 0.25 * \text{Gap (m)} \qquad \text{Eqn.34c}$$

$$\text{Receiver Area (m}^2\text{)} = \text{Capacity (mt/hr)}/\{60 * [R/(R-1)]^{0.5} * p\} \qquad \text{Eqn.34d}$$

$$\text{Reduction Ratio, R} = \text{Input feed size/Output feed size} = 4 \qquad \text{Eqn.34e}$$

Capacity (mt/hr) is the feed rate from the process feed bin plus an additional 10% to account for a recycle stream assumed to contain particles larger than the output target size (Output target size = input size/R, where input size is given in Eqn.25). The process duty cycle is 45% for plants operating with solar photovoltaic array (PV)/Regenerative fuel cell (RFC) power systems, or 90% for plants operating with nuclear power, so the solids rate from the feed bin is different than the solids entering the feed bin.

$$\text{Bulk density of feed solids, p (mt/m}^3\text{)} = 1.9 \qquad \text{Eqn.34f}$$

$$\text{Crusher inlet gap (m)} = 0.0125 * \text{Max. Input Size (cm)} \qquad \text{Eqn.34g}$$

$$\text{Crusher Length (m)} = 4 * [\text{Gap (m)}]^{0.5} \qquad \text{Eqn.35}$$

$$\text{Crusher Height (m)} = 2.2 * \text{Gap (m)} + 0.4 \qquad \text{Eqn.36}$$

Power

The Bond crushing law is used to predict crusher power requirements (91, p.8-12; 124, p.825):

$$\text{Power (kw)} = 0.3162 * W_{index} * \text{Feed} * [(1/\text{output size})^{0.5} - (1/\text{input size})^{0.5}] \quad \text{Eqn.37}$$

where,

Basalt work index = Windex = 20.41
Feed rate (mt/hr) includes 10% oversize recycle
Output size (mm) = Input Size (mm)/Reduction Ratio

A.6 Secondary Crusher (Rotary, Gyratory or Cone Crusher)

Correlations derived from Crusher data presented in literature (91, p.8-25, Table 8-11; 93, p.4.21-4.34 and p.4.40-4.55; 95, p.28.08-28.10).

Mass

$$\text{Crusher Mass (mt)} = (\text{S.G.})\pi * (\text{Diameter}/2)^2 * \text{Height} \quad \text{Eqn.38}$$

where,

$$\text{Crusher Diameter (m)} = 1.33 * \text{Crusher Bowl Diameter (m)} \quad \text{Eqn.39a}$$

$$\text{Bowl Diameter (m)} = \text{Receiver Area}/(\pi * \text{Gap}) * \text{Gap} \quad \text{Eqn.39b}$$

$$\text{Receiver Area (m}^2\text{)} = [\text{Capacity}/\{25 * (R/(R-1))^{0.5} * p\}]^{0.75} \quad \text{Eqn.39c}$$

Capacity is the feed rate (mt/hr) from the primary crusher with an additional stream of oversize from the secondary crusher outlet (10% of primary crusher feed).

$$\text{Reduction Ratio} = R = \text{Inlet Size/Outlet Size} = 10 \quad \text{Eqn.39d}$$

$$p = \text{bulk density of solids} = 1.9 \text{ mt/m}^3 \quad \text{Eqn.39e}$$

$$\text{Receiver gap (m)} = 0.012 * \text{Maximum Input Size (cm)} \quad \text{Eqn.39f}$$

$$\text{Crusher Height (m)} = 2.5 * \text{Crusher Diameter (m)} \quad \text{Eqn.40}$$

$$\text{Crusher S.G.} = 1 \text{ mt/m}^3 \quad \text{Eqn.41}$$

Power

As with the primary crusher, the Bond crushing law is used to predict crusher power requirements (91, p.8-12; 124, p.825):

$$\text{Power (kw)} = 0.3162 * W_{index} * \text{Feed} * [(1/\text{output size})^{0.5} - (1/\text{input size})^{0.5}] \quad \text{Eqn.42}$$

where,

Basalt work index = Windex = 20.41
Feed rate (mt/hr) includes 10% oversize recycle
Output size (mm) = Input Size (mm)/Reduction Ratio

A.7 Final Grinding to Desired Product Size (Ball Mill)

References Used: (91, p.8.30-8.34; 93, p.5.03-5.92 and 6.14-6.17; 125).

Mass

Mill Mass (mt) = Liner/Structure Mass (mt) + Ball Charge Mass (mt) Eqn.43

Liner/structure mass estimated from literature data (93, p.5.54-5.55) as 1-2 times ball charge mass. Accounting for lunar structural mass savings, the low end of the scale is assumed:

Structure to Charge Mass Ratio = 1 Eqn.44

From reduction of ball mill data (91, p.8-34, Table 8-18):

$$\text{Ball charge mass (mt)} = 1.116 * [\text{Mill Length (m)}]^{3.279} \quad \text{Eqn.45a}$$

$$\text{Mill Length (m)} = [0.0222 * R^{2/3} + 0.915] * \text{Capacity}^{0.237} \quad \text{Eqn.45b}$$

Capacity is the feed rate (mt/hr) from the secondary crusher.

Reduction ratio = R = Input size/Output size. Output size is set at 0.1 mm as the target size that is a compromise between substantial ilmenite liberation and generation of fines.

Power

Power (kw) = 18.9 * Length (m) Eqn.46

Size

if Length (m) > 1m, Mill Diameter (m) = Length (m) Eqn.47a
if Length (m) < 1m, Mill Diameter (m) = Length (m)/1.25 Eqn.47b

Ilmenite Liberation

The amount of ilmenite mineral fragments liberated in essentially pure form from a basalt matrix (mixture of pyroxene, olivine, plagioclase, ilmenite, and other mineral components) depends on the average size (and shape) of the ilmenite grains and the initial abundance of ilmenite.

$$F_l = 1/\{(1+x)^3 - V_o * [(1+x)^3-1]\} \quad \text{Eqn.48}$$

where,

F_l = fraction of original ilmenite liberated as pure mineral fragments. The rest of the ilmenite is contained in fragments with varying amounts of other mineral constituents.

$x = 1/r$

r = reduction ratio = ilmenite grain size in basalt ore/target size of particles produced in final grinding step = 0.5 mm/0.1 mm = 5

V_o = initial volume fraction ilmenite in ore.

Fines Generated

The final grinding step will produce undesirable fines that will be removed in subsequent steps. The Gates-Gaudin-Schumann size distribution correlation is used to predict the mass fraction of fines produced in the ball mill step (91, p.8.15-8.16):

$$F_f = (d_f/d_t)^{0.7} \qquad \text{Eqn.49}$$

where,

F_f = the mass fraction of fines produced (fraction of particles with diameter d_f and smaller).

d_f = fines particle diameter = 0.03 mm.

d_t = grinding target size = 0.1 mm.

A.8 Vibratory Screen (Fines Removal)

Scaling for the vibratory screen is basically the same as presented for the pit scalper screen.

Mass

The mass of the mechanically vibrated screen was determined by:

$$M_v = F_v * A \qquad \text{Eqn.50}$$

A factor, F_v (kg/m^2), relates vibratory screen mass to screen area; a value of 25 kg/m^2 was used. The screen area, A (m^2), is determined from a capacity relationship (91, p.21-17):

$$A = 0.4\, C_t\, e_m/(C_u\, F_o\, F_s) \qquad \text{Eqn.51}$$

where,

C_t = feed rate to the screen (mt/hr).

e_m = a factor to account for the expected inefficiencies of screening operation in the lunar low gravity conditions = 1.5.

C-3

C_u = unit capacity factor (mt/hr of feed per m^2 screen). The following unit capacity relations were derived (from 91, p.21-18, Figure 21-15):
For screen sizes greater than 2.5 cm, $C_u = 43.7 * \text{Size (cm)} + 12$. Eqn.52a
For screen sizes less than 2.5 cm, $C_u = 14.88 * [\text{Size (cm)}]^{0.5}$. Eqn.52b
A minimum value of 0.05 mt/hr of feed per m^2 of screen was used as a constraint at low capacities where equation accuracy suffers.

F_o = open area factor for the screen (91, p.21-15, Table 21-6):
$F_o = 0.1079 * [\text{Opening (mm)}]^{0.5} + 0.3354$ Eqn.52c

F_s = slotted opening factor = 1 for the square mesh assumed in this study.

Power

Power for the vibratory screen in the pit scalper is:

$$P_s = F_p * A \quad \text{Eqn.53}$$

where,

Screen area, A (m^2), is defined by Eqn.51 and the screen power factor, F_p (kw/m^2), is 0.75, which was derived from typical Earth industrial "hummer" vibratory screen data (93, p.7-42 and 7-45).

Size

Screen Width (m) = 2.5 m
Screen Length (m) = Screen Area/Width/Number of Screens
Screen Height (m) = 0.5 * (Number of Screens - 1) + 0.4

A.8 Ilmenite Separator Feed Bin

Mass calculation basis is cylindrical storage of particulate solids. Bin length, L (m), and diameter, D (m), are calculated given storage requirements (3 days), number of silos (1), length to diameter ratio (0.75 selected for manifesting purposes), and bulk density (1.9 mt/m^3). The vertical pressure exerted by the solids on the base of the storage bin is greater than the lateral pressure on the sides. For a full silo, the base pressure, P_b (Pa), is (124, p.812-815):

$$P_b = D/2 * p * 1000 * g_m/(2 * \mu * r) * \{1 - \exp[-2 * \mu * r * L/(D/2)]\} \quad \text{Eqn.54}$$

where,

p = bulk density = 1.9 mt/m^3

g_m = lunar gravity = 1.62 m/s^2

μ = coefficient of friction at the wall = tan (θ)

θ = angle of internal friction = 38°

r = ratio of lateral to vertical pressure = P_l/P_b

$r = (1 - \sin\theta)/(1 + \sin\theta)$

L = storage bin length (m)

D = storage bin diameter (m)

The lateral pressure, P_l (Pa), in the storage silo is:

$$P_l = r * P_b \qquad \text{Eqn.55}$$

The cyclinder wall thickness, t (mm), can then be calculated as:

$$t = P_l * D/2 * FOS/(\sigma_{al} * 1000) \qquad \text{Eqn.56}$$

where,

FOS = factor of safety = 1.2

σ_{al} = yield stress for aluminum = 324 MPa for Al 2024-T3

The base wall thickness, t_b (mm), is found by:

$$t_b = t/r \qquad \text{Eqn.57}$$

In all cases, a minimum skin thickness of 16 mils or 0.4 mm is assumed. Given a density of 2.8 mt/m^3 for aluminum, the bin mass, M_b (kg), becomes:

$$M_b = 2.8 * \pi * [(D/2)^2 * t_b + D * L * t + (D/2)^2 * t] \qquad \text{Eqn.58}$$

A.9 Induced Magnetic Roll Separator (for Ilmenite Separation)

Relationships for the high-tension induced magnetic roll (IMR) separator were developed from industrial data (96, 97). It is assumed that multi-staged magnetic separators will recover 98% of the pure ilmenite fragments in the feed, and final product stream purity is 90% ilmenite (the rest gangue materials).

Mass

Based on up to a five stage (5 rolls) machine (96):

IMR Mass (mt) = 1.043 * Feed Rate to the machine (mt/hr) Eqn.59

Power

For feed rates less than 0.6 mt/hr: Power (kw) = 1.362 * Feed Rate (mt/hr) Eqn.60a

For feed rates > or = 0.6 mt/hr: Power (kw) = 0.602 * Feed (mt/hr) + 0.7 Eqn.60b

Size

IMR Volume (m^3) = 1.03 * Feed (mt/hr) Eqn.61a

IMR Width (m) = (Volume/(1.8*1.2))$^{1/3}$ Eqn.61b
IMR Length (m) = 1.2 * Width Eqn.61c
IMR Height (m) = 1.8 * Width Eqn.61d

Permanent Magnetic Roll (PMR) Scaling Equations (96-98)

For Feed less than 1.5 mt/hr: Mass (mt) = 0.319 * Feed (mt/hr) Eqn.62a
For Feed > or = 1.5 mt/hr: Mass (mt) = 0.0916 * Feed (mt/hr) + 0.41 Eqn.62b

PMR Power (kw) = 0.196 * Feed (mt/hr) Eqn.63

For Feed < 1.5 mt/hr: PMR Volume (m^3) = 0.85 * Feed (mt/hr) Eqn.64a
For Feed > or = 1.5 mt/hr: PMR Volume (m^3) = 0.341 * Feed (mt/hr) + 0.967 Eqn.64b

PMR Width (m) = (Volume/(1.3*1.9))$^{1/3}$ Eqn.64c
PMR Length (m) = 1.9 * Width Eqn.64d
PMR Height (m) = 1.3 * Width Eqn.64e

Electrostatic Separator Scaling Equations

Efficient electrostatic separation requires that the input feed be heated to approximately 200°C. Because of the insulating nature of lunar soil, subsurface temperatures (> 10 cm deep) are a relatively constant 0 to -20°C (depending on latitude) even during the lunar day (86). Thus, feedstock temperatures of 0°C or less are probable.

Pre-heat Energy: 0.265 kw-hr/mt-°C (Ref.70). For 200°C delta T (0°C input, 200°C output), need 53 kw-hr/mt feed.

Electrostatic Separator Mass: 666 kg per mt/hr feed (derived from Ref.74)

Electrostatic Power: 0.244 kw per mt/hr feed (derived from Ref.46)

Electrostatic Sep. Volume: 7.3 m^3 per mt/hr feed (derived from Ref.46)

E.S. Height = 14 * Width
E.S. Length = 8 * Width

A.10 Reactor Feed Hoppers

Low-Pressure Feed Hopper:

Since the operation of the feed hoppers is such that the low-pressure feed hopper always remains in vacuum conditions (see Section 6.2.3), this hopper is sized like the magnetic separator feed bin (Section A.8).

High-Pressure Feed Hopper:

Hopper length, L (m), and diameter, D (m), is determined by assuming a cylinder, storage requirements of 3 days of feed, 1.9 mt/m^3 bulk solids density, and assigning a L/D ratio of 1.5. The design operating pressure for the hopper is 10 atm (P = 1.03 MPa). Hoop stress in a cylindrical pressure vessel is twice as great as the longitudinal stress. Sizing the wall thickness, t (mm), for the hoop stress results in:

$$t = P' * D/2 * FOS * 1000/\sigma_{al} \quad \text{Eqn.65}$$

where,

t = skin thickness (mm)

D = hopper diameter (m)

P' = hopper pressure (design pressure of 10 atm plus the pressure from the solids, which is negligible compared to the gas pressure) = P = 1.03 MPa

FOS = factor of safety = 1.2

σ_{al} = yield stress for aluminum = 324 MPa for Al 2024-T3 (assumed that the feed hopper operates at temperatures below 200°C, may require insulation or alternative materials).

Hopper mass is determined in a procedure similar to that given in Section A.8 by using the calculated skin thickness and hopper geometry, and assuming aluminum construction (S.G.=2.8).

A.11 Fluidized Bed Reactor

A three stage fluidized bed reactor is assumed. Other assumptions are:

L_i = length of cylinder section of reactor = 6.1 m
Residence time of solids in reactor = 4.2 hrs
The solids occupy a third of the reactor volume.
Operating pressure = 10 atm = 1.03 MPa
Maximum operating temperature = 1,000°C
Inside insulation (high-density) thickness = 7.6 cm
Outside insulation (low-density) thickness = 22.9 cm
Shell material is high-temperature grade alloy steel (A-286)
90% of ilmenite in feed is converted to iron and rutile
2/3rd equilibrium conversion is achieved in middle bed

Mass

Reactor consists of an inner core for counter-current gas/solids flow surrounded by tough high-density insulation, then low-density insulation, then the shell. The total mass of the reactor is the sum of the high- and low-density insulation mass and the shell mass.

$$\text{Mass of inner insulation} = V * p_i \quad \text{Eqn.66}$$

where,

V = volume of high density insulation (m^3)

$$V = \pi \{[(D_i/2 + t_i/100)^2 - (D_i/2)^2] * L_i + 4/3 * [(D_i/2+t_i/100)^3-(D_i/2)^3]\} \quad \text{Eqn.67}$$

$$D_i = \text{inside reactor diameter (m)} = 2 * [F * \theta * 3/(p * L_i * \pi)]^{0.5} \quad \text{Eqn.68}$$

F = feed rate to reactor (kg/hr) 90% ilmenite, 10% gangue
θ = residence time of solids = 4.2 hr
p = bulk density of feed solids = 1,900 kg/m^3
L_i = overall length of cylindrical section of reactor = 6.1 m (1/3 of which occupied by solids).
t_i = high-density insulation thickness = 7.6 cm
p_i = density of high-density insulation = 2,240 kg/m^3 (for superduty fire brick)

Mass of outer insulation = $V_o * p_o$ Eqn.69

where,

V_o = volume of low density insulation (m^3)
$V_o = \pi \{[(D_i/2 + (t_i+t_o)/100)^2 - (D_i/2 + t_i/100)^2] * L_i + 4/3 * [(D_i/2+(t_i+t_o)/100)^3 - (D_i/2 + t_i/100)^3]\}$ Eqn.70

t_o = low-density insulation thickness = 22.86 cm
p_o = density of low-density insulation = 140 kg/m^3 (for Orbiter-like thermal Tiles)

Mass of reactor shell = $V_s * p_s$ Eqn.71

where,

V_s = volume of shell (m^3)
$V_s = \pi \{[(D_i/2 + (t_i+t_o)/100 + t_s/1000)^2 - (D_i/2 + (t_i+t_o)/100)^2] * L_i + 4/3 * [(D_i/2+(t_i+t_o)/100 + t_s/1000)^3 - (D_i/2 + (t_i+t_o)/100)^3]\}$ Eqn.72

t_s = thickness of shell (mm) Eqn.73
$ts = P * D * FOS/(2 * \sigma_s * f_s * 1000)$
P = design pressure = 1.03 MPa
D = diameter (m) = $D_i + 2 * (t_i + t_o)/100$
FOS = factor of safety = 1.5
σ_s = room temperature yield stress for steel alloy A-286 = 655 MPa (Ref.107)
f_s = fraction of room temperature yield stress available at temperature of skin, which is assumed to be 450°F = 0.88 (Ref.107)
p_s = density of Alloy A-286 = 7,940 kg/m^3

Power

Energy requirements = sensible heat of products + heat of reaction + heat loss- sensible heat of reactants.

Heat of reaction = 294 KJ/kg ilmenite converted (@ 900°C from Ref.119)
Sensible heat added = 544 KJ/kg feed (from series of equations, including heat transfer between gas/solids in each bed of reactor, see Appendix B reactor section for details)

Heat loss is found from a simplified thermal analysis:
Thermal radiation loss to space = thermal conduction from interior

$Q_{loss} = \epsilon A_e \sigma T_o^4 = (T_i - T_o)/\Sigma[t * 10/(k * A_{lm})]$ Eqn.74

where,
ϵ = average reactor exterior emissivity = 0.1

A_e = exterior surface area of reactor (m^2)
σ = Stefan-Boltzmann Constant = 5.67 x 10^{-11} kw/m^2-K^4
T_o = exterior temperature (K)
T_i = average interior temperature = 1,173°K
Σ = summation of thermal conductive flux across both insulation layers (thermal resistance of metallic shell is so low, it is neglected in the analysis)
t = insulation thicknesses (cm) as given above
k = thermal conductivity of insulation
k of low-density insulation = 0.19 W/m-K
k of high-density insulation = 1.47 W/m-K
A_{lm} = log-mean surface area of each insulation layer (m^2)
A_{lm} = (exterior area - interior area)/$\log_e$(exterior area/interior area)

The reactor exterior temperature, T_o (K), is determined by solving Equation 74 by trial and error. An iterative technique, such as the Newton-Raphson method, could be used to solve this equation. The power loss, Q_{loss} (kw), is then found after solving for T_o.

The total power demand for the reactor, Q_r (kw), is:

Q_r = Ilmenite Reacted (kg/hr) * 294 KJ/kg + Feed (kg/hr) * 544 KJ/kg + Q_{loss} Eqn.75

This power is provided by heating the reactor gas stream in the electric heater.

Size

Overall Length (m) = $L_i + D_i + 2 * (t_i + t_o)/100 + 2 * t_s/1000$ Eqn.76

Overall Diameter (m) = $D_i + 2 * (t_i + t_o)/100 + 2 * t_s/1000$ Eqn.77

Maximum and Minimum Feed Sizes

Particle sizes in the feed to the fluidized-bed reactor must be small enough to allow fluidization to occur. An equation for fluidized beds that characterizes minimum fluidization conditions is (124, p.163):

$$[g\ p\ (p_p - p)/u^2]\ D^2 - [1.75\ p^2\ V^2/(\phi\ \epsilon^3\ u^2)]\ D - 150\ p\ (1-\epsilon)\ V/(\phi^2\ \epsilon^3\ u) = 0 \qquad \text{Eqn.78}$$

where,

D = particle size (mm) to allow fluidization to occur
g = lunar gravity = 162 cm/s^2
p = gas density in reactor (g/cc) = 0.0002 (for pure hydrogen @ 1000°C)
p = P MW Z/(R*T)
= 10 atm * 2.0158 g/gmole * 1.001765 /(82.056 cm^3-atm/gmole-K * 1273K)
p_p = particle density = 4.79 g/cc for ilmenite
u = gas viscosity (cp or g/m-s) = 0.0237 g/m-s (Ref.126)
V = gas velocity (cm/s) = 30 cm/s in fluidized beds
ϕ = shape factor of particles = surface area of sphere/surface area of particles
ϕ = 0.83 for round sand (124, p.804)
ϵ = minimum porosity of fluidized bed = 0.5 (124, p.162)

The Eqn.78 quadratic in D is solved for the maximum allowable particle size, which for these and lower temperature conditions (900-1000K) results in a maximum allowable size of 0.92-0.95 mm.

The particles in the reactor feed must also be large enough to avoid being entrained by the gas stream and carried out of the reactor. An equation relating gravity and drag forces on a particle in the gas stream is:

$$dU/dt = g\,(p_p - p)/p_p + C_d\,U_2\,p\,A_p/(2\,m) - C_d\,V_2\,p\,A_p/(2\,m) \qquad \text{Eqn.79}$$

where,

dU/dt = acceleration of the particle
g = lunar gravity
p_p = particle density
p = gas density
C_d = drag coefficient
U = particle velocity
A_p = particle projected area
m = particle mass (= $4/3\,\pi\,r^3\,p_p$ for a spherical particle)
V = gas velocity

which, if the particle is floating (U = 0, dU/dt = 0), simplifies to:

$$d = 3\,C_d\,V^2\,p/[4\,(p_p - p)\,g] \qquad \text{Eqn.80}$$

where,

d = minimum particle size to avoid excessive entrainment (cm)
C_d = drag coefficient = approximately 8.4 for a sphere in the Reynolds number of interest.
V = gas velocity = 30 cm/s
p_p = ilmenite density = 4.79 g/cc
p = gas density = 0.0002 g/cc (for pure hydrogen at 1273°K)
g = lunar gravity = 162 cm/s^2

For the given conditions, 15 micron spheres will be entrained. Based on temperatures (900-1000°K) and gas densities (higher due to water content and lower temperature) expected at the top of the reactor, 30 micron (0.03 mm) particles could be entrained.

A.12 Cyclone Separators

Reference for calculations: (91, p.20-84)

$$A = mdot/(p * v) \qquad \text{Eqn.81}$$

where,

A = Area of inlet to cyclone (m^2)
mdot = Mass flow rate of inlet gas stream (kg/sec) = known from mass balances
p = density of inlet gas stream (kg/m^3)
v = inlet gas velocity = 15.2 m/s

The width of the inlet, W (m), and height, H (m), are:

$W = (A/2)^2$
$H = 2 * W$

The cylindrical diameter of the cyclone, D (m), is:

$D = 4 * W$

The overall length of the cyclone, L (m), is:

$L = 4 * D$

Mass

The thickness, t (cm) of the cyclone is:

$t = P * D * FOS * 100/(2 * \sigma * f)$ Eqn.82

P = design pressure = 1.03 MPa
D = cyclone diameter (m)
FOS = factor of safety = 2
σ = room temperature yield stress for Inconel 718 = 1034 MPa (Ref.107)
f = fraction of room temperature yield stress available at temperature of skin, assumed to be 850°C = 0.4 (Ref.107)

Mass = cyclone skin volume * density Eqn.83

Density of Inconel = 8,220 kg/m^3

Since there at least 3 cyclones (1 for each stage), total mass = 3 * cyclone mass

Performance

Particle size with 50% removal efficiency ("cut size"):

$$d_c = 1{,}000{,}000 * [9 * u * W/(2\pi N V (p_p - p))]^{0.5}$$ Eqn.84

where,

d_c = cyclone removes 50% of this particle size (microns)
u = gas viscosity = 1.97×10^{-5} Pa-s (@ 700°C) (from Ref.124, p.996).
W = cyclone width (m)
N = number of effective turns made by gas in cyclone = 5 (typically 5-10) (Ref.91)
V = gas velocity = 15 m/s
p_p = solids density = 4500 kg/m^3.
p = gas density = 0.27 kg/m^3.

Fractional mass collection efficiency, n, for removing particles of size, d (microns), or larger is:

$$n = (d/d_c)^2/[1 + (d/d_c)^2]$$ Eqn.85

A.13 Hydrogen Makeup

Hydrogen loss rate is calculated by assuming that voids in the reactor discharge (through the solid's settling hopper) are filled by gas (mostly hydrogen):

$$mdot_{H2l} = mdot_d/p * \epsilon * p_g \qquad \text{Eqn.86}$$

where,

$mdot_{H2l}$ = mass flow rate (kg/hr) of hydrogen lost in the solids exiting the reactor.

$mdot_d$ = solids discharge rate (kg/hr)

p = solids bulk density = 1900 kg/m^3

ϵ = bed porosity = (particle density - bulk density)/particle density = (5700 - 1900)/5700
ϵ = 0.67

p_g = gas density = 0.27 kg/m^3 for case shown in Appendix B (depends on reactor conditions, temperature).

A.14 Conveyors

References: (46; 70; 91, p.7.3-7.20; 127; 128)

Belt Conveyors

Mass of belt, rolls, drive, and other components estimated by:

$$\text{Mass (kg)} = 5 * \text{Area of belt } (m^2) \qquad \text{Eqn.87}$$

$$\text{Area } (m^2) = 2 * \text{Width belt (m)} * \text{Length belt (m)}$$

Thus,

$$\text{Mass (kg)} = 10 * \text{Width} * \text{Length}$$

Factor of 10 kg/m^2 is a scaled value for lunar gravity (46, 70), typical terrestrial (128) Kevlar reinforced V-belts mass 24 kg/m^2 (for 1 m wide belt) or more for steel reinforced belts.

Belt width determined by capacity equation for V-belts:

Capacity = Belt Width * Average Burden Depth * Belt Speed * Bulk Density

Average burden depth = 0.082 * belt width

$$\text{Width (m)} = [\text{Cap}/(0.082 * \text{Speed} * 60 * p]^{0.5} \qquad \text{Eqn.88}$$

where,

Cap = Solids discharge rate (kg/hr) including tailings rate from reactor, magnetic separator, and fines screen.

Speed = belt speed = 30 m/min (typical terrestrial speeds range up to 100-200 m/min)
p = bulk density = 1900 kg/m^3

A minimum width of 15 cm was specified to ease solid's handling.

Belt length = 15 m

Power requirements: Horizontal runs: 0.0351 kw/m lenth per m^3/sec material flow
Vertical rise (30° maximum): 0.2768 kw/m lift per m^3/sec material

Stowed volume: 0.042 m^3 per m^2 of belt + 50% for other conveyor components.

Screw Conveyors

Mass: 133 kg/m length per m diameter
Diameter: 0.28 m diameter per m^3/hr material flow

Power: 0.00141 kw/m length per mt/hr material flow

Bucket Elevator Conveyor

Mass: 3.4 kg/m lift per mt/hr material flow

Power: 0.005 kw/m lift per mt/hr material flow

Capacity: Volume bucket * No. buckets/m * Speed * bulk density

Normal speeds: 45 m/min = 0.75 m/s. Assume 3 bucket/m, 0.5 m/s.

A.15 Electrolysis Cell

Sizing reference: (25)

Assume solid-state electrolysis, 1,000°C operating temperature. 95% of inlet water electrolyzed to hydrogen and oxygen. Water content of inlet gas stream determined by reactor conditions. Assume conversion approaches 2/3rd of equilibrium value. At 1,000°C, equilibrium molar water content of product gases is 0.105. The electrolysis feed gas would then contain 7% water by volume (molar content) or 40% by mass.

Mass

Mass of electrolysis cell (kg) = 35 * Oxygen production rate (kg/hr) Eqn.89

Power

From thermodynamics, the theoretical minimum power required for water electrolysis at 1000°C is 3.52 kw per kg/hr water. Given an efficiency for the solid-state cells of approximately 72% (25):

Power (kw) = 3.52/0.72 * Water electrolysis rate (kg/hr) Eqn.90

Size

Specific gravity of electrolysis cell (25) is approximately 0.6.

Volume (m^3) = Mass of cell (kg)/600 Eqn.91

Width (m) = (Volume/1.6)$^{1/3}$
Length (m) = Width (m)
Height (m) = 1.6 * Width (m)

Waste heat is effectively radiated from the surface of the cell.

A.16 Oxygen Liquefier

References: (19, 70, 101)

Mass

Refrigerator Mass (kg) = 20 * LOX Rate (kg/hr) Eqn.92

Oxygen load on liquefier includes boiloff from storage tanks. In worst case conditions (non-buried tanks with only 3" insulation, direct sun), boiloff rate from LOX storage tanks was calculated as 64% of the oxygen production rate from the process.

Power

For typical Stirling cycle oxygen liquefiers (101), power consumption is:

Power (kw) = 0.461 * LOX Rate (kg/hr) Eqn.93

Carnot efficiency of 38% is assumed, resulting in overall efficiency of 23% from theoretical cooling load (from sensible and latent heats of oxygen stream).

Volume

Volume (m^3) = Mass (kg) / 1,000 kg/m^3
L/D = 3 (Ref.19) Eqn.94
Diameter (m) = [4 * Volume/(3π)]$^{1/3}$
Length = 3 * Diameter

A.17 Oxygen Storage

Storage tank mass based on:

- N = 2 tanks
- f_u = ullage factor (un-used volume when tanks full) = 0.05 (5% of volume)
- 60 days of process LOX production storage capacity.

Mass LOX stored, M_o (kg) = LOX production rate (kg/day) * 60 days
Volume LOX stored per tank, V_o (m^3) = $M_o/(p_o*N)$, where density of liquid oxygen, p_o = 1,140 kg/m^3

- P_d = 10 atm (1.0 MPa), although nominal operating pressure of 1 atm assumed for maximum boiloff calculations. Boiling point temperature for liquid oxygen increases with pressure by (derived from data in Ref.91):

$$T_{bp}\ (^{\circ}C) = 31.4479 * [P\ (atm)]^{0.2857} - 214.268$$

LOX Data	Vapor Pressure (atm)	Temperature (°C)	
	1	-183.1	
	2	-176.0	
	5	-164.5	
	10	-153.2	
	20	-140.0	
	30	-130.7	
	40	-124.1	
	49.7	-118.9	Critical Point

Thus, the LOX tank could be operated at higher pressure to reduce boiloff (making it easier to place tanks on surface without boiloff problems), but would increase tank wall thicknesses.

$$\text{Tank Mass (kg)} = N * (M_s + M_i) \qquad \text{Eqn.95}$$

where,
N = number of tanks = 2
M_s = mass of tank shell (kg)
M_i = mass of tank insulation (kg)

Shell mass is:

$$M_s = p * 4/3\ \pi\ [(D_i/2 + t_s/1000)^3 - (D_i/2)^3] \qquad \text{Eqn.96}$$

where,
p = density of shell = 2,800 kg/m^3 for Aluminum (2219 alloy)
D_i = inside diameter of tank (m)
$D_i = 2 * [3 * (1 + f_u) * V_o/(4\pi)]^{1/3}$
f_u = tank ullage = 0.05
V_o = Volume of LOX stored in each tank at capacity (m^3)
t_s = thickness of tank shell (mm)
$ts = P * D_i * FOS * 1000/(4 * \sigma_{al})$ Eqn.97
P = design pressure = 1.0 MPa
FOS = factor of safety = 1.5
σ_{al} = Al 2219-T87 yield stress = 324 MPa

Insulation mass is:

$$M_i = p_i * 4/3\ \pi\ [(D_i/2 + t_s/1000 + t_i/100)^3 - (D_i/2 + t_s/1000)^3] \qquad \text{Eqn.98}$$

where,
p_i = Mulilayer insulation (MLI) density = 120 kg/m^3
t_i = MLI thickness = 7.6 cm

A.18 Photovoltaic Power System

References: (102-104)

Solar array sized to deliver required power load, P_L (kw), to process equipment and to regenerate reactants for regenerative fuel cells. The mass of all PV equipment (arrays, structure, and power conversion) is calculated from:

$$\text{PV Mass (kg)} = P_L \text{ (kw)} * 1000/25.5 \qquad \text{Eqn.99}$$

Surface area of PV arrays, A (m^2), found by:

$$A = P_L * 1000/[F_s * n * (1 - f_d) * \cos\theta * (1 - (T-28)*0.005) * f_p] \qquad \text{Eqn.100a}$$

where,

f_d = degradation factor = 0.3 (assume 30% in 10 yrs)
θ = sun angle = 6.5° from normal
T = operating temperature = 50°C (0.5% efficiency loss per °C)
f_p = packing factor = 0.9 (90% solar cell area)
n = cell efficiency at 28°C = 0.115 (11.5%)
F_s = solar intensity at 1 AU = 1,352 W/m^2

Given these factors:

$$A = P_L * 1000/86.6 \qquad \text{Eqn.100b}$$

Major PV factors are: 39.2 kg/kw, 86.6 W/m^2, 3.4 kg/m^2 for all photovoltaic power system equipment.

A.19 Regenerative Fuel Cell Power System

Reference: (25)

A regenerative fuel cell (RFC) system, using gaseous oxygen and hydrogen reactants, was sized based on thermal losses during lunar night from the high-temperature process equipment.

The amount of reactants required for the RFC is:

$$M_r = E_L / 2.913 \qquad \text{Eqn.101}$$

where,

M_r = Reactants (hydrogen and oxygen) required (kg)
E_L = Energy required of RFC system (kwh) = P_L * t = Power load (kw) * time period. t = 336 hrs (14 days x 24 hr/day).

The mass of oxygen, M_O (kg), and hydrogen, M_H (kg), required is:

$$M_O = 0.8881 * M_r \qquad \text{Eqn.102a}$$
$$M_H = 0.1119 * M_r \qquad \text{Eqn.102b}$$

The mass of water produced, M_W (kg) = M_r

The power required, P_R (kw), to regenerate the reactants includes the inefficiency of electrolysis (64% for high temperature electrolysis when compared to P_L) and is:

$$P_R = P_L/0.64 \qquad \text{Eqn.103}$$

Total RFC system mass was calculated as the sum of:

$$\text{RFC System Mass} = \text{RFC} + \text{Reactants} + GO_2 \text{ Tanks} + GH_2 \text{ Tanks} + H_2O \text{ Tank}$$

The regenerative fuel cell is sized with similar equations as the high-temperature electrolysis cell (Section A.15). Most of the RFC system mass is in reactants and tankage.

Two gaseous storage tanks of each reactant (O_2 and H_2) and one water tank are assumed. Estimation of tank masses begins by calculating tank diameter:

$$D_i = 2 * (M * (1+f_u) * 3/(p * N * 4\pi)^{1/3} \qquad \text{Eqn.104}$$

where,

D_i = inside tank diameter (m)
M = mass of stored material (kg)
f_u = ullage factor. For gaseous reactant tanks, f_u = 0. For water tank, f_u=0.5.
p = material density (kg/m^3).
Density of hydrogen gas at storage conditions (10 atm, 400°K) = 6.1 kg/m^3
Density of oxygen gas at 10 atm, 400°K = 97.5 kg/m^3.
Density of water = 1,000 kg/m^3.
N = number of tanks.

Wall thickness is calculated by:

$$t = P * D_i * FOS * 1000/(4 * \sigma_{go}) \qquad \text{Eqn.105}$$

where,

t = tank wall thickness (mm)
P = tank pressure = 100 atm = 10.1 MPa
FOS = factor of safety = 1.5
σ_{go} = yield stress for graphite overwrapped pressure vessels = 579 MPa (Ref.129)

Mass of tank shell is:

$$M_S = p_S * 4/3 * \pi * [(D_i/2 + t/1000)^3 - (D_i/2)^3] \qquad \text{Eqn.106}$$

where,

M_S = tank shell mass (kg)
p_S = shell density = 1,550 kg/m^3 (for thin metallic liner and graphite/epoxy overwrap)

Mass of tank thermal insulation:

$$M_i = p_i * 4/3 * \pi * [(D_i/2 + t/1000 + t_i/100)^3 - (D_i/2 + t/1000)^3] \quad \text{Eqn.107}$$

where,

M_i = tank insulation mass (kg)
p_i = insulation density = 120 kg/m^3
t_i = insulation thickness = 1 cm

Total tank mass, M_t (kg), is the summation over all 5 tanks:

$$M_t = \Sigma [N * (M_S + M_i)] \quad \text{Eqn.108}$$

A small additional mass is calculated for a RFC dedicated thermal control system to reject waste heat generated during the electrolysis step (radiator operates at high-temperature).

A.20 Nuclear Power System

Reference: (105)

The nuclear power system mass estimate includes the reactor, radiator, power converter, and instrument-rated shielding.

Power MWe(MWt)	Reactor (mt)	Radiator (mt)	Converter (mt)	Shielding (mt)	Total (mt)	(kg/kwe)
0.3 (6)	1.6	2.0	1.7	0.9	6.2	20.7
1.0 (14)	2.4	2.9	2.3	1.9	9.5	9.5
3.0 (30)	3.9	3.6	3.7	2.6	13.8	4.6
10.0 (90)	7.4	4.3	4.8	3.2	19.7	2.0

A.21 Thermal Control System

Waste heat from the process units is rejected by a thermal control system (TCS) using a central radiator. Total mass for the TCS, M_t (kg), is estimated by:

$$M_t = 20 * A \quad \text{Eqn.109}$$

where, A = the radiator area (m^2) determined by:

$$A = Q/(2 * n * \sigma * \epsilon * T^4) \quad \text{Eqn.110}$$

where,

Heat rejection from both sides of the radiator is assumed.
Q = heat rejection load (kwt)
n = efficiency of heat rejection = 0.5
σ = Stefan-Boltzmann constant = 5.67 x 10^{-11} kw/m^2-K^4
ϵ = radiator emissivity = 0.8
T = rejection temperature = 298°K

Appendix B - Sample Application of LOX Plant Scaling Program

Case: LOX Pilot Plant, 2 mt/month, PV/RFC Power System, 45% Plant Duty Cycle

28-Jul-88 LUNAR OXYGEN PRODUCTION PLANT SIZING
18:33:28

Crushed Particle Size as Fraction of Ore Grain Size	Min. Volume Fraction Ore in Concentrate (assume dispersed ore, transgranular fractures, all ore recovered)	Fraction Ore Recovered in Concentrate With 100% Purity	Volume Fraction Ore in Feed: 0.10	0.20	0.25	0.33	0.50	0.67
			Volume Fraction Ore/Volume Fraction Gangue: 0.11	0.25	0.33	0.50	1.00	2.00
			Vol.Fraction Ore Liberated					
1	0.125	0	0.14	0.15	0.16	0.18	0.22	0.30
0.5	0.296	0.125	0.32	0.34	0.36	0.39	0.46	0.56
0.333333333	0.422	0.296	0.45	0.48	0.49	0.52	0.59	0.69
0.25	0.512	0.422	0.54	0.57	0.58	0.61	0.68	0.76
0.2	0.579	0.512	0.60	0.63	0.65	0.67	0.73	0.80
0.1	0.751	0.729	0.77	0.79	0.80	0.82	0.86	0.90
0.05	0.864	0.857	0.88	0.89	0.89	0.90	0.93	0.95
0.02	0.942	0.941	0.95	0.95	0.96	0.96	0.97	0.98

Mare Soil 10084, 853 old soil

Size Range (mm)	wt.%	Min.Dia. (mm)	Cumulative wt.% >= Min.	Max.Dia. (mm)	Cumulative wt.% <=Max.	Min.Dia. (mm)	Cumulative wt.% >= Min.	Max.Dia. (mm)	Cumulative wt.% <=Max.
4-10	1.67	4	1.67	10	100	0	100	0.02	26.85
2-4	2.39	2	4.06	4	98.33	0.02	73.15	0.045	44.86
1-2	3.20	1	7.26	2	95.94	0.045	55.14	0.075	57.26
0.5-1	4.01	0.5	11.27	1	92.74	0.075	42.74	0.09	61.27
0.25-0.5	7.72	0.25	18.99	0.5	88.73	0.09	38.73	0.15	72.78
0.15-0.25	8.23	0.15	27.22	0.25	81.01	0.15	27.22	0.25	81.01
0.09-0.15	11.51	0.09	38.73	0.15	72.78	0.25	18.99	0.5	88.73
0.075-0.09	4.01	0.075	42.74	0.09	61.27	0.5	11.27	1	92.74
0.045-0.075	12.40	0.045	55.14	0.075	57.26	1	7.26	2	95.94
0.02-0.045	18.01	0.02	73.15	0.045	44.86	2	4.06	4	98.33
<0.02	26.85	0	100	0.02	26.85	4	1.67	10	100

28-Jul-88
18:33:28

LOX Production Rate (mt/month)	2.0
Annual LOX Production (mt)	24
Production During Day=0.5 (& Night=1)	0.5
Process Plant Utility Factor	0.9
Process Plant Duty Cycle	0.45
Plant LOX Capacity (kg/hr)	6.1

Approximate Soil Mining Rate (mt/hr)	2.558308	326.8 (soil/02 mass ratio)
Assumes: Mining Utility (%)	35%	
Ilmenite in Soil (wt.%)	7.5%	
Oversize (Wt.% Greater than 0.5 mm)	11.27%	
Undersize (Wt.% less than 45 micron)	44.86%	
Ilmenite Recovery in Beneficiation	98%	
Available oxygen in ilmenite	10.5%	
Reactor Conversion Efficiency	90%	

					S.G.
Basalt Layer Mining Rate (mt/hr)	1.453915	185.7 (basalt/02 mass ratio)	Ratio Overburden/Basalt Layer Mined Area	1.3	
Assumes: Mining Utility (%)	35%	(assume daylight)	Thickness Overburden Layer (m)	2	1.8
Basalt Quality as Mined	50%		Thickness Basalt Layer (m)	2	2.85
Oversize (Wt.% > than crusher inlet)	5%				
Ilmenite in Basalt (vol.%)	25%				
Specific Gravity Ilmenite	4.5				
Specific Gravity Basalt	3.4		Extent of Mine: Year:	1 2 3	

Ilmenite in Basalt (wt.%)	33%	
Ilmenite Grain size in Basalt (mm)	0.5	
Grinding Size Target (mm)	0.1	
Reduction Ratio	5	
Ilmenite Composition of Basalt (vol. %)	25%	
Ilmenite Liberated by Grinding (% of Orig Ilmen)	65%	
Minimum Size Limit Entering Reactor (mm)	0.03	
Exponent Factor for Grinding Particle Size	0.7	
Wt. Fraction Input Less than Minimum Size	0.43	0.43
Ilmenite Recovery in Beneficiation	98%	
Available oxygen in ilmenite	10.5%	
Reactor Conversion Efficiency	90%	

Basalt Mined (mt)	2229	4458	6687
Basalt Layer (mt)	4458	8915	13373
Basalt Layer Mined (m^2)	1087	2174	3262
Overburden Area Mined (m^2)	1413	2827	4240
Length Basalt Mine (m)	33	47	57
Len. Overburden Removed (m)	38	53	65
Average Depth of Pit (m)	3	3	3 (if non-basalt fraction of basalt la
Average Depth of Pit (m)	4	4	4 (if all materials removed)
Mass Overburden (mt)	5088	10177	15265
Overburden/Basalt Layer	1.14	1.14	1.14
Total Mine Mass/Oxygen Mass	397.8	397.8	397.8

Rad. System (1=central TCS,2=dedicated)	1
Power System (1=PV/RFC,2=Nuclear)	1
LOX Liquefaction? (1=Yes,2=No)	1

Summary of Mining System Mass/Power:
SOIL MINING/BENEFICIATION:

Mining Utility	Mining Rate (mt/hr)	Beneficiation Utility	Feed Rate (mt/hr)	Ilmenite Feed Conc. (wt%)	Ilmenite Recovered (mt/hr)	Gangue in Conc. (mt/hr)	Gangue in Tails (mt/hr)
35%	2.6	45%	0.87	7.5%	0.06	0.01	0.8

	Number	Tot.Mass (kg)	Power (kw)	Feed Rate (mt/hr)	Length (m)	Dia./Mid.Height (m)		Vol. (m^3)	Screen Size (mm)	Under-Size (mt/hr)	Over-Size (mt/hr)	Days Storage	Radiator/ Array/ Screen Area (m^2)	Use Factor
Front-End Loaders	1	1728	2.28		3.8	2.1	2.2	17.5						9.97%
Haulers	1	962	0.91		4.0	2.5	2.5	25.0						
Feed Bin	1	798		2.558		3.9	5.6	84.1						
Coarse Screen	1	85	2.54	1.990	2.3	1.5	0.4	1.4	0.5	1.8	0.2		3	
Fine Screen	1	1500	45	1.766	4.0	2.5	2.9	29.0	0.045	0.9	0.9		59	
Storage Hopper	1	65		0.873		3.0	4.6	42.1				3		
Magnetic Sep.		910	1.2	0.873	0.9	0.7	1.3	0.9						
Feed to Process				0.871										
			(chk)	0.871288										
Soil Mining Total		2690	3.2					42.5						
Beneficiation Total		3358	48.8					157.5						
Process Total		5235	62.5					19.0						
SubTotal		11284	114.5					219.0						
Margin	30%	3385	34.3					65.7						
Total		14669	148.8					284.7						
				(kg/kwe)										
PV Array	8	6419	163.7	39.2	108.9	17.5		15.1					1903	
Fuel Cells		3285	9.6	343.6	(Pow Req:	14.9)		33.6						
Nuclear Power		0	0.0	0.0				0.0						
Total Power		9704	173.2	56.0				48.7						
Total Plant w/ Power		24373						333.4						
Radiator Total	1	1781			29.7	3	0.01	0.9					89.0	
Alternative Beneficiation:														
Preheat			46.26											
Electrostatic Sep.		581	0.20											

BASALT MINING & BENEFICIATION:

Mining Utility	Mining Rate (mt/hr)	Beneficiation Utility	Feed Rate (mt/hr)	Ilmenite Feed Conc. (wt%)
35%	1.5	45%	0.3	21%

	Number	Tot.Mass (kg)	Power (kw)	Feed Rate (kg/hr)	Length (m)	Dia./Wid. (m)	Height (m)	Vol. (m^3)
Overburden FL Remover	0	0	1.69		3.9	2.1	2.3	0.0
Overburden Haulers	0	0	0.03		4.0	2.5	2.5	0.0
Front-End Loaders	1	1968	1.30		3.9	2.1	2.3	18.6
Haulers	1	1015	0.26		4.0	2.5	2.5	25.0
Pit Scalper	1	380	1.18	1454	4.2	2.1	3.6	31.8
Mining Total		3363	4.45					74.6
Feed Bin	1	215		691	3.9	3.9	1.5	22.7
Primary Crusher	1	724	0.38	591	1.4	0.4	0.7	0.4
Coarse Screen	1	3	0.08	591	0.4	0.3	0.4	0.04
Secondary Crusher	1	239	1.50	537		0.5	1.0	0.24
Coarse Screen	1	3	0.09	591	0.4	0.3	0.4	0.05
Ball Mill	1	1914	16.4	537	1.0	0.8		0.4
Fine Screen	1	500	15	537	4.0	2.5	0.9	9.0
Storage Hopper	1	32		306		2.7	2.0	11.6
Induced Magnetic Sep.	1	248	0.3	238	0.6	0.5	0.9	0.2
Beneficiate Total		3879	33.8					44.7
Alternatives for Ilmenite Separation:								
Electrostatic Preheater			16.2					
Electrostatic Sep.		204	0.07					
Electrostatic Total		204	16.3					
Permanent Magnetic Roll		76	0.05	238	0.8	0.4	0.6	0.20
Reactor Lo-P Hopper	1	12		71.3		1.3	2.0	2.7
Hi-Pres. Feed Hopper	1	77		71.3		1.3	2.0	2.7
Reactor	1	1963	24.0	71.3		0.9	6.6	4.4
Electric Heater	1	134		11.86	1.1	0.9		0.7
Electrolysis Cell	1	213	33.5	6.86	0.6	0.6	1.0	0.4
Blower	1	29	0.29	11.86		0.2	0.3	0.01
Cyclone Separators	3	2.5				0.1	0.3	0.01
Discharge Hopper	1	102		65.20		1.0	2.0	1.6
Tailings Conveyor	1	23	0.002	531.1	15.0	0.2	0.1	0.2
Pre-Liquifier Radiator		0			0.0			
Oxygen Liquifier	1	199	4.6	10.0	1.3	0.4		0.2
Radiator		0			0.0			
Storage Tanks	2	219				1.7		4.9
Process Piping		453			209.1			0.06
Hydrogen Makeup Sys.		27	0.06					0.3
- LH2 Storage Tank	1	24				0.8		0.3
- H2 Heater	1	0.1	0.03		0.1	0.1		0.008

Ilmenite Gangue in

Recovered (mt/hr)	Conc. (mt/hr)	Tails (mt/hr)
0.06	0.01	0.2

Screen Size (mm)	Max Input Size (cm)	Output Size (cm)	Under-Size (mt/hr)	Over-Size (mt/hr)	Days Storage	Radiator/ Array/ Screen Area (m^2)	Heat Rejection (kw)	Use Factor
								6.47%
								7.60%
								4.98%
								7.66%
25.00002	10.00001	2.500002	0.5	0.1		0.109		
2.500002	2.500002	0.250000	0.5	0.1		0.121		
0.03	0.250000	0.01	0.2	0.3	3	18.20		
							16.9	
					3			
					3			
						0.00	1.8	
							5.7	
						0.00		
					60			
							0.02	

- H2 Blower	1	3	0.03			0.1	0.1	0.001		
Radiator/TCS	1	1362			22.7	3.0	0.01	0.7		
									68.1	24.4
H2 Loss Rate (kg/year)		23.69	H2 Proc. Inv.(kg)		0.13					
LH2 Max. Storage (kg)		11.68	Days Storage		180.0					
Mining Total		3363	4.45					74.6		
Beneficiation Total		3879	33.8					44.7		0
Process Total		4817	62.5					18.8		16.9
SubTotal		12059	100.8					138.1		7.5
Margin	30%	3618	30.2					41.4		24.4
Total		15677	131.0					179.5		
				(kg/kwe)						
PV Array	7	5721	145.9	39.2	97.0	17.5		13.2		
Fuel Cells		3285	9.6	343.6	(Pow Req=	14.9)		33.6	1696	
Nuclear Power		0	0.0	0.0				0.0		
Total Power		9005	155.4	57.9				46.8		
Total Plant w/ Power		24682						226.3		

SOIL MINING:

Mining Utility Factor	35%		
Mining Hours per Year	3066		
Mining Rate (mt/hr)	2.6		
Required Mass per month (mt/month)	653.6477		
Number/Mass of Mining Equipment (Excavators, Haulers)			
Excavator Systems: Front-End Loaders			
Number of front-end loaders (FL)	1		
FL Cycle Time (sec)	120		
Bulk Density of Soil in FL Bucket (mt/m^3)	1.8		
Bucket Fill Factor	0.95		
Minimum Bucket Size Flag (1=min, 2=calc)	1		
FL Bucket Size (m^3)	0.5		
Max Bucket Load (mt)	0.9		
Factor of Safety	1.2		
Tipping Mass (mt)	1.1		
Factor Mass FL/Tipping Mass	1.6		
Mass Each Front End Loader (mt)	1.7		
Mass all FLs (mt)	1.7		
Total Material Mining Rate (mt/hr)	25.7		
Percent of mining utility time actually needed by FL	9.97%		
Time per Month FL Used Mining (hrs)	25.5	(chk) 25.48334	
Vertical Distance Bucket Travels (m)	3.5		
Fraction cycle time loaded bucket is raised	0.3	(*No longer used)	
Lunar gravity (m/s^2)	1.62		
Power efficiency factor	0.7	(*No longer used)	
Power for lifting loaded bucket (kw)	0.2025	(*No longer used)	
Power for other fraction of cycle (kw)	0.10125	(*No longer used)	
Power Factor for Wheel FLs (kw/mt empty weight)	8.5		
Peak Power for FL's (kw/vehicle)	14.688		
Avg. Power required by all FLs during mining (kw)	1.464968		
Fuel Cell Charging Efficiency	0.641995		
Avg. Power required from Base Power System (kw) -PV array	2.281897		0.13 (*No longer used)
Scoop Width to Depth Ratio	2		
Scoop Width (m)	1.59		
Scoop Depth and Height (m)	0.793700		

Distance Wheels Extend beyond sides of vehicle (m)	1		
Distance Scoop Extends beyond sides of vehicle (m)	0.5		
SG of FL	1		
Length to Height Ratio (of primary FL structure)	3		
Height bottom of FL above ground (m)	1.5		
Distance Scoop Rests from Front of FL (m)	0.8		
Excavator Width (m) overall envelope	2.1		
Excavator Length (m) overall envelope w/out scoop	2.2		
Excavator Length (m) overall envelope w/ scoop	3.8		
Excavator Height (m) overall envelope	2.2		
Haulers:			
Hauler Bed Length/Width Ratio	2		
Hauler Bed Length/Height Ratio	3		
Hauler Bed Width (m)	1.5		
Hauler Bed Length (m)	3		
Hauler Bed Height (m)	1		
Hauler/Excavator Volume Ratio	4		
Minimum Hauler Volume (m^3)	4.5		
Hauler Volume (m^3)	4.5		
Loaded Soil Bulk Density (mt/m^3)	1.8		
Hauler Fill Factor	0.95		
Time Required to Fill Hauler (min)	18.0	18	
Hauler Load (mt)	7.7		
Roundtrip distance from mine to plant to tailings pit to mine (km)		2	
Average Hauling Velocity (km/hr)	10		
Time Required for Round-Trip (min)	12.0		
Time Required to Discharge (min)	0.8	(sec/m^3) 10	
Time Required to Reload Tailings (min)	4.5	(m^3/min) 1	
Time to Discharge at tailings pit (min)	0.8		
Single Hauler Mass Rate (mt/hr)	12.8		
Number of hauler trips per month	85		
Number of hours per month loading and hauling	51		
Percent of Mining Time Used for loading and hauling	19.95%		
Number of Haulers Required	1	1	
Hauler Mass Factor (mass payload/mass hauler)	8		
Mass of single hauler (mt)	1.0		
Mass of Haulers (mt)	1.0		
Coefficient of rolling friction	0.2		
Power per round-trip (kw)	7.8		
Calculated Hauling Power Required (w-hr/kg-km)	0.090		
Avg. Power required for all haulers (kw)	0.582814	(assume power required for discharge same as hauling, and power req. for loading = zero)	
Fuel Cell Charging Efficiency	0.641995		
Avg. Power required from Base Power System (kw) -PV array	0.907816		
Distance Wheels Extend beyond sides of vehicle (m)	1		
Height bottom of FL above ground (m)	1.5		
Length Bed/Length Hauler Drive Unit	3		
Hauler Width (m) overall envelope	2.5		
Hauler Length (m) overall envelope	4.0		
Hauler Height (m) overall envelope	2.5		
Screening/Beneficiation Utility	0.45		
Feed to Storage Hopper (mt/hr)	2.558308		
Discharge to Screening Section (mt/hr)	1.989795		
Coarse Screen:			

Feed (mt/hr)	2.0
Size Screen (mm)	0.5
Percent feed less than 0.5 mm	88.7%
Undersize Flow (mt/hr)	1.8
Oversize Discard (mt/hr)	0.2

Factors to determine screen area:	
Unit Capacity Factor - Cu (mt/hr per m^2)	0.856989
Open Area Factor - Foa	0.411698
Slotted Opening Factor - Fs	1
Linear Screening Inefficiency Factor	1.5
Calc. Screen Area (m^2)	3
Size per Screen Unit: 2.5 x 4 (m^2)	10
Screen Area (m^2)	3
Number of Units	1
Screen Width (m)	1.5
Screen Length (m)	2.3
Screen Height (m)	0.4
Screen Power Factor (kw/m^2)	0.75
Power per unit (kw/unit)	2.5
Screen Mass Factor (kg/m^2)	25
Mass per unit (kg/unit)	85
Total Power (kw)	2.5
Total Screen Mass (mt)	0.084602

Fine Screen: single stage	
Feed (mt/hr)	1.8
Size Screen (mm)	0.045
Percent feed less than 0.045 mm	50.6%
Undersize Flow Discarded (mt/hr)	0.9
Oversize Flow to Storage (mt/hr)	0.9

Factors to determine screen area:	
Unit Capacity Factor - Cu (mt/hr per m^2)	0.05 (Input manually)
Open Area Factor - Foa	0.358273
Slotted Opening Factor - Fs	1
Linear Screening Inefficiency Factor	1.5
Calc. Screen Area (m^2)	59
Size per Screen Unit: 2.5 x 4 (m^2)	10
Screen Area (m^2)	10
Number of Units	6
Screen Width (m)	2.5
Screen Length (m)	4.0
Screen Height (m)	2.9
Power Scaling Factor (kw/m^2)	0.75
Power per unit (kw/unit)	7.5
Screen Mass Factor (kg/m^2)	25
Mass per unit (kg/unit)	250
Total Power (kw)	45
Total Screen Mass (mt)	1.5

Beneficiation Plant Feed Storage Hopper:

Beneficiation Utility Factor	45%

Fine Screen: three stages (screen sizes of 0.25 mm, 0.15 mm, 0.045 mm).	
Feed to first stage (mt/hr)	1.8
Size Screen (mm)	0.25
Percent feed less than 0.25 mm	91.3%
Undersize Feed to 2nd stage (mt/hr)	1.6
Oversize Flow to Storage (mt/hr)	0.2

Factors to determine screen area:	
Unit Capacity Factor - Cu (mt/hr per m^2)	0.15 (Input manually)
Open Area Factor - Foa	0.39
Slotted Opening Factor - Fs	1
Linear Screening Inefficiency Factor	1.5
Screen Area (m^2)	18
Size per Screen Unit: 2.5 x 4 (m^2)	10
Number of Units	2
Power per unit (kw/unit)	10.7
Mass per unit (kg/unit)	105
Total Power (kw)	21
Total Screen Mass (mt)	0.2

Feed to 2nd Stage (mt/hr)	1.6
Size Screen (mm)	0.15
Percent feed less than 0.15 mm	89.8%

Feed Rate to Beneficiation (mt/hr)	0.9
Days of Storage	3
Storage Capacity (mt)	63
Bulk Storage Density (mt/m^3)	1.9
Storage Volume (m^3)	33
Number of Silos	1
Length/Diameter	1.5
Length (m)	4.6
Diameter (m)	3.0
Angle of Internal Friction (deg)	38
Ratio of Lateral to Vertical pressure	0.238
Lunar gravity (m/s^2)	1.62
Coefficient of Friction	0.781285
Full Silo: Base Pressure (Vertical) (N/m^2)	8,458
Lateral Pressure at Base (N/m^2)	2,012
Al 2024-T4 Yield Stress (MPa)	324
Factor of Safety	1.2
Minimum Wall Thickness (mm)	0.4
Cylinder Wall Thickness (mm)	0.4
Base Wall Thickness (mm)	0.4
Al Density (mt/m^3)	2.8
Single Silo Mass (mt)	0.065010
Total Silo Mass (mt)	0.065010

Beneficiation:

Beneficiation Utility Factor	45%
Hours per Year for Beneficiation	3845
Feed Rate to Beneficiation (mt/hr)	0.9
Ilmenite Conc. in Feed (wt.%)	8%
Ilmenite Recovery Efficiency	98%
Ilmenite Recovered (mt/hr)	0.064
Gangue Material in Concentrate (wt.%)	10%
Gangue in Concentrate (mt/hr)	0.007
Solids flow to Reactor Feed Hopper (mt/hr)	0.07129
Ilmenite in Tailings (mt/hr)	0.017
Tails (mt/hr)	0.802

Electrostatic Separator Preheater:

Average Temperature of Input Material (deg C)	0 (Surface soil temperature range -150 to 130 C, @ 45 cm below surface, temp avg. is -20 C w/ temp cycles of ~2 deg C)
Desired Temperature (deg C)	200
Delta Temp. (deg C)	200
Soil Heat Capacity (kw/C per mt/hr)	0.265
Power for Pre-heat (kw)	46

Two-Stage Electrostatic Separator: (Recovers 98% of ilmenite in feed)

Mass Factor (kg per kg/hr feed)	0.666
Power Factor (kw per mt/hr feed)	0.233
Mass of Electrostatic Sep. (mt)	0.6
Power (kw)	0.2

Undersize Feed to 3rd stage (mt/hr)	1.4
Oversize Flow to Storage (mt/hr)	0.2

Factors to determine screen area:

Unit Capacity Factor - Cu (mt/hr per m^2)	0.08 (Input manually)
Open Area Factor - Foa	0.38
Slotted Opening Factor - Fs	1
Lunar Screening Inefficiency Factor	1.5
Screen Area (m^2)	32
Size per Screen Unit: 2.5 x 4 (m^2)	10
Number of Units	3
Power per unit (kw/unit)	10.7
Mass per unit (kg/unit)	105
Total Power (kw)	32
Total Screen Mass (mt)	0.3

Feed to 3rd Stage (mt/hr)	1.4
Size Screen (mm)	0.045
Percent feed less than 0.045 mm	61.6%
Undersize Feed Discarded (mt/hr)	0.9
Oversize Flow to Storage (mt/hr)	0.6

Factors to determine screen area:

Unit Capacity Factor - Cu (mt/hr per m^2)	0.05 (Input manually)
Open Area Factor - Foa	0.36
Slotted Opening Factor - Fs	1
Lunar Screening Inefficiency Factor	1.5

Screen Area (m^2)	49
Size per Screen Unit: 2.5 x 4 (m^2)	10
Number of Units	5
Power per unit (kw/unit)	10.7
Mass per unit (kg/unit)	105
Total Power (kw)	54
Total Screen Mass (mt)	0.5

	Multi-Stage	Single-Stage
Feed (mt/hr)	1.8	1.8
Total Flow to Storage (mt/hr)	0.9	0.9
Discard (mt/hr)	0.9	0.9
Total	1.8	1.8

Stage:	1	2	3	Total	
Mass (mt)	0.2	0.3	0.5	1.1	1.5
Power(kw)	21	32	54	107	45
Area(m^2)	18	32	49	99	59

Three-Stage Magnetic Separator (Induced Magnetic Roll)	
Beneficiation Utility Factor	45%
Hours per Year for Beneficiation	3845
Feed Rate to Beneficiation (mt/hr)	0.872923
Ilmenite Conc. in Feed (wt.%)	8%
Ilmenite Liberated (%)	100%
Liberated Ilmenite Conc. in Feed (wt.%)	8%
Ilmenite Recovery Efficiency	98%
Ilmenite Recovered (mt/hr)	0.064159
Gangue Material in Concentrate (wt.%)	10%
Gangue in Concentrate (mt/hr)	0.007128
Solids flow to Reactor Feed Hopper (mt/hr)	0.071288
Ilmenite in Tailings (mt/hr)	0.017458
Tails (mt/hr)	0.801634
Mass Factor (kg per kg/hr feed)	1.043
Mass of IMR Separator (mt)	0.910458
Volume Factor (m^3 per mt/hr feed)	1.03
IMR Volume (m^3)	0.899110
IMR Width (m)	0.746654
IMR Length (m)	0.895985
IMR Height (m)	1.343978
Capacity Power Factor (kw per mt/hr)	0.602
Constant Power Factor (kw)	0.7
Power (kw)	1.225499
Efficiency	0.7
Waste Heat (kwt)	0.367649

MINING & BENEFICIATION FOR BASALT MINING

Mining Utility	35%			
Mining Hours per Year	3066			
Mining Hours per Month	255.5			
Mining Rate (mt/hr)	1.454			
Fraction Basalt in Each Mined Bucket	0.5			
Basalt Mining Rate (mt/hr)	0.727			
Amount of Basalt Required per Month (mt)	186			
(Assume Basalt fragments separated in mining pit).				
Ilmenite Grain size in Basalt (mm)	0.5			
Grinding Size Target (mm)	0.1			
Reduction Ratio	5			
Ilmenite Composition of Basalt (vol. %)	25%			
Ilmenite Liberated by Grinding (V% of Orig. Il)	64.7%		Average Ilmenite in Ore Concentrate (Vol.%)	68.4%
Minimum Size Entering Reactor (mm)	0.03			
Exponent Factor for Grinding Particle Size	0.7			
Wt. Fraction Input Less than Minimum Size	0.430511	0.43		

Number/Mass of Mining Equipment (Excavators, Haulers)	
Excavator Systems: Front-End Loaders (FL's)	
Number of front-end loaders (FL)	1
FL Cycle Time (sec)	120
Bulk Density of Basalt Fragments in FL Bucket (mt/m^3)	2.3
Fraction Basalt > 1 cm	0.5

Bulk Density Soil/Reject Material (mt/m^3)	1.8	
Average Bulk Density of Mined Material (mt/m^3)	2.1	
Bucket Initial Fill Factor	0.95	
Minimum Bucket Size Flag (1=min., 2=calc.)	1	
FL Bucket Size (m^3)	0.50	
Max Bucket Load (mt)	1.0	
Factor of Safety	1.2	
Tipping Mass (mt)	1.2	
Factor FL Mass/Tipping Mass	1.6	
Mass Each Front End Loader (mt)	2.0	
Mass all FLs (mt)	2.0	
FL basalt mining rate (mt/hr)	14.6	
Fine Material Seived from Material in Bucket (mt/hr)	14.6	
Total Material Mining Rate (mt/hr)	29.2	
Percent of mining utility time actually needed by FL	4.98%	chk 0.049770 0.049770
Time per Month FL Used Mining Basalt (hrs)	12.7	
Vertical Distance Bucket Travels (m)	3.5	
Fraction cycle time loaded bucket is raised	0.3	(*No longer used)
Lunar gravity (m/s^2)	1.62	
Power efficiency factor	0.7	
Power for lifting loaded bucket (kw)	0.23	(*No longer used)
Power for other fraction of cycle (kw)	0.12	(*No longer used)
Power factor for wheel FLs (kw/mt empty weight)	8.5	
Peak Power for FL's (kw/vehicle)	16.7	
Avg. Power required by all FLs for mining (kw)	0.83	
Fuel Cell Charging Efficiency	0.64	
Avg. Power required by all FLs for mining (kw)	1.30	
Scoop Width to Depth Ratio	2	
Scoop Width (m)	1.59	
Scoop Depth and Height (m)	0.79	
Distance Wheels Extend beyond sides of vehicle (m)	1	
Distance Scoop Extends beyond sides of vehicle (m)	0.5	
SG of FL	1	
Length to Height Ratio (of primary FL structure)	3	
Height bottom of FL above ground (m)	1.5	
Distance Scoop Rests from Front of FL (m)	0.8	
Excavator Width (m) overall envelope	2.1	
Excavator Length (m) overall envelope w/out scoop	2.3	
Excavator Length (m) overall envelope w/ scoop	3.9	
Excavator Height (m) overall envelope	2.3	
Haulers: (assume Hauler self-propelled)		
Hauler Bed Length/Width Ratio	2	
Hauler Bed Length/Height Ratio	3	
Hauler Bed Width (m)	1.5	
Hauler Bed Length (m)	3	
Hauler Bed Height (m)	1	
Hauler/Excavator Volume Ratio	4	
Minimum Hauler Bed Volume (m^3)	4.5	
Hauler Bed Volume (m^3)	4.5	
Bulk Density Mined Material (mt/m^3)	2.3	
Swell Factor for Material Transported	1.2	
Material Bulk Density Loaded in Trailer (mt/m^3)	1.9	
Hauler Fill Factor	0.95	
Time Required to Fill Hauler (min)	33.4	
Hauler Load (mt)	8.1	

Roundtrip distance from mine to plant to tailings pit to mine (km)	2	
Average Hauling Velocity (km/hr)	10	
Time Required for Round-Trip (min)	12.0	
Time Required to Discharge (min)	9.8 (sec/m^3)	10
Time Required to Reload Hauler w/ Tailings (min)	4.5 (m^3/min)	1
Time Required to discharge at tailings area (min)	0.8	
Single Hauler Mass Rate (mt/hr)	9.5	
Number of hauler trips per month	23	
Number of hours per month loading & hauling	20	chk 19.57643
Percent of Mining Time Used for Loading & Hauling	7.66%	
Number of Haulers Required	1	
Hauler Mass Factor (mass payload/mass hauler)	8	
Mass of single hauler (mt)	1.0	
Mass of Haulers (mt)	1.0	
Coefficient of rolling friction	0.2	
Power per round-trip (kw)	8.22	
Calculated Hauling Power Required (w-hr/kg-km)	0.090	
Average Power required for all haulers (kw)	0.17	assume power for dumping hauler = hauling power, for loading = zero)
Fuel Cell Charging Efficiency	0.64	
Avg. Power required from Base Power System (kw) -PV array	0.26	
Distance Wheels Extend beyond sides of vehicle (m)	1	
Height bottom of FL above ground (m)	1.5	
Length Bed/Length Hauler Drive Unit	3	
Hauler Width (m) overall envelope	2.5	
Hauler Length (m) overall envelope	4.0	
Hauler Height (m) overall envelope	2.5	

Overburden Removal (OBR): Front-End Loaders (assume use same type FL's as exacavators)

% available time used if same FLs used for OBR & mining	11.45%
% avail. time used if same haulers used for OBR & mining	15.26%
Number of front-end loaders (FL)	0
Number of Haulers	0
Depth of Overburden (m)	2
Depth of Basalt Layer Mined (m)	2
Area Overburden removed per area basalt mined	1.3
FL Load/Unload Cycle Time (sec)	120
FL Bucket Size (m^3)	0.50
Bucket Fill Factor	0.95
Bulk Density of Soil in FL Bucket & in Hauler (mt/m^3)	1.8
Max Bucket Load (mt)	0.9
Area Basalt Layer Mined (m^2/hr)	0.355
Rate of Overburden Removal (mt/hr)	1.7
Overburden per Month (mt)	424
Time to Fill Haulers per Month (hr)	16.5
Mass Each Front End Loader (mt)	2.0
Mass all FLs (mt)	0.0
Power factor for wheel FLs (kw/mt empty weight)	8.5
Peak Power for FL's (kw/vehicle)	16.7
Avg Power required by all FLs for overburden removal (kw)	1.08
Fuel Cell Charging Efficiency	0.64
Power required by FLs fuel cells from base power (kw)	1.69
Hauler Bed Volume (m^3)	4.5
Hauler Fill Factor	0.95
Distance to Discard (m)	200
Travel Speed (km/hr)	10
Round-trip travel time (min)	2.4

Hauler Dump time (min)	0.8
Time per Month to Haul Material (hr)	2.9
Power Required for Hauling (kw)	1.53
Avg. Power required by all Haulers (kw)	0.02
Avg. Power for overburden Haulers from base power (kw)	0.03
Mass each additional Hauler (mt)	1.0
Mass overburden haulers (mt)	0.0
Mine Pit Scalper/Coarse Sizer:	
Mining Rate (mt/hr)	1.45
Grizzly Scalper - (Oversize Protection)	
Oversize Rejected Wt.% of Basalt	5%
Oversize Rate Rejected (mt/hr)	0.036
Max. Feed Size to Crushers (cm)	10
Width of Grizzly Scalper (m)	1.5
Length of Grizzly Scalper (m)	1.5
Spacing between Scalper bars (m)	0.100000
Number of grizzly spaced (inclined) bars	15
Bar Width (cm)	1
Bar Length (cm)	3
Density of bars (mt/m^3)	7.8
Length of bars (m)	1.5
Volume of bars (m^3)	0.0068
Mass of bars (kg)	52.7
Amount of Basaltic Rock in each mined bucket	50% (assume half rock & half soil, assume soil is rejected through grizzl
Minimum Size to Crusher (cm)	1
Undersize Soil Rejected (mt/hr)	0.727
Feed to Crusher Bin (mt/hr)	0.690609
Factors to size screen for crusher feed:	
Feed (mt/hr)	1.418
Size Screen (mm)	10
Feed greater than Screen Size (%)	49%
Oversize Flow to Crusher (mt/hr)	0.691
Undersize Flow Rejected in Pit (mt/hr)	0.727
Unit Capacity Factor - Cu (mt/hr per m^2)	14.70
Open Area Factor - Foa	0.68
Slotted Opening Factor - Fs	1
Lunar Screening Inefficiency Factor	1.5
Required Screen Area (m^2)	0.086
Design Width (m)	1.5
Design Length (m)	1.5
Size per Screen Unit: (m^2)	2.25
Screening Power Factor (kw/m^2)	0.75
Screen Mass Factor (kg/m^2)	25
Screen Power (kw)	1.7
Screen Utility (Fraction Time Unit On)	0.7
Pit Scalper Power (kw)	1.2
Number of Scalper Units	1
Power for all Scalpers (kw)	1.2
Screen Mass (kg)	56.3
Structure Mass Factor (kg structure/kg screens)	0.5
Structure Mass (kg)	54.5
Bin Volume (m^3)	9.0
Bin Side Length (m)	2.1
Bin Wall Thickness (mm)	5
Bin Material Density (mt/m^3)	2.8

Bin Mass (kg)	108	
Number Bins per Pit Scalper	2	
Pit Scalper/Screener Mass (kg/unit)	380	
Total Pit Scalper/Screener Mass (kg)	380	
Hauler Height (m)	2.5	(added 1 m off ground)
Height Screens (m)	1.5	
Deployed Height (m)	4	
Pre-Crusher Bin:		
Feed to Bin (mt/hr)	0.690609	
Utility of Mining	0.35	
Utility of Crusher Stages	0.45	
Feed to Crusher (mt/hr)	0.537141	
Delta Feed over mining utility (mt)	39.21129	
Factor over delta	1.1	
Bin Storage Capacity (mt)	43.1	
Bin Width (m)	3.9	
Bin Length (m)	3.9	
Bin Height (m)	1.5	
Bin Volume (m^3)	22.7	Chk 43.1
Bulk Density of Material in Bin (mt/m^3)	1.9	
Bin Fill Factor	0.95	
Days of Storage	3.3	
Hauler Capacity (mt)	8.1	
Number of Hauler Loads Capable of being Stored	5.3	
Thickness of Bin Walls (mm)	2	
Density of Al 2024-T3 (mt/m^3)	2.8	
Volume Bin Walls (m^3)	0.077	
Mass Bin (mt)	0.215	

Primary Crusher (Jaw Crusher):

Feed Rate to Primary Crusher (mt/hr)	0.537
Max. Input Size (cm)	10
Recycle Rate of Oversize (% of Mine)	10%
Feed Rate (Scalper+Recycle) (mt/hr)	0.591
Feed Density (mt/m^3)	1.9
Speed (rpm)	225
Output Size (cm)	2.5
Reduction Ratio	4.0
Work Index (Basalt)	20.41
Required Power (kw)	0.4
Crusher Inlet Gap (m)	0.13
Receiver Area (m^2)	0.004
Calc. Rec. Width to match feed rate (m)	0.036
Minimum Receiver Width (m)	0.03
Receiver Width (m)	0.04
Mass (mt)	0.72
Length (m)	1.4
Height (m)	0.7
Width (m)	0.4
Volume (m^3)	0.4
Actual Crusher Max. Capacity (mt/hr)	0.6

Coarse Screen to Recycle Crusher Oversize:

Feed (mt/hr)	0.591

Size Screen (mm)	25.00002
Feed greater than Screen Size (%)	9%
Oversize Flow Recycle (mt/hr)	0.054
Undersize Feed 2nd Crusher (mt/hr)	0.537

Factors to determine screen area:

Unit Capacity Factor - Cu (mt/hr per m^2)	25.06
Open Area Factor - Foa	0.88
Slotted Opening Factor - Fs	1
Lunar Screening Inefficiency Factor	1.5
Calc. Screen Area to achieve capacity (m^2)	0.016
Minimum Screen Area (m^2)	0.109
Screen Area (m^2)	0.109
Size per Screen Unit: (m^2)	0.109
Number of Units	1
Screen Width (m)	0.3
Screen Length (m)	0.4
Screen Height (m)	0.4
Screen Power Factor (kw/m^2)	0.75
Power per unit (kw/unit)	0.1
Screen Mass Factor (kg/m^2)	25
Mass per unit (kg/unit)	2.7
Total Power (kw)	0.1
Total Screen Mass (mt)	0.003

Secondary Crusher (Gyratory Crusher):

Feed Rate from Primary (mt/hr)		0.537
Recycle Rate of Oversize (% of Prim)		10%
Feed Rate (Prim.+Recycle) (mt/hr)		0.591
Max. Input Size (cm)		2.5
Feed Opening (m)	Gap:	0.03
	Width:	1.29
Output Size (cm)		0.3
Reduction Ratio		10.0
Work Index (Basalt)		20.41
Power (kw)		1.5
Feed Density (mt/m^3)		1.9
Receiver Area (m^2)		0.036
Bowl Diameter (m)		0.41
Mass (mt)		0.2
Diameter (m)		0.5
Height (m)		1.0
Volume (m^3)		0.24

Coarse Screen to Recycle Secondary Oversize:

Feed (mt/hr)	0.6
Size Screen (mm)	2.500002
Feed greater than Screen Size (%)	9%
Oversize Recycle to Recrush (mt/hr)	0.054
Undersize Feed to Grinder (mt/hr)	0.537

Factors to determine screen area:

Unit Capacity Factor - Cu (mt/hr per m^2)	5.79
Open Area Factor - Foa	0.51

Slotted Opening Factor - Fs	1
Lunar Screening Inefficiency Factor	1.5
Calc. Screen Area to achieve capacity (m^2)	0.121
Minimum Screen Area (m^2)	0.109
Calc. Screen Area (m^2)	0.12
Size per Screen Unit: (m^2)	0.1
Number of Units	1
Screen Width (m)	0.3
Screen Length (m)	0.4
Screen Height (m)	0.4
Screen Power Factor (kw/m^2)	0.75
Power per unit (kw/unit)	0.1
Screen Mass Factor (kg/m^2)	25
Mass per unit (kg/unit)	3.0
Total Power (kw)	0.1
Total Screen Mass (mt)	0.003

Final Grinding to desired product size (Ball Mill):

Feed Rate (mt/hr)	0.537
Feed Size (mm)	2.500002
Desired Output Size (mm)	0.1
Reduction Ratio	25.00002
Grinder Length (m)	1.0
Power (kw)	16
Ball Charge Mass (mt)	1.0
Structure to Charge Ratio	1
Mill Mass (mt)	1.9
Diameter (m)	0.8
Volume (m^3)	0.4

Fine Screen: single stage

Feed (mt/hr)	0.537
Size Screen (mm)	0.03
Percent feed less than screen size	43%
Undersize Flow Discarded (mt/hr)	0.231
Oversize Flow to Storage (mt/hr)	0.306

Factors to determine screen area:

Unit Capacity Factor - Cu (mt/hr per m^2)	0.05 (Input manually)
Open Area Factor - Foa	0.35
Slotted Opening Factor - Fs	1
Lunar Screening Inefficiency Factor	1.5
Screen Area (m^2)	18
Size per Screen Unit: 2.5 x 4 (m^2)	10
Number of Units	2
Screen Width (m)	2.5
Screen Length (m)	4.0
Screen Height (m)	0.9
Screen Power Factor (kw/m^2)	0.75
Power per unit (kw/unit)	7.5
Screen Mass Factor (kg/m^2)	25
Mass per unit (kg/unit)	250
Total Power (kw)	15
Total Screen Mass (mt)	0.5

Beneficiation Plant Feed Storage Hopper:

Beneficiation Utility Factor	45%
Feed Rate to Beneficiation (mt/hr)	0.306
Days of Storage	3
Storage Capacity (mt)	22
Bulk Storage Density (mt/m^3)	1.9
Storage Volume (m^3)	12
Number of Silos	1
Length/Diameter	0.75
Length (m)	2.9
Diameter (m)	2.7
Angle of Internal Friction (deg)	38
Ratio of Lateral to Vertical pressure	0.238
Lunar gravity (m/s^2)	1.62
Coefficient of Friction	0.78
Full Silo: Base Pressure (Vertical) (N/m^2)	4,778
Lateral Pressure at Base (N/m^2)	1,136
Al 2024-T4 Yield Stress (MPa)	324
Factor of Safety	1.2
Minimum Wall Thickness (mm)	0.4
Cylinder Wall Thickness (mm)	0.40
Base Wall Thickness (mm)	0.40
Al Density (mt/m^3)	2.8
Single Silo Mass (mt)	0.03
Total Silo Mass (mt)	0.03

Beneficiation:

Beneficiation Utility Factor	45%	
Hours per Year for Beneficiation	3845	
Feed Rate to Beneficiation (mt/hr)	0.306	
Ilmenite Conc. in Basalt (wt.%)	33%	
Ilmenite Liberated (%)	65%	
Liberated Ilmenite Conc. in Feed (wt.%)	21%	
Ilmenite Recovery Efficiency	98%	
Ilmenite Recovered (mt/hr)	0.064	
Gangue Material in Concentrate (wt.%)	10%	
Gangue in Concentrate (mt/hr)	0.007	
Solids flow to Reactor Feed Hopper (mt/hr)	0.071	
Ilmenite in Tailings (mt/hr)	0.006	(includes ilm. in gangue & lost mineral frag.)
Tails (mt/hr)	0.235	

Electrostatic Separator Preheater:

Average Temperature of Input Material (deg C)	0	(Surface soil temperature range -150 to 130 C, @ 45 cm below surface, temp avg. is -20 C w/ temp cycles of ~2 deg C)
Desired Temperature (deg C)	200	
Delta Temp. (deg C)	200	
Soil Heat Capacity (kw/C per mt/hr)	0.265	
Power for Pre-heat (kw)	16	

Two-Stage Electrostatic Separator: (Recovers 98% of ilmenite in feed)	
Mass Factor (kg per mt/hr feed)	666
Power Factor (kw per mt/hr feed)	0.233
Mass of Electrostatic Sep. (mt)	0.20
Power (kw)	0.07
Three-Stage Magnetic Separator (Induced Magnetic Roll)	
Beneficiation Utility Factor	45%
Hours per Year for Beneficiation	3845
Feed Rate to Beneficiation (mt/hr)	0.237918
Ilmenite Conc. in Basalt (wt.%)	33%
Ilmenite Liberated (%)	65%
Liberated Ilmenite Conc. in Feed (wt.%)	21%
Ilmenite Recovery Efficiency	98%
Ilmenite Recovered (mt/hr)	0.049902
Gangue Material in Concentrate (wt.%)	10%
Gangue in Concentrate (mt/hr)	0.005544
Solids flow to Reactor Feed Hopper (mt/hr)	0.055446
Ilmenite in Tailings (mt/hr)	0.004758
Tails (mt/hr)	0.182471
Mass Factor (kg per kg/hr feed)	1.043
Mass of IMR Separator (mt)	0.248149
Volume Factor (m^3 per mt/hr feed)	1.03
IMR Volume (m^3)	0.25
IMR Width (m)	0.48
IMR Length (m)	0.58
IMR Height (m)	0.87
Capacity Power Factor (kw per mt/hr)	1.362
Constant Power Factor (kw)	0
Power (kw)	0.32
Efficiency	0.7
Waste Heat (kwt)	0.10
Permanent Magnetic Roll Separator:	
Beneficiation Utility Factor	45%
Hours per Year for Beneficiation	3845
Feed Rate to Beneficiation (mt/hr)	0.237918
Ilmenite Conc. in Basalt (wt.%)	33%
Ilmenite Liberated (%)	65%
Liberated Ilmenite Conc. in Feed (wt.%)	21%
Ilmenite Recovery Efficiency	98%
Ilmenite Recovered (mt/hr)	0.049902
Gangue Material in Concentrate (wt.%)	10%
Gangue in Concentrate (mt/hr)	0.005544
Solids flow to Reactor Feed Hopper (mt/hr)	0.055446
Ilmenite in Tailings (mt/hr)	0.004758
Tails (mt/hr)	0.182471
Capacity Mass Factor (kg per kg/hr feed)	0.319
Constant Mass Factor (kg)	0
PM Roll Mass (mt)	0.075896
Capacity Volume Factor (m^3 per kg/hr feed)	0.85
Constant Vol. Factor (m^3)	0
PM Roll Volume (m^3)	0.20
PM Roll Width (m)	0.43

PM Roll Length (m)	0.83
PM Roll Height (m)	0.56
Power Factor (kw per mt/hr feed)	0.196
Power (kw)	0.05
Low-Pressure Reactor Feed Hopper:	
Feed Rate (kg/hr)	71.3
Days of Storage	3
Storage Capacity (mt)	5.1
Bulk Storage Density (mt/m^3)	1.9
Storage Volume (m^3)	2.7
Number of Silos	1
Length/Diameter	1.5
Length (m)	2.0
Diameter (m)	1.3
Angle of Internal Friction (deg)	38
Ratio of Lateral to Vertical pressure	0.238
Lunar gravity (m/s^2)	1.62
Coefficient of Friction	0.78
Full Silo: Base Pressure (Vertical) (N/m^2)	3,670
Lateral Pressure at Base (N/m^2)	873
Al 2024-T4 Yield Stress (MPa)	324
Factor of Safety	1.2
Minimum Wall Thickness (mm)	0.4
Cylinder Wall Thickness (mm)	0.40
Base Wall Thickness (mm)	0.40
Al Density (mt/m^3)	2.8
Single Silo Mass (kg)	12.2
Total Silo Mass (kg)	12.2
Hi-Pressure Reactor Feed Hopper:	
Feed Rate (kg/hr)	71.3
Days of Storage	3
Storage Capacity (mt)	5.1
Bulk Storage Density (mt/m^3)	1.9
Storage Volume (m^3)	2.7
Number of Silos	1
Length/Diameter	1.5
Length (m)	2.0
Diameter (m)	1.3
Angle of Internal Friction (deg)	38
Ratio of Lateral to Vertical pressure	0.238
Lunar gravity (m/s^2)	1.62
Coefficient of Friction	0.78
Full Silo: Base Pressure from Solids (MPa)	0.004
Lateral Pressure at Base from Solids (MPa)	0.001
Design Pressure (MPa)	1.03
Al 2024-T4 Yield Stress (MPa)	324
Factor of Safety	1.2
Minimum Wall Thickness (mm)	0.4
Cylinder Wall Thickness (mm)	2.5
Base Wall Thickness (mm)	2.5
Al Density (mt/m^3)	2.8
Single Silo Mass (kg)	77.3

Total Silo Mass (kg)	77.3							
Reactor:								
Process Utility	45%							
Reactor Space Velocity (1/hr)	0.24							
Feed Rate to Reactor (kg/hr)	71.29			Max Reactor Pressure (N/m^2)	1.03E+06	psia	150	
Inside Diameter of Reactor (m)	0.31	(ft) 1.02		Reactor Shell Diameter (m)	0.92			
Shell Wall Thickness (cm)	0.12			SS Alloy A-286 Yield Stress (MPa) @ R.T.	655			A12024-T4 Yield St
Hi-Density Insulation Thickness (cm)	7.6			Reduction of Yield Strength @ 450F (500K)	0.88			
Lo-Density Insulation Thickness (cm)	22.86			Factor of Safety	1.5			
Exterior MLI Thickness (cm)	0			Minimum Wall Thickness (mm)	0.4			
Outside Diameter of Reactor (m)	0.92			Cylinder Wall Thickness (mm)	1.24			
Length of Reactor Cylinder (m)	6.1							
Length of ID Reactor Heads (m)	0.16							
Overall Length of Reactor (m)	6.6							
Steel Shell Density (mt/m^3)	7.94							
Volume of Shell (m^3)	0.01							
Mass of Shell (mt)	0.09							
Density of Hi-Density Insulation (mt/m^3)	2.24	(superduty fire clay brick)						
Volume of Hi-Density Insulation (m^3)	0.60							
Mass of Hi-Density Insulation (mt)	1.35							
Density of Lo-Density Insulation (mt/m^3)	0.14							
Volume of Lo-Density Insulation (m^3)	3.38							
Mass of Lo-Density Insulation (mt)	0.47							
Density of Multilayer Insulation (MLI) (mt/m^3)	0.12							
Volume of MLI (m^3)	0.00							
Mass of MLI (mt)	0.00							
Total Insulation Mass (mt)	1.82							
Mass of Internals (mt)	0.05	(6 ceramic plates, 0.5 cm thick, 2 cm downcomer)						
Reactor Mass (mt)	1.96							
Internal Volume (m^3)	0.48							
Internal Surface Area (m^2)	6.2							
Exterior Surface Area (m^2)	20.3							
Hi-Dens. Insul. Thermal Conductivity (W/m-K)	1.47			Initial T T2 T3 T4 T5				
Lo-Dens. Insul. Thermal Conductivity (W/m-K)	0.19			400 400.0150 400.0301 400.0452 400.0602				
MLI Thermal Conductivity (W/m-K)	6.80E-05							
Average Reactor Exterior Emissivity	0.1							
Mean Internal Temperature (K)	1173	Max Internal Temp.(K)	1273					
Stefan Boltzmann Constant (kw/m^2-K^4)	5.7E-11							
Exterior Surface Area of Hi-Dens. Ins. (m^2)	9.5							
Exterior Surface Area of Lo-Dens. Ins. (m^2)	20.28							
Exterior Surface Area of Shell (m^2)	20.34							
Log Mean Area for Hi-Dens. Ins. (m^2)	7.78							
Log Mean Area for Lo-Dens. Ins. (m^2)	14.24							
Log Mean Area for MLI (m^2)	20.34							
Exterior Temperature (K)	502.5							
Cond. Heat Loss (kw)	7.36							
Radiative Heat Loss (kw)	7.35	(check)						
Heat Loss (kw)	7.4							
Temp. (K) at Hi-Dens./Lo-Dens. Ins. Interface	1124.1							
Temp. (K) at Lo-Dens. Ins./Shell Interface	502.5							
Temp. (K) at Shell/MLI Interface	502.5							
Temp. (K) at MLI/Exterior Interface	502.5							
Heat of Reaction @ 900C (KJ/kg ilmenite)	294							

Ilmenite in Feed to Reactor (kg/hr)	64.2				
Conversion Factor	90%				
Ilmenite Converted (kg/hr)	57.7				
Power Req. for Reaction Heat (kw)	4.7		Cp (cal/K mole) = a + bT + cT^-2		
Feed Temp (K)	273		a	b	c
Solids Exit Temp (K)	1044		28.6184	0.003851	-644287.
Sensible Heat Enthalpy Change of Solids (KJ/kg)		544	ho=	-10.7609	
Power Req. for Solids Sensible Heat (kw)	10.8		Sensible+Reaction Power per Mass Rate Ilmenite Reacted (kw/mt/hr FeTiO3)		268
Efficiency of Electric Heater	95%		Sens.+React.+Heat Loss Power (kw per mt/hr ilmenite)		395
Total Power (kw)	24.0		Heat Capacity of Solids (kw/C per mt/hr)	0.196	

Reactor Auxiliaries:

Middle Bed, Feed to Electrolysis					
Temp. Reaction (C)	1000				
Equilibrium Conc. H20 @ Rxn.Temp. (mole fract)	0.105				
Approach to Equilibrium	0.667				
Efficiency of Electrol. (H20 converted/H20 feed)	0.95				
Oxygen Production (kg/hr)	6.000				
H20 to Electrolysis (kg/hr)	7.216				
H2 to Electrolysis (kg/hr)	10.728				
Mole fraction H20 in gases above middle bed	0.07	0.07 (chk)			
Electrolysis input (kg/hr)	17.944				
Pressure (MPa)	1.03		Psia	150	
Avg. MW of Gases above middle bed	3.14				
Gas Constant (MPa-cm^3/gmole-K)	8.314				
Avg. Density of Gases above middle bed (kg/m^3)	0.306				
Superficial Gas Velocity above middle bed (m/s)	0.21		ft/s	0.71	
H20 remaining in Electrolysis H2 Output (kg/hr)	0.361				
H2 in gas flow to base of top bed (kg/hr)	11.495		(% of Feed)	16.1%	
Gas flow to base of top bed (kg/hr)	11.855				
H2 mass fraction in gas flow to top bed	0.970				
H2 mole fraction in gas flow to top bed	0.997				
Top Bed					
Estimated Exit Temp. (K)	923				
Average Heat Capacity of Solids (kw-hr/kg-K)	2.17E-04				
Average Heat Capacity of Gases (kw-hr/kg-K)	4.14E-03				
Heat Loss factor	0.25				
Heat Loss (kw)	1.84				
Gas/Solid Outlet Temperature (K)	1004.7	(C)	732		
Gas/Solid Heat Transfer (kw)	11.33	11.33			
Avg. MW of Gases above top bed	2.07				
Avg. Density of Gases above top bed (kg/m^3)	0.257				
Superficial Gas Velocity above top bed (m/s)	0.17		ft/s	0.56	
Gas Velocity in Circulation Line (m/s)	15.2		ft/s	50	
Inside Diameter of Recirculation Line (cm)	3.3		in	1.3	
Bottom Bed					
Solids Flow (kg/hr)	65.20				
Entering Solids Temp. (K)	1273				
Gas Flow (kg/hr)	11.86				
Entering Gas Temp. (K)	1004.7				
Estimated Exit Temp. (K)	1060				
Average Heat Capacity of Solids (kw-hr/kg-K)	2.50E-04				
Average Heat Capacity of Gases (kw-hr/kg-K)	4.11E-03				

Heat Loss factor	0.25				
Heat Loss (kw)	1.84				
Gas/Solid Outlet Temperature (K)	1043.7	(C)	771		
Gas/Solid Heat Transfer (kw)	1.90	1.90			
Avg. MW of Gases above bottom bed	2.07				
Avg. Density of Gases above bottom bed (kg/m^3)	0.247				
Superficial Gas Velocity above bottom bed (m/s)	0.18		ft/s	0.58	
Gas Heater (electric)					
Heat of Reaction (kw)	4.71				
Sensible Heat (kw)	10.77				
Heat Loss (kw)	7.35				
Total Heat Input (kw)	22.84				
Estimated Exit Temp. (K)	1492				
Gas Flow (kg/hr)	11.86				
Gas Inlet Temp (K)	1043.7				
Average Heat Capacity of Gases (kw-hr/kg-K)	4.22E-03				
Gas Outlet Temp (K)	1501				
Efficiency	0.95				
Power Required by Resistance Heater (kw)	24.04				
Max. Operating Temperature of Res. Heater (K)	1648				
Overall Heat Transfer Coefficient (W/m^2-K)	20				
Log Mean Temp. Diff (K)	324.0				
Surface Area of Resistance Heater (m^2)	3.52				
Dia. of Resistance Heater Element (m)	0.5				
Density of Gas at Outlet (kg/m^3)	0.172				
Velocity of Gas in Heater (m/s)	0.30		(ft/s)	1	
Diameter of Internal Passage of Heater (m)	0.57				
Thickness of Insulation (m)	0.15				
Density of Insulation (kg/m^3)	140				
Mass of Insulation (kg)	71				
Diameter of Heater (m)	0.87				
Length of Heater Surface per Linear Length	2				
Length of Heater (m)	1.1				
Thickness of Resistance Element (cm)	0.2				
Density of Resistance Element (kg/m^3)	7703		Internal Pressure (Nt/m^2)	1.03E+06	
Mass of Resistance Element (kg)	27		Diameter (m)	0.87	
Thickness of Shell (cm)	0.15		Inconel 718 Yield Stress (MPa)	414	
Density of Inconel (kg/m^3)	8221		Factor of Safety	1.5	
Mass of Shell (kg)	23		Minimum Wall Thickness (mm)	0.4	
Mass of Heater Elements (kg)	13		Cylinder Wall Thickness (mm)	3.28	
Total Mass of Electric Heater (kg)	134				
Pressure Drop Through System					
Total Static Bed Height (m)	1.83				
Average Bed Porosity	0.5				
Density of Bed Particles (kg/m^3)	4500				
Average Density of Ascending Gases (kg/m^3)	0.270				
Gravitational Parameter g/gc (Nt/kg)	1.52				
Pressure Drop (Pa)	6666		(psi)	0.97	
Pressure drop through piping:					
Gas velocity in piping (m/s)	15.2				
Inside Diameter of Piping (m)	0.033				
Gas Viscosity (Pa-s) @ 700 deg.C	1.97E-05				
Reynolds Number	6839		eqn.6.2-19 of transfer ops		
Fanning Friction Factor	0.0095		10.25978 10.86487		

Gravitational Conversion Factor gc (Kg-m/s^2-Nt)	1			
Length of Straight Pipe (m)	13.1			
Equivalent Lengths (m):		no.	E.Len	(for 1.5" Sch.40)
Sudden Enlargements (1/4)	2.7	2	1.37	
Open Globe Valves	54.9	5	10.97	
Standard Elbows	13.7	10	1.37	
Sudden Contractions (1/4)	1.5	2	0.76	
Standard T's	6.1	2	3.05	
Sudden Enlargement (>1/4)	0.9	1	0.86	
Total Equivalent Pipe Length (m)	92.9			
Pressure Loss in Piping System (Pa)	3380		(psi)	0.49
Factor for pressure drop through auxiliaries	1			
Pressure drop in auxiliaries (Pa)	6666		(psi)	0.97
Total Pressure Drop of System (Pa)	16711		(psi)	2.42

Fan

Blower	
Suction Pressure (MPa)	1.018
Discharge Pressure (MPa)	1.034
Inlet Temperature (K)	1005
H2 mass fraction in gas flow to top bed	0.970
Average Heat Capacity of Gases (kw-hr/kg-K)	4.09E-03
Avg. MW of Gases above bottom bed	2.07
Average Density of Gases (kg/m^3)	0.270
Ratio of Specific Heats of Gas	1.37
Mechanical Efficiency of Compression	0.7
Mass Flow Rate (kg/hr)	11.86
Power Required (kw)	0.29
Mass Ratio (kg/kw)	100
Blower Mass (kg)	29.0
Volume Ratio (m^3/kw)	0.027
Blower Volume (m^3)	0.008
Blower Height (m)	0.28
Blower Diameter (m)	0.19

Cyclone Separators				
Gas Velocity Entering Cyclone (m/s)	15.2			
Average Gas Flow Rate (kg/hr)	13.88		ft/s	50
Gas Viscosity (Pa-s)	1.97E-05			
Effective turns made by gas in cyclone	5			
Density of Particles (kg/m^3)	4500			
Density of Gas (kg/m^3)	0.270			
Cyclone Inlet Width (cm)	2.2			
Inlet Height (cm)	4.3			
Cyclone Diameter (cm)	8.7		(ft)	0.28
Overall Cyclone Length (cm)	34.6		(ft)	1.14
Cone (20 deg taper) length (cm)	17.3			
Exit Gas Pipe Diameter (cm)	4.3			
Exit Solids Pipe Diameter (cm)	2.2			
Particle Size w/ 50% removal efficiency (micron)	1.3			
Pressure Drop Through Cyclone (Pa)	136	(psi)	0.02	
Max. Internal Pressure (MPa)	1.03			

Part. Size (um)	Removal Eff.
0.13	1.0%
0.67	20.0%
1.0	36.0%

Inconel 718 Yield Stress (MPa)	1034			1.3	50.0%
Reduction of Inconel Yield Strength @ 1200K	0.4			2.0	69.2%
Factor of Safety	2			5.7	96.2%
Minimum Wall Thickness (cm)	0.1				
Calc. Cyclone Wall Thickness (cm)	0.02			10	98.2%
Cyclone Wall Thickness (cm)	0.1			20	99.6%
Inconel Density (kg/m^3)	8221				
Cyclone Mass (kg)	0.82				
Number of Cyclones	3				
Total Cyclone Mass (kg)	2.5				
Total Pressure Drop (Pa)	409	(psi)	0.06		
Solids Discharge Lock Hopper/Gas Separator					
Solids Rate to Discharge Hopper (kg/hr)	65.2				
Days of Storage	2				
Storage Capacity (mt)	3.1				
Bulk Storage Density (mt/m^3)	1.9				
Storage Volume (m^3)	1.6				
Number of Silos	1				
Length/Diameter	2				
Length (m)	2.0				
Diameter (m)	1.0				
Angle of Internal Friction (deg)	38				
Ratio of Lateral to Vertical pressure	0.238				
Lunar gravity (m/s^2)	1.62				
Coefficient of Friction	0.78				
Full Silo: Base Pressure from solids (MPa)	0.003				
Lateral Pressure at Base from solids (MPa)	0.000				
Max. Internal Pressure (MPa)	1.03				
Inconel 718 Yield Stress (MPa)	1034				
Reduction of Inconel Yield Strength @ 1200K	0.4				
Factor of Safety	1.2				
Minimum Wall Thickness (mm)	1.0				
Cylinder Wall Thickness (mm)	1.5				
Base Wall Thickness (mm)	1.5				
Inconel Density (mt/m^3)	8.22				
Single Hopper Mass (kg)	101.6				
Total Hopper Mass (kg)	101.6				
Hydrogen Loss:					
Solids Discharge Rate (kg/hr)	65.2				
Bulk Density (kg/m^3)	1900				
Volumetric Discharge Rate (m^3/hr)	0.034				
Particle Density (kg/m^3)	5741				
Porosity	0.67				
Density of Gas (kg/m^3)	0.270				
Mass Fraction H2	0.970				
Max. Hydrogen Loss (kg/hr)	0.006				
Hydrogen Loss (kg/day)	0.14				
Hydrogen Loss (kg/month)	1.97				
Approximate Hydrogen Inventory:					
Internal Volume of Reactor (m^3)	0.48				
Factor Volume Auxiliaries/Volume Reactor	0.06				
Density of Gas (kg/m^3)	0.270				
Mass Fraction H2	0.970				

Hydrogen Inventory Mass (kg)	0.13
Days to Lose Hydrogen Inventory	0.9
Hydrogen Makeup System:	
Liquid Hydrogen Storage (kg)	11.7
Adjusted Hydrogen Loss Rate (kg/day)	0.06
Days Storage	180
Hydrogen Density (kg/m^3)	70.9
Tank Ullage (%)	5%
Tank Volume (m^3)	0.17
Tank ID (m)	0.69
Internal Pressure (MPa)	0.10
Al 2219 Yield Stress (MPa)	324
Factor of Safety	1.5
Required Shell Thickness (mm)	0.1
Minimum Shell Thickness (mm)	0.3
Shell Thickness (mm)	0.3
Shell Density (mt/m^3)	2.8
Shell Mass per Tank (kg)	1.3
Shell Surface Area (m^2)	1.5
Multilayer Insulation Thickness (cm)	5.1
Outside Diameter of Tank (m)	0.79
MLI Density (kg/m^3)	120
MLI Volume per Tank (m^3)	0.09
MLI Mass per Tank (kg)	10.6
Empty Tank Mass (kg)	11.9
Hydrogen Heater:	
Hydrogen Flow Rate (kg/hr)	0.006
Inlet Temperature (K)	20.45
Operating Pressure (MPa)	0.10
Outlet Temperature (K)	1044
Hydrogen Gas Density (kg/m^3)	0.024
Heat of Vaporization (kw-hr/kg)	0.125
Avg. H2 gas Heat Capacity (kw-hr/kg-K)	0.00398
Required Heat Input (kw)	0.025
Efficiency	0.95
Power Required by Resistance Heater (kw)	0.027
Max. Operating Temperature of Res. Heater (K)	1648
Overall Heat Transfer Coefficient (W/m^2-K)	20
Log Mean Temp. Diff (K)	1033.0
Surface Area of Resistance Heater (m^2)	0.005
Dia. of Resistance Heater Element (m)	0.01
Velocity of Gas in Heater (m/s)	15.24
Diameter of Internal Passage of Heater (m)	0.01
Thickness of Insulation (m)	0.03
Density of Insulation (kg/m^3)	140
Mass of Insulation (kg)	0.04
Diameter of Heater (m)	0.06
Length of Heater Surface per Linear Length	2
Length of Heater (m)	0.1
Volume of Heater (m^3)	0.000
Thickness of Resistance Element (cm)	0.01
Density of Resistance Element (kg/m^3)	7703
Mass of Resistance Element (kg)	0.002
Thickness of Shell (cm)	0.1
Density of Inconel (kg/m^3)	8221

Mass of Shell (kg)	0.02		
Mass of Heater Elements (kg)	0.01		
Total Mass of Electric Heater (kg)	0.07		
Blower			
Suction Pressure (MPa)	0.101		
Discharge Pressure (MPa)	1.034		
Average Heat Capacity of Gases (kw-hr/kg-K)	3.98E-03		
Average Density of Gases (kg/m^3)	0.024		
Ratio of Specific Heats of Gas	1.40		
Mechanical Efficiency of Compression	0.7		
Mass Flow Rate (kg/hr)	0.006		
Power Required (kw)	0.03		
Mass Ratio (kg/kw)	100		
Blower Mass (kg)	3.4		
Volume Ratio (m^3/kw)	0.027		
Blower Volume (m^3)	0.001		
Blower Height (m)	0.14		
Blower Diameter (m)	0.09		
Total H2 Makeup System Mass (kg)	15		
Total H2 Makeup System Power (kw)	0.06		
Total H2 Makeup System Volume (m^3)	0.26		
Gas Velocity (m/s)	15		
Pipe Inside Diameter (cm)	0.24		
Tailings Conveyor - V-Belt			
Solids Discharge from Reactor (kg/hr)	65.2		
Tails from Beneficiation (kg/hr)	234.6		
Undersize Reject from Fine Screening (kg/hr)	231.2		
Total Tails Flow (kg/hr)	531.1		
Bulk Density of Solids (kg/m^3)	1900		
Average Belt Speed (m/min)	30		
Avg. Loaded Depth/Belt Width Ratio	0.082		
Calc. Belt Width (cm)	4.4		
Minimum Belt Width (cm)	15	(in)	6
Belt Width (cm)	15		
Req. Volumetric Flow Rate (m^3/sec)	7.76E-05		
Capacity Volumetric Flow Rate (m^3/sec)	9.52E-04		
Horizontal Flight Power Factor (kw/m - m^3/sec)	0.035		
Vertical Lift Power Factor (kw/m - m^3/sec)	0.277		
Horizontal Length (m)	7		
Belt Length (m)	15		
Belt Rise Angle (deg)	30		
Vertical Lift (m)	4		
Horizontal Power Component (kw)	0.0005		
Vertical Power Component (kw)	0.0011		
Total Power (kw)	0.0016		
Mass Factor (kg/m^2 of belt)	10		
Area of Belt (m^2)	2.3		
Mass Conveyor (kg)	23		
Stowed Volume Factor (m^3 per m^2 belt)	0.06		
Stowed Volume (m^3)	0.14		
Hauler Volume (m^3)	4.5		
Hauler Fill Factor	0.95		
Hauler Fill Time (hr)	16		

Electrolysis Cell - High Temperature					
Water Production Rate (kg/hr)	6.86				
Theo. Min. Power Required (kw/kg/hr H20)	3.52				
Efficiency	0.72				
Power Required (kw)	33.5				
Oxygen Production Rate (kg/hr)	6.09	Monthly 02 Production w/utility (kg)	2000		
Hydrogen Production Rate (kg/hr)	0.77				
Mass Factor (kg per kg/hr 02)	35				
Mass (mt)	0.213				
SG of Unit	0.6				
Volume (m^3)	0.355				
Height (m)	0.97				
Length (m)	0.61				
Width (m)	0.61				
Surface Area (m^2)	3.08				
Operating Temperature (K)	1273				
Waste Heat (kw)	9.4				
Minimum surface emissivity	0.02				
Pre-Liquefier Radiator:					
Oxygen Temperature Exit Electrolysis (K)	1273				
Oxygen Temp. Inlet to Liquefier (K)	300				
Radiator Emissivity	0.7	Absorptivity	0.3		
Rejection Heat Load (kw)	1.79			02 Cp (cal/K-mole) = a + bT + cT^-2 (300-5000 K)	
Area (m^2)	6.4	(single-side)		a b c	
Mass Factor (kg per m^2 radiator)	20			8.27 0.000258 -187700	
Mass Radiator (kg)	127.4				
Oxygen Liquefier					
Theoretical Cooling Load (kw per kg/hr 02)	0.186				
Minimum Work (kw per kg/hr 02)	0.175				
Carnot Efficiency	0.38				
Power Consumption (kw per kg/hr 02)	0.461	Eff.= 0.23			
Oxygen From Process (kg/hr 02)	6.09				
Oxygen from Storage (kg/hr)	3.89				
Total Oxygen Load (kg/hr)	9.97				
Power (kw)	4.6				
Mass Factor (kg per kg/hr 02)	20				
Mass (kg)	199.5				
Volume (m^3)	0.20				
L/D	3				
Length (m)	1.32				
Diameter (m)	0.44				
Rejection Temp. (K)	300				
Radiator Emissivity	0.8				
Rejection Heat Load (kw)	5.7				
Area (m^2)	8.8	(both sides)			
Mass Factor (kg per m^2 radiator)	20				
Mass Radiator (kg)	176.5				
Flow Velocity (m/s)	1				
LOX Density (kg/m^3)	1140				
Pipe Size (cm)	0.18				
Oxygen Storage:					

Oxygen Production (kg/hr)	6.09				
Process Plant Utility	45%				
Storage Requirements (days)	60				
LOX Density (mt/m^3)	1.14				
Max. LOX Stored (mt)	3.95				
LOX Volume (m^3)	3.46				
Number of Tanks	2				
Ullage Factor	5%				
Internal Volume per Tank (m^3)	1.82				
Internal Diameter (m)	1.5				
Tank Design Pressure (MPa)	1.0	(psi)	150		
Al 2219 Yield Stress (MPa)	324	(ksi)	47		
Factor of Safety	1.5				
Required Shell Thickness (mm)	1.8				
Shell Density (mt/m^3)	2.8				
Shell Mass per Tank (kg)	36.6				
Shell Surface Area (m^2)	7.2				
Multilayer Insulation Thickness (cm)	7.6				
MLI Density (kg/m^3)	120				
MLI Volume per Tank (m^3)	0.61				
MLI Mass per Tank (kg)	73.0				
Empty Tank Mass (kg)	109.6				
Total Tank Mass (kg)	219.3	kg Tank per kg O2 Stored =	0.056		
Thermal Conductivity of MLI (W/m^2-K)	6.80E-05				
Maximum Solar Radiation (kw/m^2)	1.373				
Tank Outside Diameter (m)	1.67				
Tank Surface Area (m^2)	8.8				
Area Per Tank Exposed to Solar Flux (m^2)	2.2				
Absorptivity of MLI	0.04				
Emissivity of Tank Shell	0.11				
Emissivity of MLI	0.72				
Interior Tank Temp. (K)	90				
Exterior Tank Temp. (K)	107				
Heat Leak per Tank (kw)	0.11				
Conductive Heat Leak (kw)	0.11	(check)	Radiative Heat Leak (kw)		0.181
Total Heat Load (kw)	0.23				
Oxygen Latent Heat (KJ/Kg O2)	213				
Additional Oxygen Vapor Load on Liquefier (kg/hr)	3.9	Boiloff per Day (% of full tank capacity)			2.4%

Piping:		
Length of 3 cm ID pipe (m)	89	(6 * Reactor Length)+Dist.From LOX Storage to Plant (50m)
Mass per Linear Length of 3 cm pipe (kg/m)	3.38	(1.25" schedule 40 steel pipe, 1.66" OD, 0.14" wall, 1.38" ID)
Mass 3 cm Pipe (kg)	302	
Length of 0.25 cm ID pipe (m)	120	(3 * Reactor Length + 50 m to LOX Storage + 50 m LH2 Storage)
Mass per length of 0.25 cm pipe (kg/m)	1.26	(0.5" sch. 40, 0.84" OD, .109" wall, 0.622" ID)
Mass 0.25 cm pipe (kg)	151	
Piping Mass (kg)	453	

Power System:		
Peak Mining + Process Power (kw)	131	
Night Process Power Requirements (kw)	7	
Power Contingency Factor	0.3	
Power For Processing @ Night (kw)	10	
Efficiency for RFC Charging	0.64	
Total PV Power (kw)	146	

Photovoltaic Array:			
Total PV Power (kw)	146		
Power/PV Mass (W/kg)	25.5	(typical oriented panels)	
PV Mass (kg)	5721		
Power/PV Area (W/m^2)	86	(for 11.5% eff, 6.5 deg pointing error, 50 C op temp, 90% packing factor)	
PV Area (m^2)	1696		
Typical Panel Length (m)	29.1		
Typical Panel Width (m)	8.74		
Number of Panels	6.7		
High Temperature Solid Oxide Regenerative Fuel Cell:			
Solid Oxide Cell Specific Performance (kg/kwe)	10.7		
Cell Stack & RFC Systems Mass (kg)	102		
Volume (m^3)	0.19		
Diameter (m)	0.49		
Length (m)	0.49		
Height (m)	0.79		
Required Power Output (kw)	10		
Days Required	14		
Energy (kwh)	3212		
Power Generated (kw per kg/hr H2O)	2.913		
Reactants Flow Rate (kg/hr)	3.3		
Oxygen Required (kg)	980		
Hydrogen Required (kg)	123		
Water Produced (kg)	1103		
Waste heat during generation (kw per kg/hr H2O)	1.54		
Waste Heat (kw)	5.0		
Tank Design Pressure (MPa)	10.1	(atm)	100
Graphite/Epoxy Wound Yield Stress (MPa)	579	(ksi)	84
Factor of Safety	1.5		
Water Density (mt/m^3)	1		
H2O Tank Volume (m^3) w/ 5% ullage	1.2		
H2 Gas Density (mt/m^3)	0.0061		
Storage Temperature (K)	400		
H2 Tank Volume (m^3)	20		
O2 Gas Density (mt/m^3)	0.0975		
O2 Tank Volume (m^3)	10		
Number H2 Tanks	2		
Number of O2 Tanks	2		
H2O Tank Internal Dia. (m)	1.3		
H2 Tank Internal Dia. (m)	2.7		
O2 Tank Internal Dia. (m)	2.1		
H2O Tank Shell Thickness (mm)	8.5		
H2 Tank Shell Thickness (mm)	17.6		
O2 Tank Shell Thickness (mm)	13.9		
Shell Density (mt/m^3)	1.55		
Shell Mass per H2O Tank (kg)	71.6		
Shell Mass per H2 Tank (kg)	621.1		
Shell Mass per O2 Tank (kg)	310.5		
MLI Thickness (cm)	1		
MLI Density (kg/m^3)	120		
MLI Mass per H2O Tank (kg)	6.7		
MLI Mass per H2 Tank (kg)	27.9		
MLI Mass per O2 Tank (kg)	17.6		
H2O Tank Exterior Dia. (m)	1.3		
H2 Tank Exterior Dia. (m)	2.7		

02 Tank Exterior Dia. (m)	2.2	
Total Tank Mass (kg)	2032.6	
Power Consumption while charging (kw per kg/hr H20)		4.537
Power Consumption (kw)	14.9	
Operating Temp. (K)	1273	
Min. Power Cons. (kw per kg/hr H20)	2.877	
Thermal Rejection (kw per kg/hr H20)	1.66	
Heat Rejection (kwt)	5.4	
Radiator Operating Temp. (K)	400	
Radiator Rejection Performance (kwt/m^2)	2.3	
Radiator Area (m^2)	2.3	
Active TCS Mass factor (kg/m^2)	20	
Thermal Control System Mass (kg)	47	
Total Regenerative FC Power System (kg)	3285	
Total RFC System Volume (m^3)	33.57527	

Nuclear Power System: (based on 300 Kwe system)

Power Requirements (kw)	131	
Waste Heat Load (kwt)	4068	
Mass Reactor (mt)	1.4	
Mass Radiator (mt)	1.8	
Mass Power Converter (mt)	1.6	
Mass Instrument Rated Shielding (mt)	0.7	
Mass Man Rated Shielding (mt)	10.5	
Total Mass w/ Inst. Shielding (mt)	5.4	
Specific Power (W/kg)	24	
SG Power System	2	
Volume (m^3)	2.4	

Central Radiator System for Basalt Mining:

Assume Heat Rejection by Mining Vehicles by on-board radiators		
Efficiency of Crushing/Beneficiation	0.5	
Power Required by Crushing/Benef. (kw)	33.8	
Heat Rejection from Crushing/Beneficiation (kw)	16.9	
Heat Rejection from Oxygen stream prior to liquefaction (kw)		1.8
Heat Rejection from Oxygen Liquefaction (kw)	5.7	
Efficiency of H2 Makeup Sys.	0.7	
Power Required by H2 Makeup Sys. (kw)	0.06	
Heat Rejection from H2 Makeup (kw)	0.02	
Total Heat Rejection (kw)	24.4	
Efficiency of Heat Rejection= A min./A req.	0.5	
Stefan Boltzmann Constant (kw/m^2-K^4)	5.7E-11	
Emissivity of Radiator	0.8	
Rejection Temperature (K)	298	
Area of Radiator (m^2)	68.1	
Width of Radiator (m)	3	
Length of Radiator (m)	22.7	
Mass Factor for ATC Sys. (kg/m^2)	20	
Radiator Mass (kg)	1362	

Central Radiator System for Soil Mining:

Assume Heat Rejection by Mining Vehicles by on-board radiators		
Efficiency of Beneficiation	0.5	
Power Required by Benef. (kw)	48.8	

Heat Rejection from Beneficiation (kw)	24.4	
Heat Rejection from Oxygen stream prior to liquefaction (kw)		1.8
Heat Rejection from Oxygen Liquefaction (kw)	5.7	
Efficiency of H2 Makeup Sys.	0.7	
Power Required by H2 Makeup Sys. (kw)	0.06	
Heat Rejection from H2 Makeup (kw)	0.02	
Total Heat Rejection (kw)	31.8	
Efficiency of Heat Rejection= A min./A req.	0.5	
Stefan Boltzmann Constant (kw/m^2-K^4)	5.7E-11	
Emissivity of Radiator	0.8	
Rejection Temperature (K)	298	
Area of Radiator (m^2)	89.0	
Width of Radiator (m)	3	
Length of Radiator (m)	29.7	
Mass Factor for ATC Sys. (kg/m^2)	20	
Radiator Mass (kg)	1781	
Power System for Soil Mining Plant Systems:		
Peak Mining + Process Power (kw)	149	
Night Process Power Requirements (kw)	7	
Power Contingency Factor	0.3	
Power For Processing @ Night (kw)	10	
Efficiency for REC Charging	0.64	
Total PV Power (kw)	164	
Photovoltaic Array:		
Total PV Power (kw)	164	
Power/PV Mass (W/kg)	25.5	(typical oriented panels)
PV Mass (kg)	6419	
Power/PV Area (W/m^2)	86	(for 11.5% eff, 6.5 deg pointing error, 50 C op temp, 90% packing
PV Area (m^2)	1903	factor, 1352 W/m^2 solar intensity)
Typical Panel Length (m)	29.1	
Typical Panel Width (m)	8.74	
Number of Panels	7.5	
Nuclear Power System: (based on 300 Kwe system)		
Power Requirements (kw)	149	
Waste Heat Load (kwt)	4272	
Mass Reactor (mt)	1.4	
Mass Radiator (mt)	1.8	
Mass Power Converter (mt)	1.6	
Mass Instrument Rated Shielding (mt)	0.7	
Mass Man Rated Shielding (mt)	10.5	
Total Mass w/ Inst. Shielding (mt)	5.5	
Specific Power (W/kg)	27	
SG Power System	2	
Volume (m^3)	2.5	

Appendix C - Unique Scaling Equations for H_2 Extraction Process

C.1 Solar Collector

Reference: (130)

A steerable, parabolic solar collector/concentrator is assumed.

$$\text{Mass (kg)} = Q_L * f_s/(Q_s * n)$$

where,

Q_L = thermal requirements (kwt)
Q_s = solar intensity = 1,352 kw/m^2
f_s = collector/concentrator mass factor = 1 kg/m^2 for all components (Ref.130 estimated 0.6 kg/m^2 for parabolic mirror, additional mass assumed for steerable mechanisms and structure, and heat transfer equipment.)
n = collector/concentrator overall efficiency = 0.7

C.2 Hydrogen Liquefier

References: (19, 101)

A two-stage refrigeration cycle must be used to liquefy hydrogen, employing either a secondary refrigerant (typically liquid nitrogen, although a lunar hydrogen liquefier might possibly use liquid oxygen) or one or more expansion engines.

$$\text{Mass (kg)} = 40 * \text{Mass Flow Rate of Hydrogen (kg/hr)}$$

Assuming the inlet gas temperature has been cooled to 300°K:

$$\text{Power (kw)} = 16.9 * \text{Mass Flow Rate of Hydrogen (kg/hr)}$$

The mass flow rate of hydrogen includes the process hydrogen production as well as boiloff rate from the hydrogen storage tanks.

Appendix D - Sample Listing of H_2 Extraction Program

Case: 1.2 mt/month LH_2, 2 mt/month LOX, Nuclear Power, 90% Plant Duty Cycle

T deg F	28-Jul-88	77	260	440	620	800	980	1160	1340	1520	1700	1880	2060	2240	2420	2600	2780	2960	3140
T deg C	05:56:41 PM	25	127	227	327	427	527	627	727	827	927	1027	1127	1227	1327	1427	1527	1627	1727
T deg K		298	400	500	600	700	800	900	1000	1100	1200	1300	1400	1500	1600	1700	1800	1900	2000
	Concentration ratio Ca	0.624575	2.023418	4.939987	10.24355	18.97745	32.37470	51.85801	79.8398	115.7221	163.8969	225.7455	303.6392	400.1389	517.9952	660.1483	829.7282	1030.054	1264.636
	concentrator rim angle radians	0.003877	0.006979	0.010906	0.015705	0.021377	0.027922	0.035342	0.043637	0.052809	0.062859	0.073791	0.085607	0.098311	0.111910	0.126409	0.141816	0.158140	0.175393
TiO2	Rutile	-212.559	-208.074	-203.723	-199.412	-195.127	-190.889	-186.67	-182.469	-178.288	-174.082	-169.839	-165.622	-161.418	-157.203	-153.022	-148.842	-144.682	-140.418
FeTiO3	Ilmentite	-277.065	-270.779	-264.682	-258.653	-252.672	-246.742	-240.822	-234.92	-229.003	-223.044	-217.062	-211.127	-205.205	-199.311	-194.238	-189.804	-185.261	-180.661
H2S	Hydrogen Sul.	-8.016	-8.903	-9.666	-10.203	-10.64	-12.209	-11.064	-9.898	-8.787	-7.549	-6.635	-5.19	-4.01	-2.832	-1.654	-0.479	0.696	1.87
FeS	Troilite	-24.219	-24.258	-24.354	-24.395	-24.655	-25.999	-24.626	-23.254	-21.84	-20.419	-19.006	-17.605	-16.388	-15.546	-14.727	-13.909	-12.942	-11.969
H20	Steam	-54.635	-53.517	-52.36	-51.155	-49.914	-48.646	-47.351	-46.04	-44.712	-43.372	-42.022	-40.663	-39.298	-37.927	-36.551	-35.171	-33.788	-32.403
FeO	Stoichiometric FeO	-60.101	-58.458	-56.901	-55.386	-53.906	-52.439	-50.971	-49.5	-47.997	-46.482	-44.971	-43.472	-41.982	-40.512	-39.086	-38.566	-37.289	-35.991
CO	Carbon Monoxide	-32.781	-34.973	-37.141	-39.308	-41.465	-43.609	-45.379	-47.854	-49.956	-52.044	-54.012	-56.182	-58.235	-60.277	-62.309	-64.33	-66.34	-68.345
CO2	Carbon Dioxide	-94.257	-94.326	-94.387	-94.445	-94.495	-94.539	-94.577	-94.609	-94.636	-94.657	-94.675	-94.688	-94.7	-94.71	-94.713	-94.716	-94.716	-94.715
SiO2	Crystobalite	-204.075	-199.679	-195.36	-191.102	-186.887	-182.701	-178.539	-174.394	-170.269	-166.165	-162.08	-157.997	-153.959	-149.919	-145.772	-141.039	-136.324	-131.621
Fe2SiO4	Fayalite	-329.668	-321.54	-313.627	-305.888	-298.067	-290.374	-282.694	-275.021	-267.294	-259.586	-251.893	-244.268	-236.827	-230.821	-224.79	-218.201	-211.328	-204.49
	Volume of H2 + H20 +H2S per cm^3 soil (2gm) in cm^3																		
	25 ppm	0.560281	0.751677	0.939597	1.127516	1.315436	1.503355	1.691275	1.879194	2.067114	2.255033	2.442953	2.630872	2.818791	3.006711	3.194630	3.382550	3.570469	3.758389
	50 ppm	1.120563	1.503355	1.879194	2.255033	2.630872	3.006711	3.382550	3.758389	4.134228	4.510067	4.885906	5.261744	5.637583	6.013422	6.389261	6.765100	7.140939	7.516778
	75 ppm	1.680845	2.255033	2.818791	3.382550	3.946308	4.510067	5.073825	5.637583	6.201342	6.765100	7.328859	7.892617	8.456375	9.020134	9.583892	10.14765	10.71140	11.27516
	100 ppm	2.241127	3.006711	3.758389	4.510067	5.261744	6.013422	6.765100	7.516778	8.268456	9.020134	9.771812	10.52348	11.27516	12.02684	12.77852	13.53020	14.28187	15.03355
	Gas Composition in equilibrium with excess Fe, FeO, FeS (mole frac.)																		
	O2	7.78E-89	1.32E-64	1.81E-50	4.49E-41	2.19E-34	2.23E-29	1.76E-25	2.31E-22	8.47E-20	1.17E-17	7.58E-16	2.68E-14	5.84E-13	8.57E-12	6.25E-11	4.32E-10	2.64E-09	1.36E-08
	H2	2.2409	3.0067	3.7199	4.3839	4.9792	5.5059	5.9729	6.3890	6.7494	7.0695	7.3602	7.6486	7.9284	8.2271	9.0231	9.5926	10.0390	10.4677
	H20	0.0002	0.0060	0.0305	0.1261	0.2824	0.5066	0.7891	1.1201	1.5018	1.9186	2.3503	2.7867	3.2221	3.6489	3.5672	3.7131	3.9718	4.2440
	H2S	0.0000	0.0000	0.0000	0.0000	0.0002	0.0009	0.0030	0.0077	0.0172	0.0320	0.0613	0.0882	0.1247	0.1509	0.1883	0.2246	0.2710	0.3218
	Total H Species	2.2411	3.0067	3.7584	4.5101	5.2617	6.0134	6.7651	7.5168	8.2685	9.0201	9.7718	10.5235	11.2752	12.0268	12.7785	13.5302	14.2819	15.0336
	Total H Species	2.2411	3.0067	3.7584	4.5101	5.2617	6.0134	6.7651	7.5168	8.2685	9.0201	9.7718	10.5235	11.2752	12.0268	12.7785	13.5302	14.2819	15.0336
	O2	7.78E-89	1.32E-64	1.81E-50	4.49E-41	2.19E-34	2.23E-29	1.76E-25	2.31E-22	8.47E-20	1.17E-17	7.58E-16	2.68E-14	5.84E-13	8.57E-12	6.25E-11	4.32E-10	2.64E-09	1.36E-08
	H2	0.9999	0.9980	0.9898	0.9720	0.9463	0.9156	0.8829	0.8500	0.8163	0.7837	0.7532	0.7268	0.7032	0.6841	0.7061	0.7090	0.7029	0.6963
	H20	0.0001	0.0020	0.0102	0.0280	0.0537	0.0842	0.1166	0.1490	0.1816	0.2127	0.2405	0.2648	0.2858	0.3034	0.2792	0.2744	0.2781	0.2823
	H2S	0.0000	0.0000	0.0000	0.0000	0.0000	0.0002	0.0004	0.0010	0.0021	0.0036	0.0063	0.0084	0.0111	0.0125	0.0147	0.0166	0.0190	0.0214
	Total H spieces	1.0000	1.0000	1.0000	1.0000	1.0000	1.0000	1.0000	1.0000	1.0000	1.0000	1.0000	1.0000	1.0000	1.0000	1.0000	1.0000	1.0000	1.0000
	Total H Species	1.0000	1.0000	1.0000	1.0000	1.0000	1.0000	1.0000	1.0000	1.0000	1.0000	1.0000	1.0000	1.0000	1.0000	1.0000	1.0000	1.0000	1.0000
	Mass per ton (gm) or ppm																		
	O2	6.23E-86	1.06E-61	1.45E-47	3.59E-38	1.75E-31	1.79E-26	1.41E-22	1.85E-19	6.78E-17	9.38E-15	6.06E-13	2.14E-11	4.67E-10	6.85E-09	5.00E-08	3.45E-07	2.11E-06	1.09E-05
	H2	99.9902	99.8007	98.9758	97.2831	94.6295	91.5602	88.2904	84.9961	81.6289	78.3745	75.3210	72.6813	70.3176	68.4061	70.6111	70.8975	70.2920	69.6288
	H20	0.0886	1.7939	9.2243	25.1657	48.2984	75.8173	104.9822	134.1134	163.4664	191.4340	216.4689	238.3242	257.1906	273.0544	251.2414	246.9854	250.2932	254.0740
	H2S	0.0000	0.0000	0.0006	0.0112	0.0679	0.2667	0.7658	1.7457	3.5479	6.8498	10.6824	14.2843	18.8405	21.3769	25.1029	28.2816	32.3352	36.4779
	Total H spieces	100.0788	101.5945	108.2000	122.3801	142.9958	167.6442	194.0384	220.8552	248.6431	275.8583	302.4723	325.2897	346.3487	362.8373	346.9554	346.1645	352.9204	360.1807
	Frac. gas released from nature soil	0.000	0.000	0.000	0.071	0.348	0.602	0.694	0.733	0.767	0.801	0.839	0.881	0.929	0.987	1.000	1.000	1.000	1.000
	Mass per ton (gm) or ppm (100 ppm H)																		
	O2	0.00E+00	0.00E+00	0.00E+00	2.56E-39	6.09E-32	1.08E-26	9.77E-23	1.36E-19	5.20E-17	7.52E-15	5.09E-13	1.89E-11	4.34E-10	6.77E-09	5.00E-08	3.45E-07	2.11E-06	1.09E-05
	H2	0.0000	0.0000	0.0000	6.9386	32.8968	55.1648	61.2886	62.3364	62.5760	62.7974	63.2070	64.0456	65.3519	67.5345	70.6111	70.8975	70.2920	69.6288

T deg F	28-Jul-88	77	260	440	620	800	980	1160	1340	1520	1700	1880	2060	2240	2420	2600	2780	2960	3140
T deg C	05:56:41 PM	25	127	227	327	427	527	627	727	827	927	1027	1127	1227	1327	1427	1527	1627	1727
T deg K		298	400	500	600	700	800	900	1000	1100	1200	1300	1400	1500	1600	1700	1800	1900	2000
H20		0.0000	0.0000	0.0000	1.7964	16.7904	45.6797	72.8755	90.3593	125.3120	153.3860	181.6537	210.0074	239.0282	269.5753	251.2414	246.9854	250.2932	254.0740
H2S		0.0000	0.0000	0.0000	0.0000	0.0236	0.1607	0.5316	1.2803	2.7198	4.8474	8.9643	12.5871	17.5100	21.1045	25.1029	28.2816	32.3352	36.4779
Total H apieces		0.0000	0.0000	0.0000	0.7358	49.7108	101.0052	134.6958	161.9760	190.6078	221.0308	253.8250	286.6400	321.0900	350.2143	346.9554	346.1645	352.9204	360.1807
MINING RATE (assumes no H2 from H2S recovered)																			
Quantity H2 desired (mt/year)	14.08756																		
kg/hr of soil at 50 ppm		1,000	1,000	1,000	1.29E+06	2.64E+05	1.52E+05	1.32E+05	1.25E+05	1.20E+05	1.15E+05	110,011	104,970	99,780	94,060	93,083	93,263	93,486	93,715
CYCLE RATE																			
cycles/hour (1/solid's residence tim		1	1	1	1	1	1	1	1	1	1	1	1	1	1	1	1	1	1
PRODUCTION RATE																			
H2 (ppm)	50																		
H2 (kg/hr)		0	0	0	4.47	4.35	4.21	4.06	3.91	3.75	3.61	3.48	3.36	3.26	3.18	3.29	3.31	3.29	3.26
H20 (kg/hr)		0	0	0	1.16	2.22	3.48	4.82	6.16	7.52	8.81	9.99	11.02	11.93	12.68	11.69	11.52	11.70	11.91
Mining Utility:	35.0%																		
H2 (mt/year)		0	0	0	13.69	13.33	12.89	12.43	11.97	11.51	11.06	10.66	10.31	10.00	9.74	10.08	10.14	10.07	10.00
H20 (mt/year)		0	0	0	3.54	6.80	10.68	14.78	18.89	23.05	27.02	30.64	33.79	36.56	38.87	35.85	35.31	35.87	36.50
After Water Split:																			
H2 (mt/year)		0	0	0	14.09	14.09	14.09	14.09	14.09	14.09	14.09	14.09	14.09	14.09	14.09	14.09	14.09	14.09	14.09
02 (mt/year)		0	0	0	3.15	6.04	9.48	13.13	16.78	20.47	24.00	27.21	30.01	32.47	34.52	31.84	31.36	31.86	32.42
THERMAL ENERGY																			
Heat Req. (MW) to heat soil		0	0	0	39	11	8	9	10	11	12	13	13	14	15	16	17	19	20
Heat Recovery Factor through staged fluidized beds:			49%																
kw to heat soil less recovered heat		0	5	10	19851	5613	4151	4415	4960	5529	6049	6523	6936	7294	7561	8188	8910	9639	10373
Approx. Exterior Temp. (K)	500																		
Heat Loss per surface area per temperature difference (kw/m^2-K)					0.002														
kw emission from reactor		0	1	2	271	127	111	124	141	159	177	193	208	222	233	252	272	293	314
1st guess exterior temp. (K)		500	500	500	500	500	500	500	500	500	500	500	500	500	500	500	500	500	500
2nd guess exterior temp. (K)		360.4	379.8	398.8	417.8	436.9	455.9	475.0	494.0	513.0	532.1	551.1	570.1	589.2	608.2	627.3	646.3	665.3	684.4
3rd guess exterior temp. (K)		281.0	325.0	362.7	395.7	424.7	450.4	473.3	493.9	512.6	529.8	545.0	560.7	574.8	588.3	601.3	613.9	626.1	638.2
4th guess exterior temp. (K)		260.6	315.8	358.9	394.3	424.3	450.3	473.3	493.9	512.6	529.8	545.8	560.7	574.8	588.3	601.3	613.9	626.1	638.2
5th guess exterior temp. (K)		259.6	315.6	358.9	394.3	424.3	450.3	473.3	493.9	512.6	529.8	545.7	560.5	574.4	587.4	599.7	611.4	622.6	633.2
6th guess exterior temp. (K)		259.6	315.6	358.9	394.3	424.3	450.3	473.3	493.9	512.6	529.8	545.7	560.5	574.4	587.4	599.7	611.4	622.5	633.2
HEAT TRANSFER SYSTEM																			
optical area of reactors (m2) ***HOT		5.6	5.6	5.6	659.5	229.5	159.1	144.7	139.6	135.6	131.8	128.0	124.0	119.9	115.3	114.5	114.6	114.8	115.0
pumps and gas lines (kg)		28.7	28.7	31.7	2736.6	879.8	600.8	554.5	604.1	660.4	831.0	799.9	1208.1	1467.8	1906.8	2270.7	2274.8	2279.9	2285.2
SUBTOTAL		28.7	28.7	31.7	2736.6	879.8	600.8	554.5	604.1	660.4	831.0	799.9	1208.1	1467.8	1906.8	2270.7	2274.8	2279.9	2285.2
REACTOR																			
Pressure (atm)	5	(psi)	73.48	(MPa)	0.506626														
Factor of Safety	2																		
Diameter of reactor (m)		0.47	0.47	0.47	5.12	3.02	2.52	2.40	2.36	2.32	2.29	2.26	2.22	2.18	2.14	2.13	2.14	2.14	2.14
Room Temperature Yield Stress (MPa)		352	352	352	1034	1034	1034	1034	1034	1034	1034	517	517	517	517	517	517	517	517
Strength Reduction due to Temperatur		1	1	0.54	1	0.91	0.89	0.81	0.48	0.33	0.18	0.45	0.21	0.15	0.1	0.08	0.08	0.08	0.08
Allowable Hoop stress (MPa)		175.8	175.8	94.9	517.1	470.6	460.2	418.9	248.2	170.6	93.1	116.3	54.3	38.0	25.9	20.7	20.7	20.7	20.7
nominal thickness (in)		0.03	0.03	0.05	0.10	0.06	0.05	0.06	0.09	0.14	0.25	0.19	0.41	0.56	0.83	1.03	1.03	1.03	1.03
thickness (mm)		0.678519	0.678519	1.256516	2.509464	1.626819	1.384736	1.451369	2.404988	3.447887	6.231244	4.912890	10.36431	14.26684	20.98326	26.13797	26.15475	26.17560	26.19695

T deg F	28-Jul-88	77	260	440	620	800	980	1160	1340	1520	1700	1880	2060	2240	2420	2600	2780	2960	3140
T deg C	05:56:41 PM	25	127	227	327	427	527	627	727	827	927	1027	1127	1227	1327	1427	1527	1627	1727
T deg K		298	400	500	600	700	800	900	1000	1100	1200	1300	1400	1500	1600	1700	1800	1900	2000
density (g/cc)		2.71	2.71	8.22	8.22	8.22	8.22	8.22	8.22	8.22	8.22	10.22	10.22	10.22	10.22	10.22	10.22	10.22	10.22
Number Reactors:		2																	
Volume of Reactor Feed (m^3/cycle)		0.097222	0.097222	0.097222	125.1369	25.69123	14.82225	12.86563	12.18161	11.66389	11.17337	10.69550	10.20544	9.700856	9.144740	9.049784	9.067223	9.088927	9.111187
Volume Reactor/Volume Solids Fed		6																	
Volume Reactor (m^3)		0.583333	0.583333	0.583333	750.82	154.15	88.93	77.19	73.09	69.98	67.04	64.17	61.23	58.21	54.87	54.30	54.40	54.53	54.67
L/D Ratio of Reactor		4																	
Length Reactor (m)		1.88	1.88	1.88	20.49	12.09	10.06	9.60	9.43	9.29	9.16	9.03	8.89	8.74	8.57	8.54	8.54	8.55	8.56
Thickness of Insulation (cm)		30																	
Density of Insulation (kg/m^3)		140																	
Volume of Insulation (m^3)		2.0	2.0	2.0	134.7	49.1	34.8	31.9	30.8	30.0	29.2	28.4	27.6	26.8	25.8	25.7	25.7	25.7	25.8
Mass of Insulation (kg)		281	281	281	18863	6879	4876	4465	4317	4202	4092	3983	3869	3750	3616	3593	3597	3603	3608
weight of reactor 1 (kg)		287	287	317	27366	8798	6008	5545	6041	6604	8310	7999	12081	14678	19068	22787	22748	22799	22852
weight of reactor 2 (kg)		287	287	317	27366	8798	6008	5545	6041	6604	8310	7999	12081	14678	19068	22787	22748	22799	22852
weight of molds (kg)		50.0	50.0	50.0	84356.1	13212.6	7622.9	6616.6	6264.8	5998.6	5746.3	5500.5	5248.5	4989.0	4703.0	4654.2	4663.1	4674.3	4685.8
weight of mold stripper (kg)		150.0	150.0	150.0	1.93E+05	39637.9	22868.6	19849.8	18794.5	17995.7	17238.9	16501.6	15745.5	14967.0	14109.0	13962.5	13989.4	14022.9	14057.3
SUBTOTAL		774.3	774.3	833.4	3.12E+05	70445.6	42506.6	37555.8	37141.6	37202.0	39605.1	38000.0	45155.3	49311.4	56947.9	64031.0	64149.0	64295.9	64446.6
GAS PURIFACATION																			
condensor (kg)		15.0	15.0	15.0	15.0	15.0	15.0	15.0	15.0	15.0	15.0	15.0	15.0	15.0	15.0	15.0	15.0	15.0	15.0
H2S scrubber (kg)		48.0	48.0	48.0	48.0	48.0	48.0	48.0	48.0	48.0	48.0	48.0	48.0	48.0	48.0	48.0	48.0	48.0	48.0
H2-CO-CO2 separator (kg) MAG		100.0	100.0	100.0	100.0	100.0	100.0	100.0	100.0	100.0	100.0	100.0	100.0	100.0	100.0	100.0	100.0	100.0	100.0
fluid lines and pumps (kg)		50.0	50.0	50.0	50.0	50.0	50.0	50.0	50.0	50.0	50.0	50.0	50.0	50.0	50.0	50.0	50.0	50.0	50.0
SUBTOTAL		213.0	213.0	213.0	213.0	213.0	213.0	213.0	213.0	213.0	213.0	213.0	213.0	213.0	213.0	213.0	213.0	213.0	213.0
SOLAR COLLECTOR																			
Solar Intensity (W/m^2)		1352																	
(not used) focal length (meters)		26.1	26.1	26.1	936.9	424.4	4062.2	3610.1	3449.5	3326.9	3209.9	3095.8	2976.4	2853.2	2716.3	2692.8	2697.1	2702.5	2708.0
(not used) Concentrator Diameter D (meters)		0.2	0.4	0.6	29.4	18.1	226.9	255.2	301.1	351.5	403.7	457.0	509.9	561.5	608.6	681.7	766.3	856.5	952.4
(not used) D energy balance		0.6	2.3	3.2	135.6	72.4	62.4	64.4	68.3	72.1	75.4	78.3	80.8	82.9	84.4	87.8	91.6	95.2	98.8
(not used) D diamter ratio		2.1	3.8	5.9	92.7	74.5	81.0	97.8	118.5	141.3	165.8	191.8	219.0	247.2	275.7	310.2	348.0	388.0	430.3
(not used) Old Conc. Area (m^2)		3.5	11.3	27.5	14435.1	4356.0	4.04E+04	5.12E+04	7.12E+04	9.70E+04	1.28E+05	1.64E+05	2.04E+05	2.48E+05	2.91E+05	3.65E+05	4.61E+05	5.76E+05	7.12E+05
Collector Efficiency Factor		70%																	
D (en bal) compensated w/ efficiency		0.8	2.7	3.9	164.5	87.9	75.7	78.1	82.9	87.5	91.5	95.1	98.0	100.6	102.4	106.6	111.1	115.6	119.9
Concentrator Area (m^2) Based on Ene		0.5	5.9	12.0	21261.7	6064.5	4503.4	4795.3	5398.3	6010.2	6578.7	7096.1	7549.2	7941.7	8236.4	8917.9	9702.6	10495.3	11292.4
Nominal Heat Flux (kw)		0.6	8.0	16.3	28745.9	8199.2	6088.6	6483.3	7298.5	8125.8	8894.3	9594.0	10206.6	10737.1	11135.7	12057.0	13117.9	14189.6	15267.3
Collector Mass Factor (kg/m^2)		1	(0.6 kg/m^2 for collector surface and 0.4 kg/m^2 for support, misc.)																
Weight of Concentrator (kg)		0.5	5.9	12.0	21261.7	6064.5	4503.4	4795.3	5398.3	6010.2	6578.7	7096.1	7549.2	7941.7	8236.4	8917.9	9702.6	10495.3	11292.4
SUBTOTAL		0.5	5.9	12.0	21261.7	6064.5	4503.4	4795.3	5398.3	6010.2	6578.7	7096.1	7549.2	7941.7	8236.4	8917.9	9702.6	10495.3	11292.4
RADIATOR																			
area (m2)		5.2	5.2	5.2	5.2	5.2	5.2	5.2	5.2	5.2	5.2	5.2	5.2	5.2	5.2	5.2	5.2	5.2	5.2
weight (kg)		52.0	52.0	52.0	52.0	52.0	52.0	52.0	52.0	52.0	52.0	52.0	52.0	52.0	52.0	52.0	52.0	52.0	52.0
SUBTOTAL		52.0	52.0	52.0	52.0	52.0	52.0	52.0	52.0	52.0	52.0	52.0	52.0	52.0	52.0	52.0	52.0	52.0	52.0
SCREENS																			
sieve size (mm)		0.5	0.5	0.5	0.5	0.5	0.5	0.5	0.5	0.5	0.5	0.5	0.5	0.5	0.5	0.5	0.5	0.5	0.5
Area of screens		29.2	29.2	29.2	37585.0	7716.4	4451.9	3864.2	3658.8	3503.3	3355.9	3212.4	3065.2	2913.7	2746.6	2718.1	2723.3	2729.9	2736.6
Mass of screens		730.0	730.0	730.0	9.40E+05	1.93E+05	111296.9	96605.1	91469.0	87581.5	83898.3	80310.1	76630.4	72841.5	68665.8	67952.8	68083.7	68246.7	68413.8
SYSTEM WEIGHT (kg)		1039.7	1045.2	1110.4	3.34E+05	7.68E+04	4.73E+04	4.26E+04	4.28E+04	4.35E+04	4.64E+04	4.54E+04	5.30E+04	5.75E+04	6.54E+04	7.32E+04	7.41E+04	7.51E+04	7.60E+04
Desired H2 Extraction (mt/year)		14.08756	3.28																
Extraction Temp. (K)		1200	(C)=	927	(F)=	1700													
Process Power Flag (Nuclear=1, PV/RFC=2)		1																	

T deg F	28-Jul-88			980	1160	1340	1520	1700
T deg C	05:56:41 PM			527	627	727	827	927
T deg K				800	900	1000	1100	1200

H2 Reactor Heat (Nuclear=1, Solar Conc.=2)	1	Process Utility:	90%		
Mining Utility	35%				
Number of Front Loader Excavators	3				
H2 Production (mt/year)	14.08756	(mt/month)	1.2	(kg/hr)	1.79
O2 Production (mt/year)	24.0	(mt/month)	2.0	(kg/hr)	3.04
O2/H2 Ratio	1.703630	1.703630			

SUMMARY:

	28-Jul-88 05:56:43 PM	Total Mass (mt)	Power (kwe)	Heat (kwt)	Total (kw)	
Mining		12.82	84.4			
Process		23.34	1611.3	4669.5		
Margin	0.3	10.85	41.7			
RFC Power Consumption			0.0			
Subtotal Process Plant		47.00	1737.4	4669.5	6406.9	
				0.0	(We/kg)	(kg/kwe)
Solar Concentrator Thermal Input		12.98	1737.4	22427.3	134	7.5
Nuclear Power		0.00	0.0		0	0.0
Photovoltaic Power		0.00	0.0		0	0.0
Regenerative Fuel Cells		12.98	1737.4	22427.3	134	7.5
Subtotal Power						
Total Plant & Power Mass		59.98				

Detailed Summary:

	Number	Total Mass (mt)	Power (kwe)	Heat (kwt)	Total Power (kw)
Front End Loaders	3	7.7	65.81		
Haulers	5	5.1	18.6		
Mining Subtotal:		12.8	84.4		
Feed Bin	1	0.37			
Tailings Bin	1	0.37			
H2 Extraction Reactors	2	16.62	1557	4670	
Solar Collectors	2	0.0		0	
Other H2 Extraction Equipment		1.10			
H2 Extraction Subtotal:		18.46	1557	4670	6226
Electrolysis	1	0.11	16.8		
O2 Liquifier	1	0.07	1.7		
H2 Liquifier	1	0.09	36.3		
O2 Storage	2	0.30			
H2 Storage	2	1.31			
Radiator & Thermal Control System		3.00		48	
Process Subtotal (include H2):		23.34	1611.3	4670	6281

Extraction Temperature (K)	1200	(C)	927	(F)	1700

T deg F	28-Jul-88			980	1160	1340	1520	1700
T deg C	05:56:41 PM			527	627	727	827	927
T deg K				800	900	1000	1100	1200

Heat Transfer Equipment (kg)	831		
Reactors (kg)	16620	Heat Req. (kwt)	6226
Gas Purification (kg)	213		
Solar Collector (kg)	0	Heat Flux (kwt)	0
Radiator (kg)	52		
Subtotal H2 Extraction Process (kg)	17716		
Soil Required (mt/hr)	115		
Mining Utility	35.0%		
H2 Extracted (kg/hr)	3.61		
H2O Extracted (kg/hr)	8.81		
Annual H2 Prod. (after Electrolysis) (mt/yr)	14	Soil/H2 Ratio =	25012
Annual O2 Prod. (after Electrolysis) (mt/yr)	24	Soil/O2 Ratio =	14682
SOIL MINING:			
Mining Hours per year	3066		
Required Mass per Month (mt/month)	29364		
Number of Front-End Loaders (FL)	3		
FL Cycle Time (sec)	120		
Bulk Density of Soil in FL Bucket (mt/m^3)	1.9		
Bucket Fill Factor	0.95		
Minimum Bucket Size Flag (1=min, 2=calc)	2		
FL Bucket Size (m^3)	0.707455		
Max Bucket Load (mt)	1.344165		
Factor of Safety	1.2		
Tipping Mass (mt)	1.612998		
Factor Mass FL/Tipping Mass	1.6		
Mass Each FL (mt)	2.6		
Mass all FLs (mt)	7.742390		
Total Material Mining Rate (mt/hr)	114.9261		
Percent of mining utility needed by FL	100.00%		
Time per month FL used mining (hrs)	255.5		
Vertical Distance Bucket Travels (m)	3.5		
Fraction cycle time raising bucket	0.3	(*No Longer Use)	
Lunar Gravity (m/s^2)	1.62		
Power efficiency factor	0.7	(*No Longer Use)	
Power for lifting loaded bucket (kw)	0.30	(*No Longer Use)	
Power for other fraction of cycle (kw)	0.15	(*No Longer Use)	
Power Factor for Wheel FLs (kw/mt empty)	8.5		
Peak Power for FL's (kw/vehicle)	21.93677		
Avg. Power required for all FLs (kw)	65.81		
Scoop Width to Depth Ratio	2		
Scoop Width (m)	1.782090		
Scoop Depth and Height (m)	0.891045		
Dist. Wheels extend beyond sides vehicle (m)	1		
Dist. Scoop extends beyond sides vehicle (m)	0.5		
S.G. of FL	1		
Length to Heigth Ratio (of primary FL)	3		
Height bottom of FL above ground (m)	1.5		
Dist. Scoop Rests from front of FL (m)	0.8		
Excavator Width (m) overall envelope	2.282090		
Excavator Length (m) overall w/o scoop	2.457413		
Excavator Length (m) overall w/ scoop	3.257413		
Excavator Height (m) overall envelope	2.319137		

T deg F	28-Jul-88		980	1160	1340	1520	1700
T deg C	05:56:41 PM		527	627	727	827	927
T deg K			800	900	1000	1100	1200

Haulers:	
Hauler Bed Width (m)	1.5
Hauler Bed Length (m)	3
Hauler Bed Height (m)	1
Hauler Bed Volume (m^3)	4.5
Bulk Density of Soil in Hauler (mt/m^3)	1.9
Hauler Fill Factor	0.95
Time Required to Fill Hauler (min)	4.24
Hauler Load (mt)	8.1
Roundtrip Distance from Mine to Reactor (km)	2
Average Hauling Velocity (km/hr)	10
Time Required for Roundtrip (min)	12
Time Required to Discharge at mine (min)	0.15
Tailings refill Rate (m^3/min)	1
Time to Refill Hauler with Tailings (min)	4.5
Time to discharge tailings (min)	0.15
Total Hauler fill time (min/cycle)	8.74
Total Hauler discharge time (min/cycle)	0.30
Single Hauler Mass Rate (mt/hr)	23.16241
Number of Hauler trips per month	3615.096
Number of hours per month loading and hauling	1267.727
Percent of Mining Time Used for loading/haul	496%
Number of Haulers Required	5
Hauler Mass Factor (p/l to hauler mass)	8
Mass of single hauler (mt)	1.02
Mass of Haulers (mt)	5
Coefficient of Rolling Friction	0.2
Power per round trip (kw)	8.224031
Calculated Hauling Power Factor (w-hr/kg-km)	0.090
Avg. Power for hauling/unload/load cycle (kw)	4.690389
Power Required for Haulers (kw)	18.58214
Dist. wheels extend beyond sides vehicle (m)	1
Height bottom of hauler above ground (m)	1.5
Length bed/length hauler drive unit	3
Hauler width (m) overall envelope	2.5
Hauler length (m) overall envelope	4
Hauler height (m) overall envelope	2.5
MINING SYSTEM SUBTOTAL, mass (mt)	12.81895
MINING SYSTEM SUBTOTAL, power (kw)	84.39246

Storage/Feed Hopper:			
Volume Charge to single Reactor (m^3)	11		
Number Reactors	2		
Number of charges store in feed hopper:	4		
Storage Volume (m^3)	45	Hauler trips to fill storage:	10
Bulk Density of Material Stored (mt/m^3)	1.9		
Mass Stored (mt)	85		
Width to Height Ratio	5		
Bin Width (m)	6.1		
Bin Height (m)	1.2		
Wall Thickness (mm)	2		
Wall Density (mt/m^3)	2.8		

T deg F	28-Jul-88			980	1160	1340	1520	1700
T deg C	05:56:41 PM			527	627	727	827	927
T deg K				800	900	1000	1100	1200
Bin Mass (mt)		0.4						
Discharge Hopper Mass (mt)		0.4						
Electrolysis Cell - High Temperature								
Utility of Process		0.9						
Inlet Water Flow Rate (kg/hr)		3.427679						
Theo. Min. Power Req. (kw-hr/kg H20)		3.52						
Efficiency		0.72						
Power Required (kw)		16.8						
Oxygen Production (kg/hr)		3.044140	Prod. (kg/month)	2000	Prod. (mt/year)		24	
Hydrogen Production (kg/hr)		0.383537						
Mass Factor (kg per kg/hr O2)		35						
Mass (kg)		106.5449						
Sg of Unit		0.6						
Volume (m^3)		0.177574						
Height (m)		0.768906						
Width (m)		0.480566						
Surface Area (m^2)		1.708989						
Operating Temperature (K)		1200						
Waste Heat (kw)		4.692110						
Minimum Surface Emissivity		0.02						
Heat Rejection:								
O2 Flow (kg/hr)		3.044140						
H2 Flow (kg/hr)		1.786854	Prod. (kg/month)	1173.963	Prod. (mt/year)		14.08756	
Start Temperature (K)		1200	cal/K-mole = a + bT + cT-2					
End Temperature (K)		300	a	b	c			
O2 Heat Capacity (kw/kg-K)		0.000288	8.27	0.000258	-187700			
H2 Heat Capacity (kw/kg-K)		0.004167	6.62	0.00081				
O2 Heat Rejection Load (kw)		0.790311						
H2 Heat Rejection Load (kw)		6.701332						
Oxygen Liquifier:								
Theoretical Cooling Load (kw per kg/hr O2)		0.1963						
Minimum Work (kw per kg/hr O2)		0.1753						
Carnot Efficiency		0.38						
Power Consumption (kw per kg/hr O2)		0.461315	Eff.= 0.230427					
Oxygen from Process (kg/hr)		3.044140						
Factor for O2 Boiloff/O2 from Process		0.2						
Oxygen from storage (kg/hr)		0.608828						
Total O2 Load (kg/hr)		3.652968						
Power (kw)		1.685171						
Mass Factor (kg per kg/hr O2)		20						
Mass (kg)		73.05936						
SG of Unit		1						
Volume (m^3)		0.073059						
L/D		3						
Length (m)		0.942488						
Diameter (m)		0.314162						
Rejection Heat Load (kw)		2.073482						

T deg F	28-Jul-88		1160	1340	1520	1700
T deg C	05:56:41 PM		627	727	827	927
T deg K			900	1000	1100	1200

Hydrogen Liquifier:			
Theoretical Cooling Load (kw per kg/hr H2)	1.069		
Minimum Work (kw per kg/hr H2)	3.386		
Carnot Efficiency	0.2		
Power Consumption (kw per kg/hr H2)	16.93055	Eff.= 0.063117	
Hydrogen from Process (kg/hr)	1.786854		
Factor for H2 Boiloff/H2 from Process	0.2		
Hydrogen from storage (kg/hr)	0.357370		
Total H2 Load (kg/hr)	2.144225		
Power (kw)	36.30293		
Mass Factor (kg per kg/hr H2)	40		
Mass (kg)	85.76903		
SG of Unit	1		
Volume (m^3)	0.085769		
L/D	3		
Length (m)	0.994247		
Diameter (m)	0.331415		
Rejection Heat Load (kw)	38.59427		
Oxygen Storage:			
O2 Production (kg/hr)	3.044140		
Process Plant Utility	0.9		
Storage Requirements (days)	90		
LOX Density (mt/m^3)	1.14		
Max. LOX Stored (mt)	5.917808		
LOX Volume (m^3)	5.191059		
Number of Tanks	2		
Ullage Factor	5%		
Intenal Volume per Tank (m^3)	2.725306		
Internal Diameter (m)	1.733027		
Tank Design Pressure (MPa)	1.034213	(psi) 150	
Al 2219 Yield Stress (MPa)	324.0536	(ksi) 47	
Factor of Safety	1.5		
Required Shell Thickness (mm)	2.074102		
Shell Density (mt/m^3)	2.8		
Shell Mass per Tank (kg)	54.92731		
Multilayer Insulation Thickness (cm)	7.62		
MLI Density (kg/m^3)	120		
MLI Volume per Tank (m^3)	0.787655		
MLI Mass per Tank (kg)	94.51863		
Empty Tank Mass (kg)	149.4459		
Total Tank Mass (kg)	298.8919		
Tank Outside Diameter (m)	1.889576		
Hydrogen Storage:			
H2 Production (kg/hr)	1.786854		
Process Plant Utility	0.9		
Storage Requirements (days)	60		
LH2 Density (mt/m^3)	0.0709		
Max. LH2 Stored (mt)	2.315763		
LH2 Volume (m^3)	32.66239		
Number of Tanks	2		

T deg F	28-Jul-88			1340	1520	1700
T deg C	05:56:41 PM			727	827	927
T deg K				1000	1100	1200

Ullage Factor	5%		
Intenal Volume per Tank (m^3)	17.14775		
Internal Diameter (m)	3.199407		
Tank Design Pressure (MPa)	1.034213	(psi)	150
Al 2219 Yield Stress (MPa)	324.0536	(ksi)	47
Factor of Safety	1.5		
Required Shell Thickness (mm)	3.829078		
Shell Density (mt/m^3)	2.8		
Shell Mass per Tank (kg)	345.6053		
Multilayer Insulation Thickness (cm)	7.62		
MLI Density (kg/m^3)	120		
MLI Volume per Tank (m^3)	2.581040		
MLI Mass per Tank (kg)	309.7249		
Empty Tank Mass (kg)	655.3302		
Total Tank Mass (kg)	1310.660		
Tank Outside Diameter (m)	3.359465		

Central Thermal Control - Radiator System	
Heat Rejection from O2 prior to Liquifier(kw)	0.790311
Heat Rejection from H2 prior to Liquifier(kw)	6.701332
Heat Rejection from O2 Liquifier (kw)	2.073482
Heat Rejection from H2 Liquifier (kw)	38.59427
Total Heat Rejection (kw)	48.15940
Efficiency of Rejection, A min/A actual	0.5
Emissivity of Radiator	0.8
Rejection Temperature (K)	290
Area of Radiator (m^2)	150.1122
Mass factor for TCS (kg/m^2)	20
TCS Mass (kg)	3002.244
Width of Radiator (m)	6
Length of Radiator (m)	25.01870

Power System:	
Mining Power (kw)	84.4
Electrolysis Power (kw)	16.8
O2 Liquifier (kw)	1.7
H2 Liquifier (kw)	36.3
Process Power (kw)	139.1
Contingency Factor	0.3
Process Power (kw)	180.9
Reactor (kwt)	6226

Nuclear Power Plant:	
Reactor Heat Provided by Nuclear Waste Heat:	75%
Nuclear Waste Heat Conversion Efficiency	0.5
Reactor Heat Provided by Nuc. (kwt)	4670
Reactor Power Provided by Nuc. (kwe)	1557
Process Power Provided by Nuc. (kwe)	180.9
Total Nuc. Electric Power Required (kwe)	1737.4
Waste Heat Load (kwt)	22427
Additional Electric Energy for Heat (kwe)	0
Total Nuc. Electric Power Required (kwe)	1737.4

T deg F	28-Jul-88	77	260	440	620	800	980	1160	1340	1520	1700	1880	2060	2240	2420	2600	2780	2960	3140
T deg C	05:56:41 PM	25	127	227	327	427	527	627	727	827	927	1027	1127	1227	1327	1427	1527	1627	1727
T deg K		298	400	500	600	700	800	900	1000	1100	1200	1300	1400	1500	1600	1700	1800	1900	2000

Waste Heat Load (kwt)	22427		
Mass Reactor (mt)	3.24		
Mass Radiator (mt)	3.85		
Mass Power Converter (mt)	2.93		
Mass Instrument Shielding (mt)	2.95		
Mass Man-Rated Shielding (mt)	14.60		
Total Mass w/ Instru. Shielding (mt)	13.0		
Specific Power (W/kg)	134	(kg/kw)	7.47
Photovoltaic and Regenerative Fuel Cell Power:			
Process Power provided by PV (kw)	0		
RFC Power Requirements (kw)	0		
RFC Charging Efficiency	0.64		
Power provided by PV (kw)	0		
Power/PV Mass (W/kg)	25.5		
PV Mass (kg)	0		
Power/PV Area (W/m^2)	86		
PV Area (m^2)	0		
Typical Panel Length (m)	29.1		
Typical Panel Width (m)	8.74		
Number of Panels	0		
RFC Scaling:			
Reactor Heat Loss at Night (kw)	177		
Contingency Factor for other power users	0.5	0.3	
RFC Power Requirements (kw)	0	176.6035	
Specific RFC Mass (W/Kg) for Lunar Night	3		
RFC Mass (kg)	0		

heat to heat from 298.15K to

anorthite kcal/mole	0	5.57	11.75	18.45	25.41	32.57	39.91	47.43	55.13	62.97	70.93	79.05	87.45	96.17	105.23
kw-hr/ton	0	23.28024	49.11002	77.11318	106.2838	136.1288	166.8069	198.2373	230.4200	263.1879	296.4573	330.3955	365.5039	401.9498	439.8168	477.6838	515.5507	553.4177
kw-hr/ton-C		0.228573	0.243299	0.255468	0.264285	0.271253	0.277156	0.282449	0.287360	0.291831	0.295989	0.299855	0.304117	0.308752	0.313740	0.318063	0.321847	0.325185

Appendix E - Analysis of Lunar Oxygen Production

(Update to Ref.48)

TABLE 1 - PROJECTED MARKET

PROJECTED ANNUAL
LEO MARKET (Reference 48)

Program (Year 2005)	Total Mass to LEO, MT	Fraction of Mass assumed to be prop.	Total Propellant in LEO, MT	Assumed Mixture Ratio	Oxygen Propellant in LEO, MT	Hydrogen Propellant in LEO, MT
LEO Servicing	118	0.3	35	7	31	4
LEO Communication	59	0.6	35	7	31	4
LEO DOD	118	0.3	35	7	31	4
LEO Space Station	136	0.3	41	7	36	5
GEO Manned Sortie	45	0.6	27	7	24	3
Planetary	30	0.7	21	7	18	3
Lunar Base	630	0.7	441	7	386	55
SDI	11,272	0.3	3,382	7	2,959	423
Mars Missions	1,307	0.7	915	7	801	114
Total	13,715		4,933		4,316	617
Total less SDI	2,443		1,551		1,357	194
Total less SDI and Mars Missions	1,136		636		556	80

ANNUAL MARKET LUNAR SURFACE AND LOW LUNAR ORBIT	Total Mass to Lunar Orbit, MT	Fraction of Mass assumed to be prop.	Total Propellant MT	Assumed Mixture Ratio	Oxygen Propellant MT	Hydrogen Propellant MT
Lunar Orbit Market	140	0.4	56	7	49	7
Lunar Surface Market	140	1.71	239	7	209	30

(LS and LO Market numbers are estimated based on placement of large lunar base)

TABLE 2 - O2 & H2 PLANTS AND MINIMUM BASE

SURFACE INFRASTRUCTURE	Large O2 Plant for Total O2 Market	Medium O2 Plant for Total less SDI	Small O2 Plant for Total less SDI & Mars Mis.	Large H2 Plant	Medium H2 Plant	Small H2 Plant	Minimum Base to Support Plant
				(H2 is used only in OTVs and landers, not sold)			
Plant specific mass, MT/MT per year product	0.187	0.19	0.19	3	3	3	-
Ratio of LOX/LH2 Produced by H2 Plant				1.7	1.7	1.7	
LEO market, MT/year	4,316	1,357	556	0	0	0	-
Lunar propellant production ratio (Total prop. produced/O2 delivered to LEO) O2 plant only case - from col. 1 in Table 7	4.52	4.52	4.52				
Lunar propellant production ratio (Total prop. produced/O2 delivered to LEO) O2 & H2 plant case - from col. 2 in Table 7	2.17	2.17	2.17				
MT H2 prod. req./MT O2 del. to LEO	0	0	0	0.28	0.28	0.28	
Total production, O2 only case, MT/year	19,527	6,140	2,518				
Total production, O2 & H2 case, MT/year	9,355	2,942	1,206	1,192	375	154	
Plant Mass, MT (O2 only case)	3,652	1,148	471				35
Plant Mass, MT (O2 & H2 case)	1,370	431	177	3,576	1,124	461	35
Power Req., O2 only case, MW	46	14	6				100
Power Req., O2 & H2 case, MW	22	7	3				
Fraction of base or plant mass that is resupplied each year	0.01	0.01	0.01	0.01	0.01	0.01	0.01
Resupply mass, O2 only case, MT/year	37	11	5				0.35
Resupply mass, O2 & H2 case, MT/year	14	4	2	35.76	11.24	4.61	0.35
Crew on lunar surface/MT per year prod.							
Crew on the lunar surface, O2 only case O2 plt:	4	4	2	0	0	0	
Crew on the lunar surface, O2 & H2 case add-on for H2 plt:	4	4	2	2 (add-on crew for H2 plant)	0	0	
Plant life, years	20 (wild guess)	20 (wild guess)	20 (wild guess)	20 (wild guess)	20 (wild guess)	20 (wild guess)	
Development cost, O2 only case, billion $ (5,000 $/KG of plant mass)	18 (guess)	6 (guess)	2 (guess)				5 (guess)

Development cost, O2 & H2 case, billion $ (5,000 $/EG of plant mass)	7 (guess)	2 (guess)	1 (guess)	17.88 (guess)	5.62 (guess)	2.31 (guess)	
Operations cost, million $/year	100 (wild guess)	100 (wild guess)	100 (wild guess)	100 (wild guess)	100 (wild guess)	100 (wild guess)	100 (guess)

TABLE 3 - EARTH LAUNCH SYSTEMS

EARTH LAUNCH SYSTEMS (Surface to 500 km LEO)	Shuttle	Small SDV	Large SDV	Heavy Lift Launch Veh.
Max. possible payload, MT	25	68	100	250
Max. O2 payload, MT (.95 multiplier for tank factor)	23.75	64.6	95	237.5
Max. H2 payload, MT (.7 multiplier for tank factor)	17.5	47.6	70	175
Launch cost (one mission, operations only), million $	114	177	134	150
General payload transportation to LEO cost, K$/Kg	4.56	2.60	1.34	0.60
O2 transportation to LEO cost, K$/Kg	4.80	2.74	1.41	0.63
H2 transportation to LEO cost, K$/Kg	6.51	3.72	1.91	0.86
Development cost, billion $	7.3	2.8	3.5	8
Years required to develop	10	5	5	10

TABLE 4 - PROPELLANT CARRIER OTVS

SPACE BASED, AEROBRAKED OTV PROPELLANT CARRIER	Cryogenic O2/H2 LEO-GEO-LEO	Cryogenic O2/H2 LEO-LLO-LEO	Cryogenic O2/H2 LLO-LEO-LLO	Cryogenic O2/H2 LLO-LEO-LLO	Cryogenic O2/H2 LLO-LEO-LLO	Cryogenic O2/H2 LLO-GEO-LLO	O2 Nuc.Elec. 5,000 sec Isp LLO-LEO-LLO	Solar Sai LLO-HLEO-L
Mission	round trip retrn empty	round trip retrn empty	round trip retrn empty	round trip retrns H2	round trip retrn empty	round trip retrn empty	round trip retrn empty 1 yr r-trip	round trip retrn empty or with pay
Load H2 in:, O2 in:	LEO, LEO	LEO, LEO	LLO, LLO	LEO, LLO	LEO,LLO	LLO,LLO	LLO	
Inert mass, MT	7	7.6	26.4	25 (guess)	24	6.8	40 (5 MW/MPD)	400 (JPL veh. scale up, may need operate f high LEO)
Aerobrake fraction, %	15	10	10	5	10	0	0	
Boiloff, MT/day	0	0.2	0.2	0	0.2	0.2	0	
Start burn mass, MT	58	158.8	243.6	177.5	220	237.6	340 (guess)	500
Max. possible payload, MT	9 (to GEO)	51.2 (to LLO)	117.2 (to Earth)	52.5 *(to Earth)	96 (to Earth)	130.8 (to GEO)	240 (guess)	100
Max. O2 payload, MT (.95 of max. payload)	8.55	48.64	111.34	49.875	91.2	124.26	228	95
Max. H2 payload, MT (.7 of max. payload)	6.3	35.84	82.04	36.75	67.2	91.56	168	70
Total Propellant Mass, MT	42	100	100	100	100	100	63 (guess)	(lose 10% of sail every 4 years)
Mixture Ratio	7	7	7	7	7	7		
O2 Propellant, MT	36.75	87.5	87.5	87.5 (load LLO)	87.5 (load LLO)	87.5 (load LLO)	60 (load LLO)	
H2 Propellant, MT	5.25	12.5	12.5	12.5 (load LEO)	12.5 (load LEO)	12.5 (load LLO)		
One mission costs, I$ (ops and airframe amortization)	18,500	18,500	18,500	18,500	18,500	18,500	56,000	18,500
General payload transportation cost, $/Kg	2,056	361	158	352	193	141	233	185
O2 transportation cost, $/Kg	2,164	380	166	371	203	149	246	195
H2 transportation cost, $/Kg	2,937	516	225	503	275	202	333	264
No. of missions veh. can fly	40 (guess)	40 (guess)	40 (guess)	40 (guess)	40 (guess)	40 (guess)	20 (wild guess)	40 (wild guess
Development cost, billion $	3.6 (guess)	5 (guess)	5 (guess)	5 (guess)	5 (guess)	5 (guess)	5 (wild guess)	5 (wild guess
Unit cost of veh., million $	500 (wild guess)	500 (wild guess)	500 (wild guess)	500 (wild guess)	500 (wild guess)	500 (wild guess)	1,000 (wild guess)	500 (wild guess
Years to develop	5 (wild guess)	5 (wild guess)	5 (wild guess)	5 (wild guess)	5 (wild guess)	5 (wild guess)	5 (wild guess)	5 (wild guess

* This OTV must return a payload of 12.6/.7 = 18 MT of H2 to LLO for the lunar lander.

TABLE 5 - TWO STAGE SMALL OTV (BASE LANDER)

Space based, aerobraked, two identical stages load O2 & H2 in LEO. Mission is LEO-LLO-LEO. First stage drops off before LLO insertion.

Inert mass, MT (for one stage)	7
Start burn mass, MT (for entire stack)	133
Max. possible payload, MT	35 (to LLO)
Max. O2 payload, MT (.95 x max.)	33.25
Max. H2 payload, MT (.7 x max.)	24.5
Total Propellant Mass, MT (for total stack)	84
Mixture Ratio	7
O2 Propellant, MT	73.5
H2 Propellant, MT	10.5
One mission costs, K$ (ops and airframe amortization)	37,000
General payload transportation cost, $/Kg	1,057
O2 transportation to LLO cost, $/Kg	1,113
H2 transportation to LLO cost, $/Kg	1,510
Development cost, billion $	3.6 (guess)
One airframe unit cost, mil. $	500 (wild guess)
No. of missions one airframe can fly	40 (guess)

TABLE 6 - LUNAR LANDER/LAUNCHERS

	Expendable Cryogenic	Reusable Cryogenic LS based and fueled	Mass Driver (Numbers scaled from Ref.5)
Deorbit or launch mass, MT	34.9	78.2	1,500
Inert mass, MT	3.8	5.2	1,500
Max. payload up, MT	0	43 *(dwn empty)	2,000 (MT/year)
Max. payload dwn, MT	17.5	17.5 (up empty)	0
Total Propellant Mass, MT (for total stack)	13.6	30	0
Mixture Ratio	7	7	
O2 Propellant, MT	11.9	26.25	
H2 Propellant, MT	1.7	3.75	
No. engines	1	3	
Missions between overhaul or replacement	1	30	
New engine cost, K$		10,000 (guess)	
Manhours maintenance per mission		200 (wild guess)	
$/manhour, LS		50,000 (guess)	
Total airframe life (No. of missions)	1	500 (wild guess)	
Development cost, billion $	2 (guess)	2 (guess)	10 (guess)
Operations cost, per mission, K$ (includes airframe replacement, engine replacement, and maintenance)	92,000	12,500	
Unit cost, K$	75,000 (wild guess)	750,000 (wild guess)	1,897,500 (guess)

* Carries 38.2 MT up if H2 loaded in LLO, 26.7 up if H2 & O2 loaded in LLO

TABLE 7 - STEADY STATE MASS PAYBACK RATIO CALCULATIONS

	O2 produc. only, all cyogenic propulsion	O2 & H2 prod., all cryogenic propulsion	O2 prod. only, mass driv.to LLO, cryo to LEO	O2 prod. only, cryo to LLO,sol. sail to LEO	O2 prod. only, cryo to LLO, elec.to LEO	O2 & H2 prod., cryo to LLO,sol. sail to LEO	Mass driv. to LLO, solar sail to LE
OTV delivered O2 to LEO, MT/flight	49.875	111.34	91.2	95	228	95	95
OTV O2 propellant req., MT/flight (load LLO, LLO-LEO-LLO)	87.5	87.5	87.5	0	59.85	0	0
OTV H2 propellant req., MT/flight	12.5 (load LEO)	12.5 (load LLO)	12.5 (load LEO)	0		0	0
Reus. lunar lander O2 del.to LLO, MT/flight (.95 x maximum payload)	40.85	40.85	1 (mass driv.)	40.85	40.85	40.85	0
No. of lunar lander flights req. per OTV flight	3.36	4.87	178.70	2.33	7.05	2.33	0
Lunar lander O2 prop. req., MT/flight (for one round trip)	26.25	26.25	0	26.25	26.25	26.25	0
Lunar lander H2 prop. req., MT/flight (for one round trip)	3.75	3.75	0	3.75	3.75	3.75	0
OTV H2 del. to LLO from Earth, MT/flight	12.61	0	0	8.72	26.42	0	0
Total payload, LEO to LLO, of OTV, MT (hydrogen plus tankage)	18.02	0	0	12.46	37.75	0	0
Steady state best case mass payback ratio (Total inbound payload/(outbound payload + OTV H2))	1.63	infinity	7.30	7.63	6.04	infinity	infinity
1/(steady state best case mass payback ratio)	0.61	0	0.14	0.13	0.17	0.00	0
Lunar launch ratio (Total propellants launched from LLO/O2 del. to LEO)	2.75	1.90	1.96	1.00	1.26	1.00	1
Lunar propellant production ratio (Total prop. produced/O2 delivered to LEO)	4.52	2.17	1.96	1.64	2.07	1.64	1

TABLE 8 - AVE. MASS PAYBACK RATIO CALCULATIONS

O2 LEO MARKET = 1,357 MT/year	O2 produc. only, all cyogenic propulsion	O2 & H2 prod., all cryogenic propulsion	O2 prod. only, mass driv.to LLO, cryo to LEO	O2 prod. only, cryo to LLO,sol. sail to LEO	O2 prod. only, cryo to LLO, elec.to LEO	O2 & H2 prod., cryo to LLO,sol. sail to LEO	Mass driv. to LLO, solar sail to LE
System lifetime, years	20	20	20	20	20	20	20
O2 LEO Market, MT/year	1,357	1,357	1,357	1,357	1,357	1,357	1,357
H2 LEO market, MT/year	194	194	194	194	194	194	194
Base mass, MT	35.0	35	35	35	35	35	35
Annual O2 production, MT/year	6,140	2,941	2,659	2,229	2,814	2,229	1,357
MT H2 prod. req./MT O2 del. to LEO	0	0.28				0.09	0
Annual H2 plant production, MT/year	0	375				125	0
O2 Plant multiplier,plant mass/annual prod.	0.19	0.19	0.19	0.19	0.19	0.19	0.19
H2 Plant multiplier,plant mass/annual prod.		3.00				3.00	
LOX Produced per LH2 Produced in H2 Plant		1.7				1.7	
O2 plant mass, MT	1,148	431	497	417	526	377	254
H2 plant mass, MT	0	1,124	0	0	0	374	0
Total base & plant, MT	1,183	1,590	532	452	561	786	289
Fraction of base and plant mass that must be resupplied each year	0.01	0.01	0.01	0.01	0.01	0.01	0.01
Annual base and plant resupply, MT/year	12	16	5	5	6	8	3
No. base and plant personnel	4	4	4	4	4	4	4
Life support resupply, MT/person-year (estimate based on water & O2 recycling)	1.1	1.1	1.1	1.1	1.1	1.1	1.1
Annual life support resupply, MT/year	4	4	4	4	4	4	4
Total mass on LS for plant & life support resupply over lifetime of plant, MT	325	406	194	178	200	245	146
Base placement system, mass in LEO over mass del. to LS	6.8	6.8	6.8	6.8	6.8	6.8	6.8
*Total base and plant mass and all resupply LEO mass charge for system life,MT	8,370	11,220	3,814	3,251	4,017	5,590	2,109
Steady state MT from Earth/MT del. to LEO 1/SS MPBR	0.61	0.00	0.14	0.13	0.17	0.00	0.00
Total LOX market for plant lifetime	122,791	58,829	53,179	44,580	56,282	44,580	27,140

Total LEO market for plant lifetime	27,140	27,140	27,140	27,140	27,140	27,140	27,140
Total LOX Market/Total LEO Support	4.92	5.24	7.06	6.55	6.61	7.98	12.87
Total LOX & LH2 Market/Total LEO Support		5.91				8.42	
Ave. mass payback ratio = total lifetime LEO LOX market/(Total LEO charge for base, plant, and all resupply mass + (1/SS MPBR) x(Total LEO market for plant lifetime))	1.09	2.42	3.60	3.99	3.19	4.86	12.87

* LS base and plant(s) mass are multiplied by a factor of 6.8 to get this number. Resupply mass is not multiplied by a factor and is therefore a best case number.

TABLE 9 - BASE PLACEMENT TRANSPORTATION COST

ANNUAL LEO O2 MARKET (MT) = 1,357	O2 produc. only, all cyogenic propulsion	O2 & H2 prod., all cryogenic propulsion	O2 prod. only, mass driv.to LLO, cryo to LEO	O2 prod. only, cryo to LLO,sol. sail to LEO	O2 prod. only, cryo to LLO, elec.to LEO	O2 & H2 prod., cryo to LLO,sol. sail to LEO	Mass driv. to LLO, solar sail to LE
Support base mass, MT	35	35	35	35	35	35	35
Annual O2 plant production, MT/year	6,140	2,941	2,659	2,229	2,814	2,229	1,357
O2 plant size, MT	1,148	431	497	417	526	377	254
Annual H2 plant production, MT/year	0	375	0	0	0	125	0
H2 plant size, MT	0	1,124	0	0	0	374	0
Mass driver, MT	0	0	1,500	0	0	0	1500
Total mass on lunar surface, MT	1,183	1,590	2,032	452	561	786	1,789
MT one lunar lander mission can place on LS	17.5	17.5	17.5	17.5	17.5	17.5	17.5
No. of missions req. to place base & plants	68	91	116	26	32	45	102
Mass in LEO of one mission, MT	119	119	119	119	119	119	119
Shuttle flights req. to support one mission	1.5	1.5	1.5	1.5	1.5	1.5	1.5
SDV flights req. to support one mission	1	1	1	1	1	1	1
Cost per Shuttle flight, million $	114	114	114	114	114	114	114
Cost per SDV flight, million $	134	134	134	134	134	134	134
Total Earth surface to LEO cost to support one lunar surface mission, million $	305	305	305	305	305	305	305
Ave. Earth surface to LEO cost, $/KG	2,218	2,218	2,218	2,218	2,218	2,218	2,218
OTV operations cost/mission, million $	37	37	37	37	37	37	37
Expendable lander cost/mission, million $	92	92	92	92	92	92	92
Total LEO to LS cost per mission, million $	129	129	129	129	129	129	129
Total LEO to LS cost per KG, $/KG	7,371	7,371	7,371	7,371	7,371	7,371	7,371
Total cost to place base and plants, million $	29,341	39,441	50,399	11,205	13,919	19,491	44,361
$/KG, Earth surface to lunar surface	24,800	24,800	24,800	24,800	24,800	24,800	24,800
Max. possible number of devoted Shuttle missions per year	24	24	24	24	24	24	24

No. of years required to place base & plant limited by max. number of Shuttle missions	4.23	5.68	7.26	1.61	2.00	2.81	6.39

TABLE 10 - PROPELLANT DELIVERY TRANSPORTATION COST CALCULATIONS

	O2 produc. only, all cyogenic propulsion	O2 & H2 prod., all cryogenic propulsion	O2 prod. only, mass driv.to LLO, cryo to LEO	O2 prod. only, cryo to LLO,sol. sail to LEO	O2 prod. only, cryo to LLO, elec.to LEO	O2 & H2 prod., cryo to LLO,sol. sail to LEO	Mass driv. to LLO, solar sail to LE
MT del. to LEO per one OTV mission	50	111	96	95	228	95	95
OTV operational cost per mission (round trip), million $	19	19	18.5	18.5	56	18.5	18.5
$/KG, LLO to LEO	371	166	193	195	246	195	195
MT payload of reusable lander	43	43		43	43	43	
No. of reusable lunar lander missions per OTV mission	3.36	4.87		2.33	7.05	2.33	
Reusable lunar lander operational cost per mission, million $	12.50	12.50		12.5	12.5	12.5	
$/KG, Lunar surface to LLO	291	291	0	291	291	291	0
Total lander operations cost per OTV mission, million $	42.04	60.84	0.00	29.07	88.08	29.07	
Steady state best case mass payback ratio (total inbound payload/(outbound payload + OTV H2))	1.63	infinity	7.30	7.63	6.04	infinity	infinity
No. large SDV missions per OTV mission (70 MT H2 per SDV mission)	0.36	0.00	0.18	0.12	0.38	0.00	0.00
SDV launch costs/OTV mission, million $ (134 million $ per SDV launch)	48.07		23.93	16.69	50.58	0.00	0.00
Total operations cost per OTV mission including lander missions, million $	108.61	79.34	42.43	64.26	194.67	47.57	18.50
$/KG, Lunar surface to LEO	2,178	713	442	676	854	501	195

TABLE 11 - OPERATIONS COST SUMMARY

ANNUAL LEO O2 MARKET (MT) = 1,357	O2 produc. only, all cyogenic propulsion	O2 & H2 prod., all cryogenic propulsion	O2 prod. only, mass driv.to LLO, cryo to LEO	O2 prod. only, cryo to LLO,sol. sail to LEO	O2 prod. only, cryo to LLO, elec.to LEO	O2 & H2 prod., cryo to LLO,sol. sail to LEO	Mass driv. to LLO, solar sail to LE
BASE PLACEMENT ERA (before lunar propellant production begins)							
Total lunar surface mass, MT	1,183	1,590	2,032	452	561	786	1,789
$/KG, Earth surface to lunar surface	24,800	24,800	24,800	24,800	24,800	24,800	24,800
Billion $ transport cost for infrastructure	29	39	50	11	14	19	44
PROPELLANT PRODUCTION ERA (after lunar base & plant placed)							
O2 del. per year to LEO, MT/year	1,357	1,357	1,357	1,357	1,357	1,357	1,357
$/KG, lunar surface to LEO	2,178	713	442	676	854	581	195
Total annual O2 transport cost, million $/year	2,955	967	600	918	1,159	679	264
Annual mass del. to LS for plant & life support resupply, MT/year	16	20	10	9	10	12	7
Resupply $/KG, Earth surface to lunar surf. (Earth surface to LEO - large SDV $/KG, plus LEO to LS, prop. transfer $/KG)	3,518	2,053	1,782	2,016	2,194	1,841	1,535
Annual resupply cost, million $/year	57	42	17	18	22	23	11
Base and plant operations costs, million $/year	200	300	200	200	200	300	200
Total annual ops. cost, prop. prod. era, million $/year	3,212	1,309	817	1,136	1,381	1,002	475
Total annual ops. cost, $/Kg O2 to LEO	2,367	964	602	837	1,017	738	350

TABLE 12 - DEVELOPMENT COSTS

ANNUAL LEO
O2 MARKET (MT) = 1,357

	O2 produc. only, all cyogenic propulsion	O2 & H2 prod., all cryogenic propulsion	O2 prod. only, mass driv.to LLO, cryo to LEO	O2 prod. only, cryo to LLO,sol. sail to LEO	O2 prod. only, cryo to LLO, elec.to LEO	O2 & H2 prod., cryo to LLO,sol. sail to LEO	Mass driv. to LLO, solar sail to LE
Min. surf. base dev., billion $	5.00	5.00	5.00	5.00	5.00	5.00	5.00
O2 plant dev., billion $	5.74	2.15	2.49	2.08	2.63	2.08	1.27
H2 plant dev., billion $	0.00	5.62	0.00	0.00	0.00	5.62	0.00
Base lander OTV dev., billion $	3.6	3.6	3.6	3.6	3.6	3.6	3.6
Expendable lunar lander dev., billion $	2.00	2.00	2.00	2.00	2.00	2.00	2.00
Reusable lunar lander dev., billion $	2.00	2.00	2.00	2.00	2.00	2.00	2.00
Propellant carrier OTV dev., billion $	5.00	5.00	5.00	0.00	5.00	0.00	0.00
Mass driver dev., billion $	0.00	0.00	10.00	0.00	0.00	0.00	10.00
Elec. prop. dev., billion $	0.00	0.00	0.00	0.00	5.00	0.00	0.00
Prop. carrier solar sail dev., billion $	0.00	0.00	0.00	5.00	0.00	5.00	5.00
Large SDV dev. cost, billion $	3.50	3.50	3.50	3.50	3.50	3.50	3.50
Total dev., billion $	26.84	28.88	33.59	23.18	28.73	28.81	32.37
Total dev. less large SDV, base lander OTV, and 50% of min. surf. base costs, billion $	17.24	19.28	23.99	13.58	19.13	19.21	22.77

TABLE 13 - SIMPLE COST COMPARISON

LEO MARKET 1,357 MT/YEAR	O2 produc. only, all cyogenic propulsion	O2 & H2 prod., all cryogenic propulsion	O2 prod. only, mass driv.to LLO, cryo to LEO	O2 prod. only, cryo to LLO,sol. sail to LEO	O2 prod. only, cryo to LLO, elec.to LEO	O2 & H2 prod., cryo to LLO,sol. sail to LEO	Mass driv. to LLO, solar sail to LE
System life, years	20	20	20	20	20	20	20
Total O2 del. to LEO in system lifetime, MT	27,140	27,140	27,140	27,140	27,140	27,140	27,140
Total dev. less large SDV, base lander OTV, and 50% of min. surf. base costs, billion $	17	19	24	14	19	19	23
Billion $ transport cost for infrastructure	29	39	50	11	14	19	44
Total ops. cost for system lifetime, includes prop. transport, resupply, and plant and base ops., billion $	64	26	16	23	28	20	10
Total dev., ops, and initial transport cost for system life, billion $	111	85	91	48	61	59	77
Total costs/total prop. del. to LEO in system lifetime, $/KG	4,083	3,128	3,343	1,750	2,235	2,164	2,824
Large SDV cost for LEO del. of O2, $/KG (Operations only)	1,411	1,411	1,411	1,411	1,411	1,411	1,411